A SIMPLIFIED SEISMIC ASSESSMENT PROCEDURE FOR BRIDGES IN INDIANA

by

Leslie S. Bonthron

A Thesis

Submitted to the Faculty of Purdue University

In Partial Fulfillment of the Requirements for the degree of

Master of Science in Civil Engineering

Lyles School of Civil Engineering

West Lafayette, Indiana

August 2020

THE PURDUE UNIVERSITY GRADUATE SCHOOL
STATEMENT OF COMMITTEE APPROVAL

Dr. Shirley Dyke, Co-Chair

Department of Mechanical Engineering and Lyles School of Civil Engineering

Dr. Julio Ramirez, Co-Chair

Lyles School of Civil Engineering

Dr. Robert Connor

Lyles School of Civil Engineering

Approved by:

Dr. Dulcy Abraham

To Grandma and Grandpa Bonthron

ACKNOWLEDGMENTS

I would first like to recognize the Joint Transportation Research Program (JTRP) for funding this project. Without them, this project nor my graduate education would have been possible.

I would like to thank my co-advisors, Dr. Shirley Dyke and Dr. Julio Ramirez, for their knowledge, guidance, and support throughout my graduate education. I am thankful for the opportunity to work with and learn from both of them. I would also like to thank Dr. Robert Connor for being on my committee and for his insightful comments.

Additionally, I would like to thank my project team, Corey Beck, Farida Mahmud, and Alana Lund. I am thankful for Corey's expertise in the development of the automated Matlab code and for our continuous exchange of ideas pertaining to the project. Farida was instrumental in the development of the detailed analysis and I am thankful for her help with various other aspects of this project. I am thankful for Alana's help and valuable input when I was stuck. Without the three of them, my experience on the project and at Purdue would not have been the same.

Special thanks to Michael Bonthron and Katie Ceglio for being supportive throughout my entire time at Purdue and for their willingness to discuss different aspects of the project with me and give a different perspective to consider. I would also like to thank my other friends who made my graduate education most memorable. Thank you for any assistance and support provided to me during the course of this project.

TABLE OF CONTENTS

LIST OF TABLES

LIST OF FIGURES

NOMENCLATURE

A_c	Area of column core (in^2)
A_v	Area of shear reinforcement (in)
b_{pg}	Width of plate girder (in)
b_v	Width of the section (in)
c_{CFT}	Coefficient for effective rigidity of CFT
c_{HP}	Coefficient for effective rigidity of H-piles
$\boldsymbol{C}_{sub}$	Inherent viscous damping rate of pier [($kips{\cdot}s$)/in]
$c_{N.A.}$	Depth to the neutral Axis (in)
d_v	Equivalent moment arm between resulting tension and compressive forces (in)
E_c	Modulus of elasticity of concrete (ksi)
E_s	Modulus of elasticity for steel (ksi)
f_c'	Compressive strength of concrete (psi)
F_{dem}	Force demand on structure ($kips$)
F_{cap}	Force capacity of substructure ($kips$)
F_{con}	Connectivity factor based on superstructure material type
F_{FB}	Frame bent factor
F_{Length}	Hammerhead length factor
f_y	Yield stress in reinforcement (ksi)
f_s	Yield stress of reinforcement (ksi)
G	Shear modulus of concrete (ksi)
g	Gravitational constant (in/s^2)
H	Clear height of pier (ft)
H_{ratio}	Height ratio of the tallest pier to the shortest pier
H_{tall}	Height of the tallest pier (ft)
H_{short}	Height of the shortest pier (ft)
h_{pg}	Height of plate girder (in)
I	Moment of inertia of substructure (in^4)

I_b	Moment of inertia of beam (in^4)
I_c	Moment of inertia of column (in^4)
$I_{CFT,dir}$	Moment of inertia of standard CFT pile in each direction (in^4)
I_d	Moment of inertia of deck (in^4)
I_{dir}	Moment of inertia of substructure element (in^4)
I_g	Gross moment of inertia (in^4)
$I_{HP,dir}$	Moment of inertia of standard H-pile shape in each direction (in^4)
$\mathbf{K}$	Stiffness matrix (*kip/in*)
K_{pier}	Stiffness of individual pier (*kip/in*)
K_v	Shear stiffness of walls (*kip/in*)
L_{ele}	Length of the substructure element (*ft*)
L_{pg}	Length of plate girder section (*in*)
L_{bridge}	Length of bridge (*in*)
l_i	Length of span (*in*)
l_{pier}	Length of superstructure supported by each pier (*ft*)
L_{pier}	Length of the top of the substructure (*ft*)
$\mathbf{M}$	Lumped mass matrix (*kips/g*)
M_b	Mass of beam (*kip/g)*
$m_{b,avg}$	Average mass of beam from sample (*kip/g)*
M_{cr}	Cracking moment (*kip·ft*)
M_{deck}	Mass of deck over each pier (*kips/g*)
M_{pier}	Mass of superstructure over each pier (*kips/g*)
M_{RC}	Mass of reinforced concrete superstructure (*kips/g*)
M_u	Ultimate moment (*kips*ft*)
M_y	Yield moment (*kips*in*)
N_b	Number of beams
N_c	Number of columns in each bent
N_{pier}	Number of piers
r_{rb}	Radius of rocker bearing (*in*)

s	Spacing of shear reinforcement (*in*)
SA	Spectral acceleration (*g*)
s_{clear}	Clear spacing of columns (*ft*)
t_{deck}	Thickness of the deck (*in*)
T	Period of structure (s)
u_i	Translational degree of freedom
V_{bs}	Base shear strength of pier (*kips*)
V_c	Shear strength of concrete (*kips*)
V_{conn}	Shear capacity of connection (*kips*)
V_n	Shear capacity (*kips*)
V_{pg}	Volume per linear foot of plate girder (in^3/lft)
V_s	Shear strength of transverse reinforcement (*kips*)
V_{sf}	Shear strength of reinforcement (*kips*)
w_{ele}	Width of substructure element (*ft*)
w_{deck}	Width of the bridge deck (out-to-out) (*ft*)
W_b	Weight of beam (*lb/lft*)
w_{rb}	Width of rocker bearing (*in*)
W_s	Weight of steel in the railing (*lbs/lft*)
x_g	Ground displacement (*in*)
$\ddot{x}_g$	Ground Acceleration (in/s^2)
x	Displacement (*in*)
$\dot{x}$	Velocity (*in/s*)
$\ddot{x}$	Acceleration (in/s^2)
α_c	Constant associated with the shear capacity of walls
γ_c	Density of Concrete (*150 pcf*)
Δ_{rb}	Allowable displacement of rocker bearing (*in*)
Δ_l	Linear displacement (*in*)
Δ_{nl}	Nonlinear displacement (*in*)
ε_c	Strain in concrete
$\varepsilon_{N.A.}$	Strain in extreme fiber for given neutral axis

ε_s	Strain in reinforcement
ε_y	Yield strain in reinforcement
ε_0	Maximum nominal concrete strain
ζ	Viscous damping ratio
θ_i	Rotational degree of freedom
λ	Light-weight concrete multiplier
λ_R	Aspect ratio
μ	Shear term
μ_s	Coefficient of static friction
ν	Poisson's ratio (assumed to be 0.15)
ρ_t	Reinforcement ratio of longitudinal (flexural) steel to concrete
ρ_s	Reinforcement ratio of transverse (shear) steel to concrete
φ_{cr}	Curvature at cracking (*rad/in*)
φ_u	Curvature at ultimate moment (*rad/in*)
φ_y	Curvature at yield (*rad/in*)

ABSTRACT

The potential for damaging earthquakes in Indiana from the New Madrid Seismic Zone (NMSZ) has been known for 200 years. However, the identification of the Wabash Valley Seismic Zone (WVSZ) has increased the awareness of the seismic risk in Indiana. The Indiana Department of Transportation (INDOT) has been preparing for the occurrence of a large event by reducing the vulnerability of its bridge network, specifically in the Vincennes district. To facilitate the work of the State of Indiana, in this thesis the development of a simplified assessment procedure for the bridges typical in Indiana is presented. The thesis also includes a proposed simplified assessment tool, Indiana Seismic Assessment Tool (INSAT) to rapidly assess the vulnerability of INDOT's bridges. To understand the behavior and vulnerabilities typical to bridges in Indiana, a set of 100 representative bridges was chosen for a detailed seismic assessment. The assessment is completed using information from the bridge drawings and 100 synthetic ground motion time-histories. The results of the detailed assessment, found in the SPR 4222 final report, are used to develop trends in mass and stiffness across bridge types, to identify vulnerability thresholds for application in the simplified assessment, and to validate the simplified assessment procedure.

The simplified seismic assessment procedure presented in this thesis and INSAT leverage information found in BIAS. However, in its current state, BIAS does not contain enough information to perform a robust seismic assessment. Eight data items are recommended for implementation into BIAS in order to carry out a simplified assessment. These eight data items are the substructure type, the abutment type, the number of elements, the element height, length, and width, the deck thickness, and a height ratio flag. While some of these items can be estimated, the best version of the simplified assessment utilizes all of the recommended data items and leads to an 87% agreement between the vulnerability classifications of the simplified assessment and the detailed assessment.

1. INTRODUCTION

1.1 Background

The two main sources for seismic hazard in Indiana are the New Madrid Seismic Zone (NMSZ) and the Wabash Valley Seismic Zone (WVSZ). Originally thought to be a part of the NMSZ, geologic evidence has identified the WVSZ as an independent system. This identification has caused an increased awareness of the seismic hazard in Indiana. The Indiana Department of Transportation (INDOT) acknowledges this and has funded SPR 4222 to assess the seismic vulnerability of their bridge network and to develop a tool, called the Indiana Seismic Assessment Tool (INSAT), which can be used to autonomously assess the seismic vulnerability of their bridge network more frequently.

In order to facilitate the autonomous assessment, INDOT's data management system, BIAS, must be updated to include necessary information. BIAS currently stores inspection reports and photos, National Bridge Inventory (NBI) fields, such as superstructure information and sufficiency ratings, and historical rehabilitation work. While many data fields can be autonomously obtained, BIAS also stores some critical information in bridge drawings and load rating information which can be obtained manually. The development and use of the seismic vulnerability tool require additional information added to BIAS in a way that allows for autonomous extraction.

The goal of this thesis is to develop a simplified assessment procedure and apply the procedure to an autonomous tool, INSAT, capable of assessing the seismic vulnerability of Indiana bridges using information currently found in BIAS as well as the critical information identified during the simplified (Level 0 and Level 1) and detailed (Level 2) assessments. The methodology and tool developed in this thesis can be expanded upon and applied to other bridge networks across the United States (Bonthron et al., 2020).

1.2 Research Objectives

The objectives of this thesis are as follows:

- Conduct a detailed vulnerability assessment, Level 2 assessment, of a representative sample of steel bridges from Indiana's bridge network. In the overall SPR-4222 project several types of bridges were analyzed using the Level 2 assessment. These included prestressed concrete and reinforced concrete superstructure types. The results from those analysis are included in this thesis in support of the Simplified Assessment.
- Examine the Level 2 assessment results to identify trends that are useful for screening criteria (Level 0).
- Develop a simplified, Level 1 assessment, and validate through a comparison with the Level 2 assessment results.
- Develop a tool (INSAT) to autonomously assess, using a combination of the Level 0 and Level 1 assessments referred to as Simplified Assessment, the vulnerability of Indiana's bridge network using information stored in BIAS.
- Identify any gaps in BIAS that can improve the Simplified Assessment procedure and provide recommendations to INDOT for addressing these gaps.

1.3 Organization

This thesis is organized into seven chapters and three appendices. Chapter 2 provides a detailed review of relevant studies and literature. Chapter 3 details the Level 2 assessment procedure and the results from this assessment. The Level 0, initial classification, and the Level 1 assessment procedure development and validation are discussed in Chapter 4. Chapter 5 outlines the development of the autonomous tool, INSAT, and identifies the gaps in data in BIAS required for the assessment. Implementation recommendations for incorporating the findings in BIAS are discussed in Chapter 6. Conclusions from the assessment and a summary of the recommendations are provided in Chapter 7. The detailed results of the Level 2 assessment on steel bridge superstructures are provided in the Appendix A. Appendix B contains a discussion of the special modelling considerations needed when a bridge has expansion joints. The methodology used to develop the Uniform Hazard Spectra (UHS) for every bridge site is given in Appendix C.

2. LITERATURE REVIEW

2.1 Introduction

This chapter focuses on a discussion of the seismicity in Indiana and the key literature relevant to a seismic evaluation of steel bridges. First, there is a discussion of the seismicity in Indiana. Following that is a discussion of literature relevant to the performance and behavior of steel superstructure bridges under seismic loading. This chapter concludes with a review of other states' methodologies for the seismic evaluation of their bridges and bridge networks.

2.2 Seismicity in Indiana

The potential for strong ground motions in Indiana has been known for many years as evident by the 1811-1812 New Madrid earthquakes and paleo liquification findings in Southern Indiana. Two fault systems contribute to the hazard in Indiana, the New Madrid Seismic Zone (NMSZ), running from northern Arkansas to southern Illinois, and the Wabash Valley Seismic Zone (WVSZ), located along the southern Illinois/Indiana boundary. Figure 2.1 shows the 2014 Seismic Hazard Map for Indiana showing the peak ground acceleration (PGA) for a probability of exceedance 2% in 50 years hazard. The contribution from the NMSZ and the WVSZ is shown by the higher expected PGA in Southern Indiana.

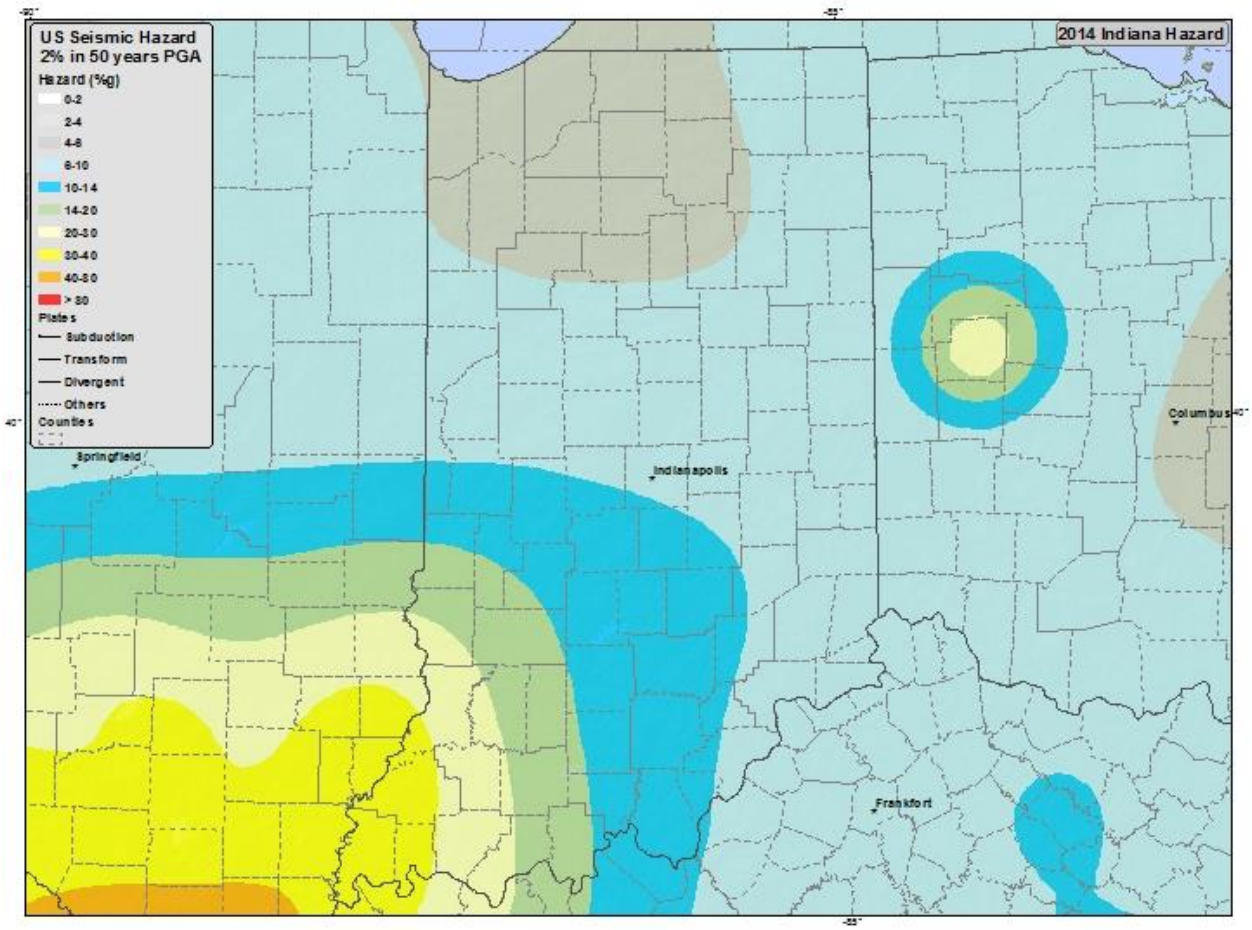

Figure 2.1. 2014 Seismic Hazard Map of Indiana (after Petersen et al., 2014)

2.2.1 New Madrid Seismic Zone

The New Madrid Seismic Zone extends from northern Arkansas to southern Illinois and contributes to the seismic hazard in Mississippi, Oklahoma, Arkansas, Tennessee, Kentucky, Illinois, and Indiana. The NMSZ is associated with the Reelfoot rift which was created about 600 million years ago when the North American Continent almost broke. The Reelfoot rift is a subsurface system of fractures and faults in the earth's crust. The seismicity of the NMSZ is contributed to movements on old faults in response to stresses related to plate movement (USGS, n.d.).

The NMSZ is responsible for the largest earthquakes Indiana has felt in recent history. In 1811-1812 NMSZ generated a series of earthquakes. Bakun and Hopper, in their paper titled

"*Magnitudes and Locations of the 1811–1812 New Madrid, Missouri, and the 1886 Charleston, South Carolina, Earthquake*" estimated the magnitudes and the locations and the epicenters of the three largest events. The first of the three occurred on December 16, 1811 with an epicenter located in northeastern Arkansas and an estimated magnitude of 7.6. The second event occurred near New Madrid, Missouri on January 23, 1812 with an estimated magnitude of 7.5. The largest of the three occurred on February 7, 1812 near New Madrid Missouri, had an estimated magnitude of 7.8, and caused damage across most of the central United States, including Indiana.

2.2.2 Wabash Valley Seismic Zone

Unlike the NMSZ, the Wabash Valley Seismic Zone has only been recently identified. Originally thought to be part of the NMZS, recent geological evidence has the WVSZ shown that it is an independent fault system. In recent history, the WVSZ has produced earthquakes with epicenters in Illinois and Indiana of magnitudes up to 5.2. The largest with an epicenter in Indiana is the 4.6 magnitude event that occurred in Evansville, Indiana on June 18, 2002 (CUSEC, n.d.). While no large magnitude events have occurred in recent history, paleo liquefaction evidence shows that prehistoric earthquakes of large magnitude have occurred and will occur again. Some researchers believe that the WVSZ poses greater threats than the NMSZ (Eagar et. al., 2006).

2.3 Performance and Behavior of Steel Bridges Under Seismic Loads

INDOT's bridge inventory consists of mainly of prestressed concrete, reinforced concrete and steel superstructures. The steel bridge inventory consists mostly of simply supported and continuous steel girder bridges resting on expansion bearings and fixed bearing. In this section, the literature available for the performance and behavior of steel bridges, with details similar to those used on bridges in Indiana, under seismic loading is reviewed. Typical damage seen in previous events includes damage to non-ductile columns, failure of fixed bearings, instability and overturning of rocker-type expansion bearings, and damage to the abutments (Choi & Jeon, 2003).

2.3.1 Typical Bridge Behavior and Vulnerabilities

The behavior of steel girder bridges, both continuous and simply supported, under low-to-moderate shaking has been studied to understand what details pose the greatest risk for damage.

Itani et al. (2004) studied the seismic behavior of steel girder bridge superstructures. Bridge superstructures, both with cross-frames and without, were modeled in SAP90 to determine the effect of cross frames on the performance of the bridge under seismic loading. For bridge superstructures without cross frames, the bridge deck was found to behave as a rigid body and displace linearly and the flexible steel girders were found to twist and deform laterally as needed with the most distortion near the supports as the bearings are the only points which counteract that movement. For bridges with intermediate cross frames, but no end cross frames, the behavior was found to not improve much as most of the distortion occurs near the supports. Analysis of bridges with intermediate and end cross frames showed that a minimal stiffness of the end cross frames was sufficient to allow the superstructure to behave as a unit (Itani et al., 2004).

The seismic fragility of typical steel bridges in moderate seismic zones was studied by Choi and Jeon (2003). They investigated the response of typical bridges with and without retrofit measures. The retrofit measures investigated included replacing steel bearings with elastomeric bearing, adding restrainer cables at supports, and using a combination of both elastomeric bearing pads and restrainer cables. The major findings were that the superstructures remain linear, but the substructure units do not. Therefore, it is important to define the moment-curvature relationship of the substructure to understand the nonlinear behavior. They found that using elastomeric bearing pads instead of steel bearings had a good isolation effect, but the bearing pads cannot protect the damage from pounding of the superstructure and abutments effectively (Choi & Jeon, 2003).

DesRoches et al. (2004) conducted an experiment to understand the effects of the 475-year earthquake and the 2.475-year earthquake on the response of multispan simply supported (MSSS) and multispan continuous (MSC) steel girder bridges in the central and southeastern United States (CSUS). 95% of bridges in CSUS were found to be are MSSS bridges, MSC bridges, or single span bridges and one third of these bridges are steel girder bridges. A bridge model, using typical details and properties found in CSUS, was developed for both a MSSS bridge and a MSC bridge using DRAIN-2DX. Each girder was supported by a fixed bearing or an expansion bearing. The bridge substructure was modelled using multi-column bents and pile bent abutments. The deck was modelled using linear elements since it is expected to remain linear. The columns were modeled as fiber elements with a defined stress-strain relationship to account for the distribution

of inelastic deformation. The steel bearings were modelled using the analytical model previously developed by Mander et al. (DesRoches et al., 2004).

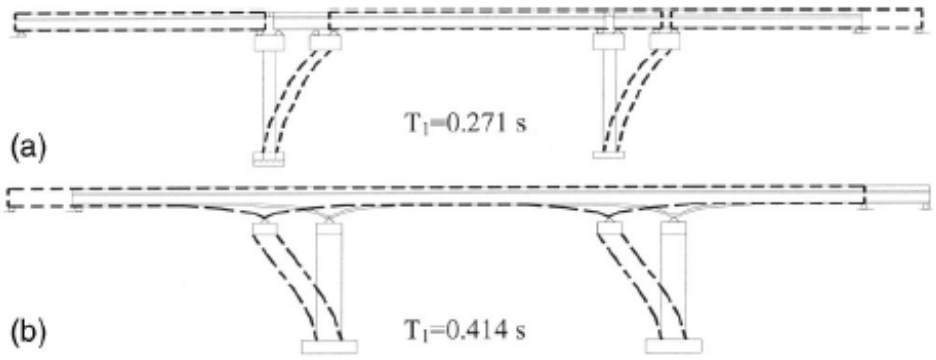

Figure 2.2. Mode Shapes for (a) Multispan Simply Supported Steel Girder Bridge and (b) Multispan Continuous Steel Girder Bridge (after DesRoches et al., 2004)

Ground motions typical for CSUS were applied to the model to determine the behavior of these bridges. The MSSS bridge had a fundamental period of 0.27s where the fundamental mode was the two frames moving linearly with one frame remaining stationary. The MSC bridge had a fundamental period of 0.41s where the fundamental mode was the longitudinal translation of the continuous deck (DesRoches, 2004). The fundamental modes can be seen in Figure 2.2.

The findings from this study reinforced the understanding of typical deficiencies seen after large event. The column demand on the MSC was two times larger than that on the MSSS due to a larger mass and displacement associated with the MSC bridges. The impact between decks of MSSS bridges and between the deck and the abutment of MSC bridges will likely lead to failure of the steel bearings. Deck displacement often exceeded the limit on rocker bearings and lead to toppling of the rocker bearing (DesRoches, 2004).

A deeper look into the seismic fragility of continuous steel highway bridges in New York was conducted by Pan, Agrawal, and Ghosn (2007). Using SAP2000, a three-dimensional model of a typical bridge was developed. In the transverse direction, displacement was restrained by both fixed and expansion bearings and inertial forces are transferred. The longitudinal direction is the critical direction and the columns were modelled as vertical cantilevers with a single plastic hinge

forming at the base of each column. The moment-curvature relationship was defined to understand the nonlinear effects. Both fixed and expansion bearings were included in the model with the fixed bearing on one intermediate pier, allowing rotation only, and the expansion bearings at the abutments and the other intermediate piers, allowing both rotation and translation. The expansion joints were modelled as gap elements to understand the effects of pounding on the behavior of the bridge (Pan, Agrawal & Ghosn, 2007).

A major finding from this study was that the gap size has a significant effect on column ductility during large ground motions. Additionally, the bridge response is more sensitive to reinforcement yield strength than column concrete compressive strength. The friction coefficient of the expansion bearing has a significant impact on the behavior. Ignoring the friction is an over-simplification of the expected bearing behavior whereas overestimating the friction factor can lead to larger forces transferred to the column. These findings were used to develop fragility curves for continuous steel highway bridges in New York (Pan, Agrawal & Ghosn, 2007).

2.3.2 Integral Abutments

Typical abutment types include integral, semi-integral, and non-integral abutments. Non-integral abutments are identified by the presence of an expansion joint. The most common problems with non-integral abutments is unseating of the superstructure from the bearing and pounding of the approach spans. This problem is eliminated for semi-integral and integral abutment bridges since the expansion joint is eliminated. The connection between the superstructure and the abutment for integral and semi-integral abutments allow the bridge to move together as a monolithic structure.

Frosch et al. studied the seismic behavior of typical integral abutment details used by INDOT to evaluate their resistance to the level of hazard expected (2009). Laboratory testing of the current integral abutment details was used to determine the displacement capacity of the current design and analytical models were used to estimate the seismic displacement at the abutments. The findings were that for bridges up to 500 *ft*, the current design for the integral abutments is adequate to provide seismic resistance, and for bridges greater than 500 *ft* in length, additional confinement at the pile head is needed for adequate seismic resistance (Frosch et al., 2009).

2.4 Other Methods for Assessing Bridge Seismic Vulnerability

The New York State Department of Transportation (NYSDOT) developed a Seismic Vulnerability Manual in 1995 which describes a detailed methodology for evaluating the highway structures for seismic vulnerability. The methodology, shown in Figure 2.3, consists of a screening processes, a classifying process and a rating process.

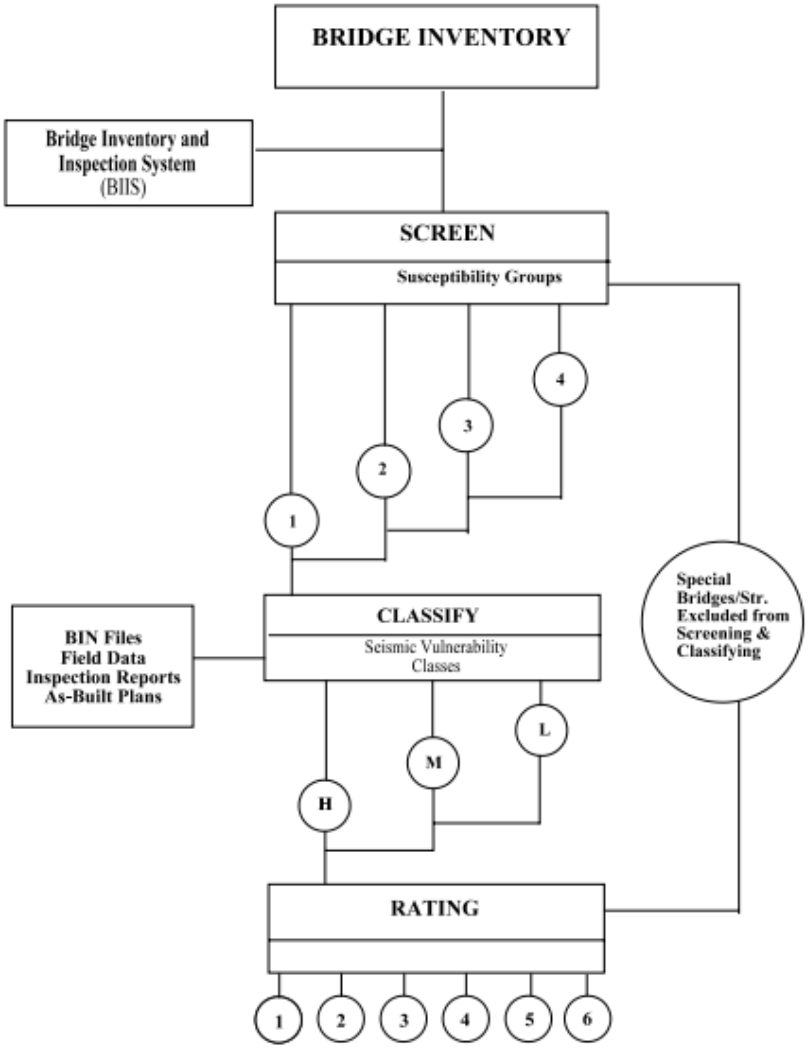

Figure 2.3. NYSDOT Seismic Vulnerability Assessment Procedure (after NYSDOT, 2004)

The screening process consists of a preliminary screening, in which bridges that do not need an assessment and bridges that need a more detailed assessment are identified, and a secondary screening, in which the bridges to be assessed are assigned a susceptibility group based on their

details. The preliminary screening removes tunnels and culverts, bridges that are currently closed, and bridges with complex structural elements, such as arch and stayed girder bridges. The secondary screening classifies bridges into one of four susceptibility groups: high seismic vulnerability, high-moderate seismic vulnerability, moderate-low seismic vulnerability, and low seismic vulnerability. Bridges identified as high seismic vulnerability consist of multispan simply supported bridges with rocker bearings, a skew greater than 30 degrees, or with fewer than four girders. Bridges identified as moderate-high seismic vulnerability consist of all the other multispan simply supported bridges, multispan continuous bridges with rocker bearings, a skew greater than 30 degrees, or with fewer than four girders, single span bridges with rocker bearings, a skew greater than 30 degrees, or with fewer than four girders, and bridges with unreinforced piers. Bridges identified as moderate-low seismic vulnerability consist of bridges with steel pile piers and bridges with a single column pier. The bridges identified as low seismic vulnerability are those with integral abutments.

The classifying process produces a score for each bridge which quantifies potential vulnerability relative to other bridges and places bridges into high, moderate, and low seismic vulnerability classes. The score is based on a vulnerability score and a seismic hazard level. The vulnerability score is calculated using various bridge details such as the substructure dimensions, the reinforcement ratio of the substructure, the bearing type, and the seat width at expansion joints. The seismic hazard level is based on an effective peak acceleration at a site with a return period of 475 years and requires the soil type at each site.

The rating process provides a uniform measure of a structure's vulnerability to failure based on a likelihood score and a consequence score. The likelihood score is based solely on the classification level whereas the consequence score is based on a failure type score and an exposure score. NYSDOT uses the ratings to determine the action required to reduce the failure vulnerability of the bridge. These actions include, but are not limited to, a safety program watch, a safety program alert, a capital program, and an inspection program (NYSDOT, 2004)

The Federal Highway Association (FHWA) created a seismic retrofitting manual for highway structures very similar to the one used by NYSDOT. This manual describes the seismic hazard, presents methodologies for screening, prioritizing, classifying, and evaluating structures, and

describes different retrofit options for different details found to be vulnerable. The screening, prioritizing and classifying methods result in a uniform measure of a structures seismic vulnerability to an upper level earthquake ground motion (that with a return period of approximately 1000 years) and a lower level earthquake ground motion (that with a return period of approximately 100 years) (FHWA, 2006).

The methodology used to develop NYSDOT's Seismic Vulnerability Manual and FHWA's Seismic Retrofitting Manual has be used in many research applications. In Kentucky, the bridges along I-24 have been evaluated and ranked using the FHWA methodology. The results from this study prioritized the bridges for a detailed evaluation (Zatar et al., 2006).

2.5 Lessons Extracted from the Literature Review

The lessons from the literature review are presented in this section. The major conclusions are as follows:

- The superstructure of steel girder bridges, given end cross-frames, behaved as a unit (Itani et al., 2004).
- The superstructure of steel girder bridges is expected to remain linear for the level of ground motion expected (DesRoches et al., 2004).
- The most common types of damage expected for steel girder superstructure bridges is damage to the substructure and damage to the bearings. (Choi & Jeon, 2003)
- Pounding on of the abutment or of two adjacent spans in simply supported continuous bridges causes damage not only to the deck, but also to the bearings (Choi & Jeon, 2003).
- Rocker-type bearings have the potential for overturning and toppling at the level of ground motion expected in the central and southeastern United States (DeRoches et al., 2004).
- For bridges under 500 ft in length or for bridges greater than 500 ft in length, with additional confinement of the pile head, INDOT details are sufficient to provide seismic resistance for the level of ground motion expected (Frosch et al., 2009)
- Other states use a rating system to determine the seismic vulnerability of their bridges and prioritize a more detailed analysis and retrofits (NYSDOT, 2004; Zatar et. al., 2006)

- Multispan simply supported steel girder bridges are more vulnerable than multispan continuous steel girder bridges because of the increased amount of bearings and the potential for pounding at the ends of the spans (DesRoches et al., 2004).

2.6 Summary

This chapter first presented discussion of the seismic hazard in Indiana and the contributions from both the New Madrid Seismic Zone and the Wabash Valley Seismic Zone. Then previous research and associated vulnerability findings were reviewed for steel girder bridges and their details. The chapter ended with a discussion of other state's methodologies used to evaluate the performance and seismic vulnerability of their bridges. The main conclusions are that the integral abutment details used on bridges in Indiana are sufficient to the level of hazard and can be excluded from a seismic analysis. The types of damage observed in bridges at approximately the same level of seismic hazard as Indiana are damage to the columns, toppling of the rocker bearings, failure of the fixed bearings, and pounding of adjacent spans.

3. DETAILED ASSESSMENT OF SELECTED BRIDGES

3.1 Introduction

The bridge selection process and the detailed (Level 2) assessment of the selected bridges to the chosen level of hazard, specific for the site conditions, is described in detail in the SPR 4222 Report for all types of bridges (Bonthron et al., 2020). The detailed analysis procedure, shown in Figure 3.3 consists of two phases, capacity (shown in purple) and demand (shown in green). The Level 2 assessment provides a basis for validating the Level 1 assessment and is useful for identifying common vulnerabilities and determining trends that can be applied to the simplified assessment including the Level 0 for initial screening of all bridges in the state. This chapter discusses the Level 2 modelling and results for the steel superstructure bridges in a representative sample set of 100 bridges. The detailed assessment of the prestressed and reinforced concrete bridges in the sample set was completed by two other project members (Bonthron et al., 2020; Mahmud, 2019). The identified trends and vulnerabilities from all three superstructure types are implemented in the simplified assessment and INSAT, discussed in subsequent chapters.

3.2 Selection of Candidate Sites

The determination of the seismic vulnerabilities of bridges in Indiana requires a seismic response analysis of representative bridges with respect to local site conditions and ground motions. As few ground-motion records have been recorded in Indiana, it is necessary to generate synthetic ground motions, compatible with the geotechnical conditions at each site. Therefore, a representative sample of 100 bridges, shown in Figure 3.1, along specified emergency (critical) routes are selected from the state bridge inventory with respect to the type of route, service under the bridge, construction material, and structure length. Half of the bridges are from the Vincennes District, which has the highest seismic hazard, according to the 2014 Seismic Hazard Map, shown in Figure 2.1. The other half of the bridges are located in the other five districts, with ten bridges chosen in each district.

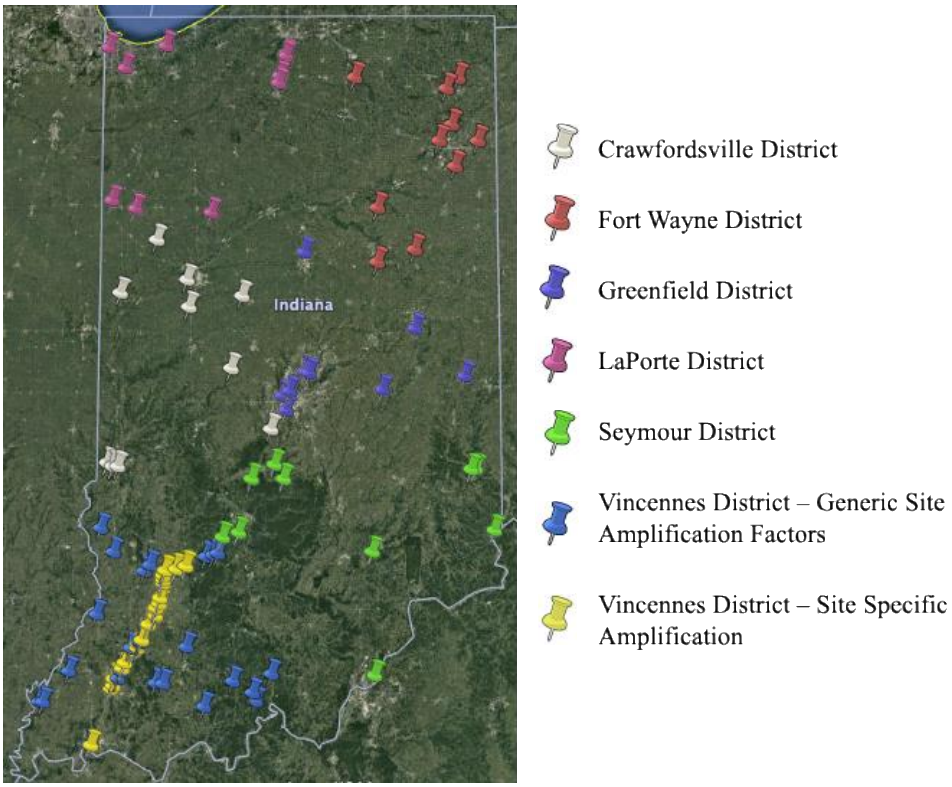

Figure 3.1. 100-bridge Sample Set

Because of the higher seismic hazard level, the selected bridges in the Vincennes district are subject to additional constraints; specifically, the availability of comprehensive geotechnical reports. Comprehensive geotechnical reports contain:

a) Boring data with a depth of at least 15 *m* (50 *ft*).

b) Shear-wave velocity profile presented in a tabular format.

c) A contract number that is assigned to a state bridge within the BIAS database

Of the 100 bridges selected, 25 bridges have reinforced concrete superstructures, 51 bridges have prestressed concrete superstructures, and 24 bridges have steel superstructures. The steel bridges are shown in Figure 3.2.

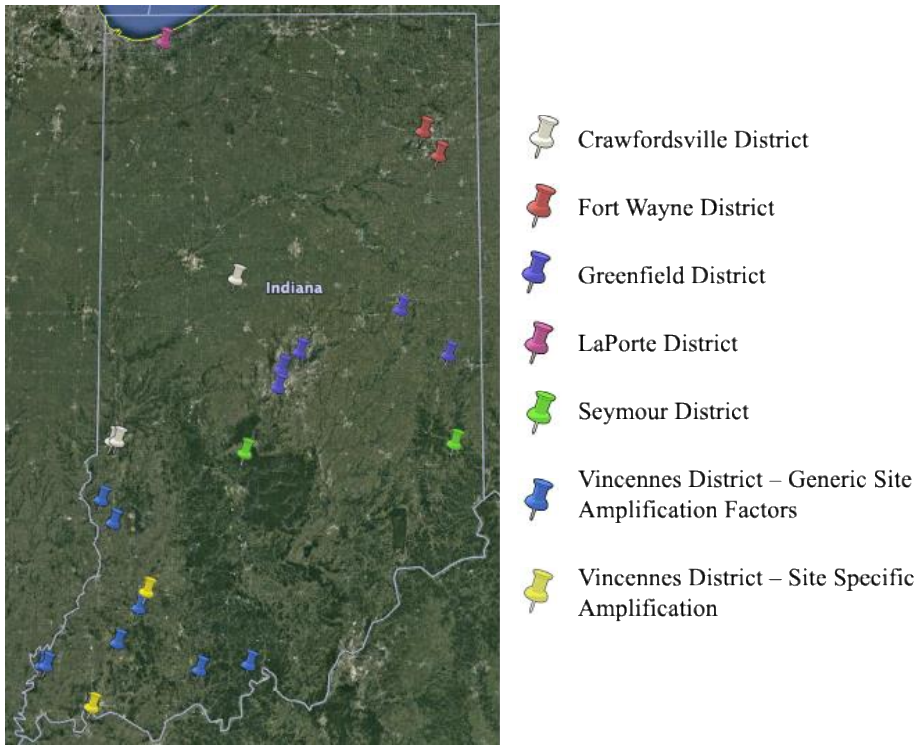

Figure 3.2. Steel Bridges in the Sample Set

The 24 steel bridges selected for the detailed assessment consists of three steel girder bridges one steel girder, truss through bridge, and twenty continuous steel girder bridges. Steel girder and continuous steel girder bridges represents 86.5% of the steel bridges in the current bridge inventory. The selected steel bridges, along with their district, number of spans, substructure type, abutment type, and if there was available geotechnical information are shown in Table 3.1.

Table 3.1. Steel Bridges in Sample Set

Asset Name	NBI	District	Number of Spans	Substructure Type	Abutment Type	Geotechnical Information
038-89-04111 B	13000	Greenfield	3	Hammerhead	Non-integral	No
052-24-06649	19430	Seymour	4	Hammerhead	Non-integral	No
062-74-06621	22190	Vincennes	2	Hammerhead	Non-integral	No
067-18-05459 D	24210	Greenfield	2	Hammerhead	Non-integral	No
154-77-01976 B	27720	Vincennes	1	-	Non-integral	No
041-82-05415 CSBL	14280	Vincennes	2	Circular Frame Bent	Integral	No
062-13-07329	22240	Vincennes	3	Hammerhead	Non-integral	No
I469-12-06947 AEB	32841	Fort Wayne	2	Rectangular Frame Bent	Integral	No
(I69)037-133-03632 JASBL	12250	Seymour	1	-	Integral	No
057-26-03322 A	20530	Vincennes	1	-	Non-integral	No
041-77-03864 JBNB	14840	Vincennes	3	Wall	Integral	Yes
I65-118-02313 JCSB	36890	Greenfield	4	Wall	Integral	No
I70-006-04712 CEBL	41130	Crawfordsville	4	Wall	Integral	No
I70-008-02344 BEBL	41230	Crawfordsville	4	Wall	Integral	No
I465-127-05274 DEBL	50340	Greenfield	3	Wall	Integral	No
I69-050-09497 NB	80182	Vincennes	3	Wall	Integral	No
I69-057-09506	80226	Vincennes	2	Wall	Integral	Yes
(421)39-12-01792 B	32200	Crawfordsville	1	-	Non-integral	No
062-82-02589 WBL	21985	Vincennes	4	Other	Non-integral	No
I64-05-05201 CEBL	33240	Vincennes	3	Other	Non-integral	No
I64-07-02367 BEBL	33280	Vincennes	3	Circular Frame Bent	Integral	No
I69-309-04548 C	40300	Fort Wayne	4	Rectangular Frame Bent	Non-integral	No
I70-074-05231 B	42020	Greenfield	4	Rectangular Frame Bent	Integral	No
I94-29-04469 CEB	49120	LaPorte	3	Circular Frame Bent	Integral	No

3.3 Generation of Synthetic Ground Motions

For each of the sample bridges, a deaggregation analysis is completed by our collaborators at the University of Notre Dame to identify the predominate seismic sources, in terms of magnitude and distance, that contribute to the seismic hazard. The results from the deaggregation analysis give scenario events that are used to generate a testbed of 100 time-histories. For the 22 steel bridges in the sample without adequate geotechnical information, synthetic ground motion time-histories were generated for the selected scenario events for NHERP site classes A to D. For the remaining two steel bridges in the sample with available geotechnical information, the ground motion time-histories were developed for the determined NHERP site class using site response analysis. The procedure used by project research team members to develop the ground motion time-histories can be found in Deliverable 1 of this project (Cao et. al., 2019).

3.4 Detailed (Level 2) Assessment Procedure

The detailed assessment is used to identify common vulnerabilities and to identify trends in the dynamic properties of Indiana bridges. The Level 2 assessment procedure, shown in Figure 3.3, is composed of two portions, capacity, shown in purple, and demand, shown in green, that are used to establish trends in vulnerability, shown in blue, of the bridge. The procedure is described in detail below and then three case studies provide detailed calculations for each of the typical substructure types: walls, hammerhead walls, and frame bents.

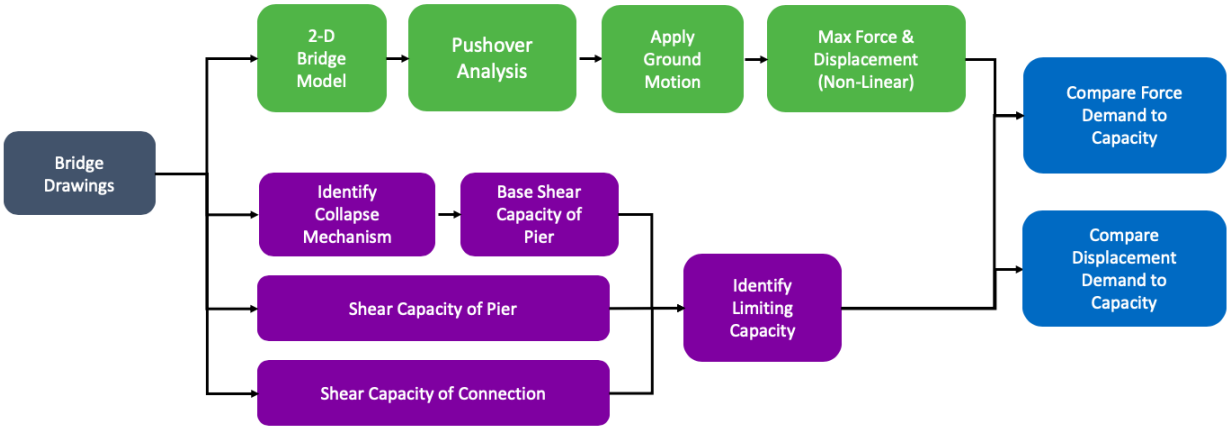

Figure 3.3. Detailed (Level 2) Assessment Procedure

3.4.1 Bridge Information

Bridge Drawings

The first step in the detailed assessment is to identify all relevant bridge geometries, and information that will impact the dynamic model and the capacity calculations for the bridge using the available bridge drawings, including rehabilitation and retrofit plans. This information includes bridge material properties, bridge superstructure geometry, bridge substructure and reinforcement layout, bearing details, and abutment details.

3.4.2 Capacity

Identify Collapse Mechanism

Each substructure's collapse mechanism depends on its ability to resists moments. For all fixed-free walls and hammerhead walls, the identified collapse mechanism is the formation of a plastic hinge at the base of the pier. For all frame bents, the identified collapse mechanism is determined through a limit analysis, comparing all potential mechanisms of failure and, ultimately choosing the mechanism with the smallest corresponding base shear. However, the capability of the substructure to exhibit this mode of failure is based on the aspect ratio (λ_R). Bridges with an aspect ratio less than 2.5 are not controlled by flexure, as seen in Figure 3.4.

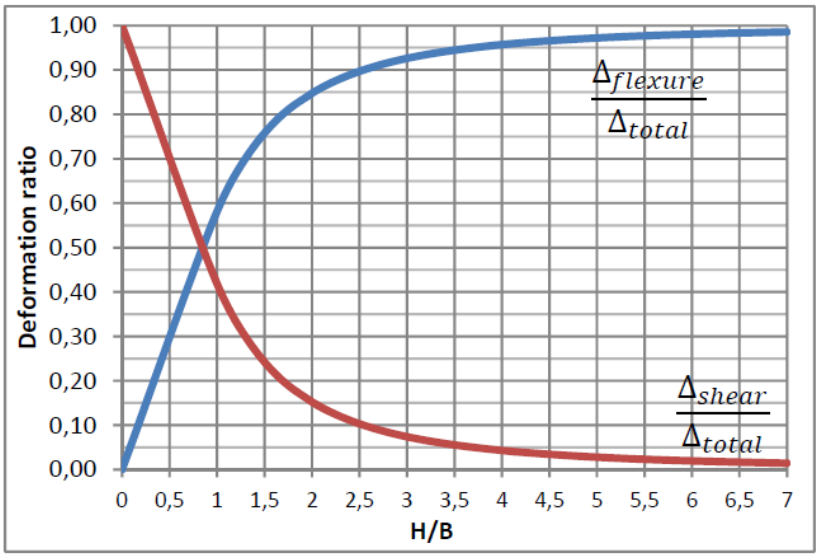

Figure 3.4. Shear and Bending Stiffness Contribution as a Function of the Aspect Ratio (Fares, 2011)

Bridges with an aspect ratio greater than 2.5 can behave in flexure and the collapse mechanism, corresponding to the formation of plastic hinges, is based on the ultimate moment capacity of substructure elements (walls, columns, and bent caps). The ultimate moment capacity for each of these elements is computed using the moment-curvature relationship. For this analysis, three points on the moment-curvature diagram are calculated: cracking, first yield, and ultimate. The first moment and corresponding curvature point calculated is the cracking moment and curvature. The moment associated with cracking is calculated using the gross moment of inertia of the pier and a centroid that is assumed to be at half the section depth. The cracking moment and curvature are calculated as

$$M_{cr} = 7.5\sqrt{f'_c} * \frac{2I_g}{H} \tag{3.1}$$

$$\varphi_{cr} = \frac{M_{cr}}{I_g * E_c}. \tag{3.2}$$

Prior to the exceedance of the cracking moment, the bridge behaves linearly. The second point on the moment-curvature diagram is the yield moment and corresponding curvature. The yield moment occurs at first yield of the extreme tension fiber of the steel and occurs when force equilibrium of the cross-section is achieved. The yield strain of the extreme fiber and resulting curvature can be calculated as

$$\varepsilon_y = \frac{f_y}{E_s} \tag{3.3}$$

$$\varphi_y = \frac{\varepsilon_c}{c_{N.A.}}. \tag{3.4}$$

The final calculated point on the moment-curvature diagram corresponds to when the substructure fully develops its plastic hinge. This corresponds to the ultimate moment and curvature. The ultimate moment is calculated at the point where strain hardening in the extreme tension fiber of the steel ($\varepsilon_s = .01$) or a compressive concrete strain (ε_c) of .003 occurs, whichever occurs first. The solution for the ultimate moment is calculated by determining the depth of the neutral axis ($c_{N.A.}$) that leads to force equilibrium. The corresponding curvature can be calculated using Equation 3.4.

Base Shear

Using the identified collapse mechanism and the corresponding ultimate moment, the base shear in each pier is calculated. The base shear is the maximum lateral force the base of the substructure can experience based on the cross-sectional properties of the element.

Shear Capacity of the Pier

The shear capacity of each substructure type is calculated using the equations outlined in AASHTO (2017). For structures where shear reinforcement is not present (typically older walls, constructed prior to 1990), the shear capacity of the pier is solely the shear capacity of the concrete.

Horizontal Shear Capacity of the Connection

The Level 2 assessment assumes that there is a singular displacement for the substructure and the superstructure. This assumption relies on the connection between the substructure and superstructure. For steel bridges supported by fixed and expansion shoes, INDOT's standard details show a 2-*inch* fillet weld connecting the bearing to the anchor plate in the substructure. Because of the typical age of the substructures and the potential for defects and cracks in the weld, the model relies on the frictional force of the superstructure to transfer forces instead of the short welds. Therefore, the horizontal shear capacity of the connection for steel bridges with expansion and fixed shoes is calculated as the force required to overcome the frictional resistance. For steel bridge superstructures supported by elastomeric bearing pads, the shear capacity of the connection is the shear strength of the bolts connecting the beam to the top plate of the bearing.

Identify Limiting Capacity

The limiting capacity is the minimum of the base shear, shear capacity of the substructure, and the horizontal shear capacity of the connection. A capacity based on the formation of plastic hinges is the desired limiting capacity because it is ductile and the total collapse of the substructure is dictated by an allowable rotation of the substructure, assuming that the load capacity can be maintained considering P-delta effects and that the substructure provides sufficient bearing seat length. In bridges where the shear capacity exceeds the calculated base shear, or where the formation of plastic hinges is impossible due to cross-sectional properties, the substructure is unable to form plastic hinges which can result in brittle failure.

3.4.3 Demand

2-D Bridge Model

The bridge characteristics identified from the bridge drawings are used to determine the dynamic properties of the structure, and, in turn, to calculate the force and displacement demand on a bridge. As is typical in design, each orthogonal direction is considered independently. Thus, a 2-D finite element modeling procedure is adopted to determine the fundamental dynamic characteristics of each bridge to develop equations-of-motion for both the transverse and longitudinal direction, shown in Figure 3.5 (Metzger, 2014; Garcia, 1998).

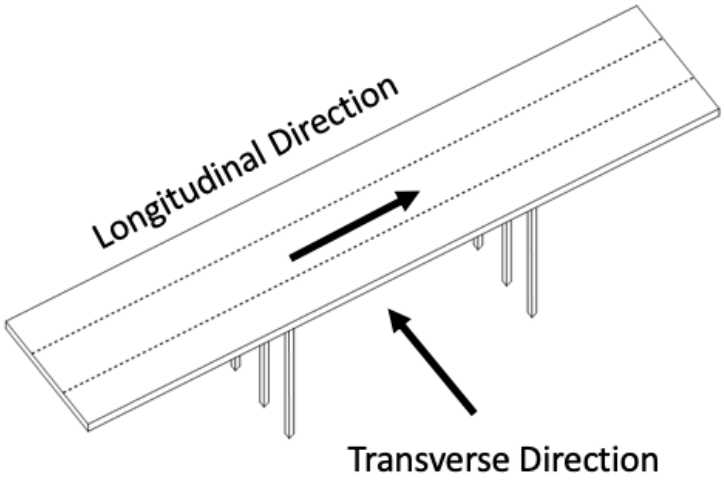

Figure 3.5. Fundamental Bridge Directions

Longitudinal Mass

The mass of the bridge is calculated using superstructure geometry (bridge deck out-to-out and bridge length), bridge railing geometry, beam type and geometry, and the applicable material types. The entire mass of the bridge superstructure is used in the longitudinal direction.

Transverse Mass

The mass of the bridge is calculated using superstructure geometry (bridge deck out-to-out and bridge length), bridge railing geometry, beam type and geometry, and the applicable material types. In the transverse direction, a lumped mass model is used, and the activated mass is determined using the tributary mass supported by each pier.

Longitudinal Stiffness

Steel girder bridges are modelled as SDOF systems in the longitudinal direction with all applicable intermediate piers behaving as springs in parallel. The bearing at each pier determines whether the pier adds stiffness.

The bearing must be able to transfer forces in the longitudinal direction. Piers with expansion shoe bearings do not contribute to the stiffness of the bridge because of the behavior of the expansion shoe. Expansion shoes are used to allow thermal expansion and contraction and do not allow lateral forces to be transferred from the superstructure to the substructure. Fixed shoes allow the transfer of lateral forces from the superstructure to the substructure and are considered to add stiffness to the bridge model in the longitudinal direction. Piers with elastomeric bearing pads that are confined in the longitudinal direction are assumed to add stiffness however, if the movement of the elastomeric bearing pads is not confined in the longitudinal direction, the piers do not contribute to the overall stiffness.

For modelling, each pier is assumed to be fixed at the based while the top is assumed to be free. The longitudinal stiffness is then modelled as the summation of the stiffness of the piers that contribute.

Transverse Stiffness

The lateral stiffness of steel girder bridges depends primarily on the substructure, specifically the piers with connections capable of transferring forces from the superstructure to the substructure. All bearing types and connections between the substructure and the superstructure are assumed to be capable of transferring forces up to the point where the strength of the connection has not been exceeded. The deck and the connection between the substructure and superstructure is assumed to be sufficiently rigid to allow the intermediate piers to behave as springs in parallel, but not so rigid that it adds to the overall stiffness of the system, meaning the bridge is modelled as a single-degree-of-freedom (SDOF) systems with a singular displacement to represent the motion of the continuous sections of the bridge in the transverse direction.

Equation of Motion

Knowing the mass and the stiffness, the viscous damping matrix can be computed. Because steel bridges are modelled as SDOF systems, the viscous damping matrix is a 1x1 matrix. A viscous damping ratio (ζ) of 5% was used for this analysis. The damping is computed as

$$\boldsymbol{C}_{dir} = 2\zeta\sqrt{(\boldsymbol{KM})_{dir}}. \quad (3.5)$$

The equations-of-motion of the bridge subject to a ground motion input, $\ddot{x}_g$, can be written, for each direction, as

$$\boldsymbol{M}\ddot{x} + \boldsymbol{C}\dot{x} + \boldsymbol{K}x = -\boldsymbol{M}\ddot{x}_g. \quad (3.6)$$

Displacement-Controlled Pushover Analysis

For bridges where all intermediate piers have the same dynamic height and stiffness, the displacement-controlled pushover analysis is bypassed, and it is assumed that the force is equally distributed to each pier. For bridges that have piers with varying heights, a displacement-controlled pushover analysis is conducted because piers may exhibit non-simultaneous nonlinear responses. The pushover analysis determines the redistribution of forces after one pier has entered the nonlinear region. Prior to the first pier entering the nonlinear region, the forces are distributed based on the relative stiffness of each pier, with the stiffest pier drawing the most force.

The pushover analysis is conducted for a displacement ranging from first yield of the stiffest pier through the formation of plastic hinges in all piers. For the nonlinear, static pushover analysis, a displacement is incrementally applied to the structure and at each increment, the force drawn to each pier is controlled by the assumption that each pier will equally displace and is calculated using the moment-area theorem. The percent of the total force drawn to each pier (force ratio) is then calculated.

SAP2000 is used to validate the pushover analysis procedure. The bridge chosen for the validation is I64-07-02367 BEBL (NBI 33280). A 3-span, continuous steel girder bridges with circular reinforced concrete frame bent piers. The SAP model makes the same assumptions as the computational model. The deck and the top of each pier is constrained such that there is a singular

displacement. The calculated moment-curvature relationship for the substructure is defined in the material properties to ensure the same forces corresponding to the cracking, yield, and ultimate moments. A displacement-controlled, nonlinear, static pushover load case is defined and applied to the model. The results from this load case are used to validate the computational model assumptions and results. The comparison of the force-force ratio of the computational model and the SAP model for the longitudinal direction is shown in Figure 3.6 and shows that the assumptions made in the computational model are valid.

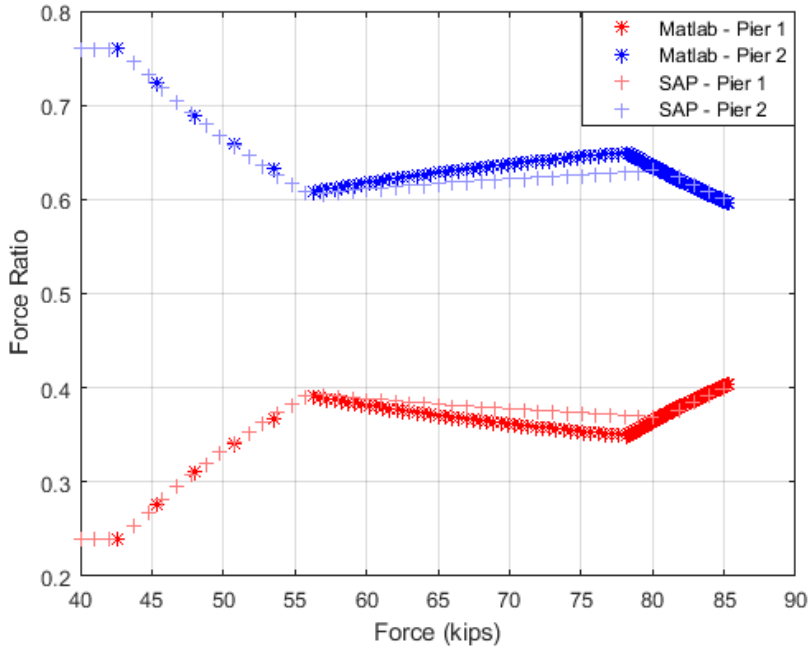

Figure 3.6. Pushover Analysis Comparison

Apply Ground Motions

The detailed assessment utilizes the time histories developed specifically for the site location, the site class, and the period of the structure, as described in Section 3.2. The site class, if not identified through detailed geotechnical reports and boring data, is determined from the "Predicted Responses of Geologic Materials to Seismically Induced Ground Shaking in Indiana, 2011" map developed by Indiana Geological and Water Survey in 2011, shown in Figure 3.7, using the latitude and longitudinal coordinates of the bridge.

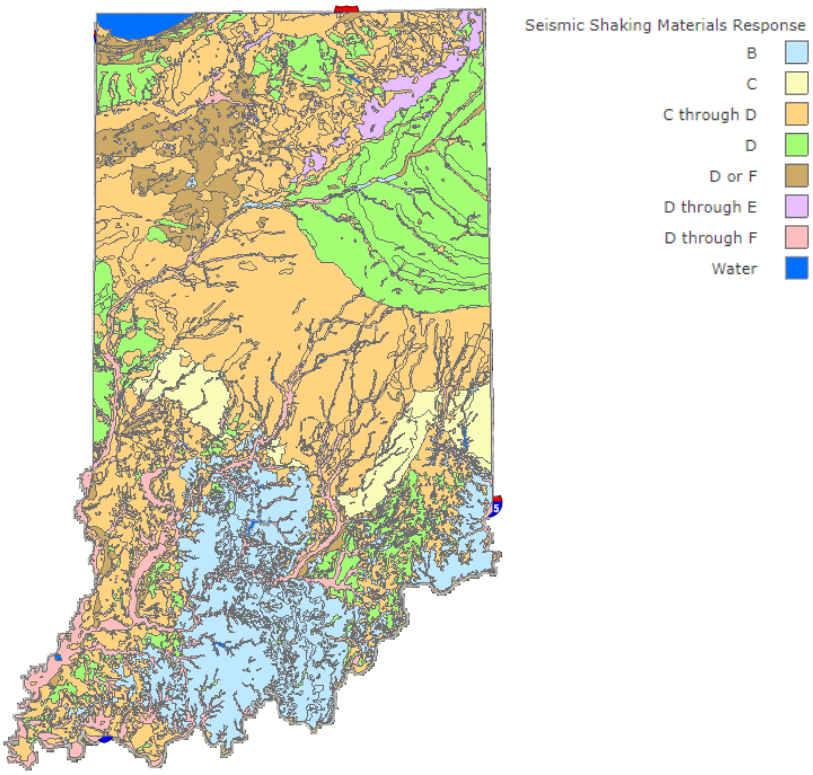

Figure 3.7. Predicted Responses of Geologic Materials to Seismically Induced Ground Shaking in Indiana, 2011 (IGS, 2011).

Maximum Force and Displacement

The detailed assessment assumes that the total force drawn to the structure remains the same for both the linear and nonlinear approach. The outputted linear displacement at each time step is used to calculate the liner force. The linear force is distributed to each pier, using the results from the displacement-controlled pushover analysis if applicable. The redistributed forces are compared to the equivalent forces for cracking, yielding, and ultimate moment. Using the moment-area theorem and the calculated moment-curvature diagram, the nonlinear displacement is calculated, and the total displacement is the sum of the linear displacement and the nonlinear displacement. If the pier remains linear, the displacement is calculated using the linear spring relationship and if any of the piers were to behave nonlinearly,

Once again, the SAP model was used to validate the redistribution of forces and the corresponding nonlinear displacement of the bridge. The results from this validation are shown in Figure 3.8.

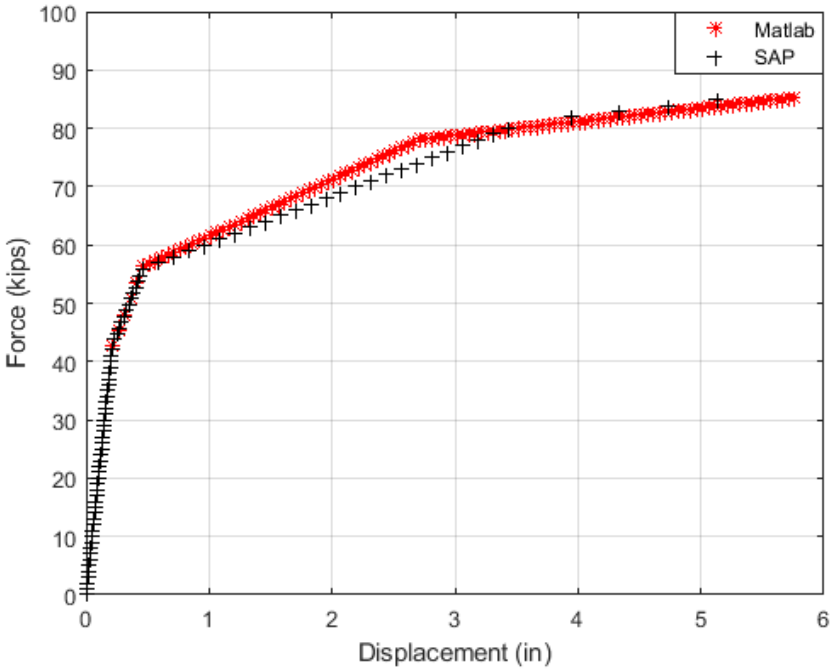

Figure 3.8. Force vs. Displacement Comparison and Validation

Compare Demand to Capacity

The potential for vulnerability comes from the force demand on the substructure exceeding the limiting capacity. The level of vulnerability, above low vulnerability, depends on the limiting capacity. Brittle failures correspond to high vulnerability whereas ductile failures correspond to moderate vulnerability. Because the detailed analysis uses a suite of ground motions with varying magnitude and distance combinations, the vulnerability classification of the bridges is not based on these results. The detailed analysis is used for identifying common vulnerabilities and determining trends that can be applied to the simplified assessment.

3.5 Application of the Detailed Assessment on Typical Bridges

From the 24 selected steel girder bridges, the detailed assessment and corresponding calculations for three typical bridges are described in detail below. The three bridges correspond to the typical substructure types seen in Indiana: a wall, a hammerhead, and a frame bent. The results from the detailed assessment for the other 18 multispan steel girder bridges are discussed in Section 3.7 and can be found in Appendix A and Appendix B.

3.5.1 Continuous Steel Girder Bridge with Walls Piers

Bridge Information

Structure I69-057-09506 (NBI 80226) is a two-span steel girder bridge located in the Vincennes district. The bridge was originally constructed in 2012 and at this time, there has been no additional rehabilitation work done on the bridge. The superstructure is composed of four plate girders with an 8-*inch* reinforced concrete deck, shown in Figure 3.10. The bridge is skewed at 55 degrees, is 32'-4" wide, and has two equal, 162'-0" spans, shown in Figure 3.9.

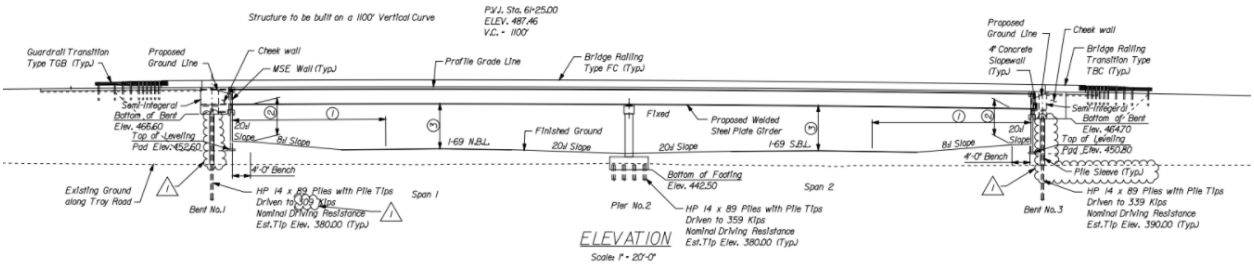

Figure 3.9. Elevation View of Structure I69-057-09506 (NBI 80226) (INDOT, 2010)

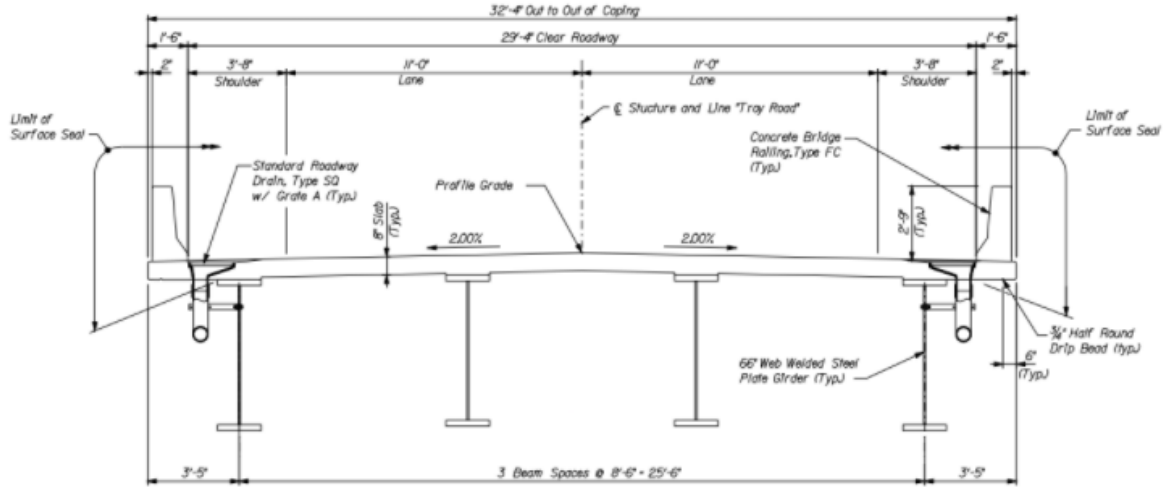

Figure 3.10. Typical Superstructure Section of Structure I69-057-09506 (NBI 80226) (INDOT, 2010)

The bridge is supported by two semi-integral abutments and one interior wall, shown in Figure 3.9. At each abutment, the bridge superstructure is supported by expansion elastomeric bearing

pad assemblies (Figure 3.11) and at the intermediate pier, Pier 2, the superstructure is supported by fixed elastomeric bearing pad assemblies (Figure 3.12). The semi-integral abutments prevent differential displacement of the substructure and the superstructure, and therefore prevent inertial forces from being transferred (Frosh et al., 2009). Because of this, only the calculations for the transverse direction are presented for this structure.

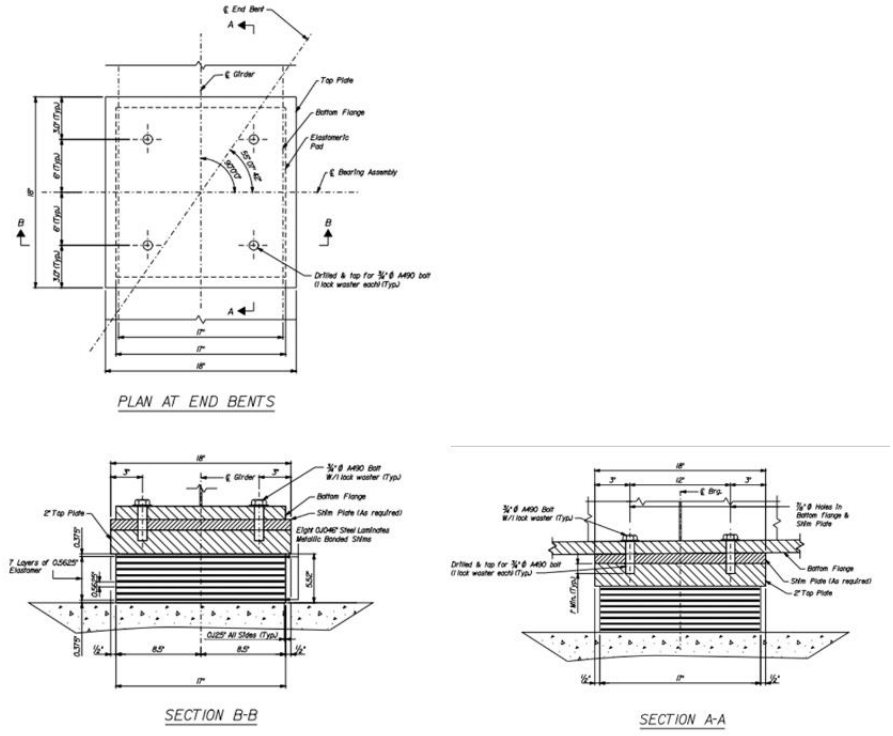

Figure 3.11. Bearing Pad Assembly at Abutments for Structure I69-057-09506 (NBI 80226) (INDOT, 2010)

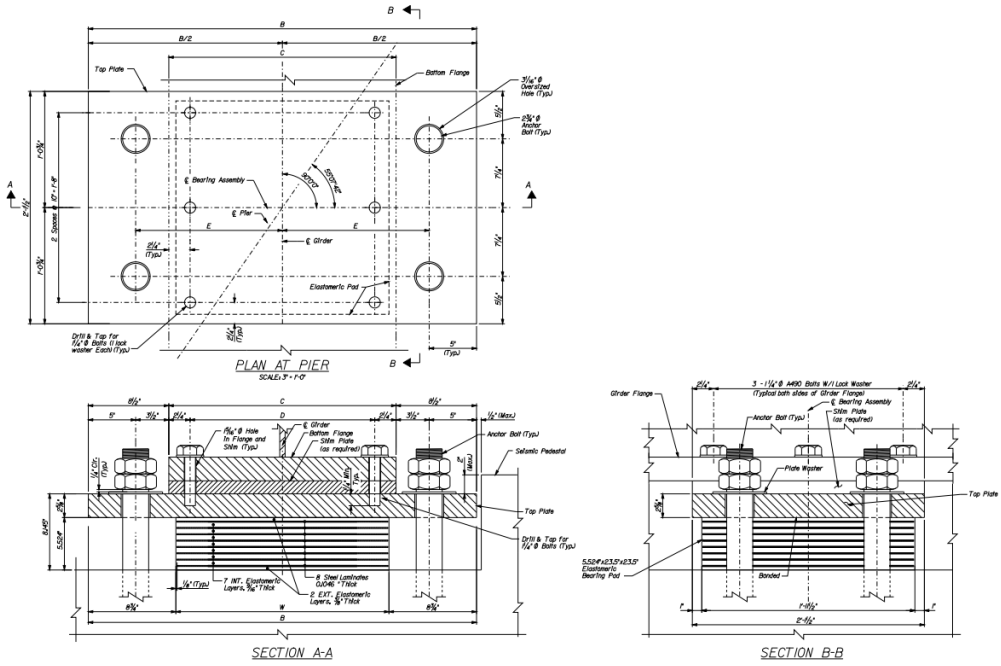

Figure 3.12. Bearing Pad Assembly at Pier 2 for Structure I69-057-09506 (NBI 80226) (INDOT, 2010)

For this substructure type, the geometries relevant to the calculations are wall length, wall thickness, and wall height. Pier 2 is 47’-10” long, with a uniform thickness of 3’-0” and a height of 20’-6”, shown in Figure 3.13. The height of the wall is measured from the base to the top of the bent cap; however, the additional width of the bent cap is ignored in the stiffness calculations.

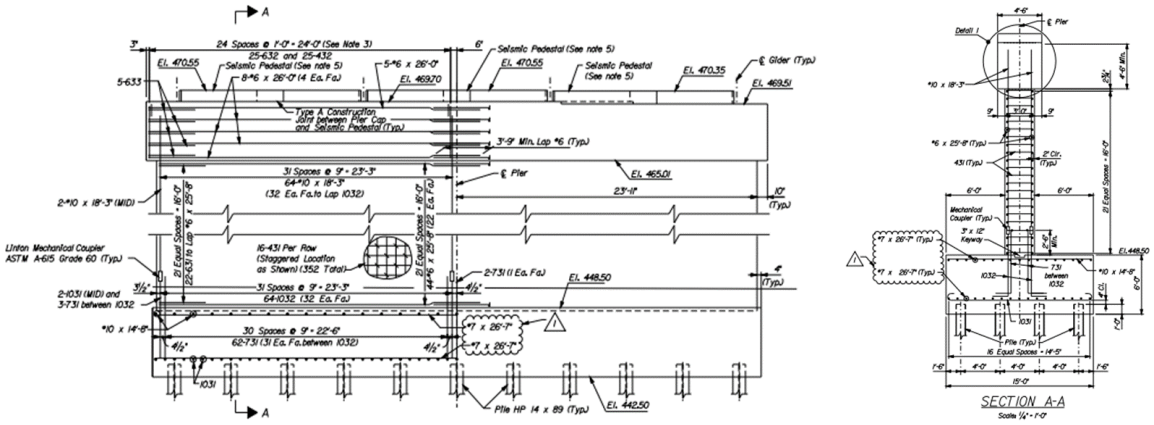

Figure 3.13. Elevation of Pier 2 for Structure I69-057-09506 (NBI 80226) (INDOT, 2010)

The results and findings for the dynamic properties, the capacity and the demand for this bridge are summarized in the Table 3.2. The results are only shown for the transverse direction because bridges with integral abutments are not vulnerable in the longitudinal direction. For more detail on the calculations, refer to the sections below.

Table 3.2. Summary of Dynamic Properties and Capacity Calculation Results for Structure I69-057-09506 (NBI 80226)

	Transverse Direction
Asset Name	I69-057-09506
NBI	80226
Mass (kip/g)	2.37
Stiffness (kip/in)	493600
Period (s)	0.014
Base Shear Capacity (kip)	-
Shear Capacity (kip)	7035
Shear Connection Capacity (kip)	1280

Capacity

Identify Collapse Mechanism

The controlling mechanism of failure for all fixed-free walls is identified as the formation of a plastic hinge at the base of the wall. The ultimate force the wall can take, in both the longitudinal and transverse direction, is calculated as

$$V_{BS} = \frac{M_u}{H}. \tag{3.7}$$

Base Shear

The ability for the substructure to experience this failure mechanism depends on its ability to behave in flexure. Figure 3.4 shows the contribution from shear and bending as a function of the aspect ratio (Fares, 2018). For substructures with an aspect ratio less than 2.5, the structural response is not governed by flexure and therefore plastic hinges cannot form at the base. The aspect ratio, λ_R, is 0.42 and is calculated as

$$\lambda_R = \frac{H}{L_{ele}}. \quad (3.8)$$

The calculated aspect ratio is less than 2.5, therefore, in the transverse direction, this bridge will not behave in flexure and base shear will not be the controlling capacity.

Shear Capacity of the Pier

In the transverse direction, the shear capacity of the wall is calculated in accordance with ACI 318-19 in order to take into account the geometric variations of the wall and its likelihood to fail in flexure or shear and is calculated as

$$V_n = w_{ele} * L_{ele} * \left(\alpha_c \lambda \sqrt{f'_c} + \rho_t f_y\right). \quad (3.9)$$

The α_c value accounts for the difference between the expected occurrence of flexure-shear cracking for slender walls and web-shear cracking in shorter walls and is based on the aspect ratio. For this bridge, the aspect ratio is less than 1.5, and therefore, an $\alpha_c$value of three is used (ACI 318-19, 11.5.4.3).

The transverse reinforcement ratio, ρ_t, is determined from the amount of distributed transverse reinforcement. Pier 2 has #6 bar spaced at 9-*inches* on center, shown in Figure 3.13, which corresponds to a transverse reinforcement ratio of 0.27%.

Assuming normal weight concrete ($\lambda = 1$) and using the material properties for the concrete and the reinforcement, the shear strength of the pier is calculated as 7035 *kips*.

Horizontal Shear Capacity of the Connection

The connection between the substructure and the superstructure for steel bridges is the capacity of the connection of the bearing to the substructure. Figure 3.12 shows the bearing assembly at each beam and the connection consists of 4 – 2 ¾-*inch* diameter anchor bolts connecting the bearing to the concrete, with a minimum embedded depth of 2'-2". The beam is connected to the bearing with 6 – 1¼-*inch* diameter bolts. The controlling shear capacity is the shear capacity of the six

bolts connecting the beam to the top plate of the bearing. The calculated shear capacity for one bearing is 320 *kips*. Therefore, the shear capacity of the connection, considering all beam-bearing connections, is 1280 *kips*.

Identify Limiting Capacity

With the capacity of the two potential failure mechanisms (shear failure and shear connection failure) calculated, the limiting capacity is identified as the minimum of these values. Thus Pier 2 is controlled by the shear connection and the limiting capacity in the transverse direction is 1280 *kips*.

Demand

Mass

The activated mass of the bridge in the transverse direction is calculated using the superstructure geometry and the beam properties. The mass attributed to each pier is based on the mass calculated using the tributary area, taken as half of each span length adjacent to the pier and consists of the mass of the deck, the mass of the barriers, and the mass of the beams. The barrier is a concrete bridge railing type FC, and the mass of the railing supported by Pier 2 calculated using INDOT standard drawing E706-BRSF-01 is 0.35 *kip/g* and is calculated as

$$M_r = 2 * l_{pier} * \frac{\gamma_c * A_c + W_s}{g}. \tag{3.10}$$

The mass of the deck is 1.36 *kip/g* and is calculated as

$$M_{deck} = \frac{l_{pier} * w_{deck} * t_{deck} * \gamma_c}{g}. \tag{3.11}$$

For built-up plate girders, as in this bridge, the weight per linear foot is calculated using the density of steel and the volume of the plates. The density of steel is taken as 0.284 *lb/in*^{3} and the average volume per linear foot of the plate girder is

$$V_{pg} = \frac{\sum_{i=1}^{n}\left(L_{pg} * b_{pg} * h_{pg}\right)_i}{L_{bridge}}. \tag{3.12}$$

The plate girder elevation is shown in Figure 3.14. The dimensions of each plate and is symmetric about the centerline of the bridge. The dimensions of each plate and the calculated volume is shown in

Table 3.3.

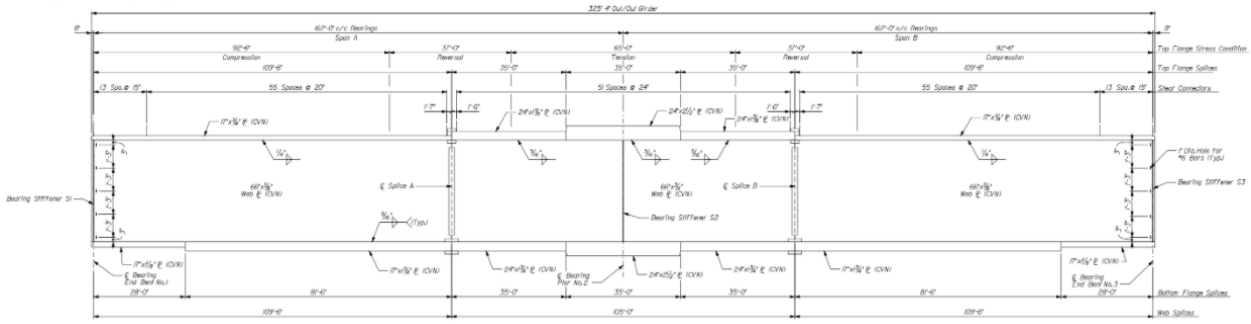

Figure 3.14. Typical Plate Girder Elevation for Structure I69-057-09506 (NBI 80226) (INDOT, 2010)

Table 3.3. Plate Girder Volume for Structure I69-057-09506 (NBI 80226)

	Length (ft)	**Width (in)**	**Height (in)**	**Volume (in^3)**
Top Plate A	28	17	0.75	4284
Web Plate A	28	0.625	66	13860
Bottom Plate A	28	17	1.125	6426
Top Plate B	81	17	0.75	12393
Web Plate B	81	0.625	66	40095
Bottom Plate B	81	17	1.75	28917
Top Plate C	35	24	1.375	13860
Web Plate C	35	0.75	66	20790
Bottom Plate C	35	24	1.75	17640
Top Plate D	17.5	24	2.5	12600
Web Plate D	17.5	0.75	66	10395
Bottom Plate D	17.5	24	2.5	12600
			Total	193860

A 15% increase in mass is applied to all steel bridges to account for the mass of the diaphragms, cross-bracing, connections, and stiffeners. The weight per linear foot of each beam is 0.39 *kip/lft* and is found as

$$W_b = 1.15 * 0.284 \frac{lb}{in^3} * V_{pg}. \quad (3.13)$$

The mass of the beams supported by Pier 2 is 0.66 *kip/g* and is calculated as

$$M_{beam} = \frac{l_{pier} * W_b * N_b}{g}. \tag{3.14}$$

The mass of the superstructure over each pier is the sum of the mass of the railing, the mass of the deck and the mass of the beam and is 2.37 *kip/g*.

Transverse Stiffness

The stiffness of wall substructures in the transverse direction considers contributions from both bending and shear because the aspect ratio deviates significantly from the assumptions of traditional beam theory (Fares, 2018). For substructures with an aspect ratio greater than 2.5, Figure 3.4 shows that the response is dominated by flexure and traditional beam theory assumptions can be used. However, for substructures with an aspect ratio less than 2.5, the response is a combination of flexure and shear, and is calculated as

$$K_{pier} = \frac{3E_c I}{H^3} + \frac{G w_{ele} L_{ele}}{1.2H} \tag{3.15}$$

where the shear coefficient, G, is

$$G = \frac{E_c}{2(1+\nu)}, \tag{3.16}$$

and the stiffness of Pier 2 in the transverse direction is 493,660 *kip/in*.

Equation-of-Motion

As mentioned previously, the deck is assumed to be rigid enough to ensure uniform movement in both directions. Because of this, continuous steel girder bridges are modelled as SDOF systems and the mass and stiffness used in the equation-of-motion is the summation of the individual pier masses and stiffnesses. For two-span bridges, the mass and stiffness in the transverse direction are the mass supported by and the stiffness of the intermediate pier and are 2.35 *kip/g* and 493,660 *kips/in*, respectively. Using a viscous damping ratio of 5%, the equation of motion, used in the dynamic analysis of the transverse direction, is

$$2.37\frac{kips}{g}\ddot{x} + \left(108.15\frac{kips * s}{in}\right)\dot{x} + \left(493660\frac{kips}{in}\right)x = -2.37\frac{kips}{g}\ddot{x}_g. \tag{3.17}$$

Displacement-Controlled Pushover Analysis

Because the structure is not expected to behave in flexure it the transverse direction and because the controlling mechanism of failure is shear, the forces are not expected to vary from a linear model and the displacement-controlled pushover analysis is bypassed.

Apply Ground Motions

This bridge had adequate geotechnical information that allowed the project team to use site response analysis to develop site specific ground motion time-histories. The shear wave velocity profile and the boring data from this site classified the site as NHERP site class D. The project team also developed synthetic ground motion time-histories for comparison. Because of this, the response of the bridge to 200 ground motion time-histories was evaluated.

Maximum Force and Displacement

The linear displacement and the linear stiffness are used to calculate the total force applied to the bridge. Since there is only one pier and the bridge is expected to behave linearly, the force experienced by Pier 2 is the total force calculated. With the force, the corresponding displacement is calculated, for this case, it is a linear displacement.

Compare Demand to Capacity

In the transverse direction, the maximum force resulting from the application of each of the 200 time-histories is compared to the capacity to assess if the capacity is exceeded. The maximum resulting force (605.4 *kips*) never exceeds the capacity (1280 *kips*) in the transverse direction, controlled by the shear connection between the substructure and the superstructure.

Key Vulnerabilities/Trends

As shown though this case study, wall substructures in the transverse direction are not vulnerable to the level of hazard in Indiana due to the large stiffness of the walls. However, if the bridge was not integral, the longitudinal direction would need to be checked for vulnerabilities.

3.5.2 Continuous Steel Girder Bridge with Hammerhead Piers

Bridge Information

Structure 052-24-06649 (NBI 19430) is a four-span, continuous steel girder bridge located in Franklin County which is in the Seymour District. The bridge was originally constructed in 1983 and has no additional rehabilitation work done at this time. The superstructure is composed of eight plate girders with an 8-*inch* reinforced concrete deck, shown in Figure 3.16. The bridge is skewed at 27-degrees, is 53'-6" wide, and has span lengths (from left to right) of 65'-0", 81'- 4", 81'-4", and 65'-0", as shown in Figure 3.15.

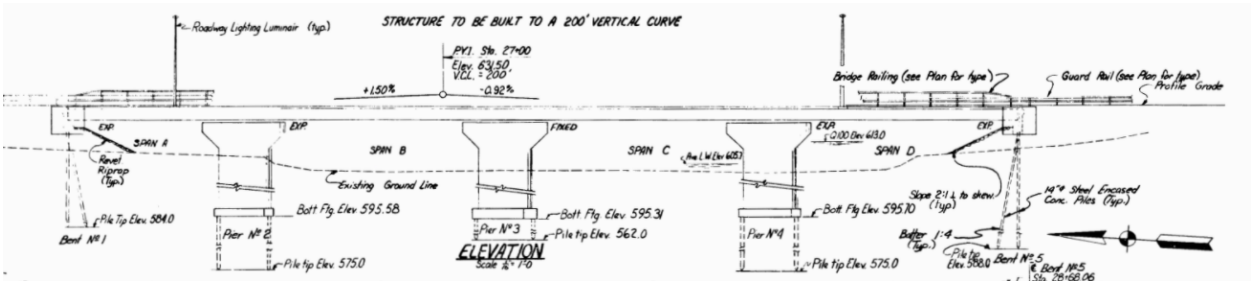

Figure 3.15. Elevation View of Structure 052-24-06649 (NBI 19430) (INDOT, 1982)

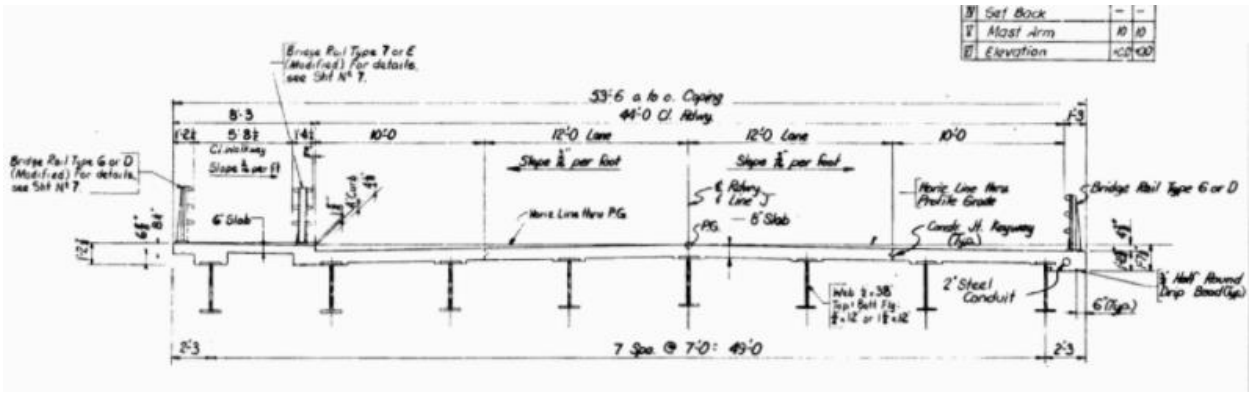

Figure 3.16. Typical Superstructure Section of Structure 052-24-06649 (NBI 19430) (INDOT, 1982)

The bridge is supported by two abutments and three interior hammerhead piers, shown in Figure 3.15. At each abutment and the two outermost piers, the superstructure is supported by expansion shoes (Figure 3.17). At the middle pier (Pier 3), the superstructure is supported by eight fixed shoes

(Figure 3.18). The dimensions for the fixed bearing and the expansion bearing assembly can be found in INDOT standard drawings E 711-BSTS-01 and E 711-BSTS-02, respectively.

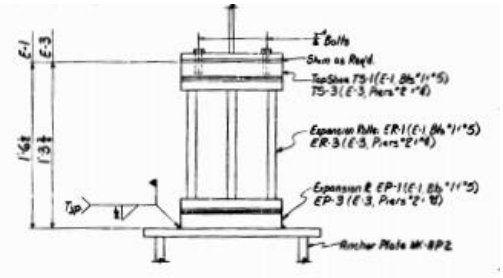

Figure 3.17. Expansion Shoe Assembly at Abutments and Piers 2 and 4 of Structure 052-24-06649 (NBI 19430) (INDOT, 1982)

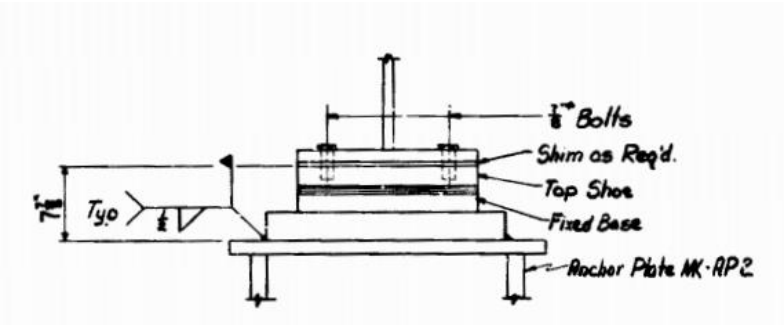

Figure 3.18. Fixed Shoe Assembly at Piers 3 of Structure 052-24-06649 (NBI 19430) (INDOT, 1982)

For this substructure type, the geometries relevant to the calculations are wall length at the base, wall thickness, and wall height. Each pier has a uniform thickness of 2’-6”, and an equivalent rectangular base length of 42’-0”. The typical pier elevation is shown in Figure 3.19. The base length is used, rather than the length at the top, because the base of the pier is where yielding will occur. The additional length of the top of the pier is ignored when determining the stiffness. The total heights of Piers 2, 3, and 4 are 26’-6”, 27’-6”, and 26’-6”, respectively.

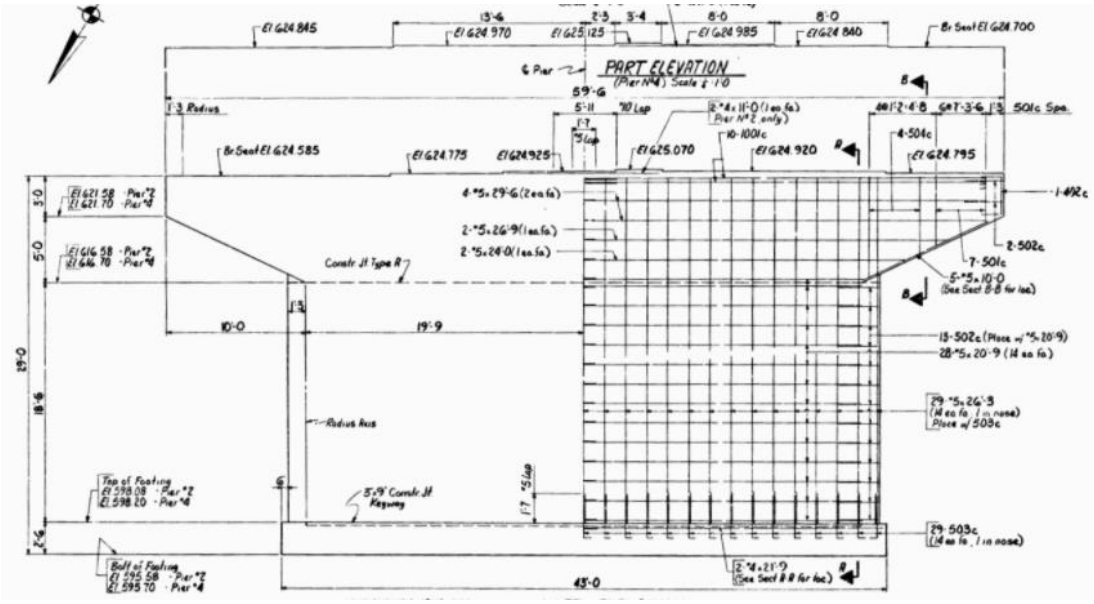

Figure 3.19. Typical Elevation of Piers of Structure 052-24-06649 (NBI 19430) (INDOT, 1982)

The results and findings for the dynamic properties, the capacity and the demand for this bridge are summarized in Table 3.4. For more detail on the calculations, refer to the sections below.

Table 3.4. Summary of Dynamic Properties and Capacity Calculation Results for Structure 052-24-06649 (NBI 19430)

	Longitudinal Direction	**Transverse Direction**
Asset Name	I69-057-09506	
NBI	19430	
Mass (kip/g)	5.07	3.95
Stiffness (kip/in)	300	433000
Period (s)	0.82	0.0019
Base Shear Capacity (kip)	97.7*	-
Shear Capacity (kip)	1440	3180
Shear Connection Capacity (kip)	280	

Capacity

Identify Collapse Mechanism

The controlling mechanism of hinge formation for all fixed-free hammerheads is identified as the formation of a plastic hinge at the base of the pier. On this basis, the ultimate force the pier can

take, in either direction, is calculated using Equation 3.7. This force (Base Shear Capacity) is then compared to the available transverse shear capacity, and horizontal shear capacity of connections between the pier and the superstructure in order to determine the controlling mechanism in terms of force.

Base Shear

As described earlier, walls in the transverse direction with aspect ratios less than 2.5 are controlled by shear. The aspect ratio for this bridge is 0.63 which means the bridge will not develop a hinge in the transverse direction.

In the longitudinal direction, the moment-curvature diagram and the base shear, controlled by the flexure mechanism, of each pier is calculated using the reinforcement layout shown in and the moment-curvature procedure described previously. The elongated oval shape is modeled as an equivalent rectangular section with a total reinforcement ratio of 0.11 percent or 0.41 $in^2/ft.$ A 12-*inch* section of the wall is used for the longitudinal direction calculations and then multiplied by the total length to get the total base shear.

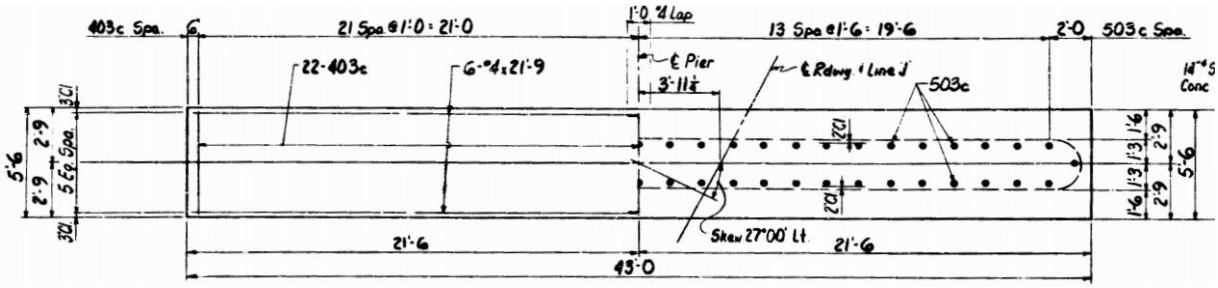

Figure 3.20. Cross-Section of Typical Interior Pier of Structure 052-24-06649 (NBI 19430) (INDOT, 1982)

Table 3.5 shows the results of the moment-curvature analysis for each pier in the longitudinal direction. The cracking moment is larger than the yield moment and the ultimate moment for every pier because of low flexural reinforcement ratio, 0.11%. If the cracking moment is ever exceeded, brittle failure may occur unless an alternate load path can be established. The cracking moment is therefore conservatively taken as the controlling moment for this case study and a linear response

of the bridge is used in all further calculations. The shear force that causes cracking is calculated as

$$V_{cr} = \frac{M_{cr}}{H}. \quad (3.18)$$

and the shear force, over the entire length of the wall, that causes cracking of Piers 2, 3, and 4, in the longitudinal direction, is 97.7 *kips*, 94.1 *kips*, and 97.7 *kips*, respectively.

Table 3.5. Moment Curvature Relationship for the Longitudinal Direction of Structure 052-24-06649 (NBI 19430)

	Pier 2		**Pier 3**		**Pier 4**	
	Moment *(kip*ft)*	φ	**Moment *(kip*ft)***	φ	**Moment *(kip*ft)***	φ
Cracking	2588	8.70E-06	2588	8.70E-06	2588	8.70E-06
Yield	768	5.96E-05	768	5.96E-05	768	5.96E-05
Ultimate	819	3.77E-04	819	3.77E-04	819	3.77E-04

Shear Capacity

In the transverse direction, the shear capacity of each pier is calculated using Equation 3.9. An α_c value of three is used based on the height to length ratio and a lambda (λ) value of one is used for normal-weight concrete. The transverse reinforcement ratio for each pier is 0.11%. The yield strength of the longitudinal reinforcement is assumed to be 40 *ksi* because the bridge was built during or after 1945 (Manual for Bridge Evaluation Table 6A.5.2.2-1). The resulting shear capacity of the three piers in the transverse direction is 3,180 *kips*, 3180 *kips*, and 3180 *kips*, respectively.

The shear capacity in the longitudinal direction is calculated in accordance with AASHTO 5.8.3.3 (AASHTO, 2017). The minimum value of Equation 3.19 and 3.20 is taken as the controlling shear capacity.

$$V_n = 0.25 * f'_c * b_v * d_v \quad (3.19)$$

$$V_n = V_c + V_s, \quad (3.20)$$

where V_c and V_s are calculated as

$$V_c = 0.0316 * 2 * \sqrt{f'_c} * b_v * d_v \quad (3.21)$$

$$V_s = \frac{A_v * f_y * d_v}{s}. \quad (3.22)$$

The value b_v corresponds to the width of the section considered, so for walls and hammerhead piers, this value is 12-*inches*. The value of d_v corresponds to the equivalent moment arm between the resulting tensile and compressive forces. For the three piers in this bridge, the value for V_c, per linear foot, is 34 *kips/ft*.

The area of steel, A_v, is the area of shear ties connecting the two faces of longitudinal steel. However, for this bridge, there are no shear ties and therefore, the value of V_s is 0. The value of V_n, per linear foot is the minimum of 135 *kips/ft* (Equation 3.19) and 35 *kips/ft* (Equation 3.20) and the total shear capacity of Pier 2, 3 and 4 in the longitudinal direction is 1,440 *kips*, 1440 *kips*, 1440 *kips*, respectively.

Horizontal Shear Capacity of the Connection

The shear connection capacity between the substructure and the superstructure for steel bridges is the capacity of the connection of the bearing to the substructure. For steel bridges on expansion and fixed shoes, the bottom plates are connected to anchor plates using a 2-*inch* long, ½-*inch* fillet weld (shown in Figure 3.17 and Figure 3.18). Because these welds were not designed to transfer shear forces and because of the age of the bridges with these bearings, these welds cannot be expected to perform reliably during earthquakes. Therefore, the shear capacity of the connection is conservatively taken as the frictional force between the substructure and the superstructure. A value of 0.57 is used for the coefficient of static friction (μ_s) (Rabbat & Russell, 1985) and the weight is taken as the tributary weight supported by each pier. The shear capacity of the connection is found as

$$V_{conn} = \mu_s * M_{pier} * g. \quad (3.23)$$

Because the shear capacity of the connection is based only on the mass supported by each pier, it is the same in the transverse and the longitudinal direction. Therefore, the shear capacity of the connections of Piers 2, 3, and 4 are 280 *kips*, 310 *kips*, and 280 *kips*, respectively.

Identify Limiting Capacity

The limiting capacity is the minimum value of the potential failure mechanism in each direction. For this bridge, the limiting capacity in the transverse direction considers shear failure and shear connection whereas in the longitudinal direction, the limiting capacity considers brittle failure in addition to shear failure and shear connection failure. Table 3.6 and Table 3.7 show the capacity and the controlling mechanism in the transverse and the longitudinal direction.

Table 3.6. Limiting Capacity of Substructure in the Transverse Direction of Structure 052-24-06649 (NBI 19430)

Pier No.	Capacity – Trans.	Mechanism
2	280 $kips$	Shear Connection Failure
3	310 $kips$	Shear Connection Failure
4	280 $kips$	Shear Connection Failure

Table 3.7. Limiting Capacity of Substructure in the Longitudinal Direction of Structure 052-24-06649 (NBI 19430)

Pier No.	Capacity – Long.	Mechanism
2	98 $kips$	Brittle Failure of Pier
3	94 $kips$	Brittle Failure of Pier
4	98 $kips$	Brittle Failure of Pier

Additional Longitudinal Displacement Capacity

In the longitudinal direction, when expansion shoe bearings are present, the displacement must be compared to the allowable displacement of the expansion shoe bearing because of their potential to overturn.

The allowable displacement of the bridge is limited by the rotation of the expansion shoe-type bearings. The allowable displacement is taken as one-half of the arc length of the bearing. For this bridge, the expansion shoe-type bearing is E1-types at the abutments and E3-types at Piers 2 and 4. E1-type bearings have a height of 12-*inches* and a width of 8-*inches*. E3-type bearings have a height 12-*inches* and a width of 6-*inches*. The bearing with the smaller width will govern. Using the geometry of the smaller bearing, maximum displacement before overturning, assuming the bearing is vertical, is 3.1-*inches* and is calculated as

$$\Delta_{rb} = \frac{w_{rb} * 2 * \sin^{-1}\left(\frac{0.5 * w_{rb}}{r_{rb}}\right)}{2}. \quad (3.24)$$

Demand

Longitudinal Mass

The entire mass is activated in the longitudinal direction. The mass consists of the entire mass of the deck, the mass of the beams and the mass of the railings. The mass of the deck is calculated using Equation 3.11 and is 4.05 *kips/g*. The railings on this bridge are steel and aluminum and the 15% increase in beam mass is assumed to account for the mass of the railings as well as the mass of the diaphragms, cross-bracing, and connections. The bridge superstructure consists of eight plate girders, shown in Figure 3.21, is symmetric about the centerline. The same process used in the wall calculations, is used to calculate the mass of the beams. Table 3.8 shows the dimensions and the calculated volume for each plate. The total mass of the beams, including the 15% increase in mass is 1.02 *kip/g*.

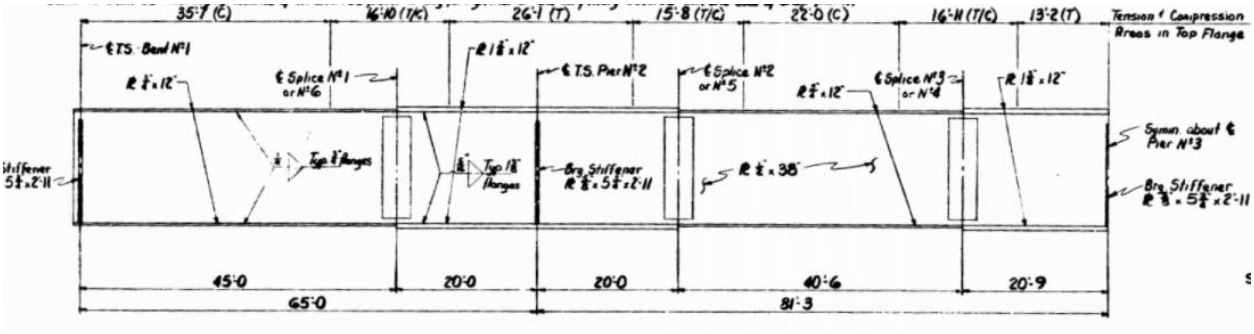

Figure 3.21. Typical Plate Girder Elevation of Structure 052-24-06649 (NBI 19430)

Table 3.8. Plate Girder Volume of Structure 052-24-06649 (NBI 19430)

	Length (ft)	Width (in)	Height (in)	Volume (in^3)
Top Plate A	45	12	0.5	3240
Web Plate A	45	0.5	38	10260
Bottom Plate A	45	12	0.5	3240
Top Plate B	40	12	1.375	7920
Web Plate B	40	0.5	38	9120
Bottom Plate B	40	12	1.375	7920
Top Plate C	40.5	12	0.75	4374
Web Plate C	40.5	0.5	38	9234
Bottom Plate C	40.5	12	0.75	4374
Top Plate D	20.75	12	1.375	4108.5
Web Plate D	20.75	0.5	38	4731
Bottom Plate D	20.75	12	1.375	4108.5
			Total	72630

The longitudinal mass is the summation of the deck mass and the beam mass and is 5.07 *kip/g*.

Transverse Mass

The activated mass of the bridge in the transverse direction is calculated using the superstructure geometry and the beam properties. The mass attributed to each pier is based on the mass calculated using the tributary area, taken as half of each span length adjacent to the pier, and the mass of the deck and the beams. Using the information used to calculate the mass in the longitudinal direction, the mass of the superstructure over Piers 2, 3 and 4 is 1.27 *kips/g*, 1.41 *kips/g*, and 1.27 *kips/g*, respectively.

Longitudinal Stiffness

The stiffness of hammerhead piers in the longitudinal direction is derived solely from bending and is assumed to behave as a fixed-free column. For steel bridges, the type of bearing on each pier determines if the pier adds stiffness. Piers with expansion shoe bearings do not contribute to the stiffness of the bridge in the longitudinal direction because of the behavior of the expansion shoes. Expansion shoes are used to allow thermal expansion and contraction and do not allow lateral forces to be transferred from the superstructure to the substructure in the longitudinal direction. Fixed shoes allow the transfer of lateral forces from the superstructure to the substructure and are considered to add stiffness to the bridge model in the longitudinal direction. Because Pier 3 is the

only pier that has fixed shoes, the longitudinal stiffness is solely the longitudinal stiffness of Pier 3. The stiffness of Pier 3 is 298.7 *kip/in* and is calculated as

$$K_{pier} = \frac{3E_c I}{H^3}. \tag{3.25}$$

Transverse Stiffness

The stiffness of hammerhead piers in the transverse direction is calculated using the same equations as a wall (Equation 3.15). The transverse length is taken as the length of the wall at the bottom of the pier. For steel superstructures, the substructure is assumed to be fixed-free. The resulting bending stiffness and the shear stiffness of Pier 2, 3, and 4 in the transverse direction is 148,560 *kip/in*, 136,670 *kip/in*, and 148,560 *kip/in*.

Equation-of-Motion

The mass activated in the longitudinal direction is the total mass of the superstructure (5.07 *kip/g*). However, the total stiffness in the longitudinal direction is calculated as the sum of the individual pier stiffnesses whose bearings allow them to participate. Because of this, the stiffness used in the dynamic analysis in the longitudinal direction is the stiffness of only Pier 3 (298.7 *kip/in*). Therefore, the equation-of-motion in the longitudinal direction, to be used for the dynamic analysis, is

$$5.07\frac{kips}{g}\ddot{x} + \left(3.89\frac{kips * s}{in}\right)\dot{x} + \left(298.7\frac{kips}{in}\right)x = -5.07\frac{kips}{g}\ddot{x}_g. \tag{3.26}$$

The rigidity of the deck ensures uniform movement which means the total stiffness and mass in the transverse direction are calculated as the sum of the individual pier stiffnesses and masses, respectively. The total stiffness in the transverse direction is 433790 *kip/in* and the total mass activated in the transverse direction is 3.95 *kip/g*. Therefore, the equation-of-motion in the transverse direction, to be used for the dynamic analysis, is

$$3.95\frac{kips}{g}\ddot{x} + \left(130.89\frac{kips * s}{in}\right)\dot{x} + \left(433790\frac{kips}{in}\right)x = -3.95\frac{kips}{g}\ddot{x}_g. \tag{3.27}$$

Displacement-Controlled Pushover Analysis

As mentioned earlier, because the cracking moment of each pier is larger than the yield moment, the bridge will remain in the linear region until brittle failure. Because of this, no pushover analysis is needed.

Apply Ground Motions

This bridge did not have any available geotechnical information, so 100 synthetic ground motions were developed for the dynamic analysis. The site class for this bridge was determined from the IGS map (Figure 3.7) and is classified as site class C through D. The ground motion time-histories developed for site class D were used in the analysis for this bridge.

Maximum Force and Displacement

The linear displacement and the linear stiffness are used to calculate the total force applied to the bridge. Since the pushover analysis is not applicable to this bridge, the force is distributed to each pier based on the relative stiffness of the piers. With the force, the corresponding displacement is calculated.

Compare Demand to Capacity

In each direction, the maximum force resulting from the application of each of the seismic ground motions is compared to the capacity to assess if the capacity is exceeded. In the longitudinal direction, the maximum force resulting from 100 ground motions (555.4 *kip*) exceeds the capacity (94.1 *kip*), controlled by brittle failure of the pier. In the transverse direction, the maximum force resulting from 100 ground motions (127.5 *kip*) never exceeds the capacity in the transverse direction (279 *kip*), controlled by the shear connection between the substructure and superstructure. The maximum displacement in the longitudinal direction from the 100 ground motions 0.3-*inches* never exceeded the allowable displacement (3.1-*inches).*

Key Vulnerabilities/Trends

As shown through this case study, hammerhead substructures, and structures that are older with a low longitudinal reinforcement ratio, are unable to behave in flexure and have the potential for brittle failure in the longitudinal direction. As with wall substructures, bridges with hammerhead

substructures are not vulnerable to the level of hazard in Indiana in the transverse direction due to the large stiffness of the walls.

3.5.3 Continuous Steel Girder Bridge with Frame Bent Piers

Bridge Information

Structure I64-07-02367 BEBL (NBI 33280) is a three-span steel girder bridge located in the Vincennes district. The bridge was originally constructed in 1967 and has had the bridge deck replaced two times, once in 1979 and a second time in 2002. In 2002, the expansion shoe bearings at the abutments and Pier 3 were replaced with elastomeric bearing pads. The superstructure is composed of seven W33x118 steel beams with a 6¾”-*inch* reinforced concrete deck, shown in The bridge is skewed at 9 degrees, is 42’-6” wide, and has span lengths of 72’-0”, 87’-0”, and 56’-0”, shown in Figure 3.22.

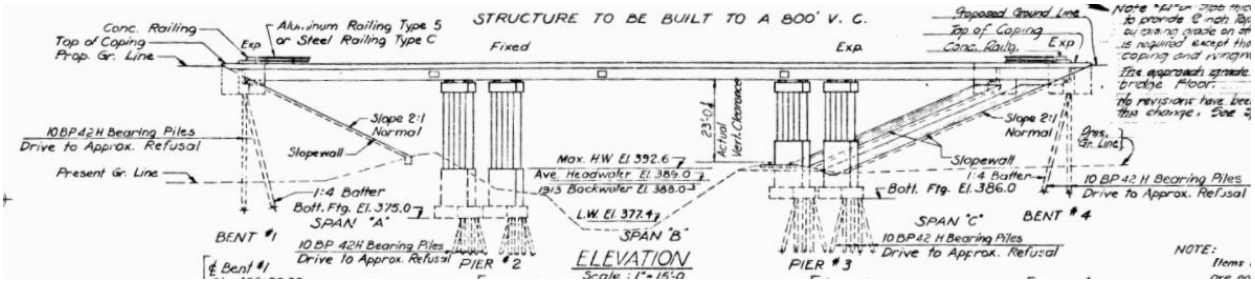

Figure 3.22. Elevation View of Structure I64-07-02367 BEBL (NBI 33280) (INDOT, 1964)

The bridge is supported by two non-integral abutments and two intermediate frame bent piers with five circular columns. At each abutment and at Pier 3, the superstructure is supported by elastomeric bearing pads, shown in Figure 3.24. At Pier 2, the superstructure is supported by fixed shoes at each beam, shown in Figure 3.25.

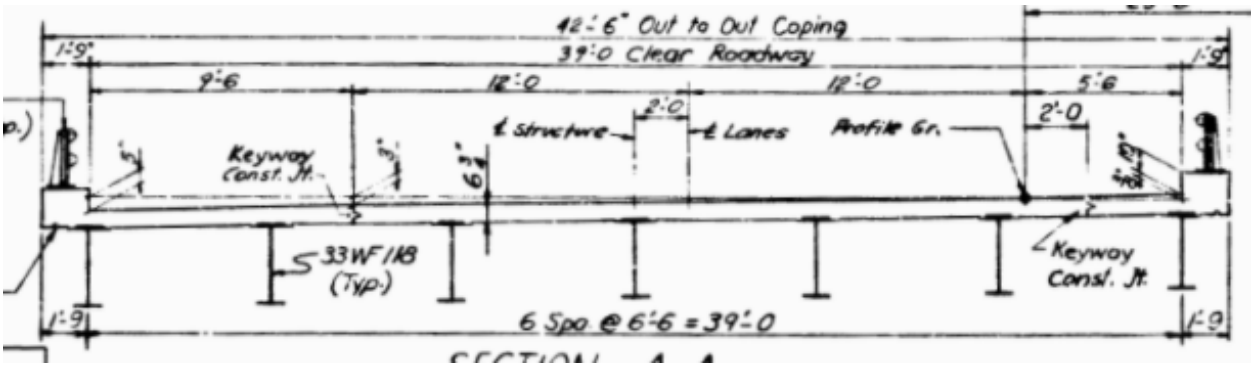

Figure 3.23. Typical Superstructure Section of Structure I64-07-02367 BEBL (NBI 33280) (INDOT, 1964)

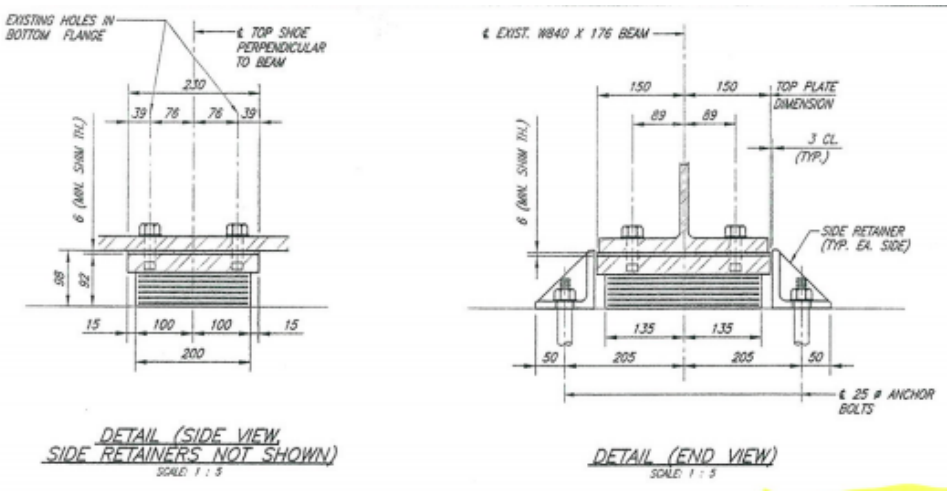

Figure 3.24. Bearing Pad Assembly at Abutments and Pier 3 for Structure I64-07-02367 BEBL (NBI 33280) (INDOT, 2001)

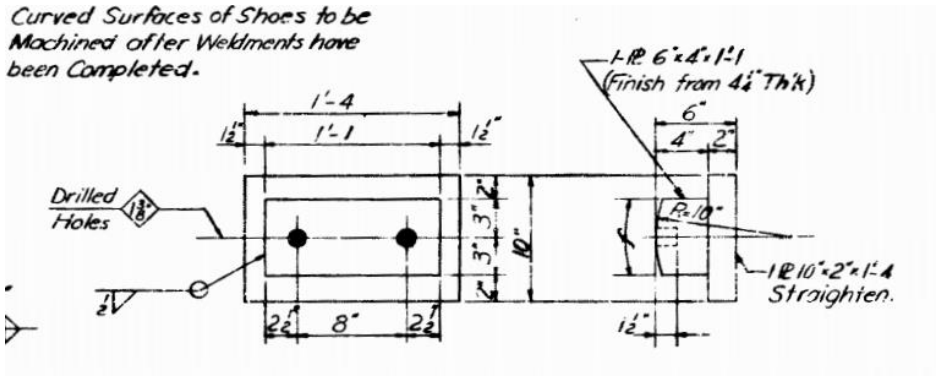

Figure 3.25. Fixed Bearing Assembly at Pier 2 for Structure I64-07-02367 BEBL (NBI 33280) (INDOT, 1964)

For this substructure type, the geometries relevant to the capacity and demand calculations are the number of columns, column dimensions, column clear span, bent cap dimensions, and column height. Each frame bent consists of five, 2'-0" diameter circular reinforced concrete columns, with a clear span of 7'-0". The bent cap on each pier is 30"x30". The columns in Pier 2 have a clear height of 20'-4" and the columns in Pier 3 have a clear height of 13'-4".

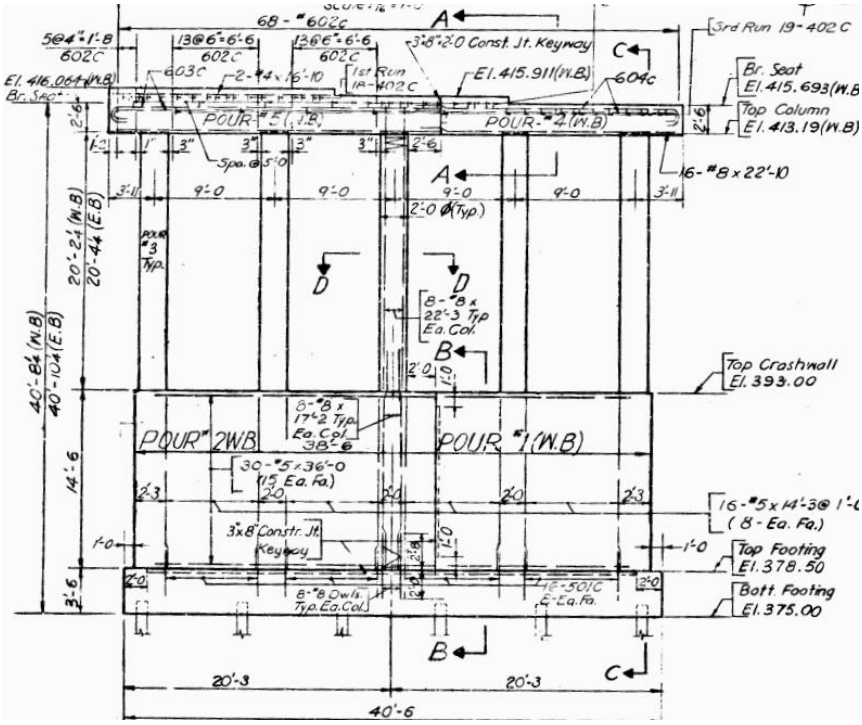

Figure 3.26. Typical Elevation of Piers for Structure I64-07-02367 BEBL (NBI 33280) (INDOT, 1964)

The results and findings for the dynamic properties, the capacity and the demand for this bridge are summarized in the Table 3.9. The bridge is not vulnerable in the longitudinal direction because of the integral abutments, however calculations for both directions are given for completeness. For more detail on the calculations, refer to the sections below.

Table 3.9. Summary of Dynamic Properties and Capacity Calculation Results for Structure I64-07-02367 BEBL (NBI 33280)

	Transverse Direction
Asset Name	I64-07-02367 BEBL
NBI	33280
Mass (kip/g)	2.15
Stiffness (kip/in)	1000
Period (s)	0.29
Base Shear Capacity (kip)	93
Shear Capacity (kip)	290
Shear Connection Capacity (kip)	210

Capacity

Identify Collapse Mechanism

In the longitudinal direction, the columns are modelled as fixed-free and the controlling collapse mechanism is the formation of plastic hinges at the base of every column. A moment-curvature analysis is done for the columns in the longitudinal direction to calculate the ultimate moment. Because the columns are circular, the moment-curvature results are assumed to be the same in both the longitudinal and transverse directions. The results for Pier 2 and Pier 3 can be found in Table 3.10.

A limit analysis is used to determine the controlling collapse mechanism for frame bent substructures in the transverse direction. Two mechanisms of hinge formation are considered: one where plastic hinges form at the base and the top of every column, and another where plastic hinges form at the base of the columns and at either end of each beam, shown in Figure 3.27 and Figure 3.28, respectively.

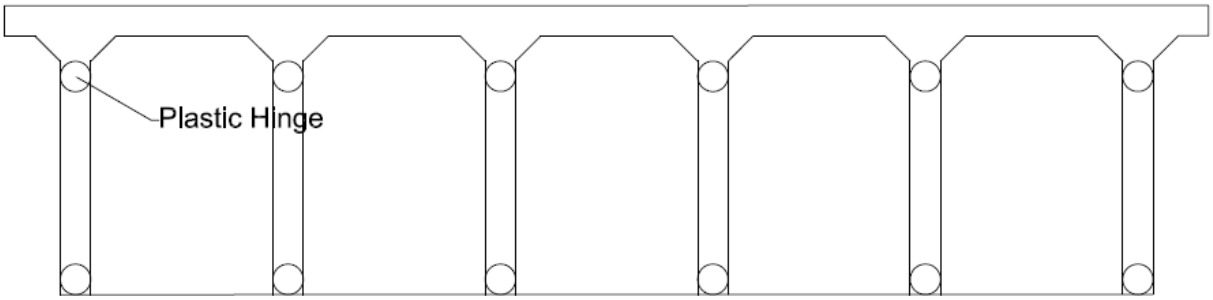

Figure 3.27. First Collapse Mechanism: Plastic Hinges Formed at Base and Top of Columns

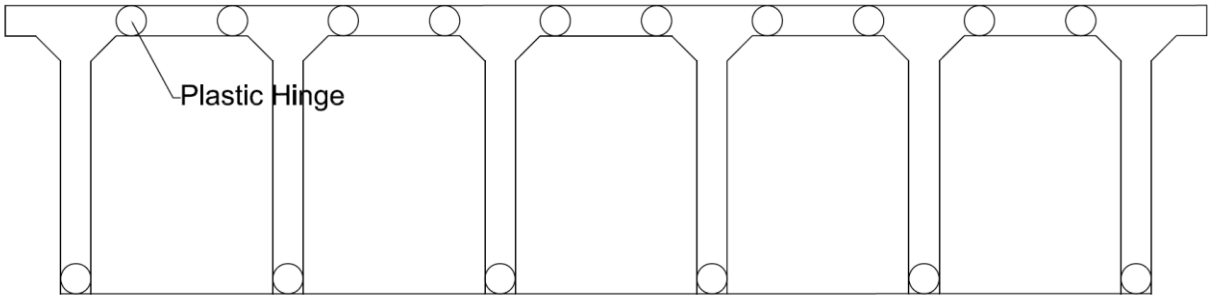

Figure 3.28. Second Collapse Mechanism: Plastic Hinges Formed at Base of Columns and End of Beams

The controlling mechanism of hinge formation is the mechanism that results in the smallest base shear, calculated as

$$V_{bs} = \frac{\sum M_u}{H}, \tag{3.28}$$

where M_u, is the ultimate moment calculated using the moment-curvature procedure described previously. The reinforcement layouts used to calculate the cracking, yield, and ultimate moments of the columns in Pier 2 and Pier 3 and the beams are shown in Figure 3.29, Figure 3.30, and Figure 3.31, respectively. This bridge is unique because the reinforcement layout for the columns in Pier 2 and 3 are not identical. Pier 2 has a reinforcement ratio of 1.4% and Pier 3 has a reinforcement ratio of 1%. The moment curvature relationship is calculated for a single column and beam for each pier. Table 3.10 and Table 3.11 show the moment-curvature results for the columns and the beams in the transverse direction, respectively.

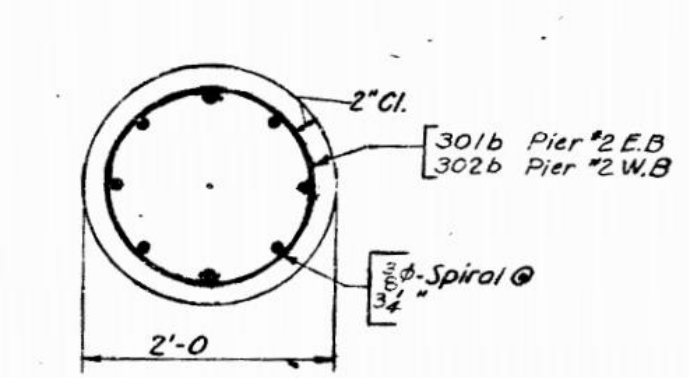

Figure 3.29. Cross-Section of Pier 2 Column for Structure I64-07-02367 BEBL (NBI 33280) (INDOT, 1964)

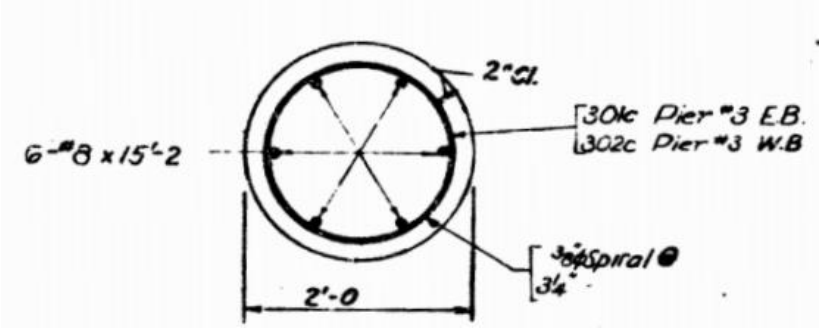

Figure 3.30. Cross-Section of Pier 3 Column for Structure I64-07-02367 BEBL (NBI 33280) (INDOT, 1964)

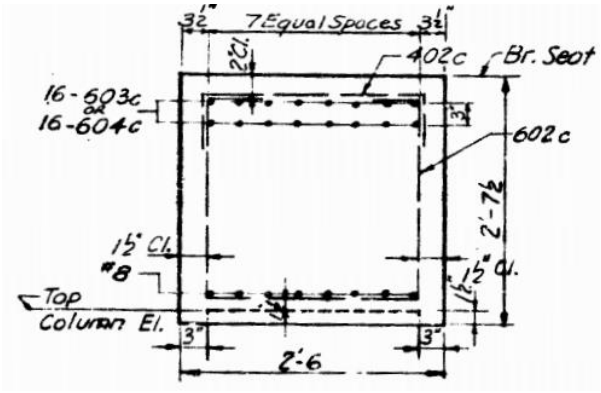

Figure 3.31. Bent Cap Cross-Section for Structure I64-07-02367 BEBL (NBI 33280) (INDOT, 1964)

Table 3.10. Transverse Column Moment-Curvature Results for Structure I64-07-02367 BEBL (NBI 33280)

	Pier 2		Pier 3	
	Moment (*kip*ft*)	**φ**	**Moment (*kip*ft*)**	**φ**
Cracking	50	1.08E-05	50	1.08E-05
Yield	122	9.73E-05	94	9.37E-05
Ultimate	188	6.09E-04	150	6.03E-04

Table 3.11. Transverse Beam Moment-Curvature Results for Structure I64-07-02367 BEBL (NBI 33280)

	Pier 2		Pier 3	
	Moment (*kip*ft*)	**φ**	**Moment (*kip*ft*)**	**φ**
Cracking	183	8.03E-06	18	8.03E-06
Yield	654	5.40E-05	654	5.40E-05
Ultimate	721	3.19E-04	721	3.19E-04

Using the ultimate moment and the number of hinges formed, the shear resultant of Pier 2 for the first collapse mechanism is 93 *kips* and the shear resultant of Pier 2 for the second collapse mechanism is 330 *kips*. For both piers, the first collapse mechanism governs, meaning plastic hinges will form at the base and the top of the columns, the preferred collapse mechanism for bridge structures.

Base Shear

The base shear in the longitudinal direction, using the calculated ultimate moment capacity is 43 *kips* and 51 *kips*, for Piers 2 and 3 respectively. In the transverse direction, the base shear for the controlling collapse mechanism is 93 *kips* and 112 *kips*, for Piers 2 and 3 respectively.

Shear Capacity

The shear capacity of the substructure is the same in both the longitudinal and the transverse direction because the column is circular. The shear strength of a single circular column is calculated as the minimum of Equation 3.19 and Equation 3.20, using the cross-sections shown in Figure 3.29 and Figure 3.30. The results for a single column in Pier 2 are 295 *kips* (Equation 3.19) and 59 *kips* (Equation 3.20). The results for a single column in Pier 3 are 299 *kips* (Equation

3.19) and 59 *kips* (Equation 3.20). The controlling shear capacity for Pier 2 is 294 *kips* and for Pier 3 is 299 *kips*.

Horizontal Shear Capacity of the Connection

The horizontal shear capacity of the connection between the substructure and the superstructure depends on the bearing type. For this bridge, the bearing at Pier 2 is the fixed shoe, shown in Figure 3.25. This bearing is attached to the substructure using a 2-inch long, ½-inch fillet weld. As mentioned previously, these welds were not designed to transfer shear forces and because of the age of the bridges with these bearings, these welds cannot be expected to perform reliably during earthquakes. Therefore, the shear capacity of the connection is conservatively taken as the frictional force between the substructure and the superstructure, using Equation 3.23, and is 211 *kips*. At Pier 3, there are 5 elastomeric bearing pad assemblies. As shown in Section 3.5.1, the capacity of the elastomeric bearing pad assemblies is much greater than the capacity of the shear friction connection and therefore, the shear friction connection at Pier 2 will govern.

Identify Limiting Capacity

The limiting capacity is the minimum value of the potential failure mechanism in each direction. For this bridge, the limiting capacity in both directions considers, base shear, shear failure and shear connection failure. Table 3.12 and Table 3.13 show the controlling mechanism for the transverse and the longitudinal direction, respectively.

Table 3.12. Limiting Capacity of Substructure in the Transverse Direction of Structure I64-07-02367 BEBL (NBI 33280)

Pier No.	Capacity – Trans.	Mechanism
2	93 *kips*	Base Shear (1)
3	112 *kips*	Base Shear (1)

Table 3.13. Limiting Capacity of Substructure in the Longitudinal Direction of Structure I64-07-02367 BEBL (NBI 33280)

Pier No.	Capacity – Long.	Mechanism
2	43 *kips*	Base Shear
3	51 *kips*	Base Shear

Demand

Longitudinal Mass

The entire mass is activated in the longitudinal direction. The mass consists of the entire mass of the deck, the mass of the beams and the mass of the railings. The mass of the deck is calculated using Equation 3.11 and is 1.99 *kips/g*. The railings on this bridge are steel and aluminum and the 15% increase in beam mass is assumed to account for the mass of the railings as well as the mass of the diaphragms, cross-bracing, and connections. The bridge superstructure consists of seven W33x118 steel beams. Using 118 *lb/ft* as the weight of each beam, the total mass of the beams, including the 15% increase in mass is 0.528 *kip/g*. The longitudinal mass is the summation of the deck mass and the beam mass and is 2.52 *kip/g*.

Transverse Mass

The activated mass of the bridge in the transverse direction is calculated using the superstructure geometry and the beam properties. The mass attributed to each pier is based on the mass calculated using the tributary area, taken as half of each span length adjacent to the pier, and the mass of the deck and the beams. Using the information used to calculate the mass in the longitudinal direction, the mass of the superstructure over Piers 2 and 3 and 4 is 0.96 *kips/g* and 0.86 *kips/g*, respectively.

Longitudinal Stiffness

In the longitudinal direction, the bridge is modeled as a SDOF system with the piers behaving as springs in parallel. Each column is assumed to be fixed at the base and free at the top, due to the connection between the deck and the substructure. The stiffness is calculated as

$$K_{pier} = N_c * \frac{3E_c I}{H^3}. \quad (3.29)$$

Because Pier 3 is supported by elastomeric bearing pads, which are designed to allow thermal expansion in the longitudinal direction without transferring forces, it does not add to the total stiffness in the longitudinal direction. Thus, the stiffness of this bridge in the longitudinal direction is the stiffness of Pier 2 and is 47 *kip/in*.

Transverse Stiffness

Frame bent substructures are modelled as a planar moment resisting frame with translation allowed at top of the pier and rotation allowed at each node, shown in Figure 3.32, to determine the transverse stiffness.

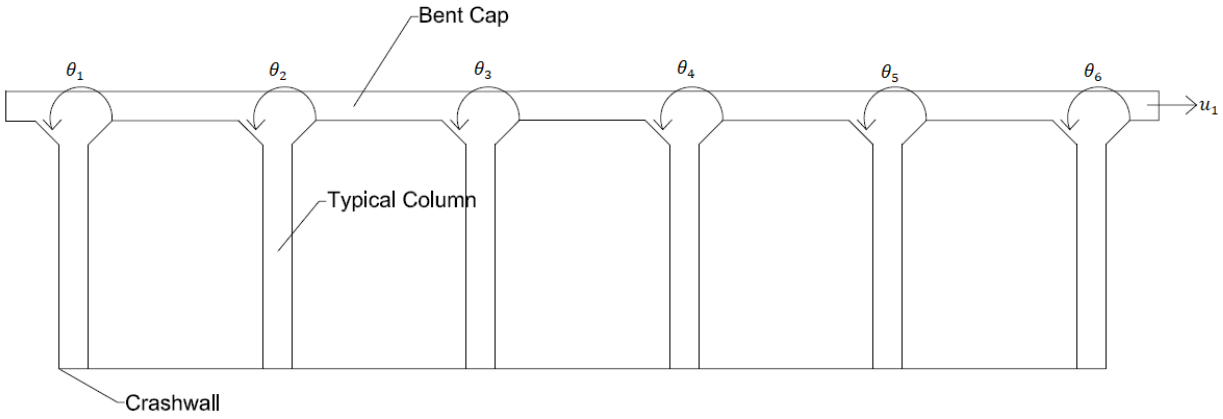

Figure 3.32. Transverse Elevation of Interior Bent with Degrees of Freedom Shown (Mahmud, 2019)

The stiffness matrix for each bent is assembled using the stiffness matrix of a single bay frame as the elemental matrix. The assembled pier stiffness matrix is shown in

Table 3.14. The pier stiffness matrix is then condensed to obtain the stiffness for the translational degree-of-freedom. The stiffness of Pier 2 and Pier 3 is 222 *kip/in* and 770 *kip/in*, respectively. The total stiffness in the transverse direction is taken as the sum of the pier stiffnesses because steel girder bridges are modelled as SDOF systems. This stiffness of this bridge in the transverse direction is 993 *kip/in*.

Table 3.14. Interior Pier Stiffness Matrix in the Transverse Direction (NBI 33280)

Degree of freedoms	u_1	θ_1	θ_2	θ_3	θ_4	θ_5
u_1	$N_c \frac{12A}{H^3}$	$\frac{6A}{H^2}$	$\frac{6A}{H^2}$	$\frac{6A}{H^2}$	$\frac{6A}{H^2}$	$\frac{6A}{H^2}$
θ_1	$\frac{6A}{H^2}$	$\frac{4A}{H} + \frac{4B}{s_{clear}}$	$\frac{2B}{s_{clear}}$	0	0	0
θ_2	$\frac{6A}{H^2}$	$\frac{2B}{s_{clear}}$	$\frac{4A}{H} + 2\frac{4B}{s_{clear}}$	$\frac{2B}{s_{clear}}$	0	0
θ_3	$\frac{6A}{H^2}$	0	$\frac{2B}{s_{clear}}$	$\frac{4A}{H} + 2\frac{4B}{s_{clear}}$	$\frac{2B}{s_{clear}}$	0
θ_4	$\frac{6A}{H^2}$	0	0	$\frac{2B}{s_{clear}}$	$\frac{4A}{H} + 2\frac{4B}{s_{clear}}$	$\frac{2B}{s_{clear}}$
θ_5	$\frac{6A}{H^2}$	0	0	0	$\frac{2B}{s_{clear}}$	$\frac{4A}{H} + \frac{4B}{s_{clear}}$

Where: $A = E_c I_c \quad B = E_c I_b$

Equation-of-Motion

The mass activated in the longitudinal direction is the total mass of the superstructure (2.52 *kip/g*). However, the total stiffness in the longitudinal direction is calculated as the sum of the individual pier stiffnesses whose bearings allow them to participate. Because of this, the stiffness used in the dynamic analysis in the longitudinal direction is the stiffness of only Pier 2 (47 *kip/in*). Therefore, the equation-of-motion in the longitudinal direction, to be used for the dynamic analysis, is

$$2.52\frac{kips}{g}\ddot{x} + \left(1.09\frac{kips * s}{in}\right)\dot{x} + \left(47\ \frac{kips}{in}\right)x = -2.52\frac{kips}{g}\ddot{x}_g. \qquad (3.30)$$

The rigidity of the deck ensures uniform movement which means the total stiffness and mass in the transverse direction are calculated as the sum of the individual pier stiffnesses and masses, respectively. The total stiffness in the transverse direction is 993 *kip/i*n and the total mass activated in the transverse direction is 1.82 *kip/g*. Therefore, the equation-of-motion in the transverse direction, to be used for the dynamic analysis, is

$$1.82\frac{kips}{g}\ddot{x} + \left(4.25\frac{kips * s}{in}\right)\dot{x} + \left(993\ \frac{kips}{in}\right)x = -1.82\frac{kips}{g}\ddot{x}_g. \qquad (3.31)$$

Displacement Controlled Pushover Analysis

A displacement-controlled pushover analysis is performed in the transverse direction to better understand the redistribution of forces as piers progressively exhibit nonlinear behavior. By incrementally applying a displacement to the structure beginning with the first yield of the stiffest pier through the formation of plastic hinges in all piers, the force redistribution is quantified. The results of the pushover analysis in the transverse direction are shown in Figure 3.33. The displacement-controlled pushover analysis step is bypassed in the longitudinal direction because only one pier contributes to the overall stiffness.

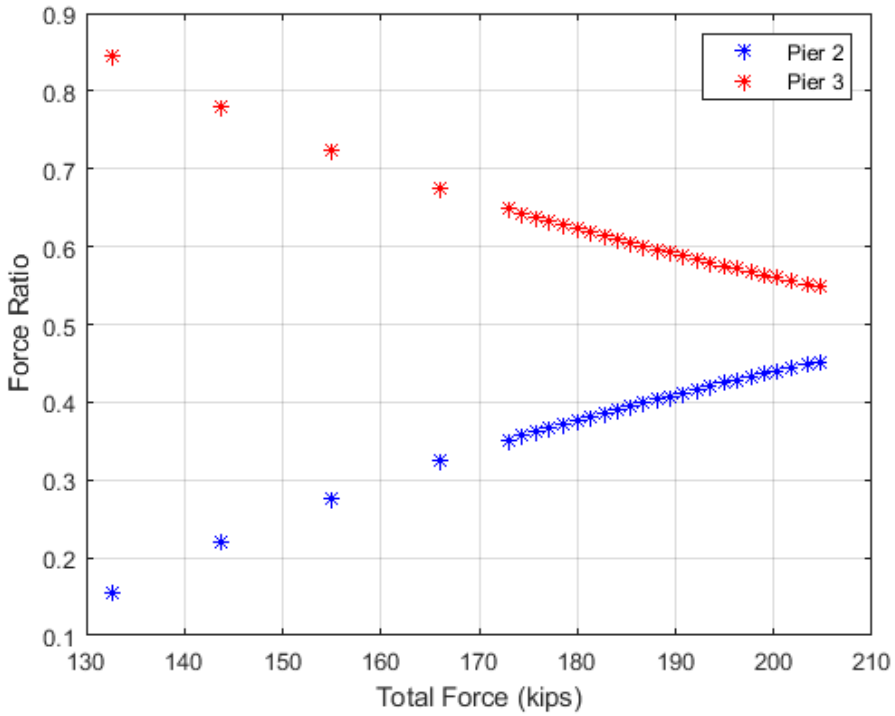

Figure 3.33. Pushover Analysis Results in the Transverse Direction for Structure I64-07-02367 BEBL (NBI 33280)

Apply Ground Motions

This bridge did not have any available geotechnical information, so 100 synthetic ground motions were developed for the dynamic analysis. The site class for this bridge was determined from the IGS map (Figure 3.7) and is classified as site class D and the corresponding ground motions were used to assess the performance of the bridge.

Compare Demand to Capacity

In each direction, the maximum force resulting from the application of each of the seismic ground motions is compared to the capacity to assess if the capacity is exceeded. In the longitudinal direction, the maximum force resulting from 100 ground motions exceeds the capacity controlled by the base shear of the pier. In the transverse direction, the maximum force resulting from 100 ground motions exceeds the capacity in the transverse direction, controlled by the base shear of the pier.

Key Vulnerabilities/Trends

As shown through this case study, frame bent substructures have the ability to behave in flexure in both the longitudinal and transverse direction. Both directions have the potential to form plastic hinges, and for this bridge plastic hinges formed for the majority of the developed time histories.

3.6 Discussion of Special Modelling Cases

The sample set of 24 steel superstructure bridges mainly consists of bridges that fall into the three categories of sample calculations above. However, the sample does include three single-span bridges and two bridges with expansion joints. Single span bridges are typically excluded from a seismic evaluation due to a low vulnerability (Choi, 2002 & Nielson, 2005). However, single span bridges with rocker bearings have the potential for damage due to the bearings overturning which should be classified as moderately vulnerable in the simplified analysis (NYSDOT, 2004).

The two bridges with expansion joints require a few adjustments to the analysis previously discussed. Structure (421)39-12-01792 B (NBI 32200) and Structure I64-05-05201 CEBL (NBI 33240) are unique because the deck is broken up by expansion joints. The presence of expansion joints allows the bridge deck to move as separate bodies. The modelling of bridges with expansion joints is, for the most part, very similar to what is discussed. However, because expansion joints allow portions of the deck to move separately from one another, the model must be divided into separate systems based on the location of the expansion joints. For the subsystems that include an abutment, the abutment is not included in the analysis and, typically, the end pier is also not included in the analysis and for interior subsystems, typically, the exterior piers are not included in the analysis because of the bearing type. If an expansion type bearing in present on these piers, they are not included. Once the bridge is broken into subsystems based on the location of the expansion joints, each subsystem is modelled using the procedures described in Section 3.5, based on the substructure type. An example of the application of the detailed assessment on a bridge with expansion joints can be found in Appendix B.

3.7 Results for Sample Set

Appendix A and Appendix B contain the detailed assessment results for the remaining multispan bridges in the sample set. The major results and conclusions from the detailed assessment for the longitudinal and transverse direction for each bridge is shown in Table 3.15 and Table 3.16, respectively.

Table 3.15. Longitudinal Direction Steel Bridge Dynamic Properties and Controlling Capacity Results

Asset Name	NBI	Substructure Type	Abutment Type	Mass (kip/g)	Stiffnes (kip/in)	Period (s)	Controlling Capacity	Potential Vulnerability
038-89-04111 B	13000	Hammerhead	Non-integral	2.77	1160	0.31	Force at Cracking	Brittle Failure
052-24-06649	19430	Hammerhead	Non-integral	5.07	300	0.82	Force at Cracking	Brittle Failure
062-74-06621	22190	Hammerhead	Non-integral	2.9	1000	0.34	Force at Cracking	Brittle Failure
067-18-05459 D	24210	Hammerhead	Non-integral	3.49	160	0.93	Force at Cracking	Brittle Failure
154-77-01976 B	27720	-	Non-integral	N/A	N/A	N/A	N/A	N/A
041-82-05415 CSBL	14280	Circular Frame Bent	Integral	3.1	416.4	0.54	Base Shear	None
062-13-07329	22240	Hammerhead	Non-integral	4.83	175	1.04	Force at Ultimate	Plastic Hinge
I469-12-06947 AEB	32841	Rectangular Frame Bent	Integral	3.87	225.4	0.82	Base Shear	None
(I69)037-133-03632 JASBL	12250	-	Integral	N/A	N/A	N/A	N/A	N/A
057-26-03322 A	20530	-	Non-integral	N/A	N/A	N/A	N/A	N/A
041-77-03864 JBNB	14840	Wall	Integral	2.37	325.4	0.54	Force at Cracking	None
I65-118-02313 JCSB	36890	Wall	Integral	6.12	1297.8	0.43	Force at Cracking	None
I70-006-04712 CEBL	41130	Wall	Integral	3.32	1630	0.28	Force at Ultimate	None
I70-008-02344 BEBL	41230	Wall	Integral	4.32	446	0.62	Force at Ultimate	None
I465-127-05274 DEBL	50340	Wall	Integral	3.24	420	0.55	Force at Ultimate	None
I69-050-09497 NB	80182	Wall	Integral	7.83	1752	0.42	Force at Ultimate	None
I69-057-09506	80226	Wall	Integral	4.74	1533	0.35	Force at Ultimate	None
(421)39-12-01792 B	32200	Wall	Non-integral	2.59	3400	0.17	Force at Cracking	Brittle Failure
062-82-02589 WBL	21985	Rectangular Frame Bent	Non-integral	7.11	366.8	0.87	Base Shear	Plastic Hinge
I64-05-05201 CEBL	33240	Other	Non-integral	5.94	230	1.01	Force at Cracking	Brittle Failure
I64-07-02367 BEBL	33280	Circular Frame Bent	Integral	3.06	198	0.78	Base Shear	None
I69-309-04548 C	40300	Rectangular Frame Bent	Non-integral	4.1	555	0.54	Base Shear	Plastic Hinge
I70-074-05231 B	42020	Rectangular Frame Bent	Integral	8.38	8930	0.19	Shear Connection	None
I94-29-04469 CEB	49120	Circular Frame Bent	Integral	4.25	800	0.46	Base Shear	None

Table 3.16. Transverse Steel Bridge Dynamic Properties and Controlling Capacity

Asset Name	NBI	Substructure Type	Abutment Type	Mass (kip/g)	Stiffnes (kip/in)	Period (s)	Controlling Capacity	Potential Vulnerability
038-89-04111 B	13000	Hammerhead	Non-integral	1.9	171000	0.21	Shear Connection	None
052-24-06649	19430	Hammerhead	Non-integral	3.95	433000	0.0019	Shear Connection	None
062-74-06621	22190	Hammerhead	Non-integral	1.45	265000	0.015	Shear Connection	None
067-18-05459 D	24210	Hammerhead	Non-integral	1.74	60200	0.034	Shear Connection	None
154-77-01976 B	27720	-	Non-integral	N/A	N/A	N/A	N/A	N/A
041-82-05415 CSBL	14280	Circular Frame Bent	Integral	1.55	2530	0.15	Collapse Mechanism 1	Plastic Hinge
062-13-07329	22240	Hammerhead	Non-integral	3.34	189000	0.026	Shear Connection	None
I469-12-06947 AEB	32841	Rectangular Frame Bent	Integral	1.93	2300	0.182	Collapse Mechanism 1	Plastic Hinge
(I69)037-133-03632 JASBL	12250	-	Integral	N/A	N/A	N/A	N/A	N/A
057-26-03322 A	20530	-	Non-integral	N/A	N/A	N/A	N/A	N/A
041-77-03864 JBNB	14840	Wall	Integral	1.64	273000	0.015	Shear Connection	None
I65-118-02313 JCSB	36890	Wall	Integral	5.05	2240000	0.009	Shear Connection	None
I70-006-04712 CEBL	41130	Wall	Integral	2.66	1040000	0.01	Shear Connection	None
I70-008-02344 BEBL	41230	Wall	Integral	3.37	437000	0.017	Shear Connection	None
I465-127-05274 DEBL	50340	Wall	Integral	2.24	1620000	0.007	Shear Connection	None
I69-050-09497 NB	80182	Wall	Integral	5.58	520000	0.021	Shear Connection	None
I69-057-09506	80226	Wall	Integral	1.9	7120000	0.003	Shear Connection	None
(421)39-12-01792 B	32200	Wall	Non-integral	2.18	696000	0.011	Shear Connection	None
062-82-02589 WBL	21985	Rectangular Frame Bent	Non-integral	5.47	4400	0.22	Collapse Mechanism 1	Plastic Hinge
I64-05-05201 CEBL	33240	Other	Non-integral	4.16	218000	0.027	Shear Connection	None
I64-07-02367 BEBL	33280	Circular Frame Bent	Integral	2.15	1000	0.29	Collapse Mechanism 1	Plastic Hinge
I69-309-04548 C	40300	Rectangular Frame Bent	Non-integral	3.37	22400	0.077	Collapse Mechanism 1	Plastic Hinge
I70-074-05231 B	42020	Rectangular Frame Bent	Integral	7.01	448000	0.025	Collapse Mechanism 2	Plastic Hinge
I94-29-04469 CEB	49120	Circular Frame Bent	Integral	3.08	4300	0.17	Collapse Mechanism 1	Plastic Hinge

3.8 Discussion of Vulnerabilities

The detailed assessment of the steel bridges in the sample set is used to identify potential vulnerabilities and vulnerability thresholds to be applied to the simplified assessment. No matter the substructure type, bridges with integral abutments are not vulnerable in the longitudinal direction. However, bridges with non-integral abutments and expansion shoe type bearings are especially vulnerable in the longitudinal direction because of the small stiffness and the potential for the bearings to overturn. The rest of the specific vulnerabilities are broken up, first by substructure type, and then further if needed.

3.8.1 Wall Vulnerabilities

Transverse Direction

As shown through the detailed calculations for wall-type substructures, Section 3.5.1, walls are not vulnerable to the level of hazard in the transverse direction because of the large stiffness of the walls in that direction.

Longitudinal Direction

While the sample calculation was an integral wall and is not vulnerable in the longitudinal direction, there is the possibility for wall substructures with non-integral abutments to be vulnerable in the longitudinal direction. For all of the wall bridges in the sample set, in the longitudinal direction, the base shear controlled over the shear strength and the shear connection however, two different vulnerabilities were identified for wall substructures with non-integral abutments based on the year of construction.

The older bridges, constructed prior to 1990, have a lower grade of steel and a lower reinforcement ratio, often below the minimum 0.25% required by current code (ACI, 2019). Because of this, and shown through the moment-curvature analysis, the bridge cannot behave in flexure, a brittle failure would occur because cracking moment of the concrete was greater than the calculated yield and ultimate moment. This means that once the concrete cracks, the steel almost immediately yields and reaches its ultimate strength and brittle failure may occur unless an alternate load path can be

established. This type of moment-curvature relationship, and corresponding potential failure method is dangerous and if it were to occur, the bridge would not be useable.

Newer walls, constructed after 1990, use a higher grade of reinforcement and often have a larger reinforcement ratio. The combination of this leads to the expected moment-curvature relationship, in which the ultimate moment is greater than the yield moment which is greater than the cracking moment. This means that the substructure is able to behave in flexure and a plastic hinge will form at the base of each wall.

3.8.2 Hammerhead Vulnerabilities

Transverse Direction

Hammerhead substructures are very similar to wall substructures in their behavior and the vulnerabilities seen. Just like walls, hammerheads are not vulnerable to the level of hazard in the transverse direction because of the large stiffness in that direction.

Longitudinal Direction

As seen in the sample calculations for hammerhead substructures, in the longitudinal direction, there is the potential for vulnerability in the longitudinal direction. Like the wall substructures, in the longitudinal direction, the base shear controlled over the shear strength and the shear connection however, two different vulnerabilities were identified for wall substructures with non-integral abutments based on the year of construction.

The older bridges, constructed prior to 1990, have a lower grade of steel and a lower reinforcement ratio, often below the minimum 0.25% required by current code (ACI, 2019). Because of this, and shown through the moment-curvature analysis, the bridge cannot behave in flexure, a brittle failure would occur because cracking moment of the concrete was greater than the calculated yield and ultimate moment.

Newer hammerheads, constructed after 1990, use a higher grade of reinforcement and often have a larger reinforcement ratio. The combination of this leads to the expected moment-curvature relationship, in which the ultimate moment is greater than the yield moment which is greater than

the cracking moment. This means that the substructure is able to behave in flexure and a plastic hinge will form at the base of each wall.

3.8.3 Frame Bent Vulnerabilities

Transverse Direction

Unlike walls and hammerheads, frame bents have the potential for vulnerability in the transverse direction. In the sample set, the base shear and the formation of a plastic hinge, in the transverse direction, controlled over the shear strength and the shear friction connection. However, the governing collapse mechanism depends specifically on the cross-section of the beam and the column. For the majority of bridges, collapse mechanism 1 (Figure 3.27), governed. However, as seen in Table 3.16, collapse mechanism 2 (Figure 3.28) governed occasionally. Brittle failure was not seen in any of the frame bents because, even if they were older and had a lower grade of reinforcement, the reinforcement ratio was large enough to allow the pier to behave in flexure.

Longitudinal Direction

Frame bents also have the potential for vulnerability in the longitudinal direction. As shown in the detailed calculations, frame bents have the potential to form plastic hinges at the base of each column. In the sample set, the base shear, and the formation of a plastic hinge, controlled over the shear strength and the shear friction connection. Brittle failure, as discussed in the section above, was not seen in any of the frame bents. Therefore, frame bent piers will behave in flexure in the longitudinal direction.

3.9 Indicators of Vulnerabilities

The information that can be used in the simplified assessment has to be information that is already available in BIAS or information that can be easily identified during routine inspections. Information like reinforcement ratio and layout, used to develop the moment-curvature relationship for each element and determine the controlling capacity, is not available for the simplified assessment. Because of this, the results from the detailed assessment, in addition to identifying potential vulnerabilities, are used to identify displacement and drift indicators for the potential vulnerabilities. Displacement and drift indicators are used to identify the vulnerabilities

because the displacement demand and drift demand can easily be determined using information available whereas force demand cannot. These indicators link the force capacity to a displacement or drift level and are shown in Table 3.17.

Table 3.17. Vulnerability Indicators for Steel Bridges

		Walls		Hammerheads		Frame Bents
		Year Built < 1990	Year Built > 1990	Year Built < 1990	Year Built > 1990	RC Columns
Low Vulnerability	Longitudinal	Δ_{lin} < 0.1"	Δ_{NL} < 1"	Δ_{lin} < 0.1"	Δ_{NL} < 1"	Δ_{NL} < 1"
	Transverse					Drift < 0.5%
Moderate Vulnerability	Longitudinal		1" < Δ_{NL} < 6"		1" < Δ_{NL} < 6"	1" < Δ_{NL} < 6"
	Transverse					0.5% < Drift < 1.5%
High Vulnerability	Longitudinal	Δ_{lin} > 0.1"	Δ_{NL} > 6"	Δ_{lin} > 0.1"	Δ_{NL} > 6"	Δ_{NL} > 6"
	Transverse					Drift > 1.5%

3.9.1 Wall Vulnerability Indicators

As mentioned earlier, walls are not vulnerable in the transverse direction, so only displacement indicators for the longitudinal direction are identified. The indicator is dependent on the year of construction. If the wall was constructed prior to 1990, there is the potential for brittle failure, which would classify the bridge as highly vulnerable. In the detailed analysis, a longitudinal displacement of approximately 0.1-*inch* corresponded to the concrete cracking. If the displacement was less than 0.1-*inch*, the concrete will not have cracked, and the bridge is classified as low vulnerability. If the wall was constructed after 1990, the detailed assessment results show that the substructure can behave in flexure, and if the steel were to yield, the bridge would be classified as moderately vulnerable. In the detailed analysis for the newly constructed walls, a displacement of 1-i*nch* or greater corresponded to the steel yielding in the substructure and leads to a vulnerability classification of moderately vulnerable. However, if the displacement were to exceed 6-*inches*, the ultimate rotation of the plastic hinge is assumed to be reached and the bridge would then be classified as highly vulnerable.

3.9.2 Hammerhead Vulnerability Indicators

Hammerhead substructures behave in the same manner as walls. In the transverse direction, hammerhead substructures are not vulnerable. In the longitudinal direction, the older walls, constructed prior to 1990, have the potential for brittle failure corresponding to a displacement of 0.1-*inch.* The newer walls, constructed after 1990, behave in flexure with a displacement of 1-*inch* corresponding to the yielding of the longitudinal reinforcement and the formation of a plastic hinge. If the displacement were to exceed 6-*inches*, the ultimate rotation of the plastic hinge is assumed to be reached and the bridge would then be classified as highly vulnerable.

3.9.3 Frame Bent Vulnerability Indicators

Unlike walls and hammerheads, frame bents are vulnerable in both the longitudinal and the transverse direction. In the transverse direction, drift percentages are used as indicators of the different levels of vulnerability. A drift calculated as

$$Drift = \frac{2 * \Delta_{NL}}{H}, \tag{3.32}$$

greater than 0.5% corresponds to a plastic hinge forming and classifies the bridge as moderately vulnerable. If the drift exceeded 1%, the plastic hinge had reached its ultimate rotation and the bridge is classified as highly vulnerable. In the longitudinal direction, the detailed assessment showed the same 1-*inch* and *6-inch* displacements corresponding to the formation of a plastic hinge and the ultimate rotation of the plastic hinge, respectively.

3.10 Conclusions

Based on the results presented in this chapter, conclusions from the detailed (Level 2) assessment can be categorized by substructure features are as follows:

- **Walls and Hammerheads with a low amount of reinforcement and a low grade of reinforcement** – Walls and hammerheads with a combination of a low amount of reinforcement and a low grade of reinforcement (40 *ksi*) had a cracking moment larger than the ultimate moment. When the cracking moment is exceeded, the reinforcement will yield and rupture almost instantaneously. Because of this, these bridges have the potential for

brittle failure and are highly vulnerable. This behavior was seen in the analysis of most bridges constructed prior to 1990.

- **Walls and Hammerheads with an adequate amount of reinforcement and an adequate grade of reinforcement** – Walls and hammerheads with a combination of an adequate amount of reinforcement and a higher grade (60 *ksi)* had an ultimate moment that was larger than the cracking moment and the yield moment. This outcome means that these substructures are able to yield and will behave in flexure in the longitudinal direction and the formation of a plastic hinge will govern. This behavior was seen in bridges constructed after 1900.
- **Frame Bent Substructures** – Frame bent substructures were found to have an adequate amount of reinforcement to allow them to behave in flexure. In the transverse direction, the strong beam-weak column failure mechanism governed for six of the seven frame bent substructures in the sample set. In the longitudinal direction, the formation of a plastic hinge at the base of each column governed.
- **Bridges with Rocker Bearings** – Bridges with rocker bearings, as opposed to elastomeric bearing pads, have an additional allowable displacement constraint because of the potential for the rocker bearings to overturn. While this chapter assumed all rocker bearings were perfectly vertical to calculate the allowable displacement, in the field, this would need to be verified and updated based on the actual position of the bearing.

3.11 Summary

This chapter presented the detailed (Level 2) assessment procedure for the steel bridges in the 100-bridges in the chosen sample set and demonstrated its application on each of the three most common substructure types in the state. The force and displacement demand, from the generated time-histories was compared to the force and displacement capacities of the substructure units in order to determine the potential vulnerabilities of bridges in Indiana. The results from the detailed assessment of the remaining 21 bridges can be found in Appendix B. These assessments will be used to develop a simplified assessment in the following chapter.

4. SIMPLIFIED VULNERABILITY ASSESSMENT PROCEDURE

4.1 Introduction

The development of the simplified seismic assessment procedure and the identification of critical items to be added to BIAS is described in detail in this chapter. The development consists of identifying trends from the detailed (Level 2) analysis, applying those trends to develop a simplified SDOF model, and using capacity threshold levels to classify the vulnerability of each bridge. The results from the detailed assessment for the reinforced concrete and prestressed bridges can be found in the SPR 4222 final report (Bonthron et al., 2020). The simplified assessment is applicable to 31 of the 100 bridges in the chosen sample set. The rationale for excluding bridges with certain characteristics is described in the initial classification (Level 0) section below. This chapter first presents the vulnerability analysis results obtained using the best models which use all of the recommended additional data items. Then it discusses potential methods for estimating those data items and the impact of using the estimate on the results. The best models for the simplified assessment are then used in the associated tool, which is discussed in the following chapter.

4.2 Identification of Required Data Items

4.2.1 Available Utilized Data Items

The primary purpose of BIAS is asset management which includes the storage of inspection reports and information about superstructures that are useful for prioritizing rehabilitations, planning preventative maintenance, and scheduling bridge replacements. In its current state, BIAS does not contain all the information required to perform an automated Level 1 assessment of the bridge inventory. However, it does contain some of the information that is needed for the Level 1 assessment, specifically, the National Bridge Inventory (NBI) data items listed below:

- Asset Name
- Asset Code (NBI Number)
- District
- Latitude
- Longitude
- Number of Spans
- Max Span
- Bridge Length
- Skew
- Year Built
- Superstructure Type
- Minimum Vertical Under Clearance

4.2.2 Required Additional Data Items

Greater detail on the rationale for recommendations to add additional data items to BIAS is given in subsequent sections. Simply put, without these data items, the number of bridges for which a simplified assessment can be conducted decreases substantially. If estimates are used for these data items, there is a reduction in the accuracy of the simplified assessment results. Throughout the development of the simplified assessment process, eight additional data items were identified as critical. These items, in no particular order, are:

- *Substructure Type* – defined as the structural system supporting the superstructure.
- *Abutment Type* – defined as the connection between the connection of the superstructure to the abutments.
- *Number of Elements in Substructure* – defined as the number of elements making up a single pier. For walls and hammerheads, this value is one. For frame bents, this value is the number of columns.
- *Element Height* – defined as the dynamic height of the tallest pier (in feet)
- *Element Length* – defined as the transverse dimension of a substructure element (in feet)
- *Element Width* – defined as the longitudinal dimension of a substructure element (in feet)
- *Deck Thickness* – defined as the thickness of deck (in inches)
- *Height Ratio Flag* – defined as yes or no to signify when two piers in a bridge have a height ratio of 1.10 or greater.

4.3 Initial Classification (Level 0)

Prior to performing the Level 1 assessment, certain bridges can be identified as having low vulnerability or moderate vulnerability or as having details that require a detailed (Level 2) assessment based on the bridge details.

4.3.1 Low Vulnerability

Based on the below pre-determined screening criteria, the details that can be automatically identified as low vulnerability are:

- **Short, Single Span Bridges –** The entire mass is attributed to abutments in both longitudinal and transverse direction. Assuming no differential movement at the abutments, the bridge will move together entirely and is categorized as low vulnerability.
- **Wall Substructures in the Transverse Directions –** Bridges with wall substructures have a large stiffness and capacity in the transverse direction. The large stiffness results in a low period and correspondingly low structural displacement, making them less vulnerable to the level of ground motion expected in Indiana.
- **Bridges with Integral Abutments in the Longitudinal Direction –** Bridges with integral abutments are not vulnerable in the longitudinal direction because there is no differential displacement between the substructure and the superstructure. The combination of a wall with integral abutments means there is no potential for vulnerability in the longitudinal and the transverse direction at the level of hazard expected for Indiana. These bridges can be automatically classified as low vulnerability.
- **Hammerhead Substructures in the Transverse Direction –** For the same reason as walls, hammerhead substructures supporting reinforced concrete and steel superstructures is not vulnerable the transverse direction due to the large stiffness of intermediate piers. Hammerhead walls supporting prestressed concrete superstructures do not fall into this category and require a simplified assessment.

4.3.2 Moderate Vulnerability

Bridge details that can be automatically identified as having moderate vulnerability are as follows:

- **Long, Single Span Bridges on Rocker Bearings –** Unlike short span, single span bridges, long, single span bridges have the potential for the rocker bearings to overturn. This makes long, single span bridges on rocker bearings vulnerable to damage during seismic activity. In order to account for this, single span bridges with a length greater than 60'-0" are classified as long, single span bridges is used to classify long span. Steel bridges that are non-integral and long, are then marked as moderately vulnerable because of this.

4.3.3 Detailed Analysis Required

Bridge details that require a detailed assessment are as follows:

- **Bridges with Expansion Joints –** Bridges with expansion joints must be divided into separate models at each expansion joint. Thus, it is not possible to apply a simplified assessment. While there is no NBI data that directly corresponds to the expansion joints, bridges with approach spans, bridges with more than six spans, and bridges that have a total length larger than 1000 ft are assumed herein to have expansion joints based on trends observed in the detailed analysis.
- **Bridges with "Other" Type Substructures –** Unique substructures require additional modeling assumptions be considered in the procedure presented in Chapter 3.4 on a case-by-case basis. Therefore, it is not possible to apply a simplified assessment to these bridges.
- **Bridges with Piers having a Height Ratio Greater than 1.1 –** A height ratio equal to or exceeding 1.1 (between the height of the tallest pier to that of the shortest pier) increases the likelihood of one pier exhibiting a non-linear response while the pier remains linear. It is not possible to capture this complicated response with a single value for the pier height; thus, a detailed analysis must be leveraged to account for the force redistribution due to non-linear behavior and structural softening.
- **Reinforced Concrete Superstructures with Reinforced Concrete Column Frame Bents –** Reinforced concrete superstructures with reinforced concrete column frame bents are excluded from the simplified assessment because they do not follow the same trends in vulnerability and vulnerability thresholds as the other superstructure materials. In order to

accurately assess the vulnerability of these bridges, the reinforcement layout and details are required (Level 2). The simplified assessment does not consider these details.

- **Frame Bent Substructures whose Columns have an Aspect Ratio Less than Three –** An aspect ratio (the ratio of the height of the substructure over the length of the substructure) less than three means that the likelihood of the pier behaving in flexure decreases and the pier is likely to fail in shear. The simplified assessment is unable to capture accurate capacity estimates if the pier does not behave in flexure because the required information needed to calculate the shear capacity.

4.3.4 Simplified (Level 1) Assessment Applicable Bridges

After the Level 0 screening of the 100 bridges in the sample set, the simplified assessment is applicable to 31 bridges. Table 4.1 lists these bridges, and each of their superstructure type, substructure type, and abutment type. The number in the first column of Table 4.1 corresponds to the bridge identification number and is used in the plots in the following sections, unless otherwise noted.

Table 4.1. Bridges for which a Simplified (Level 1) Assessment is Applicable

Bridge ID #	Asset Name	NBI #	Superstructure Material	Substructure Type	Abutment Type
1	028-79-07672	7640	Reinforced Concrete	CFT Frame Bent	Integral
2	044-55-06793 A	16310	Reinforced Concrete	CFT Frame Bent	Integral
3	057-14-06739	20690	Reinforced Concrete	CFT Frame Bent	Integral
4	064-19-03723 A	22960	Reinforced Concrete	CFT Frame Bent	Non-integral
5	067-42-07298	23760	Reinforced Concrete	CFT Frame Bent	Integral
6	252-24-06934 A	30780	Reinforced Concrete	CFT Frame Bent	Integral
7	327-17-06419 A	31350	Reinforced Concrete	CFT Frame Bent	Integral
8	I69-334-04590 BNB	40720	Reinforced Concrete	CFT Frame Bent	Non-integral
9	(237)37-13-07277	11840	Reinforced Concrete	H-pile Frame Bent	Integral
10	055-45-07366	19880	Reinforced Concrete	H-pile Frame Bent	Integral
11	056-63-07286 A	19933	Reinforced Concrete	H-pile Frame Bent	Integral
12	067-55-03831 ANBL	24100	Reinforced Concrete	H-pile Frame Bent	Non-integral
13	252-55-08713	30721	Reinforced Concrete	H-pile Frame Bent	Integral
14	018-05-06573 B	4880	Reinforced Concrete	Wall	Non-integral
15	063-86-05970 BNBL	22810	Reinforced Concrete	Wall	Non-integral
16	066-13-05443 A	23670	Reinforced Concrete	Wall	Non-integral
17	I70-112-05137 DEBL	42960	Reinforced Concrete	Wall	Non-integral
18	I69-087-09551 NB	80356	Prestressed Concrete	Frame Bent	Integral
19	064-26-09191	80372	Prestressed Concrete	Frame Bent	Integral
20	(265)I265-11-09604	80482	Prestressed Concrete	Frame Bent	Integral
21	I69-112-09708 SB	51350	Prestressed Concrete	Hammerhead	Integral
22	I69-106-09739 SB	51385	Prestressed Concrete	Hammerhead	Integral
23	024-02-09089 A	76840	Prestressed Concrete	Hammerhead	Integral
24	356-63-09491	80374	Prestressed Concrete	Hammerhead	Integral
25	041-82-05415 CSBL	14280	Steel	Frame Bent	Integral
26	I469-12-06947 AEB	32841	Steel	Frame Bent	Integral
27	038-89-04111 B	13000	Steel	Hammerhead	Non-integral
28	052-24-06649	19430	Steel	Hammerhead	Non-integral
29	062-74-06621	22190	Steel	Hammerhead	Non-integral
30	062-13-07329	22240	Steel	Hammerhead	Non-integral
31	067-18-05459 D	24210	Steel	Hammerhead	Non-integral

4.4 Simplified Assessment Procedure with All Recommended Data Items

A Level 1 assessment is intended to utilize all recommended data items. The results obtained with models generated using accurate dimensions and details will be used herein as a basis of

comparison to demonstrate the impact of estimating specific data items on the accuracy of the vulnerability assessment results. The procedure developed to perform the simplified assessment, shown in Figure 1, is described in detail below. Then the following sections demonstrate and discuss the importance of the additional data items and, if applicable, methods for estimating them.

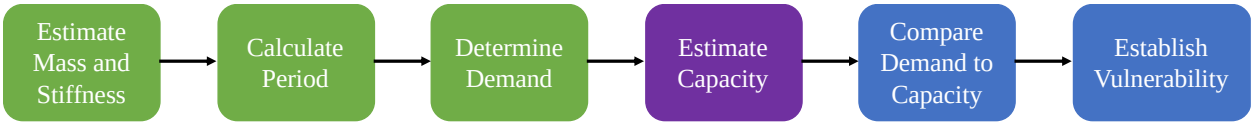

Figure 4.1. Simplified (Level 1) Assessment Procedure

4.4.1 Estimate Mass

The calculation of the mass used in the Level 1 assessment is based on superstructure dimensions that currently exist in BIAS as well as trends and averages identified in the detailed (Level 2) assessment. The calculations for mass are superstructure dependent. The following three sections describe the mass calculations for prestressed, steel, and reinforced concrete superstructures.

Prestressed Superstructure Mass – Longitudinal Direction

For prestressed girder superstructures, the mass calculation is based on estimated values for the number of beams, the average mass per linear foot of the beams, the volume of the deck, and the unit weight of concrete. The average mass of the beams ($M_{b,avg}$) is 3.3x10^{-3} *kips/g/ft*, based on the detailed assessment calculations. The number of beams is estimated using trends identified during the detailed assessment based on the deck width. For deck widths less than 44.4 *ft*, the estimated number of beams is four. Then, for every additional ten feet of deck width, one beam is added. Thus, for deck widths greater than 44.4 *ft*, the number of beams is calculated as

$$N_b = 4 + RoundUp\left(\frac{w_{deck} - 44.4ft}{10ft}\right). \quad (4.1)$$

Once the number of beams is estimated, the total mass of a bridge with a prestressed girder superstructure is calculated as

$$M_{PS} = (t_{deck} * L_{bridge} * w_{deck}) * \gamma_c + N_b * L_{bridge} * m_{b,avg}. \quad (4.2)$$

Steel Superstructure Mass – Longitudinal Direction

For steel girder superstructures, the mass calculation is based on the deck area and an estimated value of average mass per deck area. The average mass per deck area ($m_{b,avg}$) is taken as the average over the sample set of bridges and is 3.63x10^{-4} *kips/g/ft*^{2}. Thus, the total mass of a bridge with a steel superstructure is calculated as

$$M_{steel} = m_{b,avg} * L_{bridge} * w_{deck}. \quad (4.3)$$

Reinforced Concrete Slab Deck Superstructure Mass – Longitudinal Direction

For reinforced concrete slab deck superstructures, the mass calculation is based on the volume of the deck, using the actual deck thickness, the estimated value of the average mass per linear foot of railings, and the unit weight of concrete. The total mass of a bridge with a reinforced-concrete superstructure is calculated as

$$M_{RC} = (t_{deck} * L_{bridge} * w_{deck}) * \gamma_c + 0.002 * L_{bridge}. \quad (4.4)$$

Transverse Mass Estimate

In the transverse direction, the percent of the mass that is activated is based on the number of spans. This is because the abutments carry a portion of the end-span mass. Table 4.2 shows the percentage of mass activated ($\%_{act}$) for different number of spans in the main unit. The simplified assessment is not applicable to bridges with more than six spans because of the high likelihood of expansion joints being present.

Table 4.2. Percent of Total Mass Activated in the Transverse Direction

Number of Spans	Percent of Mass Activated
2	50%
3	71.5%
4	80%
5	82.5%
6	85%

For prestressed and steel superstructures, this activated mass percentage is all that is needed to calculate the transverse mass. However, because the transverse direction of reinforced concrete slab deck superstructures is modelled as a MDOF system in the Level 2 assessment, the decoupled

mass is needed for the simplified assessment calculations (Mahmud, 2019). This value is calculated as

$$M_{trans} = \frac{M_{RC} * \%_{act}}{N_{pier}}. \quad (4.5)$$

Impact of Estimates on Averages and Mass

Figure 4.2 shows a comparison between the Level 1 mass and the Level 2 mass for the 31 bridges. The mass used in the simplified assessment is calculated using the estimates and averages described above, whereas the mass used in the detailed assessment is calculated using information from the bridge drawings.

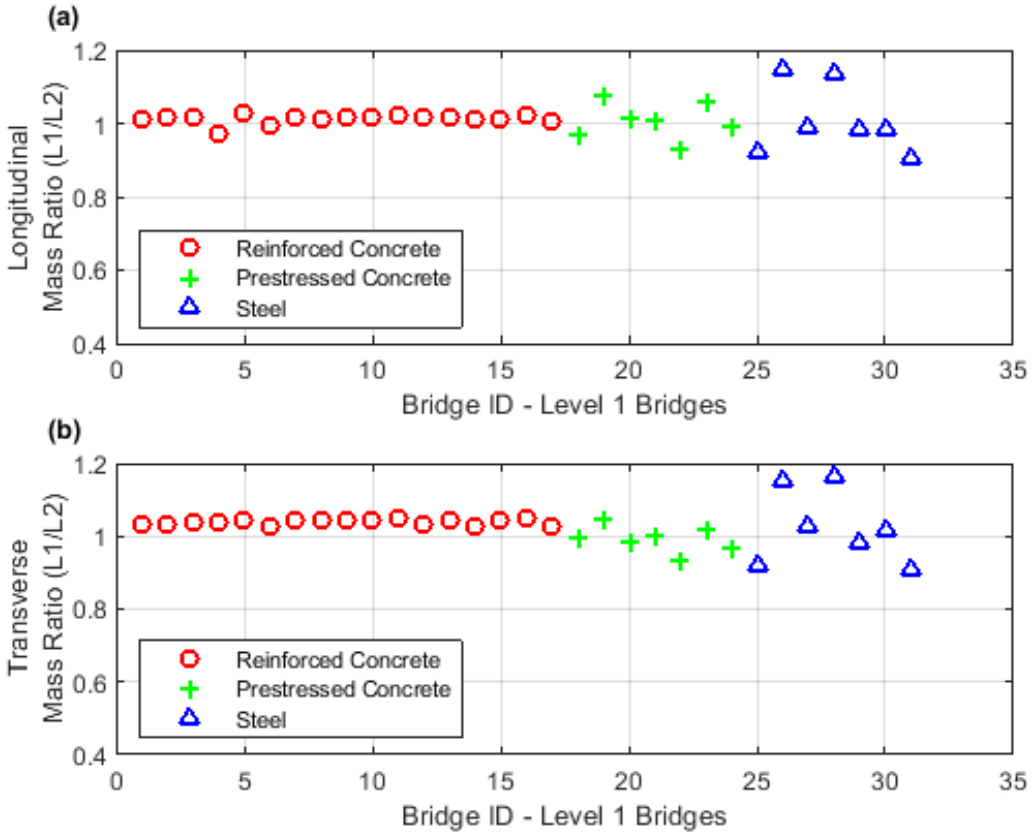

Figure 4.2. Comparison of Mass Values Used for the Simplified Assessment and Detailed Assessment in the (a) Longitudinal Direction and (b) Transverse Direction

4.4.2 Estimate Stiffness

The stiffness of a bridge is dependent on both the substructure and superstructure types. The substructure type determines the specific modeling procedure and necessary geometric properties to be used. The superstructure type determines which elements contribute stiffness as well as the connectivity factor. This factor describes the fixity of the connection between the substructure and the superstructure. The connectivity factors, F_{con}, are three, six, and twelve for steel, prestressed, and reinforced concrete superstructures, respectively. The required substructure geometry includes the clear height of the substructure, the number of elements in one pier, the length of the element (dimension in the transverse direction), and the width of the element (dimension in the longitudinal direction).

Wall Stiffness – Longitudinal Direction

The stiffness of a single wall in the longitudinal direction is calculated, using the same equations as the Level 2 assessment, as

$$K_{wall,L} = \frac{F_{con} * E_c * I_{dir}}{H^3}. \quad (4.6)$$

Wall Stiffness – Transverse Direction

As discussed previously, walls are already found to be not vulnerable in the transverse direction to the level of hazard chosen for this report (a 7% probability of exceedance in 75 years) because of the large stiffness of walls. Thus, the simplified assessment need not be applied to any walls in the transverse direction.

Hammerhead Stiffness – Longitudinal Direction

For hammerhead substructures, the stiffness in the longitudinal direction is calculated using the same equation as walls (Equation 4.6). The length used in the moment of inertia calculation is the length of the stem of the hammerhead.

Hammerhead Stiffness – Transverse Direction

Hammerhead walls supporting prestressed concrete superstructures have been identified as having the potential for vulnerability due to the combination of the large superstructure mass and the

narrowing at the base, corresponding to an increased period. For prestressed bridges with hammerhead substructures, the stiffness of a single pier in the transverse direction is calculated as

$$K_{HH,T} = \frac{F_{con} * E_c * I_{dir}}{H^3} + \frac{G * w_{ele} * L_{ele}}{1.2H}, \quad (4.7)$$

Where G is the shear coefficient and is calculated as

$$G = \frac{E_c}{2 * (1 + \nu)}. \quad (4.8)$$

Hammerhead walls supporting steel and reinforced concrete superstructures are already found to not be vulnerable in the transverse direction and therefore, the above equations only apply to prestressed superstructures.

Frame Bent Stiffness

For frame bent substructures, it is important to know whether the elements are composite piles (concrete filled tubes (CFT) or H-piles) or reinforced concrete columns. In addition, the shape of the element (circular or rectangular) also influences the response. The substructure category identifies the shape of the element but does not differentiate between composite pile and reinforced concrete columns. Rather, this distinction is made using information currently available in BIAS. Pile substructures are only identified in the state for bridges with reinforced concrete superstructures, but not for bridges with steel or prestressed superstructures. Therefore, if a bridge superstructure is prestressed or steel, the frame bent is assumed, for both the simplified assessment and tool, herein to be composed of reinforced concrete columns. For reinforced concrete superstructures, the feature intersected is used to differentiate between composite piles and reinforced concrete columns. If the feature intersected is a waterway, like a creek or a river the substructure is assumed to be composed of composite piles, and if the feature intersected is a road or railroad the substructure is assumed to be composed of reinforced concrete columns.

Frame Bent Stiffness – Longitudinal Direction

Calculations for the longitudinal stiffness for frame bents are dependent on superstructure type to determine the connectivity factor. The factors for steel, prestressed, and reinforced concrete superstructures are three, six and twelve, respectively.

Reinforced Concrete Column

For reinforced concrete column frame bents, the longitudinal stiffness of one bent is based only on the number of columns, the connectivity factor, and the column geometry (length, width, and height). The stiffness of RC frame bents is

$$K_{RCFB,L} = N_c * \frac{F_{con} * E_c * I_{dir}}{H^3}. \quad (4.9)$$

H-pile Composite Piles

For H-pile composite substructures, the standard shape is an HP 12x53 (Standard Drawing No. E 701-BPIL-01, IN). This standard has been identified as typical in Indiana and the shape properties of the pile have been leveraged to calculate the stiffness as

$$K_{HPFB,L} = N_c * \frac{F_{con} * EI_{dir}}{H^3}. \quad (4.10)$$

The EI_{dir} component is calculated as

$$EI_{dir} = E_s * I_{HP,dir} + c_{HP} * I_c * E_c, \quad (4.11)$$

Where $I_{HP,dir}$ is the moment of inertia of the steel shape in the longitudinal direction (127 in^4), c_{HP} is the coefficient for the HP 12x53 pile identified as typical in the Level 2 analysis (0.3528) and I_c is the moment of inertia of the concrete (77.06 *kip*ft*).

Concrete Filled Tube (CFT) Composite Piles

CFT piles typically are 14-inch diameter piles which includes a 0.2-inch steel encasement (Standard Drawing No. E 701-BPIL-01, IN). The stiffness of one pier is calculated as

$$K_{CFTFB,L} = N_c * \frac{F_{con} * EI_L}{H^3}. \quad (4.12)$$

The EI_{dir} component is calculated as

$$EI_{dir} = E_s * I_{CFT,L} + c_{CFT} * I_c * E_c, \quad (4.13)$$

where $I_{CFT,L}$ is the moment of inertia of the steel (105.47 in^4), c_{CFT} is the coefficient for CFTs based on the typical shape (0.5351), and I_c is the moment of inertia of the concrete (1780.3 *kip*ft*).

Frame Bent Stiffness – Transverse Direction

The calculations for the transverse stiffness of reinforced concrete column frame bents are based on a frame bent factor (F_{FB}), determined from trends identified in the detailed analysis, the superstructure type, the number of columns, and the column geometry. The frame bent factor

relates the pre-condensed pure translational degree-of-freedom term ($N_c \frac{12A}{H^3}$) of the bent stiffness matrix (

Table 3.14) to the condensed stiffness of the frame bent. Figure 4.3 provides the calculated frame bent factor for all frame bents in the sample set (note that the bridge number on the x-axis here does not correspond to the bridge ID in Table 4.1). The average frame bent factor is 0.88 with a standard deviation of 0.06 for prestressed and steel superstructures, and the average frame bent factor is 0.96 with a standard deviation of 0.04 for reinforced concrete superstructures. For the simplified assessment, these averages are used in the transverse stiffness calculations.

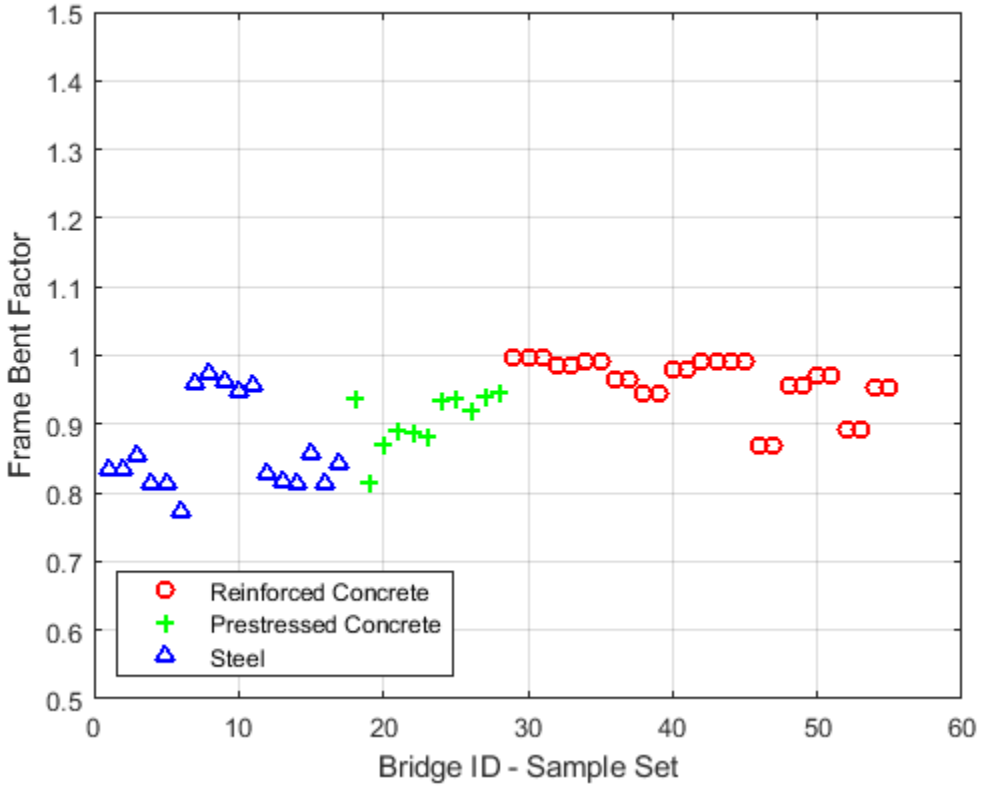

Figure 4.3. Frame Bent Factor Spread for All Frame Bent Piers in the Sample Set

Reinforced Concrete Columns

The transverse stiffness of a frame bent with reinforced concrete columns, independent of the superstructure type, is calculated as, where F_{FB} is 0.88,

$$K_{RCFB} = F_{FB} * N_c * \frac{12 * E_c * I_{dir}}{H^3}. \quad (4.14)$$

H-pile Composite Piles

Due to the difference in the moment of inertia of the steel shape about the *x*- and *y*-axes, the transverse stiffness of the H-pile substructures is equal to the longitudinal stiffness. The stiffness in the transverse direction of one pier with H-piles is calculated as, where F_{FB} is 0.96,

$$K_{HPFB} = F_{FB} * N_c * \frac{12 * EI_{dir}}{H^3}, \quad (4.15)$$

The EI_T term is calculated as

$$EI_{dir} = E_s * I_{HP,dir} + c_{HP} * I_c * E_c, \quad (4.16)$$

and $I_{HP,L}$ is the moment of inertia of the steel shape in the transverse direction (393 in^4), c_{HP} is the average coefficient for H-piles from the detailed analysis (0.3528), and I_c is the moment of inertia of the concrete (176.18 *kip*ft*).

Concrete Filled Tube (CFT) Composite Piles

The calculation for the transverse stiffness of frame bents with CFT piles is the same as that for the longitudinal direction, Equation 4.12, because the shape is symmetric about all axes.

Bridge Stiffness

Equations 4.6 through 4.16 are used to calculate the stiffness of one pier in the two fundamental directions. The calculation for the total stiffness of the bridge is dependent on the superstructure type. The following sections detail the calculations of the stiffness in the two fundamental directions for steel girder, prestressed girder, and reinforced concrete slab deck superstructures.

Steel Superstructure Bridge Stiffness – Longitudinal Direction

Only the piers with fixed bearings (not sliding, expansion, or roller bearings) add to the total stiffness of the bridge, due to their ability to transfer inertial forces from the superstructure to the substructure. In the Level 2 analysis, each bridge typically has one fixed bearing at an intermediate pier and expansion bearings at the other piers and the abutments. The fixed connection means that pier will draw most, if not all of the force, therefore eliminating the softening effects of the expansion bearings. Thus, the piers with expansion bearings are excluded from the stiffness

calculation in the longitudinal direction, and the stiffness of steel superstructure bridges in the longitudinal direction is the stiffness of one pier. This stiffness is taken as

$$K_{Long} = K_L, \tag{4.17}$$

Steel Superstructure Bridge Stiffness –Transverse Direction

Steel bridges in the transverse direction are modelled as SDOF systems, thus the intermediate piers behave as springs in parallel. Therefore, the total stiffness in the transverse direction is the sum of the stiffness of each pier. The Level 1 assessment assumes identical piers, in cross-sectional geometry and height. The stiffness of bridges with steel superstructures in the transverse direction is taken as

$$K_{Trans} = N_{pier} * K_T. \tag{4.18}$$

Prestressed Superstructure Bridge Stiffness – Longitudinal Direction

Unlike bridges with steel superstructures, the connection between the substructure and the superstructure for prestressed bridges is adequate to transfer forces in the longitudinal direction. Therefore, the stiffness of bridges with prestressed superstructures in the longitudinal direction is calculated as

$$K_{Long} = N_{pier} * K_L. \tag{4.19}$$

Prestressed Superstructure Bridge Stiffness – Transverse Direction

Following the same logic as the calculation for the transverse stiffness of bridges with steel superstructures, the transverse stiffness of bridges with prestressed superstructures is calculated using Equation 4.18.

Reinforced Concrete Slab Deck Superstructures – Longitudinal Direction

Because the longitudinal bars extend from the substructure into the superstructure in reinforced concrete slab deck bridges, each pier adds stiffness in the longitudinal direction, and the stiffness is calculated using Equation 4.19.

Reinforced Concrete Slab Deck Superstructures – Transverse Direction

Unlike bridges with prestressed and steel superstructures, bridges with reinforced concrete slab deck superstructures are modelled as MDOF systems in the detailed analysis. However, the simplified assessment is unable to handle MDOF systems, so an equivalent SDOF system is developed. In the detailed assessment, the deck is modelled as a deep beam with the stiffness of each pier added to the pure translation degrees-of-freedom in the deck stiffness matrix (Mahmud, 2019).

The Level 1 assessment assumes that the contributions from the fundamental mode of the MDOF system control and all other modes do not affect the results significantly. As with the calculation for frame bent stiffness in the transverse direction, the stiffness calculation for reinforced concrete slab deck bridges uses a deck stiffness factor (F_{RCDS}). This deck stiffness factor relates the pure translational degree-of-freedom term, $\frac{12*E_c*I_d}{(1+\mu_1)l_1^3} + \frac{12*E_c*I_d}{(1+\mu_2)l_2^3} + K_{RCFB,T}$, for the pier that supports the maximum mass to the first modal stiffness in the decoupled stiffness matrix.

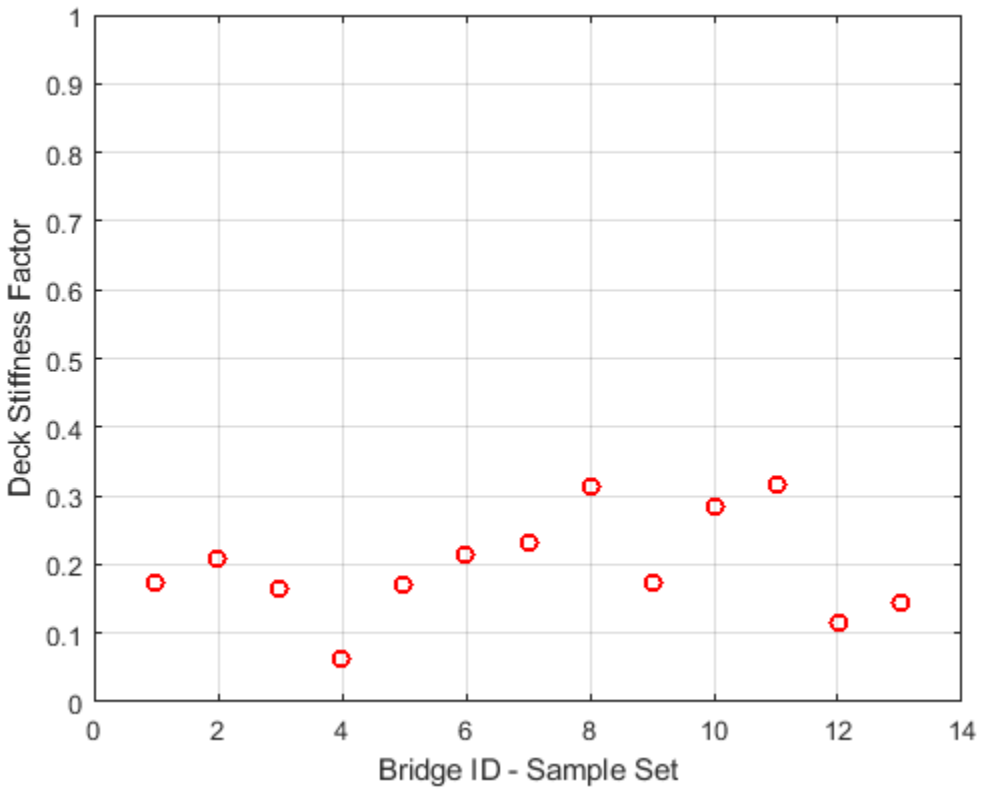

Figure 4.4. Deck Stiffness Factor for RC Bridges with Pile Substructures

The entire suite of three-span reinforced concrete slab deck bridges with pile substructures is used to determine an appropriate value for the deck stiffness factor. The outlier, bridge 4, is a four-span bridge that does not follow these trends and is excluded from the average calculations. The average deck stiffness factor (F_{RCDS}) of these results is 0.217 with a standard deviation of 0.07, as shown in Figure 4.4. The average value is used to calculate the stiffness of these bridges for the simplified assessment as

$$K_{Trans} = F_{RCFB} * \left(\frac{12 * E_c * I_d}{(1+\mu_1) l_1^3} + \frac{12 * E_c * I_d}{(1+\mu_2) l_2^3} + K_{RCFB,dir} \right), \quad (4.20)$$

Where

$$\mu_1 = \frac{12 * E_c * I_d}{G * t_{deck} * L_{bridge} * w_{deck} * l_1^2}, \quad (4.21)$$

And

$$\mu_2 = \frac{12 * E_c * I_d}{G * t_{deck} * L_{bridge} * w_{deck} * l_2^2}. \quad (4.22)$$

Because reinforced concrete slab deck superstructures are the only superstructure type in which the deck adds stiffness, they are the only type of bridge that require knowledge of the adjacent span length, (l_1 and l_2). Span lengths other than the maximum span are not given in BIAS and must be estimated based on trends seen during the detailed assessment. Since the pier supporting the maximum mass will be one that is adjacent to the maximum span, l_1 is always taken as the maximum span. The other span length used in the calculations is determined based on the number of spans, the bridge length, and the maximum span length. For two-span bridges, the remaining length, l_2, is calculated as

$$l_2 = L_{bridge} - l_1. \quad (4.23)$$

For three-span bridges, the simplified assessment procedure assumes symmetry about the middle of the bridge. Therefore, l_2 is calculated as

$$l_2 = \frac{L_{bridge} - l_1}{2}. \quad (4.24)$$

For bridges with four or more spans, the simplified assessment conservatively assumes that there are two adjacent spans of the maximum span length and therefore $l_2 = l_1$.

Impact of Estimates on Stiffness

Figure 4.5 shows the comparison of the stiffness used in the simplified assessment and the detailed assessment for all 31 bridges. The stiffness used for the simplified assessment is calculated using the estimates and averages described above, whereas the stiffness used for the detailed assessment is calculated using information from the bridge drawings. If a particular bridge does not have a data point shown in Figure 4.5, the simplified assessment is not performed in that direction for that bridge (e.g. bridges 13-17 in the transverse direction because they are reinforced concrete superstructures with wall substructures). The bridge ID on the x-axis corresponds to the bridge ID found in Table 4.1.

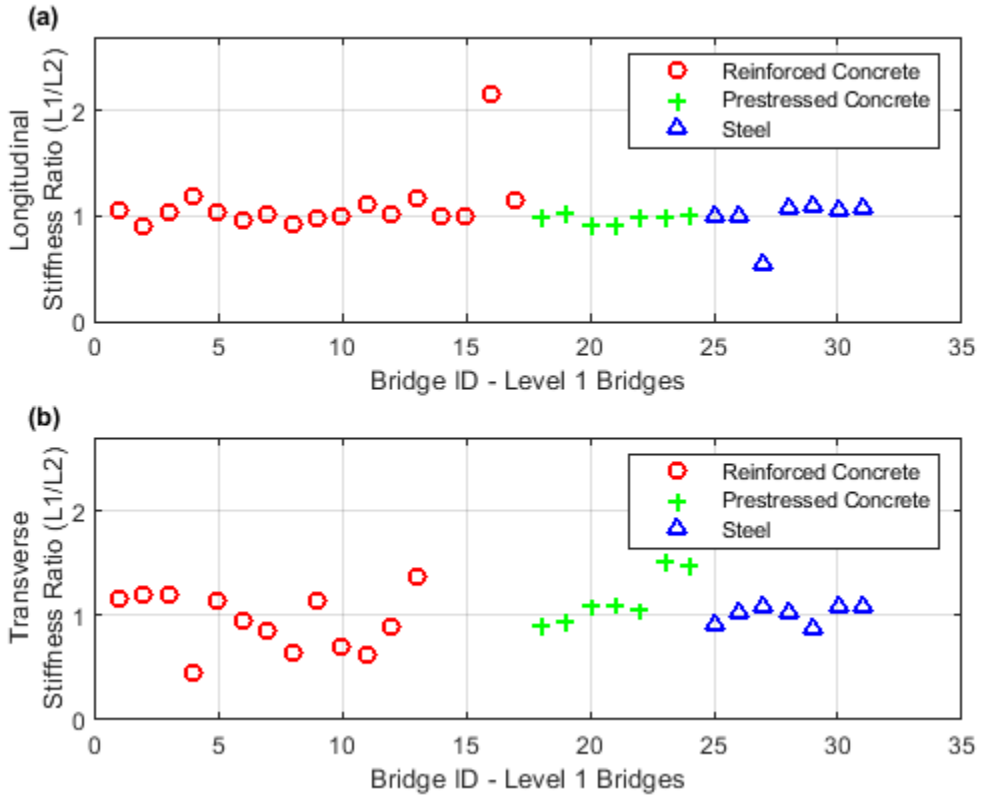

Figure 4.5. Comparison of Simplified Assessment and Detailed Assessment Stiffness in the (a) Longitudinal Direction and (b) Transverse Direction

While most of the stiffness ratios are approximately 1, there are a few outliers. In the longitudinal direction, the Level 1 stiffness for bridge 16 is approximately double the Level 2 stiffness. This outcome occurs because in that bridge one of the two intermediate piers is not stiffly connected to the deck. Therefore, the Level 1 assessment assumption that both intermediate piers add stiffness

is not suitable for this specific case. In the longitudinal direction, the Level 1 stiffness for bridge 27 is approximately half of the Level 2 longitudinal stiffness because this bridge does not follow the "one fixed bearing per bridge" assumption that is made in the simplified assessment. Each of the two intermediate piers on this bridge are connected to the superstructure with a fixed bearing, and thus, the Level 2 analysis considers the fact that both piers add stiffness. In the transverse direction, the Level 1 stiffness of bridge 4 is approximately half of the level 2 stiffness. This result is because this bridge is the only example of a four-span reinforced concrete superstructure with pile substructures in the sample set, and it does not follow the same stiffness trends those identified for three-span bridges.

4.4.3 Calculate Period

The period of the structure, which is used to determine the demand, is calculated as

$$T = 2\pi\sqrt{\frac{M}{K}}. \tag{4.25}$$

Figure 4.6 compares the actual period obtained in the detailed assessment to the estimated period from the simplified assessment. The bridge ID on the *x*-axis corresponds to the bridge ID found in Table 4.1. As in Figure 4.5 bridge IDs that do not have a period calculated are bridges that do not require a simplified assessment in that direction. From these results, the methods described above appear to provide a practical approach to estimate the period of each bridge for the superstructure and substructure combinations identified in the sample set. Recall that the sample set was carefully selected to be representative of the Indiana bridge inventory. The outliers shown in Figure 4.6 are a result of carrying forward the outlying cases described earlier for the mass and stiffness estimates.

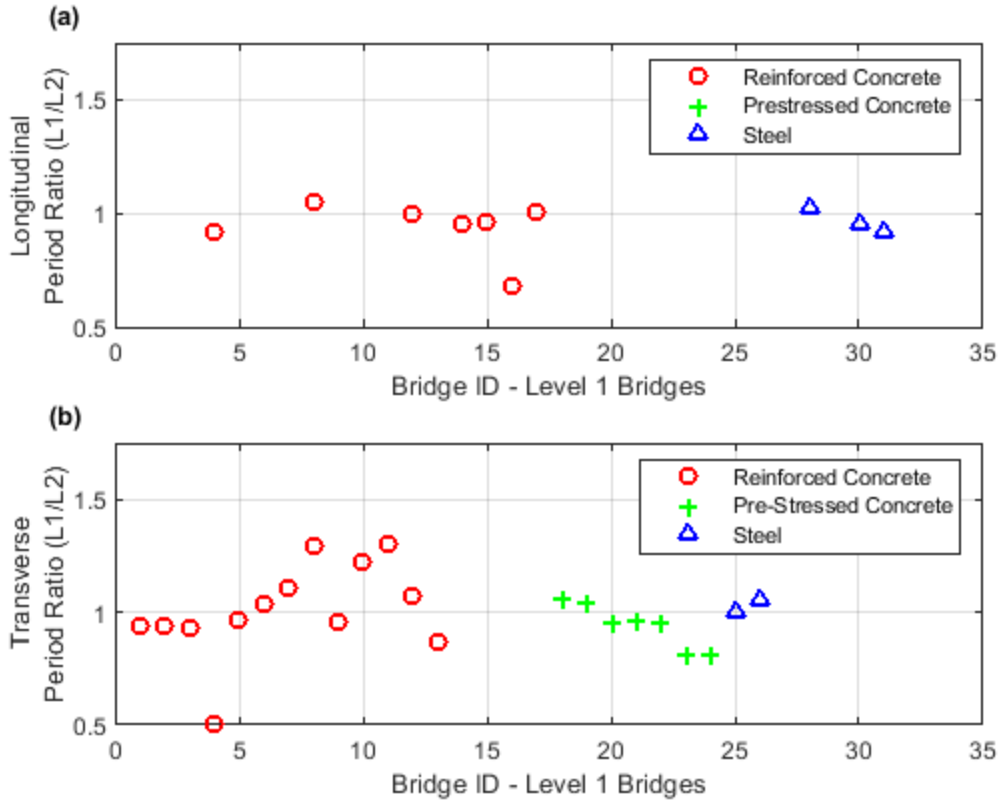

Figure 4.6. Comparison of Simplified Assessment and Detailed Assessment Period in the (a) Longitudinal Direction and (b) Transverse Direction

4.4.4 Determine Demand

Demand in the simplified assessment procedure includes both a displacement demand and a force demand. The controlling demand depends on the substructure/superstructure combination because a force capacity cannot be determined using a simplified assessment for some combinations. Because all bridges are modelled as SDOF systems in the Level 1 assessment, the spectral acceleration and displacement can easily be determined using a response spectrum. For purposes of validating the simplified assessment process, the response spectra for the 100 simulated time-histories used in the detailed assessment are used to determine the spectral acceleration. An example of the 100 acceleration response spectra, from the simulated time-histories is shown in

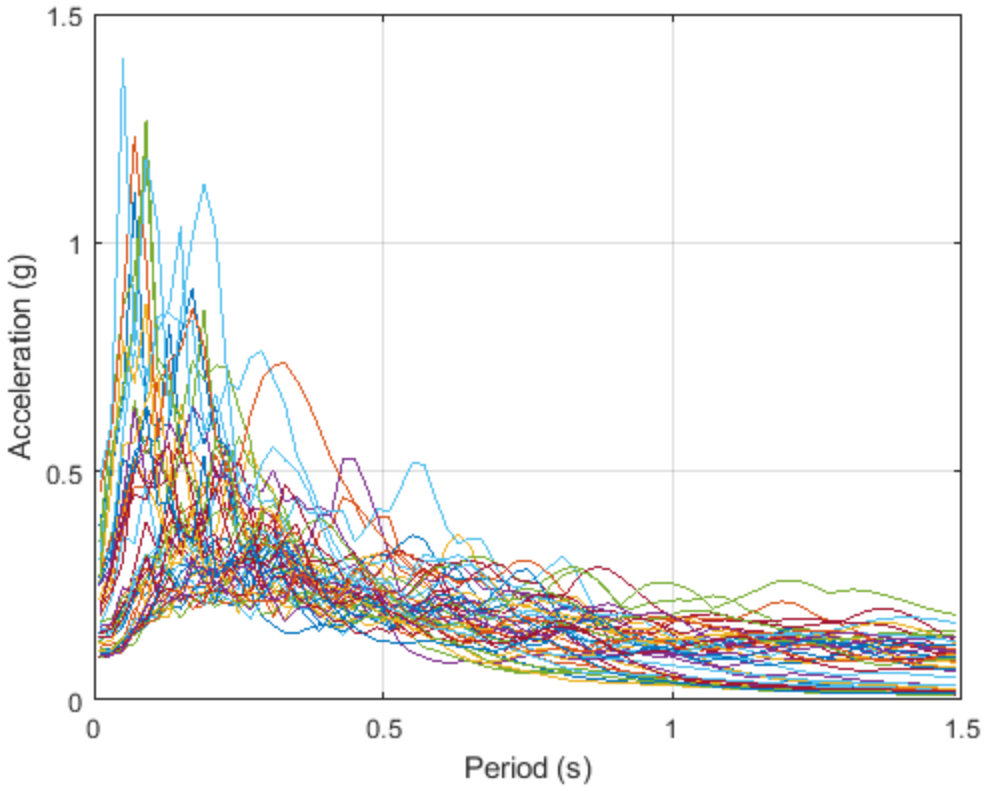

Figure 4.7. Acceleration Response Spectra for a Sample Site

Each response spectrum is used to obtain the spectral acceleration value associated with the period of the bridge, which is then used to calculate the equivalent linear spectral displacement.

$$\Delta_{lin} = \frac{SA}{(\frac{2\pi}{T})^2}. \tag{4.26}$$

This spectral displacement assumes that the substructure remains in the linear region. However, as is shown in Chapter 3, this assumption is not valid for the reinforced concrete substructures that have adequate reinforcement ratios. For these bridges, a multiplier of $\sqrt{2}$ is used to calculate an expected nonlinear displacement (Δ_{NL}) (Sozen, 2003).

$$\Delta_{NL} = \sqrt{2} * \Delta_{lin}. \tag{4.27}$$

The detailed assessment assumes that the linear force is equal to the nonlinear force which is carried to the simplified assessment. Using force-displacement relationships, the force on the bridge is calculated as

$$F_{dem} = K * \Delta_{lin}. \quad (4.28)$$

4.4.5 Determine Capacity

Table 4.3 shows the predetermined capacity thresholds for the substructure/superstructure combinations typical in Indiana. For bridges that have a displacement capacity threshold, the limits found in Table 4.3 are compared to the displacement demand, calculated using Equations 4.26 and 4.27. For bridges that have a drift capacity threshold, the limits found in Table 4.3 are directly compared to the drift demand based on the type of substructure and the direction being considered. For frame bents in the transverse direction, the drift is thus calculated as

$$drift = \frac{2 * \Delta_{NL}}{H}. \quad (4.29)$$

For bridges that require a force demand to capacity comparison, the force capacity is calculated using trends and averages seen in the detailed assessment (Beck, 2019). The force capacity is dependent on the substructure/superstructure columns. For prestressed hammerhead substructures, the force capacity in the transverse direction is calculated as

$$F_{cap} = M_{Trans} * g * \left(1.9 - 0.4 * \frac{H}{L_{ele}}\right). \quad (4.30)$$

For pile substructure types, the force capacity in the transverse direction is a base shear capacity and is calculated as

$$F_{cap} = \frac{2 * N_c * N_{pier} * M_u}{H}, \quad (4.31)$$

Where M_u is the ultimate moment for the typical piles used by INDOT. For concrete filled tubes, this moment is 63.21 *kip*ft* and for H-piles, this value is 176.18 *kip*ft*.

4.4.6 Compare Demand to Capacity Thresholds

For each bridge location and period, 100 time-histories were generated in each direction (Chapter 3.3). The demand obtained from the simplified assessment must be compared to the vulnerability thresholds to classify the vulnerability of the bridge. The vulnerability thresholds for steel, prestressed, and reinforced concrete superstructures are shown in Table 4.3.

For each of the 100 time-histories, the classification obtained with the simplified assessment is compared to that obtained with the detailed analysis to show the robustness of the simplified assessment. If the Level 1 assessment classification matches the Level 2 assessment classification, then the Level 1 assessment results are considered correct. If the Level 1 assessment classifies the bridge as having a higher level of vulnerability than the Level 2 assessment, the Level 1 assessment results overestimate the level of vulnerability of the bridge. If the Level 1 assessment classifies the bridge as having a lower level of vulnerability than the Level 2 assessment, the Level 1 assessment results underestimate the vulnerability of the bridge.

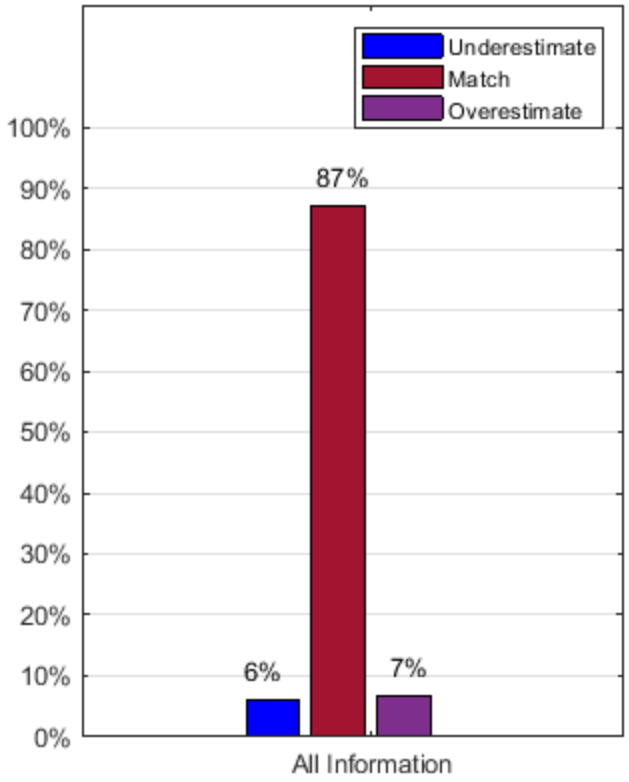

Figure 4.8. Comparison of Classification Results for a Detailed Assessment and Simplified Assessment when All Information is Known

The results for all 3,400 time-histories are shown in Figure 4.8. The results show that the simplified assessment results either matches or overestimates the vulnerability of the bridge for the majority

of bridges and time-histories. This shows that the simplified assessment, given all of the requested data items, is robust enough to assess the potential vulnerability of bridges across the state.

There are a few instances where the simplified assessment procedure underestimates the vulnerability of a given structure, even when all of the recommended information is used. This outcome occurs because some of the assumptions or estimates are violated for a small portion of the bridges.

Table 4.3. Vulnerability Thresholds by Superstructure Material

		Steel Superstructures				
		Walls		**Hammerheads**		**Frame Bents**
		Year Built < 1990	**Year Built > 1990**	**Year Built < 1990**	**Year Built > 1990**	**RC Columns**
Low Vulnerability	Longitudinal	Δ_{lin} < 0.1"	Δ_{NL} < 1"	Δ_{lin} < 0.1"	Δ_{NL} < 1"	Δ_{NL} < 1"
	Transverse					Drift < 0.5%
Moderate Vulnerability	Longitudinal		1" < Δ_{NL}< 6"		1" < Δ_{NL}< 6"	1" < Δ_{NL} < 6"
	Transverse					0.5% < Drift < 1.5%
High Vulnerability	Longitudinal	Δ_{lin} > 0.1"	Δ_{NL} > 6"	Δ_{lin}> 0.1"	Δ_{NL} > 6"	Δ_{NL} > 6"
	Transverse					Drift > 1.5%
		Prestressed Superstructures				
		Walls		**Hammerheads**		**Frame Bents**
		Year Built < 1990	**Year Built > 1990**	**Year Built < 1990**	**Year Built > 1990**	**Columns**
Low Vulnerability	Longitudinal	Δ_{lin} < 0.1"	Δ_{NL} < 1"	Δ_{lin} < 0.1"	Δ_{NL}< 1"	Δ_{NL} < 1"
	Transverse			F_{cap}> F_{dem}	F_{cap}> F_{dem}	Drift < 0.5%
Moderate Vulnerability	Longitudinal		1" < Δ_{NL}< < 6"		1" < Δ_{NL} < 6"	1" < Δ_{NL} < 6"
	Transverse			F_{cap}< F_{dem}	F_{cap}< F_{dem}	0.5% < Drift < 1.5%
High Vulnerability	Longitudinal	Δ_{lin} > 0.1"	Δ_{NL}<> 6"	Δ_{lin} > 0.2"	Δ_{NL} > 6"	Δ_{NL}> 6"
	Transverse				N/A	Drift > 1.5%
		Reinforced Concrete Superstructures				
		Walls		**Hammerheads**		**Frame Bents**
		Year Built < 1990	**Year Built > 1990**	**Year Built < 1990**	**Year Built > 1990**	**Composite Piles**
Low Vulnerability	Longitudinal	Δ_{lin} < 0.1"	Δ_{NL} < 1"	Δ_{lin} < 0.1"	Δ_{NL}< 1"	F_{cap}> F_{dem}
	Transverse					F_{cap}> F_{dem}
Moderate Vulnerability	Longitudinal		1" < Δ_{NL} < 6"		1" < Δ_{NL}< 6"	F_{cap}< F_{dem}
	Transverse					F_{cap}< F_{dem}
High Vulnerability	Longitudinal	Δ_{lin} > 0.1"	Δ_{NL}> 6"	Δ_{lin} > 0.1"	Δ_{NL} > 6"	
	Transverse					

4.5 Methods for Estimating Recommended Data Items

The calculations and results discussed above assume that all the recommended data items have been added for all of the bridges. However, there is some potential to run a Level 1 assessment without all of the recommended data items, provided that more errors can be accepted in the results. The following sections discuss each data item, the methods for estimating the values, and the impact of these estimates on the accuracy of the results.

4.5.1 Substructure Type

Substructure type is a critical data item for the simplified seismic assessment. At this time, there is no way to determine the substructure type of a bridge given only the information that is currently in BIAS. While BIAS does contain images of the substructure in the inspection reports, this information is not in a format that is currently minable. Without knowing the substructure type, there is no way to estimate the stiffness of a bridge to apply the Level 1 assessment procedure. Therefore, without the substructure type, all 31 bridges that were previously eligible for analysis with the simplified assessment methodology would require a detailed assessment.

4.5.2 Abutment Type

The abutment type is used in the simplified assessment to determine if the longitudinal direction of the bridge needs to be checked. As with the substructure type, the abutment type is not currently in BIAS and there is no way to assume the abutment type based on what is currently in BIAS. However, unlike the substructure type, if the abutment type is not given, the Level 1 assessment can still be applied to a bridge. This approach could, and will, classify more bridges as moderately or highly vulnerable, when they would accurately be classified as low vulnerability if the abutment type were available

4.5.3 Height Ratio Flag

The height ratio flag is used in the Level 1 assessment to determine which bridges the simplified assessment applies to. The height ratio is calculated as

$$H_{ratio} = \frac{H_{tall}}{H_{short}}. \quad (4.32)$$

The detailed assessment procedure would require a nonlinear pushover analysis for bridges with piers of varying heights to consider the potential for non-simultaneous nonlinear response due to structural softening. The simplified assessment procedure is unable to capture this response.

This idea is shown using a representative hypothetical three-span bridge model with two piers of varying heights. As the structure is exposed to ground motions, the shorter, stiffer pier will initially take the most force, causing it to yield first. At this point, it will start to soften and redistribute the force to the adjacent pier, which has yet to yield. The simplified assessment procedure is incapable of capturing this region of non-simultaneous yielding. The hypothetical model, with height ratios ranging from 1 to 1.2, was passed through a nonlinear pushover analysis to determine the height ratio that corresponds to this region. The results for a height ratio of 1.15 are shown in Figure 4.9. The green box shows the region where non-simultaneous yielding occurs.

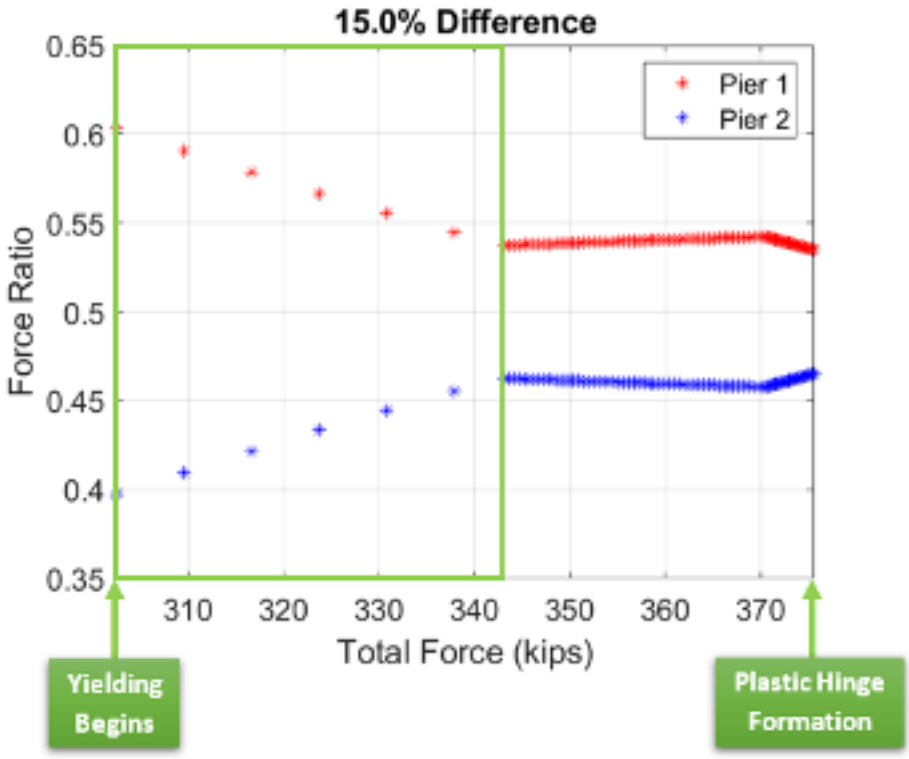

Figure 4.9. Nonlinear Pushover Analysis of Adjacent Piers with a Height Ratio of 1.15

Table 4.4 shows the percentage of the bridge responses to all 100 ground motions which land in the region of non-simultaneous yielding as a function of the height ratio and resulting stiffness ratio of the two piers. It is clear that once the height ratio exceeds 1.10, the percent of responses that land in the non-simultaneous yielding region increases substantially. This analysis is further confirmed after a review of California Department of Transportation (CalTrans) Seismic Design Criteria (CalTrans, 2019) which calls for a balanced stiffness for adjacent frames to be between 0.75 and 1.33.

Table 4.4. Results of the Nonlinear Pushover Analysis for Varying Pier Heights

Height Ratio (H2/H1)	**EQ in Green Zone**	**Stiffness Ratio (H2/H1)**
1	0	1
1.025	0	0.93
1.05	0	0.86
1.075	2	0.81
1.1	1	0.75
1.125	6	0.70
1.15	6	0.65
1.175	6	0.62
1.2	7	0.58

Because the simplified assessment procedure only considers a single height (the maximum dynamic height of all of the piers), bridges with piers of varying heights must be excluded from the simplified assessment. From BIAS, there is no way to estimate whether or not piers have a height ratio greater than 1.1 with current data items. Not having this information does not prohibit the use of the simplified assessment, but the likelihood for unfavorable misclassification (e.g. underestimating the vulnerability) is increased considerably.

4.5.4 Element Height

While the actual dynamic height of the substructure is important for the accuracy of a Level 1 assessment, there are a few data items currently stored in BIAS that can be used to estimate the relevant height. For bridges over roadways or railroads, the minimum vertical under clearance (NBI Data Item 054B) gives the minimum clear height from the road or railroad to the bottom of

the beam. For bridges over waterways, there are no minable data items currently in BIAS. However, the scour channel profile is recorded during inspections. This value includes the depth to the top and the bottom of fixed items, like piers, in the channel. If these data were to be made minable, they could be used to estimate the height of bridges over waterways. Figure 4.10 shows the comparison of the dynamic height determined from the bridge drawings and the height determined using the minimum vertical under clearance or the scour channel profile. The bridge ID on the x-axis corresponds to the bridge ID found in Table 4.1. The height from the scour channel profile was manually obtained to show the effects of using this data. If there is no scour channel profile or minimum vertical under clearance in BIAS, the height is zero and no simplified assessment can be performed on those bridges. Figure 4.10 shows that these approaches for estimating the dynamic height result in significant variability, suggesting the importance of adding the dynamic height of the structure as a data item in BIAS.

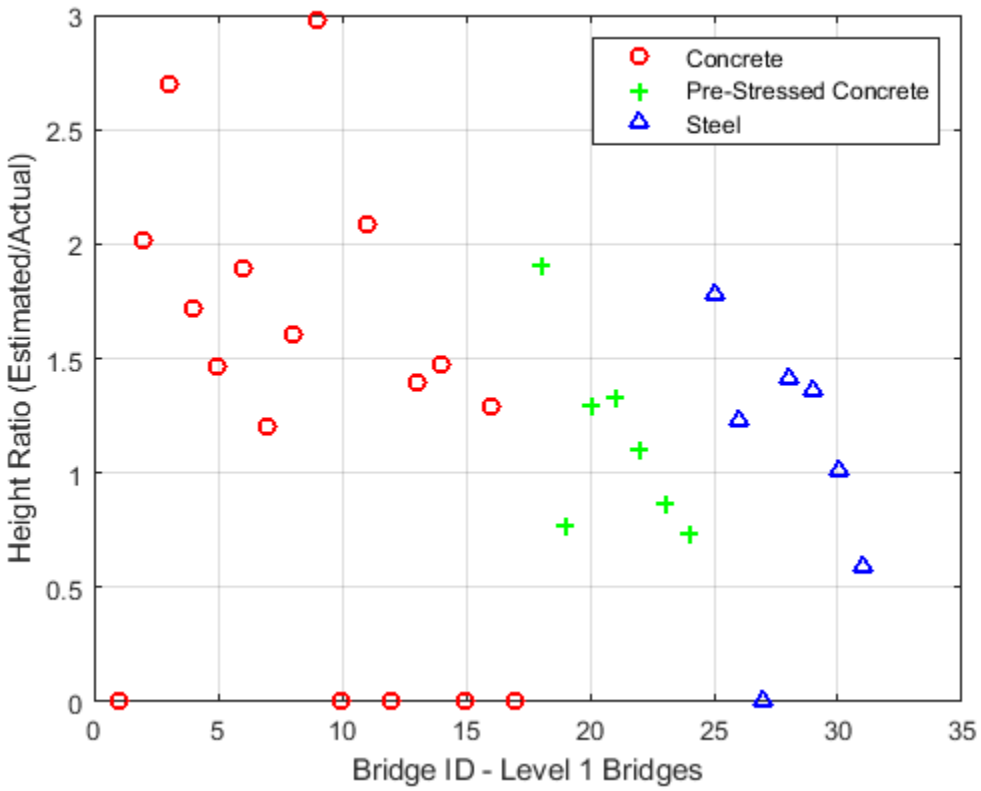

Figure 4.10. Comparison of Estimated Height and Actual Dynamic Height

Figure 4.11 shows the new comparison between the Level 2 analysis and the Level 1 analysis when the element height is not given, for all 3,400 ground motions. It is important to note that six bridges

did not have a value for the minimum vertical under clearance and did not have any information in the scour channel profile. These gaps in the data items result in 21% of results classified as "No Data". Without adding the dynamic height, a simplified assessment is not possible on these six bridges.

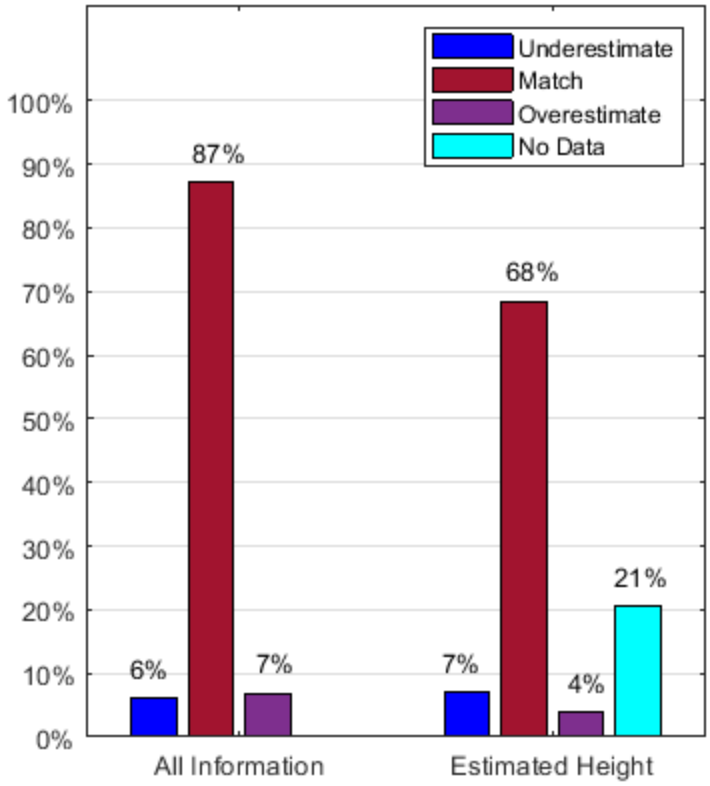

Figure 4.11. Comparison of Detailed and Simplified Classification using a Height Estimate

Comparing the "All Information" results with the "Estimated Height" results in Figure 11, the total percent of matching results between the Level 2 assessment and the Level 1 assessment decreases considerably when the height is estimated. It also shows a decrease in the number of bridges for which a simplified assessment applies due to a lack of consistent data in BIAS. This outcome shows the importance of including an accurate element height to perform the simplified assessment.

4.5.5 Number of Elements in the Substructure

The number of elements in the substructure refers to the number of columns in a single pier. For walls and hammerhead substructures, this value is one. For frame bent substructures the number of elements in the substructure is critical for the stiffness calculations. Without this information, a simplified assessment for frame bent substructures is not possible. Figure 4.12 relates the number of columns to the tributary area that a given pier supports for our sample set of bridges. It is clear that there is no definitive correlation between the number of columns in a pier and the tributary area supported by the pier. Therefore, the number of elements in the substructure is a critical data item. Without it, the simplified assessment cannot be applied to frame bent substructures with any confidence.

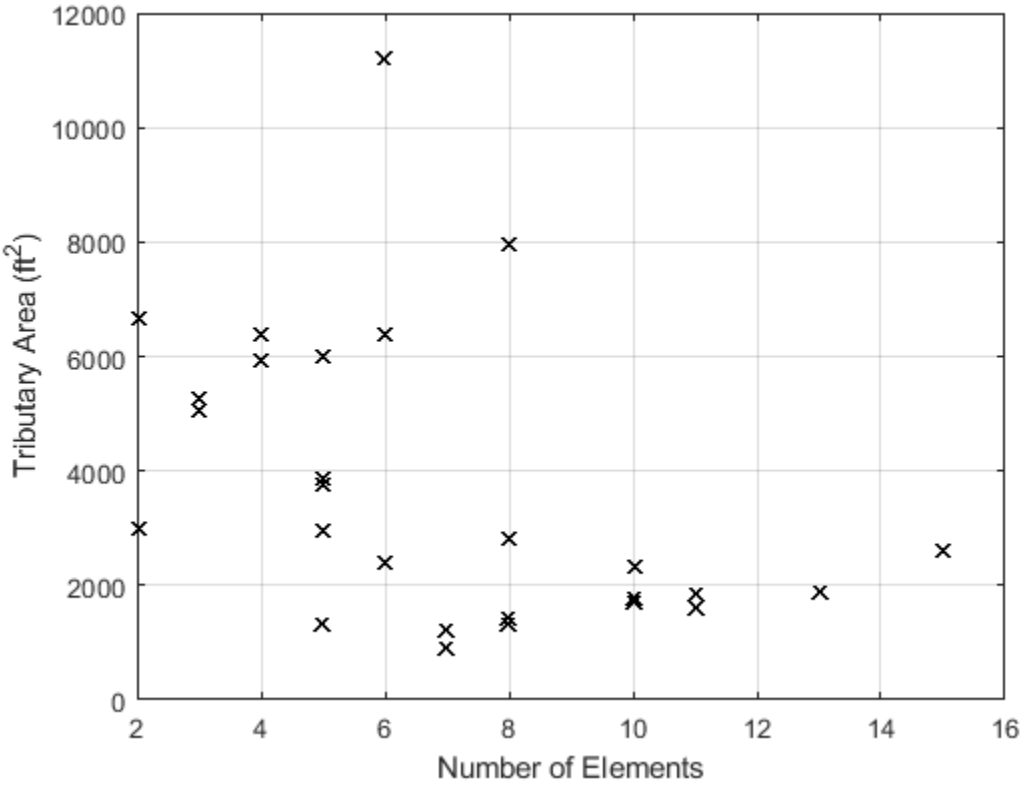

Figure 4.12. Tributary Area vs. Number of Elements for All Frame Bents in Sample Set

4.5.6 Element Length

Element length is defined as the dimension in the transverse direction of one substructure element. For walls and hammerheads, this value corresponds to the long dimension of the substructure at

the base and for frame bents, this value corresponds to the dimension in the transverse direction of a single column. This data item can be roughly estimated using information that is currently available in BIAS along with the critical information discussed in the sections above. However, estimating this data item will decrease the confidence in the Level 1 assessment results, as shown in Figure 4.13. The following three sections describe how the element length can be estimated for walls, hammerheads and frame bents.

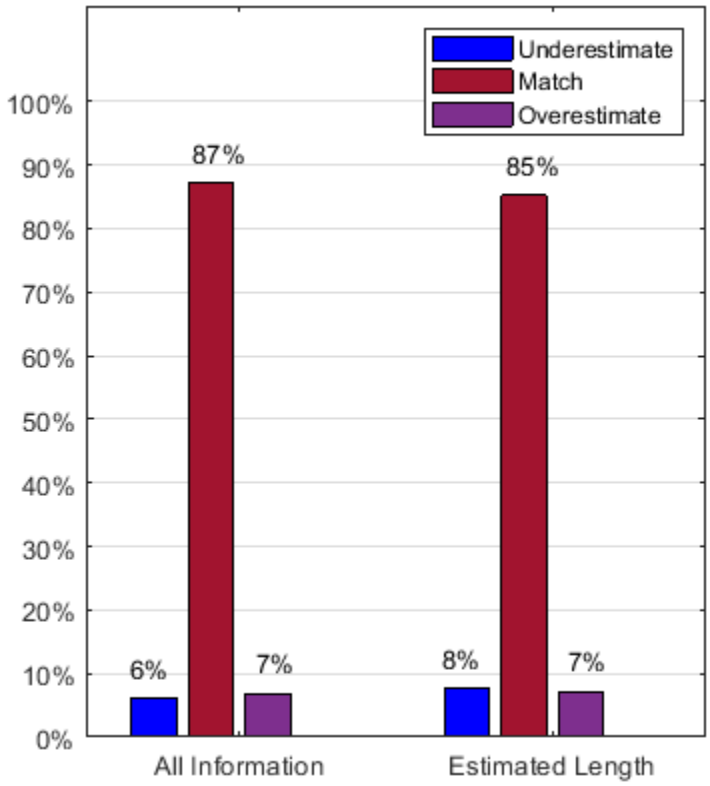

Figure 4.13. Comparison of Classification Results for the Detailed and Simplified Assessment using a Length Estimate

Walls

BIAS currently contains information on the deck out-to-out width and the skew of the bridge. Some bridges in the inventory maintain a skew of 99 which indicates a major variation in skews of substructure units (NBI Coding Guide, 1995). Therefore, if the skew is listed as 99 for a given bridge, the simplified assessment is not applicable to the bridge and a detailed assessment is required. For bridges with a skew less than 90-degrees, the length of the pier is estimated as

$$L_{ele} = \frac{w_{deck}}{\cos(skew)}. \quad (4.33)$$

Figure 4.14 shows the ratio of the estimated length to the actual length for all the wall substructures in the original sample set of 100-bridges. The bridge ID on the x-axis does not correspond to the bridge ID in Table 4.1.

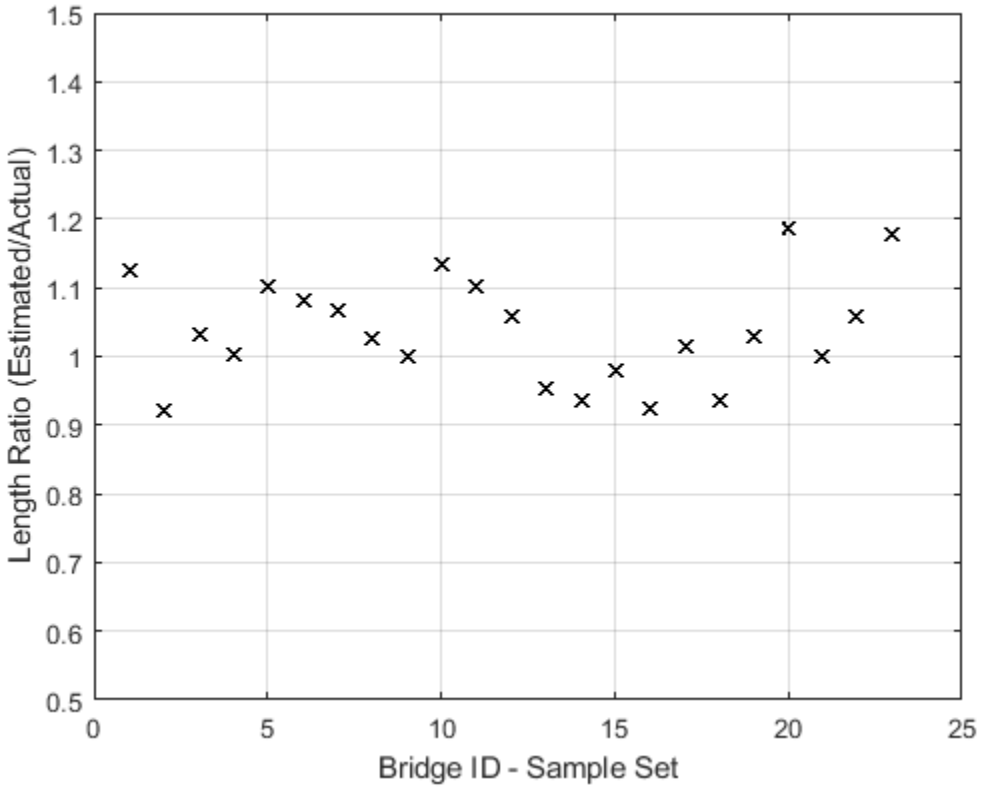

Figure 4.14. Comparison of Estimated Length to Actual Length for all Walls in the Sample Set

Hammerheads

Hammerheads are very similar to walls except for the narrowing of the cross-section in the stem. Thus, the dimension at the base of the hammerhead is the value used in all the calculations. The dimension at the top of the hammerhead can be estimated using Equation 4.33. Additionally, a ratio between the stem length and the length at the top of the sample can be calculated. Only one reinforced-concrete superstructure bridge is supported by a hammerhead substructure in the sample set. It is difficult to identify trends for the ratio depicted in Figure 15 for this class of bridges, thus if the stem length is unknown, they are excluded from the simplified assessment. For prestressed concrete and steel superstructures, Figure 15 shows the ratio of the length at the base

to the length at the top. *The bridge ID on the x-axis does not correspond to the bridge ID in Table 4.1.*

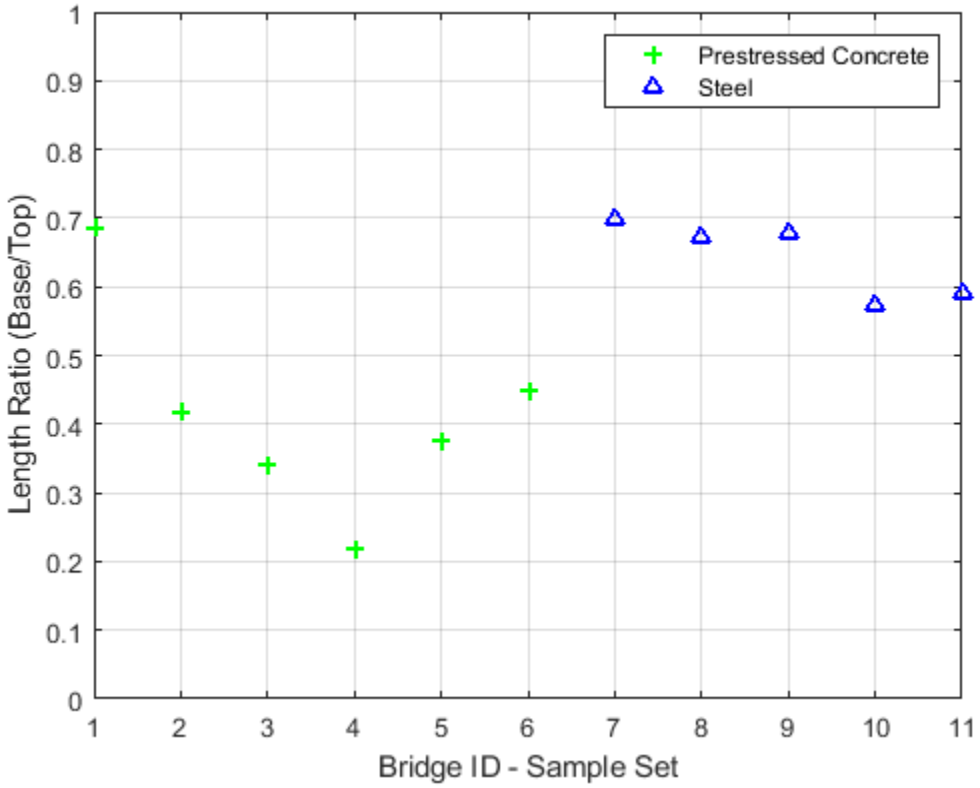

Figure 4.15. Base Length to Top Length Comparison for All Steel and Prestressed Hammerhead Bridges in the Sample Set

The average ratio for steel superstructures is 0.64 with a standard deviation of 0.05. The average ratio for prestressed superstructures is 0.36 with a standard deviation of 0.15. Due to the small number of samples and the large spread in the results, the average ratio minus one standard deviation is conservatively used to estimate the length at the base of the hammerhead pier (F_{Length}). Underestimating the length leads to an underestimate in the stiffness and an overestimate in the period, which will give results that slightly overestimate the vulnerability. An overestimate in the vulnerability is more desirable than an underestimate in the vulnerability. The length at the base of hammerhead piers is calculated as

$$L_{ele} = F_{Length} \frac{w_{deck}}{\cos(skew)}. \quad (4.34)$$

Figure 4.16 shows the ratio of the estimated length to the actual length at the base of the hammerhead substructures in the sample set. However, there is error due to the large standard deviation in the prestressed sample set. This outcome shows that while the length of the hammerhead piers can be estimated, the estimate will considerably affect the confidence in the Level 1 assessment results.

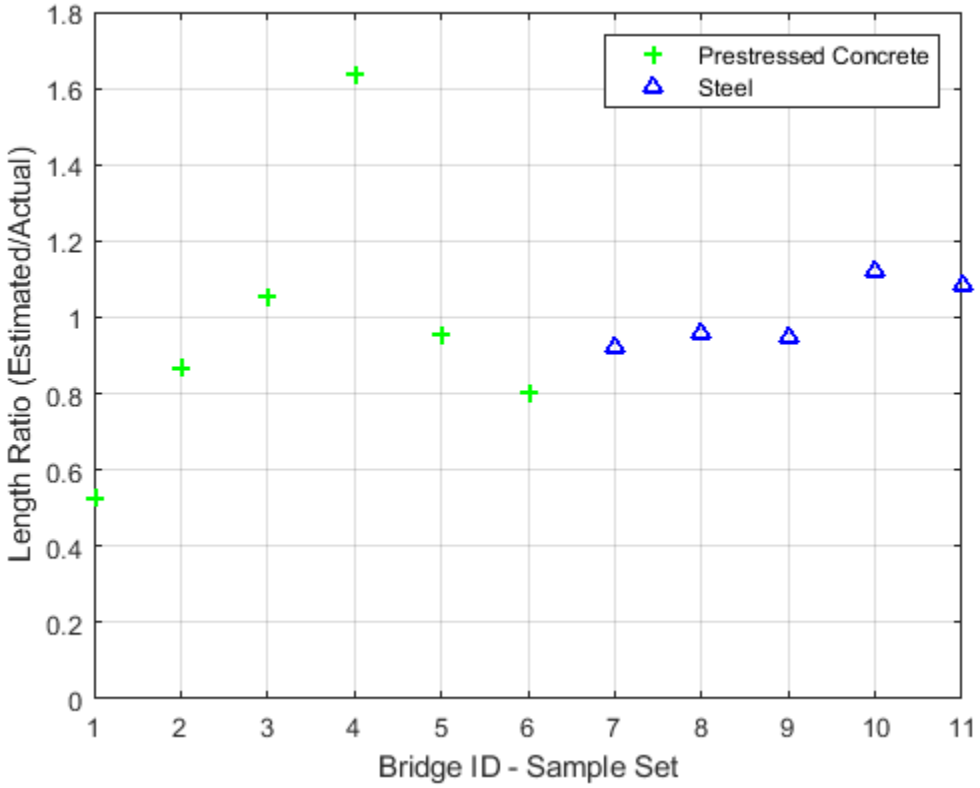

Figure 4.16. Comparison of Estimated Length to Actual Length at the Base of Steel and Prestressed Hammerheads in the Sample Set

Frame Bents

Estimating the length of multiple elements (columns) for frame bents is more difficult than estimating the length of a single element for walls and hammerheads. Given the number of elements in a pier, the deck out-to-out, and the skew, as with hammerhead substructures the total length of all columns at the base of the pier is calculated as a ratio of the total substructure out-to-out. For frame bents, this ratio (F_{Length}) is calculated as

$$F_{Length} = \frac{N_c * L_{ele,act}}{L_{pier}}, \tag{4.35}$$

where $L_{ele,act}$is the actual length of the element and L_{pier} is the length of the pier calculated using Equation 4.33. This ratio for each frame bent in the sample set is shown in Figure 4.17. The bridge ID on the x-axis does not correspond to the bridge ID in Table 4.1.

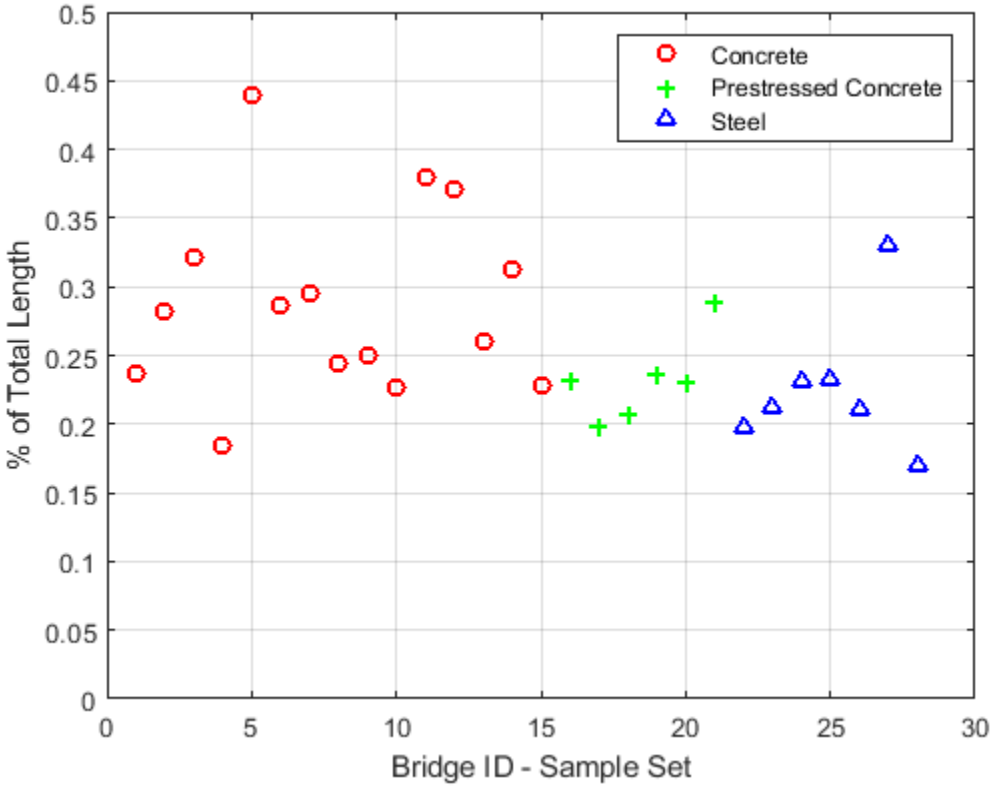

Figure 4.17. Percent of Total Length of Frame that is the Length of Elements

The values are primarily concentrated around an average value of 0.26. The standard deviation of F_{Length} for this sample set is 0.06. The average minus a standard deviation (0.2) is again used to estimate the ratio in the simplified assessment if the length is not given. This approach aims to account for the variability in the results. The ratio of the estimated length to the actual length of the element is shown in Figure 4.18.

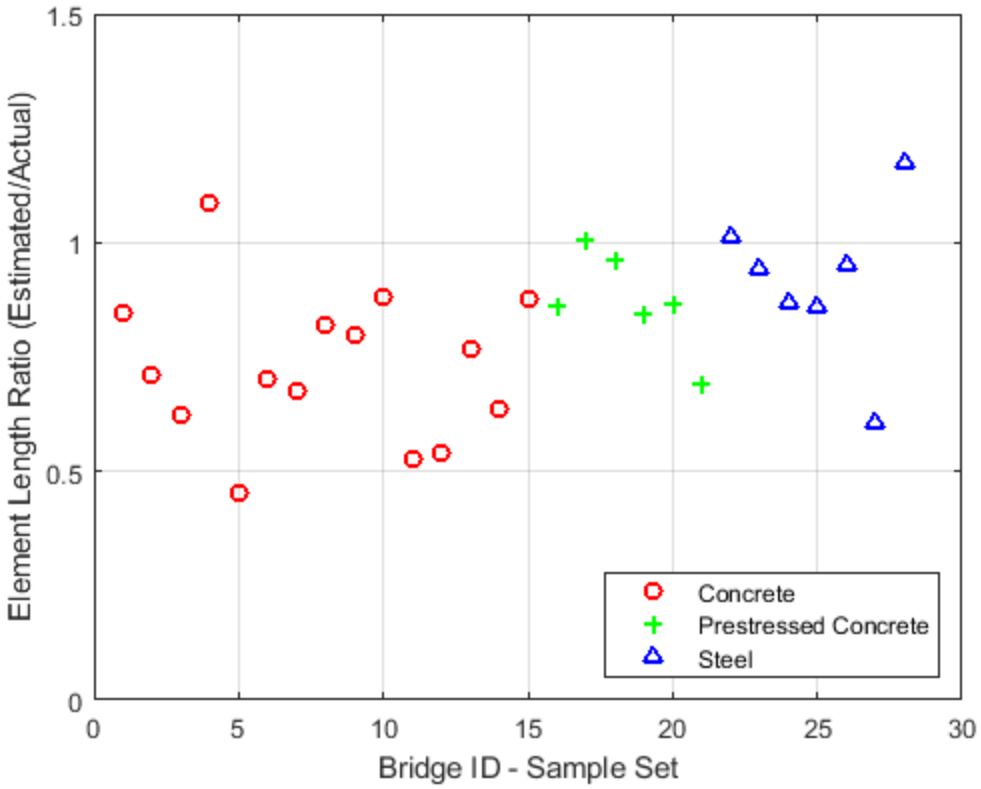

Figure 4.18. Ratio of Estimated Length of a Column to the Actual Length for All Frame Bents in the Sample Set

4.5.7 Element Width

Element width is defined as the dimension in the longitudinal direction of one substructure element. As with element length, this dimension can be approximated using an average of the values seen in the detailed assessment. If the substructure has circular elements, the element length is also the element width. For all other substructures, a width of two-feet is used as a lower-bound estimate for the width. Figure 4.19 shows the distribution of width of the non-circular substructures for all bridges in the sample set. A lower-bound estimate is used because it leads to an underestimate in the stiffness which corresponds to an overestimate in the vulnerability of the bridges. The comparison between the vulnerability classifications obtained from the Level 2 and the Level 1 assessments, when estimating the width of the elements, is shown in Figure 4.20. Note that estimating this parameter does not have a significant influence on the classification results.

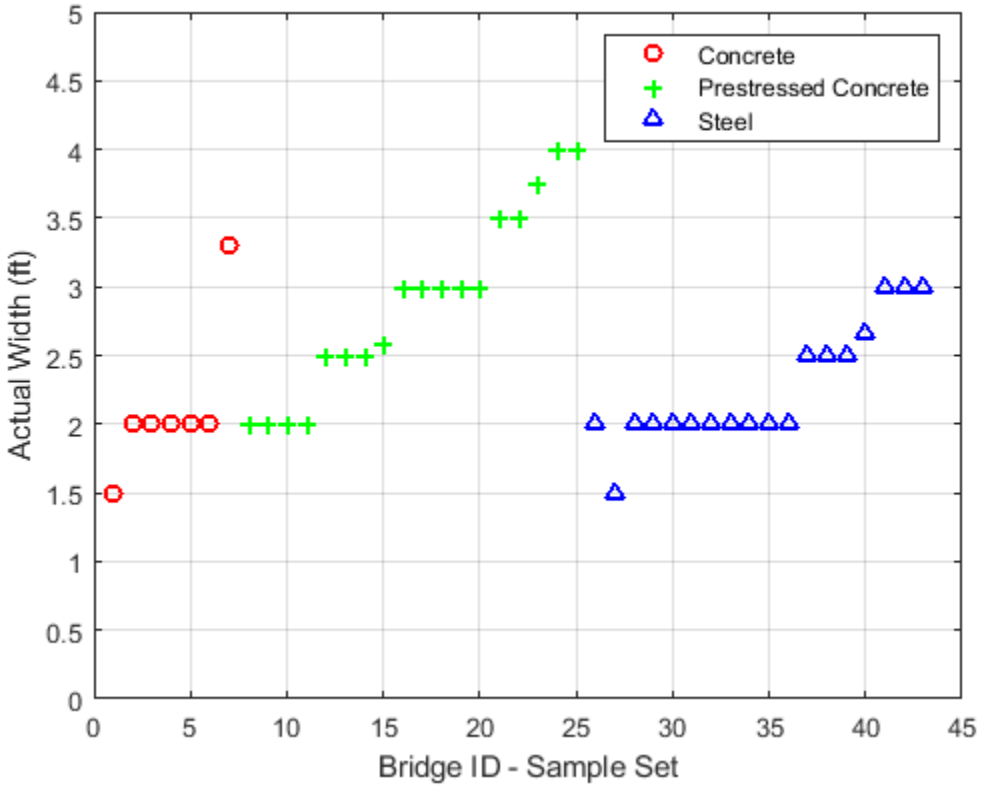

Figure 4.19. Width of Non-Circular Substructure Elements in Entire Sample Set

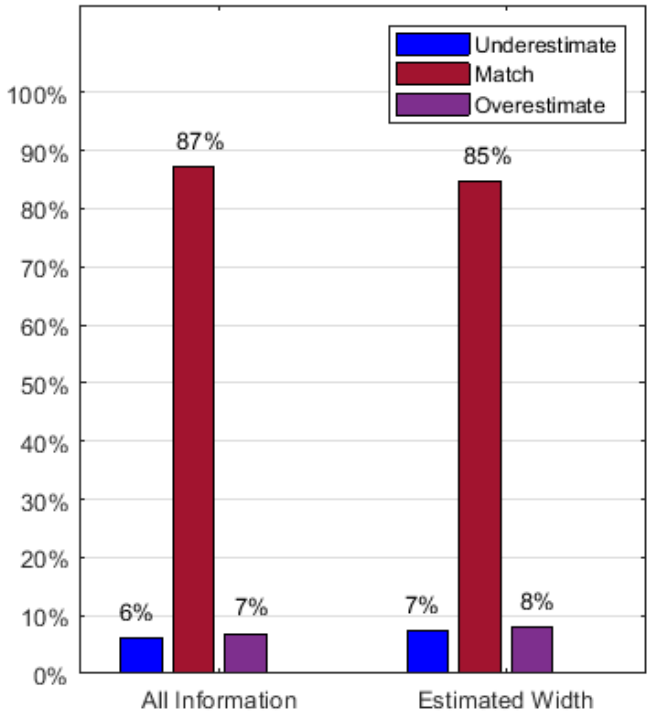

Figure 4.20. Comparison of Detailed and Simplified Assessment Classification using a Width Estimate

4.5.8 Deck Thickness

Knowing the thickness of the deck is important for the mass and stiffness calculations for reinforced concrete superstructures. For prestressed and steel superstructures, an average deck thickness of 8 inches is typical and is assumed in all Level 1 assessment calculations.

For reinforced concrete bridges, the thickness of the deck is needed for both mass and the stiffness calculations. As shown in Figure 4.21, there is a large spread in the thickness of the deck for reinforced concrete slab deck bridges, which supports the need to know the actual deck thickness.

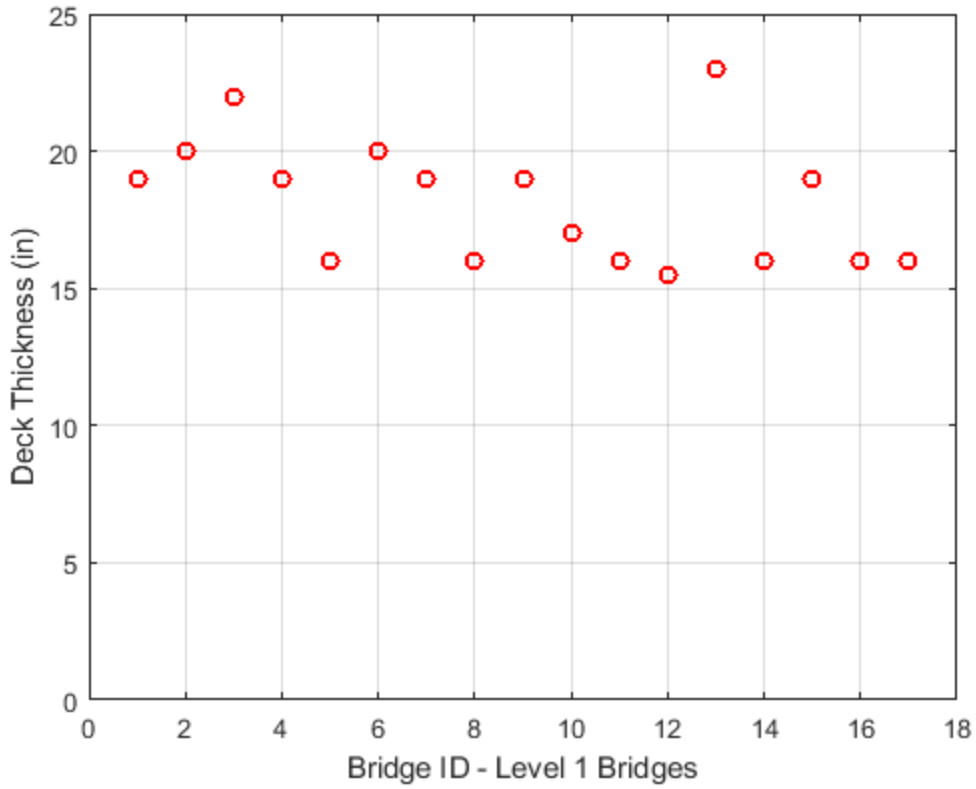

Figure 4.21. Reinforced Concrete Slab Deck Superstructure Deck Thickness Spread of Entire Sample Set

However, if the deck thickness is not given, it is assumed to be the average from the sample, 18.6-*inches*. Figure 4.22 and Figure 4.23 show the ratio of the calculated mass and stiffness using the estimated deck thickness to the calculated mass and stiffness using the actual deck thickness. The results for the stiffness results in the longitudinal direction, shown in Figure 4.23 (a), is one because deck thickness does not have an impact on the stiffness calculations in the longitudinal direction. The bridge number on the x-axis corresponds to the bridge ID number in Table 4.1.

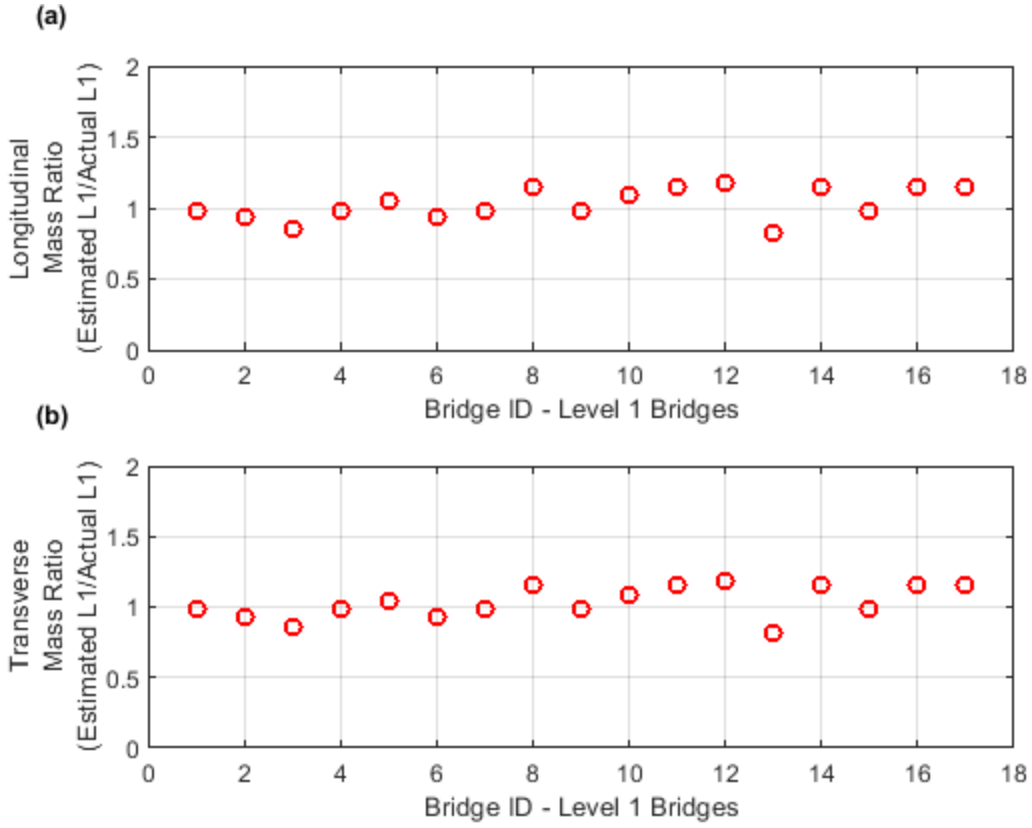

Figure 4.22. Mass Ratios (Estimated/Actual) Using an Estimated Deck Thickness for RC Slab Deck Bridges in the (a) Longitudinal Direction and (b) Transverse Direction

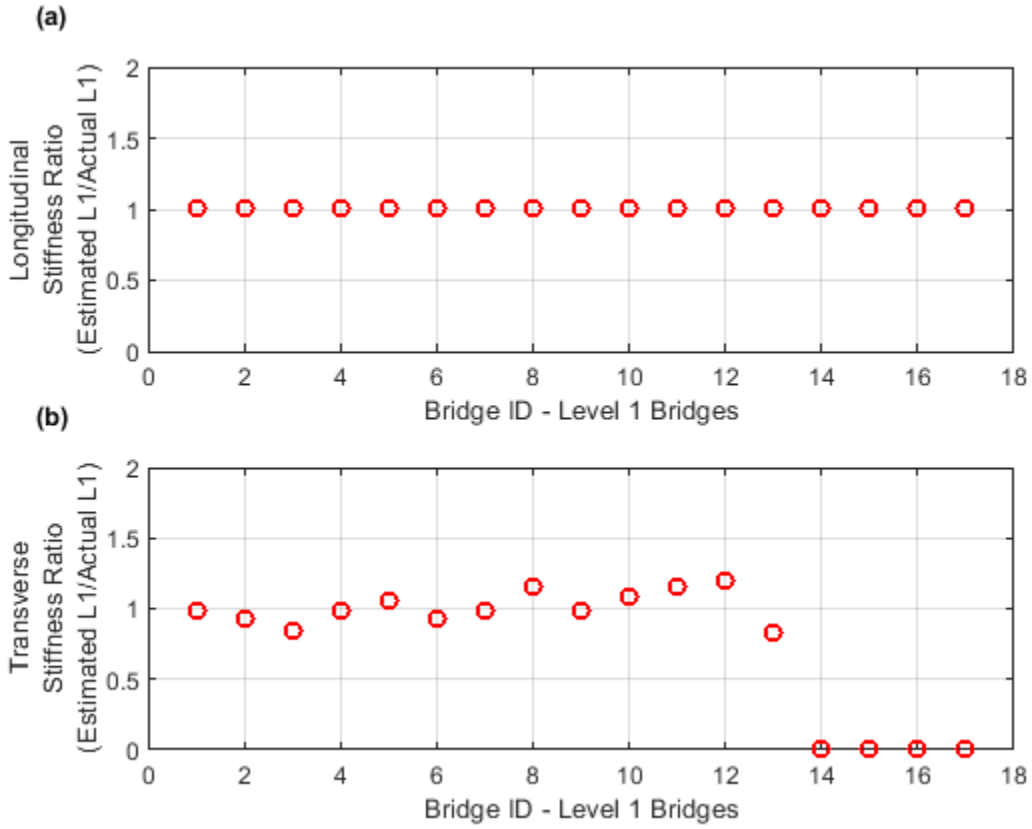

Figure 4.23. Stiffness Ratios (Estimated/Actual) Using an Estimated Deck Thickness for RC Slab Deck Bridges in the (a) Longitudinal Direction and (b) Transverse Direction

The results obtained using the average compared to those obtained using the actual deck thickness are shown in Figure 4.24. For reinforced concrete slab deck bridges, using the average deck thickness for our sample set of bridges does not change the comparison of the Level 1 and Level 2 vulnerability classifications. However, as shown in Figure 4.22 and Figure 4.23, the mass and stiffness values are impacted and these inaccuracies will potentially affect the vulnerability classification for other bridges, even though it did not for the bridges in our sample set.

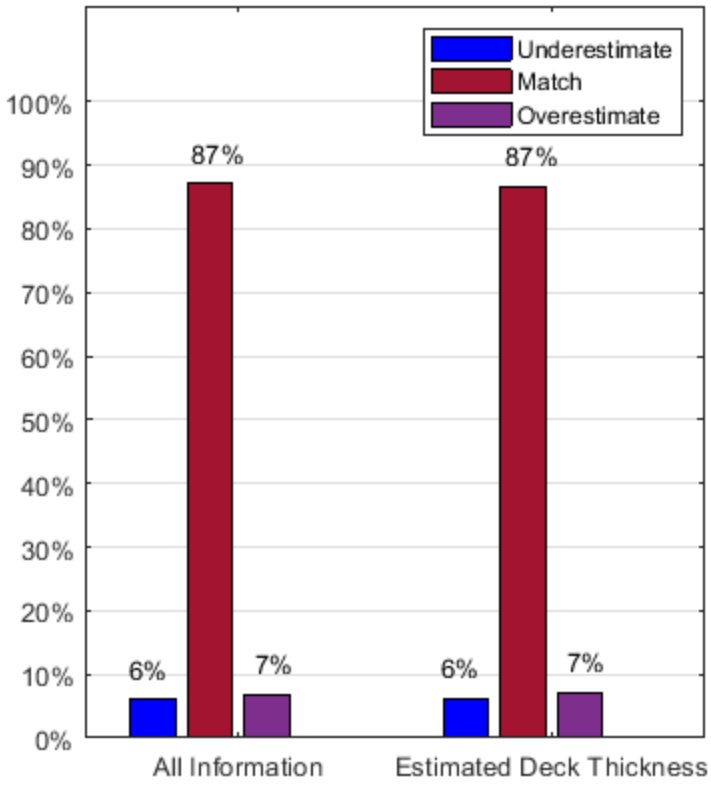

Figure 4.24. Comparison of Detailed and Simplified Classification using a Deck Thickness Estimate

4.6 Conclusion

The methodology and the results presented in this chapter show the importance of adding the requested information to BIAS. The conclusions that can be made based on this chapter are as follows:

- The simplified assessment is not applicable to all bridges. There are certain bridge details and types that automatically prohibit the use of the simplified assessment procedure, even if all the recommended information is provided. They are:
    - Bridges with expansion joints
    - Bridges whose superstructure combination is not reinforced concrete slab deck bridges, steel girder bridges, or prestressed beam or girders (both box and tee)
    - Bridges with a substructure type classified as “other”

    - Frame bents with an aspect ratio less than three
- The critical information that is needed in BIAS to run the simplified assessment is:
    - Substructure Type
    - Number of Elements
    - Element Height
    - Deck Thickness
    - Element Length
    - Element Width
    - Height Ratio Flag
    - Abutment Type
- All of the additional information we are recommending be added is critical. However, it is possible to estimate some of the information needed based on the data items that are already available in BIAS. The information that has the potential to be estimated or assumed is:
    - Element Height
    - Element Length
    - Element Width
    - Deck Thickness
- If all the recommended information is not added, more bridges will require a detailed analysis and the accuracy of the vulnerability classifications from the simplified assessments will decrease.

4.7 Summary

In this chapter, the critical additional information needed to perform the simplified assessment is introduced and the procedure to perform the simplified assessment using all of the information, is described. The importance of each additional data item is discussed, and if there is a way to estimate the value of the data item based on information that is currently available in BIAS, a method for estimating is proposed. The impact of that estimate on the vulnerability classification is evaluated through a comparison of the classification results obtained with the simplified assessment and the detailed assessment. The procedure developed in this chapter as well as the methods for estimating certain data items is implemented in the simplified assessment tool presented in the following chapter.

5. IMPLEMENTATION OF SIMPLIFIED ASSESSMENT PROCEDURE IN THE INDIANA SEISMIC ASSESSMENT TOOL (INSAT)

5.1 Introduction

The Indiana Seismic Assessment Tool (INSAT) was developed to conduct a simplified seismic assessment on INDOT's entire bridge inventory using information found in their online asset management system BIAS. Currently, BIAS does not contain enough information for the simplified seismic assessment to be applicable. However, with the addition of a few specific data items, a robust simplified seismic assessment can be performed. The recommended data items are: substructure type, the abutment type, the number of elements in the substructure (meaning the number of columns in frame bent-type substructures), the clear height of the substructure, the cross-sectional dimensions of the main substructure unit, the thickness of the deck, and a pier height ratio flag. These data items, their importance, and the effects of not having them, are discussed in Chapter 4. This chapter describes the application of the simplified assessment procedure to the sample set of 100 representative bridges using an excel macro enabled file.

5.2 Tool Built-in Information

INSAT contains six static sheets, each of which contain information needed to perform the assessment. These six sheets are locked to ensure the integrity of the data and the tool as a whole. Described in detail below is a description of each sheet, its usage, and what data would be required to update that sheet.

5.2.1 "Instructions" Sheet

The instructions sheet is the main sheet contained in the tool. This sheet contains instructions for running the tool as well as the button for running assessment.

5.2.2 "General Information" Sheet

The general information sheet contains general information about the tool and the main assumptions made. It discusses the data requirements and the format for the input files.

5.2.3 "Routes" Sheet

The routes sheet contains two columns. The first column is a list of all the roads in Indiana, shown in Table 5.2. This list is used if the user selects to run a specific road. The second column is a list of the critical routes, as defined by the INDOT Primary Disaster Routes Map (INDOT, 2012). If the primary critical routes are updated, this column should be updated to reflect the changes. The list of identified critical routes can be found in Table 5.1.

Table 5.1. List of Critical Routes as Defined by the INDOT Primary Disaster Routes Map

I-265	SR 154	SR 46	US 30
I-465	SR 161	SR 54	US 31
I-469	SR 164	SR 56	US 33
I-64	SR 18	SR 57	US 35
I-65	SR 22	SR 60	US 36
I-69	SR 237	SR 62	US 41
I-70	SR 26	SR 65	US 421
I-74	SR 28	SR 66	US 50
I-865	SR 32	US 20	US 6
I-90	SR 37	US 231	SR 2
I-94	SR 43	US 24	SR 3
SR 135	SR 44	US 27	SR 15

Table 5.2. List of Routes in Indiana

US 6	SR 68	SR 446	SR 264	SR 201	SR 129
US 52	SR 67	SR 441	SR 263	SR 2	SR 128
US 50	SR 662	SR 44	SR 262	SR 19	SR 127
US 421	SR 66	SR 431	SR 261	SR 18	SR 124
US 41	SR 650	SR 43	SR 26	SR 17	SR 121
US 40	SR 65	SR 427	SR 258	SR 168	SR 120
US 36	SR 645	SR 42	SR 257	SR 167	SR 119
US 35	SR 641	SR 4	SR 256	SR 166	SR 117
US 33	SR 64	SR 39	SR 252	SR 165	SR 116
US 31	SR 63	SR 38	SR 250	SR 164	SR 115
US 30	SR 62	SR 37	SR 25	SR 163	SR 114
US 27	SR 61	SR 364	SR 249	SR 162	SR 111
US 24	SR 60	SR 362	SR 246	SR 161	SR 110
US 231	SR 59	SR 358	SR 245	SR 160	SR 11
US 224	SR 58	SR 357	SR 244	SR 16	SR 109
US 20	SR 57	SR 356	SR 243	SR 159	SR 106
US 150	SR 56	SR 352	SR 241	SR 158	SR 105
US 136	SR 558	SR 350	SR 240	SR 157	SR 104
US 131	SR 550	SR 341	SR 237	SR 156	SR 103
US 12	SR 55	SR 340	SR 236	SR 154	SR 101
T-90	SR 545	SR 337	SR 235	SR 152	SR 10
T-80	SR 54	SR 335	SR 234	SR 15	SR 1
SR 933	SR 53	SR 332	SR 232	SR 149	I-94
SR 931	SR 524	SR 331	SR 23	SR 148	I-865
SR 930	SR 520	SR 327	SR 229	SR 145	I-80
SR 912	SR 51	SR 32	SR 227	SR 144	I-74
SR 9	SR 5	SR 312	SR 225	SR 143	I-70
SR 827	SR 49	SR 301	SR 22	SR 142	I-69
SR 8	SR 48	SR 3	SR 218	SR 140	I-65
SR 75	SR 47	SR 29	SR 213	SR 14	I-64
SR 727	SR 462	SR 28	SR 212	SR 135	I-469
SR 71	SR 46	SR 269	SR 211	SR 134	I-465
SR 70	SR 458	SR 267	SR 205	SR 130	I-275
SR 7	SR 450	SR 265	SR 203	SR 13	I-265
SR 69	SR 45	SR 265			

5.2.4 "Site Class" Sheet

This sheet contains the predetermined site class for all 5,902 state-owned bridges, at the time of writing. The site class was determined using the metadata from Indiana Geological Survey's 2011 Seismic Shaking Materials Response Map and the latitude and longitude coordinates of each structure. The first column contains the NBI number for the bridge, the second column contains a number corresponding to the site classification from the map and the third column contains the NHERP site class classification from the map. Table 5.3 shows the site class number and the corresponding site class classification. If additional bridges are added to BIAS, their site class and corresponding site class number should be included on this sheet.

Table 5.3. Site Class Classification and Corresponding Number

Site Class Classification	Site Class Number
--	0
B	1
C	2
C through D	3
D	4
D or F	5
D through E	6
D through F	7

5.2.5 "UHS Information" Sheet

INSAT uses predetermined Uniform Hazard Spectra (UHS) data for a return period of 1000 years from USGS's nshmp-haz platform (nshmp-haz, n.d.). The automated retrieval of the UHS data is not compatible with the tool, so the data must be predetermined based on the latitude and longitude data and be included in this sheet. Using the methodology found in Appendix C, one can change the return period and/or retrieve the data for additional bridges. The "UHS Information" sheet contains two rows of headings and eight columns. The first column contains the NBI number for each structure in INDOT's bridge inventory at the development of INSAT. The other seven

columns contain the acceleration data, in terms of *g*, for seven spectral periods, ranging from 0.0s to 2.0s.

5.2.6 "Site Factors" Sheet

The program provided by the USGS and used to generate the UHS data for the bridges in the state was only compatible for accessing data corresponding to a site class B/C boundary (nshmp-haz, n.d.). Because of this, AASHTO site factors (2017) are used, found in section 3.10.3.2, to amplify/de-amplify the acceleration to account for the soil conditions at the site. This sheet contains these tables, converted for a reference site class of B/C.

5.3 Simplified Assessment Application in the Tool

INSAT is used to classify the vulnerability of the bridges in Indiana using the information and trends discussed previously. The assessment procedure built into INSAT is shown in Figure 5.1. The tool requires user inputs, shown in purple, bridge information from INDOT, shown in grey, and performs various levels of assessments and calculations using built-in macros, shown in green, and outputs the vulnerability classification for each bridge, shown in blue. The procedure is described in detail below and then applied to the 100-bridge sample set to determine the vulnerability of the bridges.

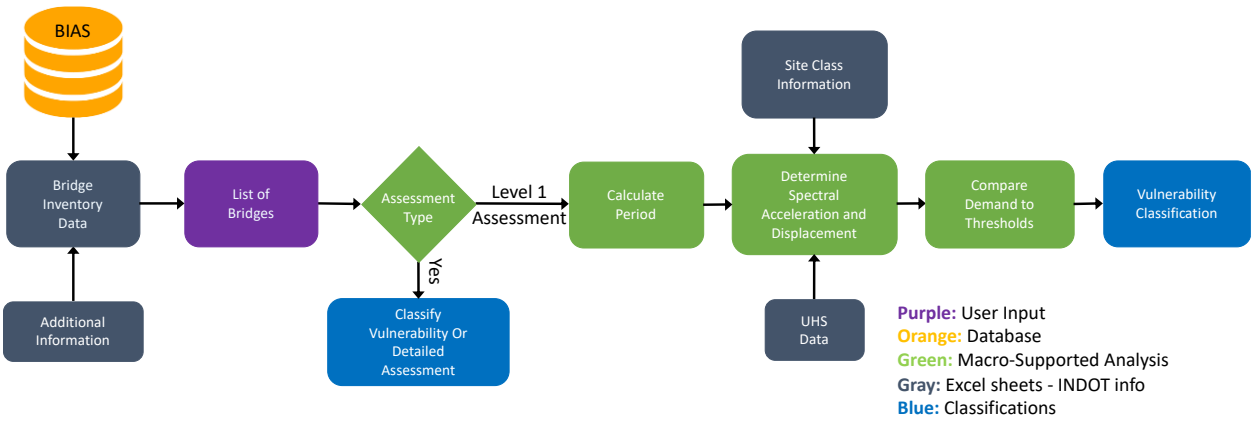

Figure 5.1. INSAT Procedure

5.3.1 Bridge Inventory Requirements

The first step is loading the required bridge inventory data items, if they have not been previously loaded. INSAT first requests that the BIAS data is loaded. This file should contain the current information found in BIAS and, must, at a minimum, contain the data items shown in Table 5.4. The user is prompted to choose the file and internally the tool searches for each of the headings, shown in Table 5.4. The headings in the BIAS data file can contain either the NBI designation or the data item name, unless denoted otherwise. If a data item is missing or the heading is not in the correct format, the user is notified and prompted to run the assessment again with the correct file.

Table 5.4. BIAS Data Requirements

NBI Designation	Data Item Name
	Asset Name*
002	District
006	Feature Intersected
007	Facility Carried
008	Structure Number **
016	Latitude
017	Longitude
027	Year Built
034	Skew
043A	Structure Type, Main: Kind of Material/Design
043B	Structure Type, Main: Type of
045	Number of Spans in Main Unit
046	Number of Approach Spans
048	Length of Maximum Span
049	Structure Length
052	Deck Width, Out-To-Out
054B	Minimum Vertical Under Clearance
106	Year Reconstructed

**Asset Name must be the heading for the column containing the asset names since no NBI designation exists.*

***The NBI designation 008 must be included in the heading of the column that contains the structure number. The Data Item Name will not work for this data item.*

As discussed in Chapter 4, a simplified assessment is not possible unless INDOT includes additional data items. INSAT is capable of handling these data items in the BIAS data file or in a separate data file. The additional data items, and the required headings for the input file, are shown in Table 5.5. If all of the data items are not found in the BIAS data file, the user is told which data items are missing and is prompted to load in an additional data item file. The tool requires at least one of the additional data items in order to run. If any additional data items are missing, the tool will make the appropriate estimates, if applicable.

Table 5.5. Additional Data Requirements

Heading Requirement	Data Description
Asset Name	Asset Name corresponding to the bridge (same as the BIAS asset name)
NBI	NBI Number corresponding to the bridge (same as the BIAS structure number)
Substructure Type	Substructure Type - Wall, Hammerhead, Circular Frame Bent, Rectangular Frame Bent, Other
Abutment Type	Abutment Type - Integral, Semi-Integral, Non-Integral
Number of Elements	The number of elements in one pier
Element Height	Dynamic height of the tallest pier (in feet)
Element Length	Transverse dimension of one substructure element (in feet)
Element Width	Longitudinal dimension of one substructure element (in feet)
Deck Thickness	Thickness of the deck (in inches)
Height Ratio	A yes or no based on a ratio of the tallest to the shortest pier

5.3.2 List of Bridges

Once the data items have been correctly loaded into the tool, the user is prompted to choose which subset of bridges to assess. INSAT prompts the user to select one of five different options: the entire bridge database, the critical routes, a specific route, a specific district(s), or a user inputted list of NBIs.

- **Entire Bridge Database:** When the user selects the entire bridge database to assess, the list of bridges stored in the inputted BIAS data file is what is used as the list of bridges.

- **District:** When the user selects this option, the tool will prompt them to select which district(s) they'd like to assess, and the tool will assess every bridge in the selected district(s).
- **Critical Routes:** When the user selects this option, tool will assess every bridge carrying or crossing one of the identified critical routes, shown in Table 5.1. This selection can be narrowed further by selecting a specific district(s) to run.
- **Specific Rote:** When the user selects this option, they will select a specific route from the list of routes, shown in Table 5.2. The tool will then identify every bridge carrying or crossing the selected route to assess. This selection can also be narrowed further by selecting a specific district(s) to run.
- **User inputted NBI List:** When the user selects this option, they will be prompted to load a .csv file that contains a list of NBI number. This list will be used as the list of bridges to assess and if an NBI on the list is not in the BIAS data file, the bridge will not be assessed, and the user will be notified of this on the "All Results" sheet.

5.3.3 Assessment Type

For every bridge the user chooses to assess, the first step is classifying the assessment type. Using the bridge data items previously loaded and bridge details discussed in Chapter 4, each bridge is assigned an assessment type. The "Level 0 Assessment" type refers to those bridges whose overall vulnerability can automatically be classified as low vulnerability or moderate vulnerability. The "Detailed Assessment" type refers to those bridges whose details dictate that a simplified assessment is not possible. The bridges that do not fall into one of these two assessment type categories, are assigned a "Level 1 Assessment" type and move forward to the simplified assessment. Figure 5.2 shows a breakdown of the assessment type for the 100-bridge sample set.

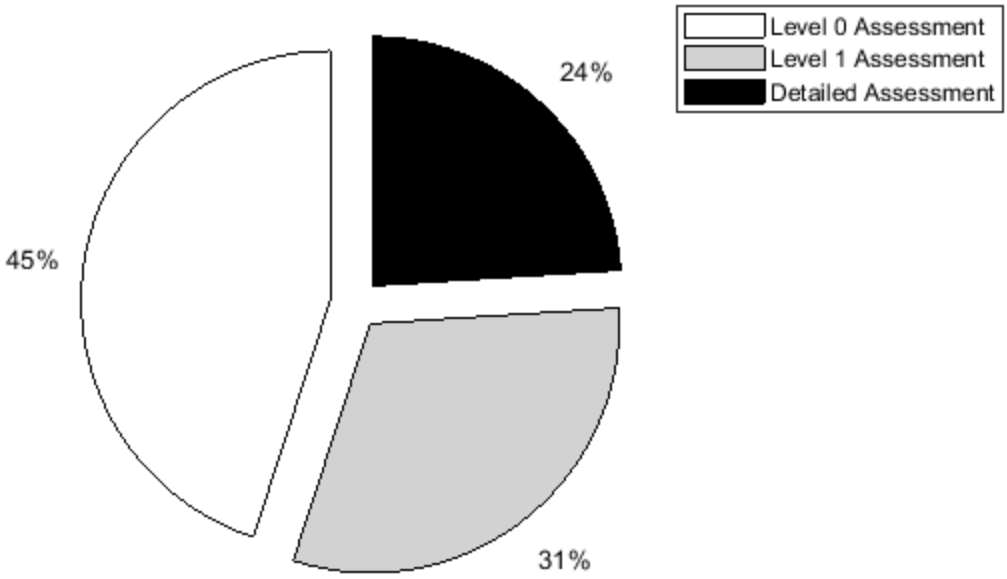

Figure 5.2. Assessment Type for 100-Bridge Sample Set

5.3.4 Calculate Period

Using the methodology presented in Chapter 4, the mass, the stiffness, and the period is calculated for each bridge that has moved forward to the simplified assessment. These calculations are done for both fundamental directions, the longitudinal direction and the transverse direction. The period of the structure, along with the location and site class, is what yields the demand on the bridge.

5.3.5 Determine Spectral Acceleration and Spectral Displacement

Once the period of the structure is calculated, the nest step in determining the demands on the structure is to calculate the spectral acceleration and spectral displacement. Unlike Chapter 3 and 4, which used the simulated ground motions to determine the typical vulnerabilities and to validate the simplified assessment procedure and assumptions, the tool imports the uniform hazard spectrum (UHS) at each specific bridge site for a return period of 1,000 years. The process for determining the UHS can be found in Appendix C. The predetermined UHS data is stored on the

"UHS Information" sheet and contains the information for every bridge in INDOT's bridge inventory at the time of writing. INSAT compares the NBI number from the list of bridges selected to the first column on the "UHS Information" sheet to determine the correct line of data to use. Then, using the period of the structure calculated, the tool interpolates between points to determine the spectral acceleration at the specific bridge site. This process is followed for both directions.

The UHS was developed for a NEHRP site class B/C at each site, so as mentioned earlier in this chapter, the spectral accelerations must be amplified/de-amplified for the actual site conditions. Site class is not a data item collected by INDOT, but it is important in determining the spectral acceleration expected for the level of hazard chosen. The map shown in Figure 3.7, shows the distribution of the NEHRP site classes in Indiana. The shapefile from this map was used to automatically predetermine the site class for all the bridges currently in the database.

INSAT uses the NBI number and matches it with the structure stored in the first column of the "Site Class" sheet. If the NBI number is not on the "Site Class" sheet, the tool assumes Site Class D for future calculations.

The tool uses AASHTO site factors, found in section 3.10.3.2, to amplify/de-amplify the spectral accelerations (AAHSTO, 2017). AASHTO developed the site factors with the reference site class of NEHRP site class B, however the UHS was developed for site class B/C. In order to apply the site factors to the UHS data, the AASHTO tables were converted to have site class B/C as the reference site class. The results of this conversion are shown in Table 5.6 through Table 5.8.

Table 5.6. Site Class Factors for Zero-Periods

Class	**Peak Ground Acceleration Coefficient**				
	PGA < 0.1	**PGA = 0.2**	**PGA = 0.3**	**PGA = 0.4**	**PGA > 0.5**
A	0.73	0.73	0.76	0.80	0.80
B	0.91	0.91	0.95	1.00	1.00
B/C	1	1	1	1	1
C	1.09	1.09	1.05	1.00	1.00
D	1.45	1.27	1.14	1.10	1.00
E	2.27	1.55	1.14	0.90	0.90

Table 5.7. Site Class Factors for Short Periods

Class	Spectral Acceleration Coefficient at Period 0.2 s				
	Ss < 0.25	**Ss = 0.5**	**Ss = 0.75**	**Ss = 0.1**	**Ss > 1.25**
A	0.73	0.73	0.76	0.80	0.80
B	0.91	0.91	0.95	1.00	1.00
B/C	1	1	1	1	1
C	1.09	1.09	1.05	1.00	1.00
D	1.45	1.27	1.14	1.10	1.00
E	2.27	1.55	1.14	0.90	0.90

Table 5.8. Site Class Factors for Long Periods

r	Spectral Acceleration Coefficient at Period 1.0 s				
	S_1 < 0.1	**S_1 = 0.2**	**S_1 = 0.3**	**S_1 = 0.4**	**S_1 > 0.5**
A	0.59	0.62	0.64	0.67	0.70
B	0.74	0.77	0.80	0.83	0.87
B/C	1	1	1	1	1
C	1.26	1.23	1.20	1.17	1.13
D	1.78	1.54	1.44	1.33	1.30
E	2.59	2.46	2.24	2.00	2.09

INSAT uses the calculated period of the structure to determine which table is applicable. For periods between 0s and 0.1s, Table 5.6 is used, for periods greater than or equal to 0.1s and less than 0.5s, Table 5.7 is used, and for periods greater than or equal to 0.5s, Table 5.8 is used. The site class determined previously tells the tool which row in the table applies. The tool uses the spectral acceleration for site class B/C to interpolate between columns to calculate the amplification factor. INSAT does these calculations for each direction and stores the results.

The spectral acceleration at each site, considering the site conditions, is calculated as

$$SA = F_{site} * SA_{B/C}. \quad (5.1)$$

The linear spectral displacement is determined using the amplified spectral and the period for each applicable direction is calculated as

$$\Delta_{lin} = g * \frac{SA}{(\frac{2\pi}{T})^2}. \quad (5.2)$$

This displacement assumes that the substructure remains in the linear region. However, as it was shown in Chapter 3.5, this assumption is not valid for the bridges that have adequate reinforcement which behave in flexure. For these bridges, the tool assumes that the nonlinear displacement is 1.41 times larger than the linear displacement based on the literature (Sozen, 2003).

5.3.6 Compare Demand to Thresholds

The tool uses the predetermined thresholds, shown in Table 4.3, to assign levels of vulnerability. The thresholds were determined using trends seen in the detailed analysis, discussed in Chapter 3. For the thresholds that are displacement limits, the threshold is directly compared to the linear displacement, in the case of old walls and hammerhead substructures, or the non-linear displacement, in the case of newer walls and hammerhead substructures and frame bent substructures with reinforced concrete columns to determine the vulnerability level. For the thresholds are not displacement limits, the calculations used in the are provided in Equations 4.30 and 4.31.

5.3.7 Classify Bridge Vulnerability

INSAT classifies each bridge's vulnerability in the longitudinal direction and the transverse direction. The overall vulnerability that is outputted on the "All Results" sheet is based on the worse vulnerability classification in either direction. For example, if a bridge was highly vulnerable in the longitudinal direction, but classified as low vulnerability in the transverse direction, the overall vulnerability of the bridge would be highly vulnerable. The vulnerability classification results for the 100-bridge sample set can be seen in Figure 5.3. A classification result of "N/A" means a detailed analysis is required.

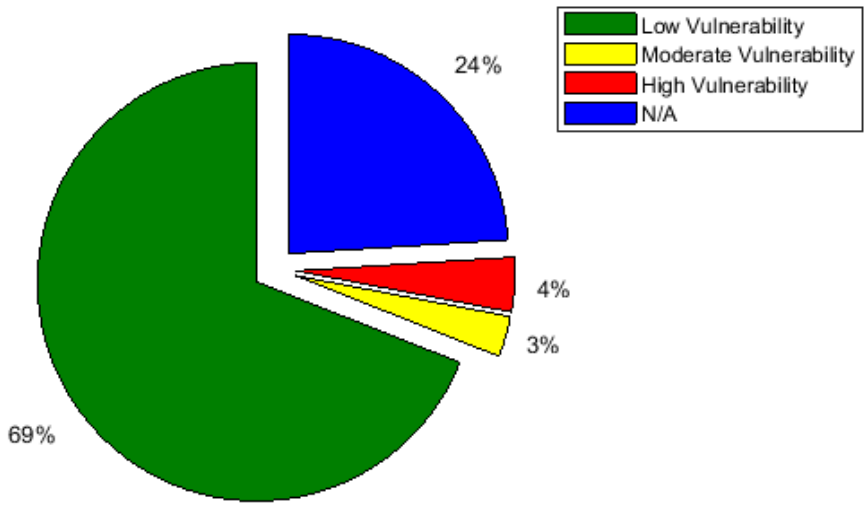

Figure 5.3. Vulnerability Classification of 100-Bridge Sample Set

5.3.8 Applying Weighting Factors

Once the seismic assessment has executed, the user has the options to apply weighting factors to help INDOT in prioritizing retrofits and replacements on other details than just the vulnerability classification. Weightings can be applied by district, for the primary disaster routes (critical routes), and for a user-provided list of NBI's with corresponding weightings. If a weighting scheme is applied, within each vulnerability classification level, the results are organized from highest weight to lowest weight. For example, the bridges that are classified as high vulnerability will be organized from the highest weight to the lowest weight. Below the high vulnerability bridges, the bridges that are classified as moderately vulnerable, will be organized from highest weight to lowest weight. Following that, the bridges classified as low vulnerability will be organized from highest weight to lowest weight. Lastly, the bridges classified as requiring a detailed analysis, with an identified vulnerability of "N/A" will be organized from highest weight to lowest weight.

5.4 Tool Outputs

5.4.1 All Results Sheet

The main output generated when executing the tool is the "All Results" sheet. This sheet contains the vulnerability classification (if applicable) for each bridge in the chosen set. Below, each of the output columns and the meaning of the data is described.

Default Options

Asset Name

The "Asset Name" column contains the asset name for each bridge as found in the BIAS Data File. If this column is left blank, the inputted NBI number was not found in the BIAS Data File.

NBI Number

The "NBI Number" column contains the NBI number (Asset Code) for each bridge as found in the BIAS Data File or from the Bridge File (if that option was chosen).

District

The "District" column contains the district for each bridge assessed as found in the BIAS Data File.

Weight Factor

This column contains the total weighting factor for each bridge. If no weighting factors are applied, this column will not be included in the outputs. If multiple weighting factor options are selected, the multiple values applied to each bridge are multiplied to get the total weighting factor.

Assessment Type

The "Assessment Type" column contains the level of assessment performed on each bridge. Three potential values for this column are described below. See the Reasons for Classification section for a description of why each bridge was classified in the way it was.

- **Level 0 Assessment –** This assessment type is assigned to bridges whose vulnerability can automatically be classified as "Low Vulnerability" or "Moderate Vulnerability". No simplified assessment is done on these bridges.

- **Level 1 Assessment –** This assessment type is assigned to bridges whose vulnerability is determined through the simplified assessment procedure.
- **Detailed Assessment –** This assessment type is assigned to bridges whose details require a more in-depth model than can be handled with the simplified assessment procedure.

Vulnerability Classification

The "Vulnerability Classification" column contains the vulnerability level for each bridge for a ground acceleration with a 7% probability of exceedance in 75 years. Four potential vulnerability classifications are described below

- **High Vulnerability** – This vulnerability classification is assigned to bridges where the demand exceeded the high vulnerability thresholds (Table 4.3)
- **Moderate Vulnerability** – This vulnerability classification is assigned to bridges where the demand exceeded the low vulnerability thresholds but does not exceed the high vulnerability thresholds (Table 4.3)
- **Low Vulnerability** – This vulnerability classification is reserved for the bridges where the demand based on the uniform hazard spectrum does not exceed low vulnerability capacity thresholds (Table 4.3)
- **N/A** – This vulnerability classification is reserved for the bridges which require a detailed analysis since the tool is not capable of estimating the dynamic properties of the bridge or the bridges which do not have any UHS data available.

Reason for Classification

The "Reason for Classification" column provides a brief description of the reasoning behind the assigned the assessment type or vulnerability classification for each bridge. Detailed discussions of each of these cases are provided in Chapter 4. The options are:

- **Assessment Type: Level 0 Assessment –** A discussion of the reasoning behind the Level 0 Assessment classification types can be found in Chapter 4.
    - **Vulnerability Classification: Low Vulnerability –** These bridge details allow the bridge to automatically be classified as moderately vulnerable to the level of hazard

chosen for this report and are automatically assigned a vulnerability classification of "Low Vulnerability"

- *Single Span or Culvert*
- *Wall and Integral*
- *RC or Steel Hammerhead and Integral*

- **Vulnerability Classification: Moderate Vulnerability –** These bridge details allow the bridge to be automatically classified as moderately vulnerable to the level of hazard chosen and are automatically assigned a vulnerability classification of "Moderate Vulnerability"
  - *Non-integral, long, single span steel bridges*

- **Assessment Type: Level 1 Assessment**
  - **Vulnerability Classification: Low Vulnerability**
    - **Substructure Capacity is Adequate –** The bridge's dynamic properties were estimated and the demand for the level of hazard expected at the site did not exceed the capacity thresholds.
  - **Vulnerability Classification: Moderate Vulnerability**
    - **Potential for Flexural Hinges to Form –** The bridge details allow a flexural mechanism to control, and this scenario is expected for the level of hazard at the bridge site.
  - **Vulnerability Classification: High Vulnerability**
    - **Potential for Brittle Failure –** The bridge details determine that a brittle failure of the substructure will control, and this scenario is expected for the level of hazard at the bridge site.
  - **Vulnerability Classification: N/A**
    - **No UHS Data Available –** The UHS data for the bridge NBI is not included on UHS Data sheet and no vulnerability assessment can be completed. The UHS data should be determined for this bridge location and added to the UHS Data sheet in order to assess the vulnerability of this bridge.
- **Assessment Type: Detailed Analysis –** a discussion of why the bridge details require a detailed analysis can be found in Chapter 4.3.3. Note that the cases with an * will not be output if all the recommended data items are incorporated into BIAS.

- *NBI Number does not exist in BIAS*
- *Superstructure combination is not supported*
- *Potential for Expansion Joints*
- *Height Ratio > 10%*
- *RC Frame Bents with RC Columns*
- *Substructure not supported*
- *Aspect Ratio < 3*
- *No substructure given**
- *No element height given **
- *Number of columns not given**
- *Frame Bent shape not given**
- *Length can't be estimated because of skew***
- *Length can't be estimate for RC hammerheads**

Estimated Properties

The "Estimate Properties" column alerts the user if any of the estimation methods, presented in Chapter 4, is used to estimate the recommended data items when they are not given. If no bridges have any estimated properties, then this column will not be included in the outputs. The following are the data items that the tool can estimate.

- Abutment Type
- Element Height
- Deck Thickness
- Element Length
- Element Width

Warning

The "Warning" column informs the user that some of the estimates and assumptions made in the simplified assessment can lead to underestimates in vulnerability. While the likelihood of this is low, it is important for the user to understand the limitations of the tool. The warnings provided in this column are given as (a), (b), and/or (c).

- **(a) – Potential for Brittle Failure:** This warning is shown for all old (constructed prior to 1990) walls and hammerheads because of the high likelihood of them having a low reinforcement ratio. The reinforcement ratio of these bridges should be verified as being larger than 0.25% to confirm the vulnerability classification as low vulnerability.
- **(b) – Confirm Deck is Connected to the Substructure at Each Pier:** This warning is shown for all reinforced concrete superstructure bridges because the assessment assumes longitudinal bars are extending from the pier into the deck. This assumption is typical, however, there is the chance that one or more piers are not connected with longitudinal bars, and this would greatly change the dynamic properties of that bridge.
- **(c) – RC Frame Bent with > 3 Spans:** This warning is shown for all RC superstructures with more than 3 spans and frame bent substructures. The transverse stiffness for these bridges does not follow the same trends assumed in the tool. Due to the limited samples for this type of bridge in the sample set, the assumption could not be improved, and the transverse stiffness should be verified.

Superstructure Material

The "Superstructure Material" column contains the superstructure material, as defined by the BIAS file.

Substructure Type

The "Substructure Type" column contains the substructure type, as define by inputted files.

Custom Outputs

Custom outputs refer to different data items found in the inputted file(s). These values are copied directly from the data files into the output sheet for convenience, and no additional explanation is needed. The possible custom outputs are:

- Latitude and Longitude
- Feature Intersected
- Facility Carried
- Abutment Type

- Number of Spans
- Skew

5.4.2 Dynamic Properties Sheet

The *Dynamic Properties* sheet is generated as an output for the tool to allow the user to verify the mass and stiffness estimates if desired. Only bridges whose assessment type is "Level 1 Assessment" will appear on this sheet. The following are the columns and the data outputs.

- **Asset Name** – used to identify the bridge
- **NBI Number** – used to identify the bridge
- **Longitudinal Mass (kip/g)** – the calculated mass used for the longitudinal direction calculations. If this value is "N/A" the details of the bridge allow it to be automatically classified as "Low Vulnerability" in the longitudinal direction, however the transverse direction needs to be checked.
- **Longitudinal Stiffness (kip/in)** – the calculated stiffness used for the longitudinal direction calculations. If this value is "N/A" the details of the bridge allow it to be automatically classified as "Low Vulnerability" in the longitudinal direction, however the transverse direction needs to be checked.
- **Longitudinal Period (s)** – the calculated period for the longitudinal direction, used to determine the spectral acceleration from the UHS. If this value is "N/A" the details of the bridge allow it to be automatically be classified as "Low Vulnerability" in the longitudinal direction, however the transverse direction needs to be checked
- **Transverse Mass (kip/g)** – the calculated mass used for the transverse direction calculations. If this value is "N/A" the details of the bridge allow it to be automatically be classified as "Low Vulnerability" in the transverse direction, however the longitudinal direction needs to be checked.
- **Transverse Stiffness (kip/in)** – the calculated stiffness used for the transverse direction calculations. If this value is "N/A" the details of the bridge allow it to be automatically be classified as "Low Vulnerability" in the transverse direction, however the longitudinal direction needs to be checked.

- **Transverse Period (s)** – the calculated period for the transverse direction, used to determine the spectral acceleration from the UHS. If this value is "N/A" the details of the bridge allow it to be automatically be classified as "Low Vulnerability" in the transverse direction, however the longitudinal direction needs to be checked.

5.5 Summary

In this chapter, the simplified assessment, presented in Chapter 4, was implemented using INSAT for a simplified assessment tool and the vulnerability classification. The assessment results for the 100 bridges in the chosen sample set were presented. The tool uses the procedure and thresholds discussed in Chapter 4, and considers the USGS uniform hazard spectrum for an acceleration with a 1,000-year return period to determine the demand on the bridge. Sixty-nine bridges are classified as "Low Vulnerability" because of their details. Twenty-four bridges require a detailed analysis due to their details, three bridges are classified as "Moderate Vulnerability" because of the potential for overturning of the rocker bearings or for the potential for plastic hinges to form, and the remaining four bridges are classified as "High Vulnerability" because of the potential for brittle failure. When any or all of the recommended items are incorporated into BIAS, INSAT can be used to rapidly assess the vulnerability of the entire bridge inventory so that INDOT can use this information to prioritize rehabilitations and retrofits.

6. IMPLEMENTATION OF DATA RECOMMENDATIONS

6.1 Introduction

The previous chapters presented and discussed various data recommendations which, if incorporated into BIAS, would allow for a rapid seismic assessment of the bridge inventory using the developed seismic assessment tool. This chapter discusses in detail, each of these data items, and how they could be gathered during routine bridge inspections and be completely incorporated into BIAS by the end of the next bridge inspection cycle (a two- to three-year period).

6.2 Implementation Recommendations by Data Item

6.2.1 Substructure Type

Substructure Type refers to the pier classification of the main spans. Five main substructure types were identified as typical in Indiana from the sample set of 100 bridges. These five substructure types are: *Circular Frame Bents, Rectangular Frame Bents, Hammerhead Walls, Walls*, and *Other*. The following points define each substructure type for easy reference, and they are shown in Figure 6.1.

- **Frame Bents, Circular and Rectangular –** a substructure with two or more unsupported columns that maintain an unsupported length greater than the column length. Additionally, the clear spacing between the columns is greater than the column length and a bent cap (or beam-type element) is present connecting the columns. The columns could have a capital, but it is not required for this classification. The cross-section shape of a single column determines whether the substructure is identified as *Circular Frame Bent* or a *Rectangular Frame Bent*.
- **Hammerhead Walls** – a concrete pier cap supported by a single reinforced concrete element. This element typically maintains a uniform width but experiences a definitive change in cross-sectional length along the height of the element.
- **Walls** – a single reinforced concrete element, similar to hammerhead walls, that do not experience a definitive change in cross-sectional length along the height. Walls may experience a slight change in cross-sectional width due to the presence of a bent cap.

- **Other** – substructures that do not definitely fit into one of the previously discussed substructure types should be classified as *Other*. If multiple substructure types are used across a single bridge, the substructure type should be classified as *Other*.

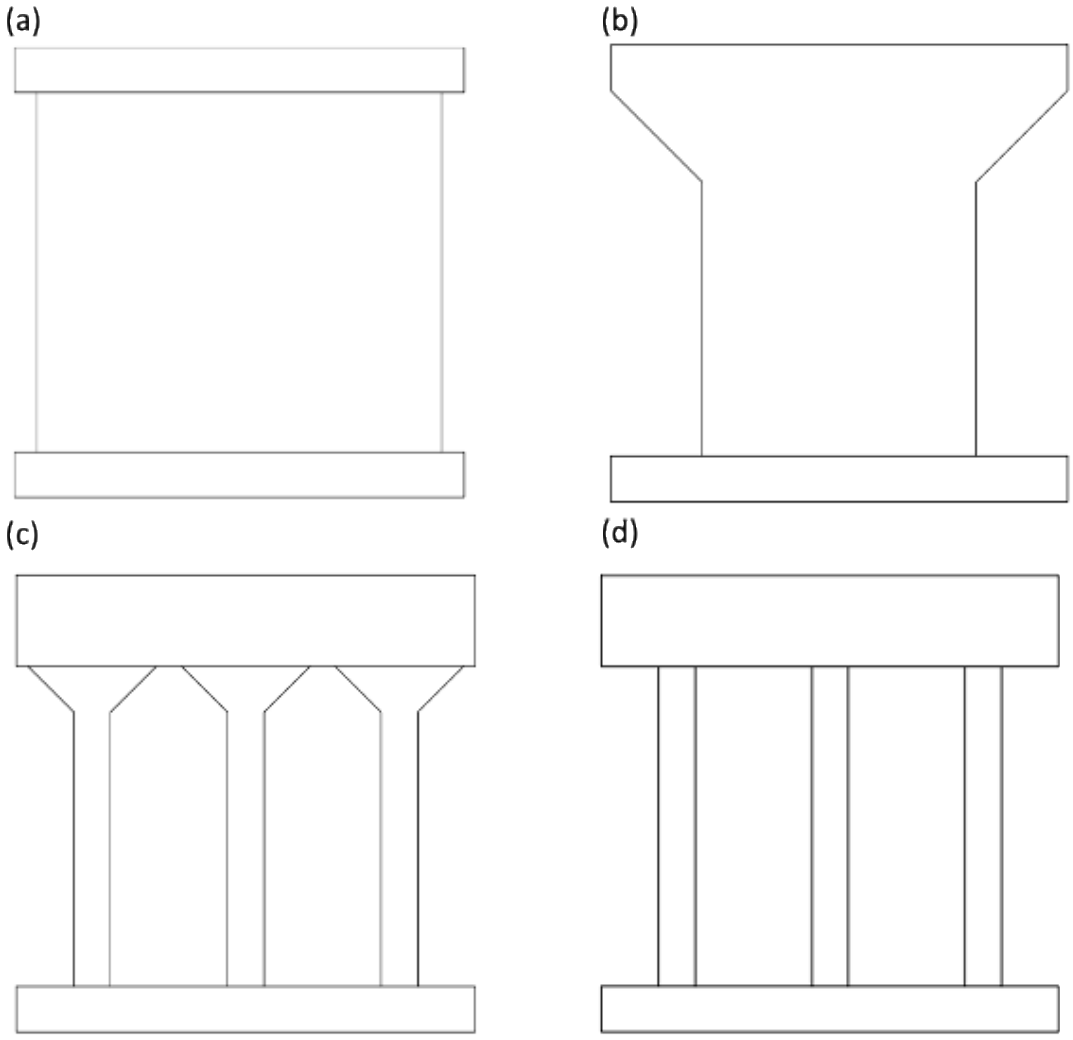

Figure 6.1. Elevation Schematic of (a) Walls, (b) Hammerhead Walls, (c) Frame Bents with a Capital, and (d) Frame Bents without a Capital

The incorporation of substructure type in BIAS would first be the identification during a routine inspection followed by a dropdown selection list in BIAS that includes the five possible substructure types. The bridge inspector, when filling out the rest of the inspection data, can easily fill out the substructure type. *Once the substructure type is identified, it does not need to be updated unless the substructure is rehabilitated.*

6.2.2 Abutment Type

Abutment Type refers to the connection of the superstructure to the abutment. Two types of abutments were identified as typical in Indiana, *integral type* and *non-integral* type. The following points define each type of abutment for easy reference

- **Integral Type** – defined by the superstructure encased in concrete at the abutment and no expansion joint between the approach span and the main span. This includes both semi-integral and integral abutments as they are expected to behave similarly under the level of ground motion expected in Indiana.
- **Non-Integral Type** – defined by the presence of an expansion joint at the abutment

The incorporation of abutment type in BIAS would first be the identification during a routine inspection followed by a dropdown selection list in BAIS that includes the two types of abutments. The bridge inspector, when filling out the rest of the inspection data, can easily fill out the abutment type. *Once the abutment type is identified, it does not change unless the abutment type is changed during a rehabilitation.*

6.2.3 Number of Elements

Number of elements refers to the number of elements in one substructure unit. For walls and hammerheads, this value is one because there is only one element per pier. For frame bents, this value is the number of columns in a single pier. If the piers have varying numbers of columns, use the smallest number of columns should be used.

The incorporation of the Number of Elements in BIAS should be implemented through a single, user-inputted box. The inspector can input the Number of Elements, when filling out the rest of the inspection data.

6.2.4 Element Height

Element Height refers to the clear height of the main substructure units recorded in feet. For wall and hammerhead wall substructures, this refers to the height measured from the ground to the top of the bent cap. For frame bents, this refers to the clear height of the column, measured from the

ground or top of the crash wall to the bottom of the bent cap. For bridges over waterways, the height is measured from the bottom of the waterway to the top or bottom of the bent cap, depending on the substructure type.

If the piers have varying heights, the largest should be recorded since the simplified assessment and tool are only capable of handling a single height. The reason for using the maximum height is discussed in Chapter 4.

Figure 6.2 shows an elevation schematic of the three main categories of substructure types: Frame Bents, with and without a capital, Hammerheads, and Walls with the height identified.

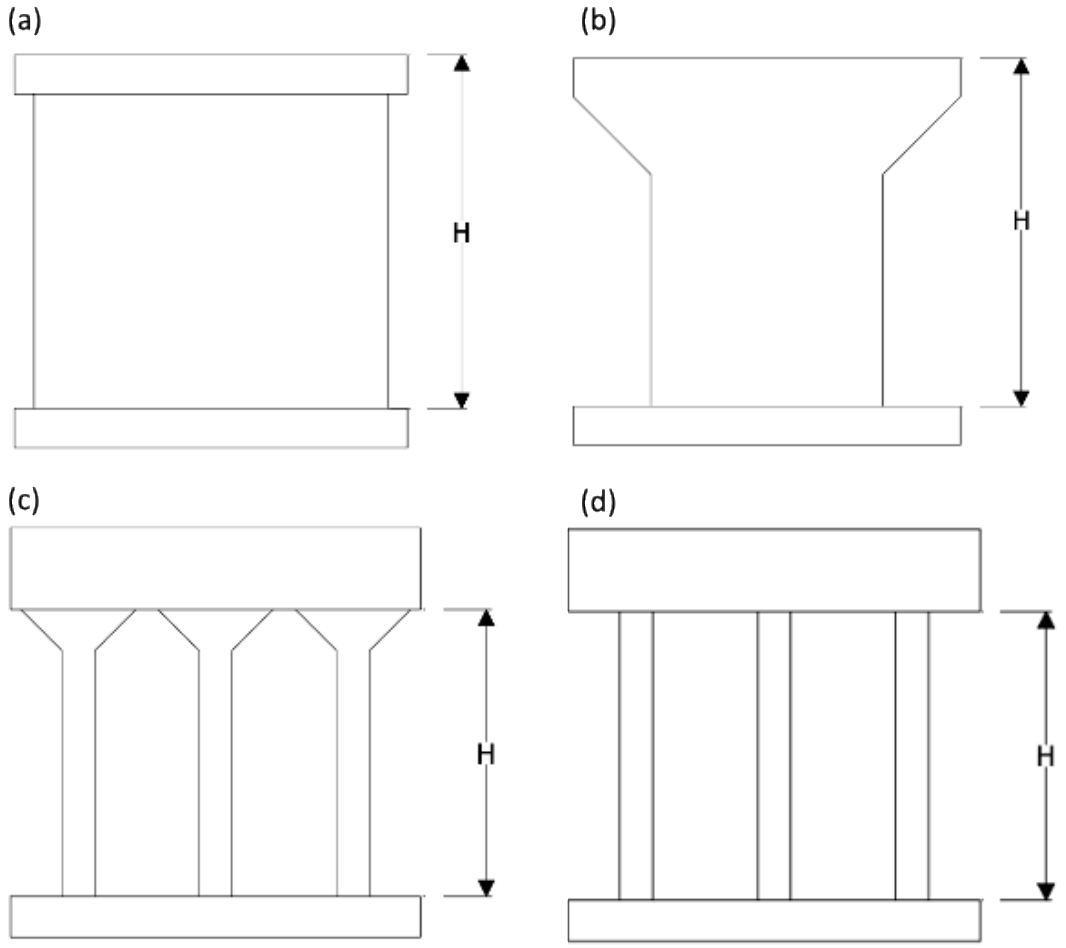

Figure 6.2. Elevation Schematic Showing Element Height Identified for (a) Walls, (b) Hammerhead Walls, (c) Frame Bents with a Capital, and (d) Frame Bents without a Capital

The incorporation of element height in BIAS should be implemented through a single user-inputted box. The inspector can input the largest element height, in feet, when filling out the rest of the inspection data. *For bridges over waterways, the height should be gathered an updated with every inspection due to the potential for change in element height due to scour. For other bridges, the height should be updated with every rehabilitation or repair.*

6.2.5 Element Length

Element length refers to the dimension of the main substructure unit in the transverse direction, recorded in feet. For walls and hammerhead walls, this dimension is the longer dimension of the substructure. For rectangular frame bents, this is the transverse dimension of a single column, and for circular frame bents, this dimension is the diameter of a single column. If the length varies across a single pier, or pier to pier, the smallest dimension should be used.

Figure 6.3 shows the cross-section of the four main categories of substructure types: Circular Frame Bents, Rectangular Frame Bents, Hammerheads, and Walls with the element length (L_{ele}) identified.

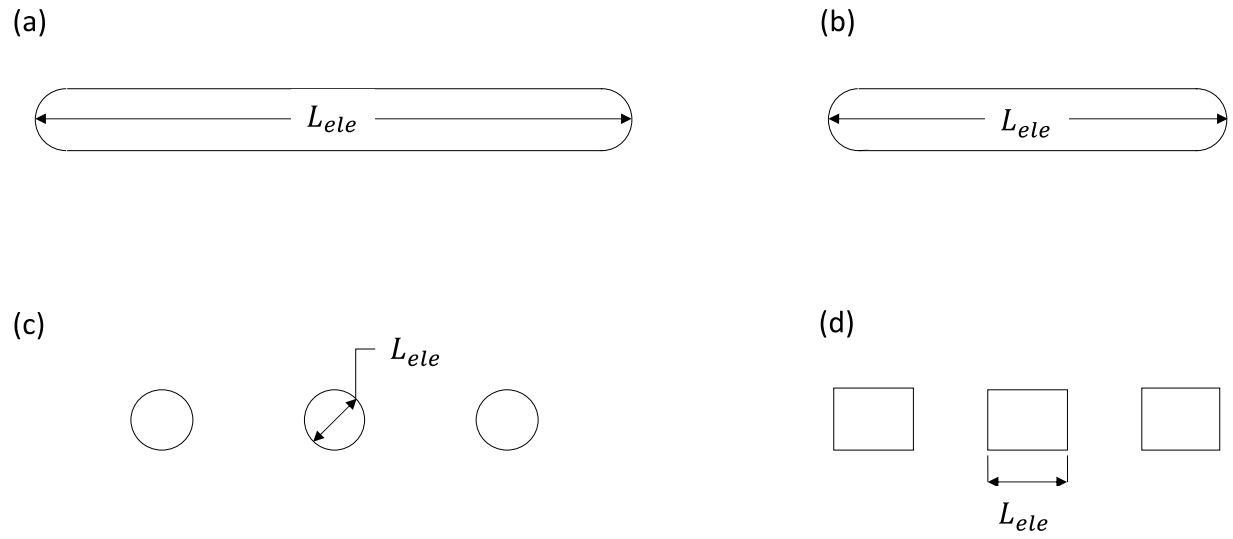

Figure 6.3. Cross-section at Base Showing Element Length Identified for (a) Walls, (b) Hammerhead Walls, (c) Circular Frame Bents, and (d) Rectangular Frame Bents

The incorporation of element length in BIAS should implemented through a single user-inputted box. The inspector can input the smallest element length, in feet, when filling out the rest of the inspection data. *Once the element length has been incorporated, it would not need to be updated unless rehabilitations or repairs were done on the bridge.*

6.2.6 Element Width

Element width refers to the dimension of the main substructure unit in the longitudinal direction, recorded in feet. For walls and hammerheads, this dimension is the shorter dimension of the substructure. If the width varies along the length, the width at the ground should be used. For rectangular frame bents, this is the longitudinal dimension of a single column. This data item is not required for circular frame bents since the diameter is recorded for the element length. If the width varies across a single pier, or pier to pier, the smallest width at the base of the pier should be used.

Figure 6.4 shows a cross-section of the three main categories of substructure types: Frame Bents, Circular and Rectangular, Hammerheads, and Walls with the element width (w_{ele}) identified. Please note that there is no dimension for Circular Frame Bents because the element width is the same as the element length previously defined.

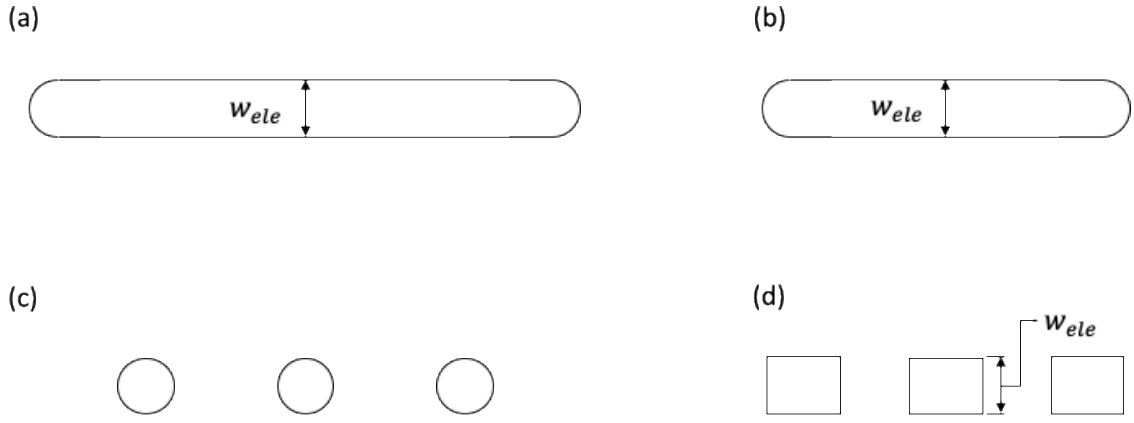

Figure 6.4. Cross-section at Base Showing Element Width Identified for (a) Walls, (b) Hammerhead Walls, (c) Circular Frame Bents, and (d) Rectangular Frame Bents

The incorporation of element width in BIAS should be implemented through a single user-inputted box. The inspector can input the smallest element width in feet, when filling out the rest of the inspection data. *Once the element width has been incorporated, it would not need to be updated unless rehabilitations or repairs were done on the bridge.*

6.2.7 Deck Thickness

Deck thickness refers to the depth of the deck of the main spans, recorded in inches. As discussed in Chapter 4, this data item is more critical for reinforced concrete slab deck bridges than steel and prestressed girder bridges because of the variability in deck thickness and the importance of the deck in the structural system. However, in order to be consistent across all bridge types and inspections, the bridge deck thickness should be recorded for all bridges.

The incorporation of deck thickness in BIAS should be implemented through a single user-inputted box. The inspector can input the thickness in inches, when filling out the rest of the inspection data. *Once the deck thickness has been incorporated, it would not need to be updated unless rehabilitations or repairs are made to the bridge deck.*

6.2.8 Height Ratio Flag

The height ratio flag refers to a yes or no check box that signifies when there is a large variation in pier height across a single bridge. As shown in Chapter 4, when a single bridge has largely varying pier heights, the simplified assessment is not applicable due to the difficulties in modeling. This data item identifies these bridges based on a 1.10 ratio of the heights of adjacent piers (H_{Ratio}). After the element height is gathered for each pier, the inspector can determine the height ratio of the tallest pier to the shortest pier using Equation (6.1).

$$H_{Ratio} = \frac{H_{tall}}{H_{short}}. \tag{6.1}$$

The incorporation of the height ratio flag in BIAS should be a check box that the inspector should check if the calculated height ratio is greater than 1.10. For all other bridges, the box would be left unchecked. *This data item must be recalculated every time heights are measured.*

6.3 Summary

This chapter presented a description of each recommended data item as well as implementation recommendations for gathering and recording each data item. Each recommended data item can be obtained during routine inspections and incorporated into BIAS through selection boxes, user-input boxes, and a check box. If INDOT were to require that bridge inspectors record these data items, along with the other data items they collect, it would take between two to four years to gather the information. Once the information has been recorded once, for the majority of the data items, updates are only needed when rehabilitations and repairs occur.

7. CONCLUSIONS AND RECOMMENDATIONS

The major conclusions from this thesis are summarized in this chapter and recommendations for future work and expanding the scope of the Indiana Seismic Assessment Tool (INSAT) are also presented.

7.1 Synthesis and Impact of Findings

The developed simplified assessment procedure and associated tool (INSAT) allows INDOT to assess the vulnerability of the bridges in their bridge network. The results from the assessment can be used to prioritize retrofits and rehabilitations for the most vulnerable bridges in the state. In order to have a robust simplified assessment, a detailed assessment on a sample set of bridges was first completed. The major conclusions from the detailed (Level 2) assessment (Chapter 3) of the selected bridges are:

- Based on the results presented in Chapter 3 and Appendix B and C, there are three main types of vulnerabilities observed in steel superstructure bridges across Indiana: brittle failure of under-reinforced substructure units, the formation of a plastic hinge for adequately reinforced substructure units, shear connection failure of the substructure to the superstructure which could result in pounding at the abutments, and the potential for rocker bearing to overturn.
- Substructures with integral abutments are not vulnerable in the longitudinal direction because there is no differential displacement between the substructure and the superstructure.
- Wall and hammerhead substructures are not vulnerable in the transverse direction to the level of hazard expected in Indiana because of the large stiffness of the substructure units in that direction.
- Walls and hammerheads were found to be highly vulnerable or moderately vulnerable in the longitudinal direction based on the amount and grade of reinforcement found in the sample steel superstructure bridges.

- Frame bents were found to be moderately vulnerable in the transverse and longitudinal direction because there is the potential for plastic hinges to form at the level of hazard expected.
- Displacement and drift thresholds are good indicators of the different levels of vulnerabilities seen in the bridge inventory.

The simplified assessment procedure utilizes trends and averages seen in the detailed (Level 2) assessment to create simplified SDOF models using available data items in BIAS and an additional eight identified data items. The major conclusions from the simplified (Level 1) assessment (Chapter 4) of all 100 bridges in the sample set are:

- A complete simplified assessment is not possible given the current information found in BIAS. Using only the current information in BIAS, 62% of the bridges in INDOT's entire bridge inventory require more information to determine the vulnerability level.
- At a minimum, the substructure type, the number of elements, the element height, and the height ratio flag needs to be added to BIAS to perform a simplified assessment because these data items cannot be estimated.
- The addition of the element length and width, the deck thickness, and the abutment type is important for the accuracy of the assessment results, however, there are methods and assumptions, presented in Chapter 4.5, that can be made. Using these estimates and assumptions will result in discrepancies in the vulnerability assessment.
- Certain bridges are excluded from the simplified assessment because a simplified assessment is not robust enough to accurately capture the unique characteristics of the bridge and its behavior under seismic loading as discussed in Chapter 4.
- With the addition of all of the recommended data items, there is an 87% agreement between the detailed assessment vulnerability classification and the simplified assessment classification. This percentage decreases considerably when data items are not included and must be estimated.

The developed tool, INSAT, applies the simplified seismic assessment procedure and determines the vulnerability classification for the bridges in Indiana. In the sample of 100 representative bridges, 69% were classified as low vulnerability, 3% are classified as moderate vulnerability, 4%

are classified as high vulnerability, and 24% have details requiring a detailed assessment. Similar results are expected when applying INSAT to the rest of the bridges in INDOT's bridge inventory as the sample set was chosen because it was representative of the whole bridge inventory based on specific data items.

INSAT gives INDOT the ability to narrow their bridge inventory from a set of nearly 6000 bridges to a smaller sample of bridges with high vulnerability. INDOT can consider this much smaller set of bridges to prioritize retrofits and note bridges for prioritization of inspection in the case of an event.

While INSAT was developed specifically for INDOT and their bridge inventory database (BIAS), the procedure can be expanded upon and applied to other states in moderate seismic zones. The bridge details, potential vulnerabilities, and trends in mass and stiffness should be confirmed with a detailed analysis on a sample set of bridges, but the methods used to estimate the structure's dynamic properties is applicable throughout moderate seismic zones.

7.2 Future Work

This thesis developed and implemented a simplified methodology suitable for assessing the seismic vulnerability of the bridge inventory across Indiana. In SPR 4222, a detailed assessment was performed on a sample set of 100 bridges, representative of INDOT's bridge inventory of prestressed concrete, reinforced concrete and steel girder superstructures to verify the results of the simplified assessment procedure and to identify trends that could be used in its implementation in INSAT (Bonthron et al., 2020). Once the additional data items are incorporated into BIAS, the trends and assumptions made in the simplified assessment can be improved upon with additional detailed analyses for specific substructure/superstructure combinations.

In addition to improving the estimates and assumptions used in the simplified assessment, INSAT can be expanded upon to offer the user more features. For example, INSAT is currently capable of determining the seismic vulnerability for a ground acceleration with a return period of 1000 years. However, INSAT could be expanded to allow the user to select different level of hazards to fit their needs. Additionally, INSAT was developed for pre-event planning and preventative decision

making, but future versions could allow the rapid assessment of bridges post-event using a user-input epicenter location and magnitude. This would allow post-disaster reconnaissance teams to understand the damage to expect at a specific site and allow them to prioritize inspections to those bridges with the highest vulnerability for the given event.

REFERENCES

AASHTO. (2017). *AASHTO LRFD Bridge Design Specifications, 8th Edition.* Washington, DC: American Association of State Highway and Transportation Officials.

AASHTO. (2018). *The Manual for Bridge Evaluation, 3rd Edition*. Washington, DC: American Association of State Highway and Transportation Officials.

ACI Committee 318. (2014). *Building Code Requirements for Structural Concrete: (ACI 318-19);* and *Commentary (ACI 318R-14).* American Concrete Institute, Farmington Hills, MI.

AISC Committee 360. (2016). *Steel Construction Manual 15th Ed*. American Institute of Steel Construction, Chicago, IL

Baker, J.W. (2008). An Introduction to Probabilistic Seismic Hazard Analysis

Bakun, W.H., Hopper, M.G. (2004). Magnitudes and Locations of the 1811–1812 New Madrid, Missouri, and the 1886 Charleston, South Carolina, Earthquakes. *Bulletin of the Seismological Society of America*; 94 (1): 64–75

BIAS (2018). Bentley® InspectTech™, INDOT, indot-it.bentley.com/login.aspx.

Bonthron, L., Beck, C., Lund, A., Mahmud, F., Zhang, X., Orellana Montano, R., Dyke, S., Ramirez, J., Cao, Y., & Mavroeidis, G. (in progress) (2020). *Empowering the Indiana Bridge Database toward Rapid Seismic Vulnerability Assessment.* Rep. JTRP No. 4222, Purdue University, IN.

CalTrans (2019). *CalTrans Seismic Design Criteria, Version 2.0.* California Department of Transportation, Sacramento, CA.

Cao, Y., & Mavroeidis, G. (2019). *Seismic Hazard Assessment and Simulation of Ground Motions*. Deliverable 1 JTRP No. 4222, University of Notre Dame, IN.

Choi, E. (2002). Seismic Analysis and Retrofit of Mid-America Bridges (Doctoral dissertation, Georgia Institute of Technology, Atlanta, United States). Retrieved from Georgia Tech Library.

Choi, E., and Jeon, J. (2003). Seismic Fragility of Typical Bridges in Moderate Seismic Zone. *KSCE Journal of Civil Engineering* 7.1: 41-51. Web.

Chopra, A. K. (2012). *Dynamics of Structures: Theory and Applications to Earthquake Engineering* (4th ed). Upper Saddle River, NJ: Prentice Hall.

CUSEC. (n.d). *Wabash Valley Seismic Zone.* Retrieved from https://cusec.org/wabash-valley-seismic-zone/

DesRoches, R., Choi, E., Leon, R. T., Dyke, S. J., & Aschheim, M. (2004). Seismic Response of Multiple Span Steel Bridges in Central and Southeastern United States. I: As Built. *Journal of Bridge Engineering*, 9(5), 464-472.

DesRoches, R., Choi, E., Leon, R. T., & Pfeifer, T. A. (2004). Seismic Response of Multiple Span Steel Bridges in Central and Southeastern United States. II: Retrofitted. *Journal of Bridge Engineering*, 9(5), 473-479.

Eagar, K.C., Pavlis. G.L., Hamburger, M.W. (2005). Evidence of Possible Induced Seismicity in the Wabash Valley Seismic Zone from Improved Microearthquake Locations. *Bulletin of the Seismological Society of America*; 96 (5): 1718–1728.

Fares, A. (2018). Simplified Equations for Rigidity and Lateral Deflection for Reinforced Concrete Cantilever Shear Walls. World Academy of Science, Engineering and Technology, Open Science Index 142, *International Journal of Civil and Environmental Engineering*, 12(10), 1051 - 1055.

Federal Highway Administration (FHWA). (2006). Seismic Retrofitting Manual for Highway Structures: Part 1—Bridges (Publication No. FHWA-HRT-06-032). McLean, VA: Research, Development, and Technology Turner-Fairbank Highway Research Center.

Frosch, R., Kreger, M., & Talbott, A. (2009). *Earthquake Resistance of Integral Abutment Bridges*. Rep. JTRP No. 2867, Purdue University, IN.

Garcia, L. E. (1998). Dinámica Estructural Aplicada al Diseño Sísmico. Bogotá: Universidad de loa Andes, Facultad de Ingeniería, Departamento de Ingeniería Civil.

IGS (2011). Predicted Responses of Geologic Materials to Seismically Induced Ground Shaking in Indiana. Indiana Geological and Water Survey. Retrieved from https://maps.indiana.edu/previewMaps/Geology/Seismic_Shaking_Materials_Response.html

INDOT (2012). *CETRP Attachment No. 4: INDOT Primary Disaster Routes*. Indianapolis, IN

INDOT (2005). *Standard Drawing No. E 711-BSTS-01: Fixed Steel Shoe Details*. Indianapolis, IN

INDOT (2005). *Standard Drawing No. E 711-BSTS-02: Expansion Steel Shoe Details*. Indianapolis, IN

INDOT (2012). *Standard Drawing No. E 726-BEBP-05: Elastomeric Bearing Pads Type S.* Indianapolis, IN.

INDOT (2013). *INDOT Design Manual Chapter 412*. Indianapolis, IN. Last Updated: 01/23/2020.

Itani, A., Bruneau, M., Carden, L., & Buckle, I. (2004). Seismic Behavior of Steel Girder Bridge Superstructures. *Journal of Bridge Engineering*, 9(3), 243-249.

Mahmud, F.I. (2019). Simplified Assessment Procedure to Determine the Seismic Vulnerability of Reinforced Concrete Bridges in Indiana (Master's thesis, Purdue University, West Lafayette, United States). Retrieved from https://hammer.figshare.com/articles/Simplified_Assessment_Procedure_to_Determine_the_Seismic_Vulnerability_of_Reinforced_Concrete_Bridges_in_Indiana/8281028

Metzger, L.E. (2004). Vulnerability of Bridges in Southern Indiana to Earthquakes (Master's thesis, Purdue University, West Lafayette, United States)

Nielson, B. G. (2005). *Analytical Fragility Curves for Highway Bridges in Moderate Seismic Zones* (Doctoral dissertation). Retrieved from Georgia Tech Library.

Nielson, B. G., & DesRoches, R. (2007). Analytical Seismic Fragility Curves for Typical Bridges in the Central and Southeastern United States. *Earthquake Spectra*, 23(3), 615-633.

nshmp-haz (n.d.). *National Seismic Hazard Mapping Project (NSHMP) Code*. Retrieved June 20, 2019, from https://github.com/usgs/nshmp-haz

NYSDOT (2004). *Seismic Vulnerability Manual*. New York State Department of Transportation, New York, NY.

Olson, S.M., Green, R.A., Obermeier, S.F. (2005). Revised Magnitude-bound Relation for the Wabash Valley Seismic Zone of the Central United States. *Seismological Research Letters* 76.6:756-71. Web.

Pan, Y., Agrawal, A., & Ghosn, M. (2007). Seismic Fragility of Continuous Steel Highway Bridges in New York State. *Journal of Bridge Engineering*, 12(6), 689-699.

Petersen, M. D., Moschetti, M. P., Powers, P. M., Mueller, C. S., Haller, K. M., Frankel, … Olsen, A. H. (2014). *Documentation for the 2014 update of the United States national seismic hazard maps* (USGS Open-File Report 2014–1091). Reston, VA: U.S. Geological Survey. h https://dx.doi.org/10.3133/ofr20141091

Rabbat, B., & Russell, H. (1985). Friction Coefficient of Steel on Concrete or Grout. Journal of Structural Engineering, 111(3), 505-515.

Ramirez, J., Frosch, R., Sozen, M., & Turk, M. (2000). *Handbook for the Post-Earthquake Safety Evaluation of Bridges and Roads*. Rep. JTRP No. 2377, Purdue University, IN. https://doi.org/10.5703/1288284315557

Ramirez, J., Peeta, S., Sozen, M., Garcia, L., & Viswanath, K. (2005*). Emergency Earthquake Routes; Part I, Criteria for Selection of Primary Routes; and Part II: Route Seismic Vulnerability Aspects*. Rep. JTRP No. 2480, Purdue University, IN. https://doi.org/10.5703/1288284313203

Sozen M.A. (2003) The Velocity of Displacement. In: Wasti S.T., Ozcebe G. (eds) *Seismic Assessment and Rehabilitation of Existing Buildings*. NATO Science Series (Series IV: Earth and Environmental Sciences), vol 29. Springer, Dordrecht

USGS. (n.d). *The New Madrid Seismic Zone.* Retrieved from https://www.usgs.gov/natural-hazards/earthquake-hazards/science/new-madrid-seismic-zone?qt-science_center_objects=0#qt-science_center_objects

Zatar, W. Harik, I.E., Yuan, P., & Choo, C.C. (2006). *Preliminary Seismic Evaluation and Ranking of Bridges along I-24 in Western Kentucky.* Rep. KTC-06-22/SPR206-00-3F

APPENDIX A. DETAILED ANALYSIS RESULTS

1. Bridge Asset Name: 038-89-04111 B – NBI 13000

Table A.1. Specifications and Information on Bridge 038-89-04111 B (NBI 13000)

Geographical Information	Asset Name	038-89-04111 B
	NBI Number	13000
	County	Wayne
	District	Greenfield
	Year of Construction	1957
	Year of Reconstruction	2003
	Facility Carried	SR 38
	Feature Intersected	GREENS FORK
Superstructure Information	No. Beams + Beam Type	7; Plate Girder
	Number of Spans	3
	Span Lengths	60'-0", 72'-0", 60'-0"
	Deck Width	38'-6"
	Deck Thickness	8"
	Skew	48.00 degrees
Substructure Information	Substructure Type	Hammerhead
	Height of Wall	19'-1", 19'-1"
	Width of Element (Base)	22'-9", 22'-9"
	Thickness of Wall	2'-8", 2'-8"
	Abutment Type	Expansion Shoe
	Concrete Compressive Strength	3000 psi
	Yield Strength of Reinforcement	40000 psi

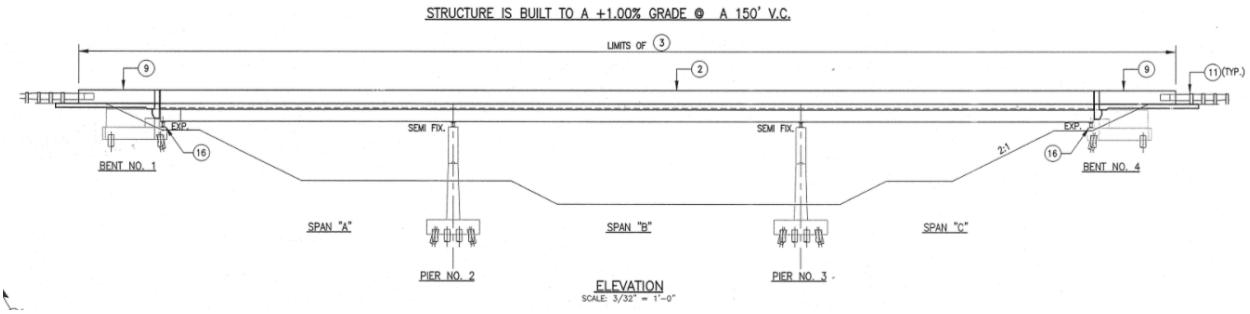

Figure A.1. Elevation View of the Bridge (NBI 13000) (2002)

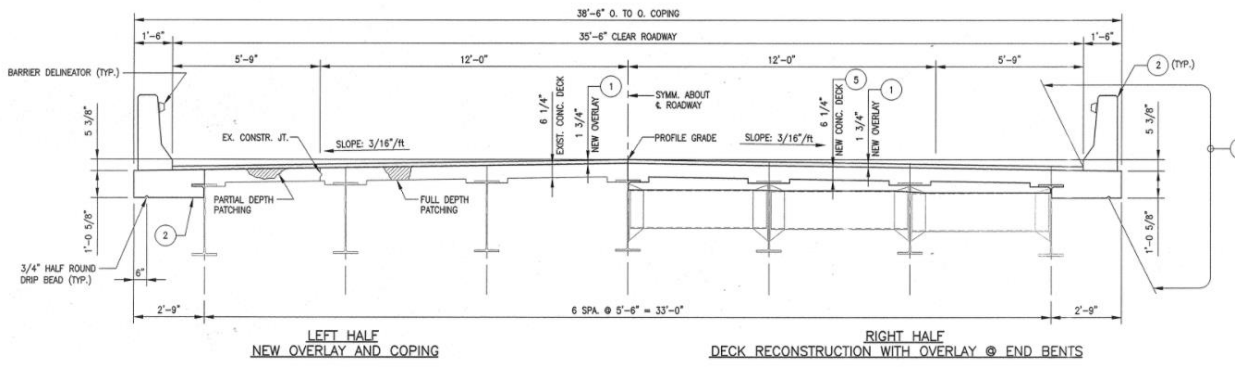

Figure A.2. Typical Section of the Bridge (NBI 13000) (2002)

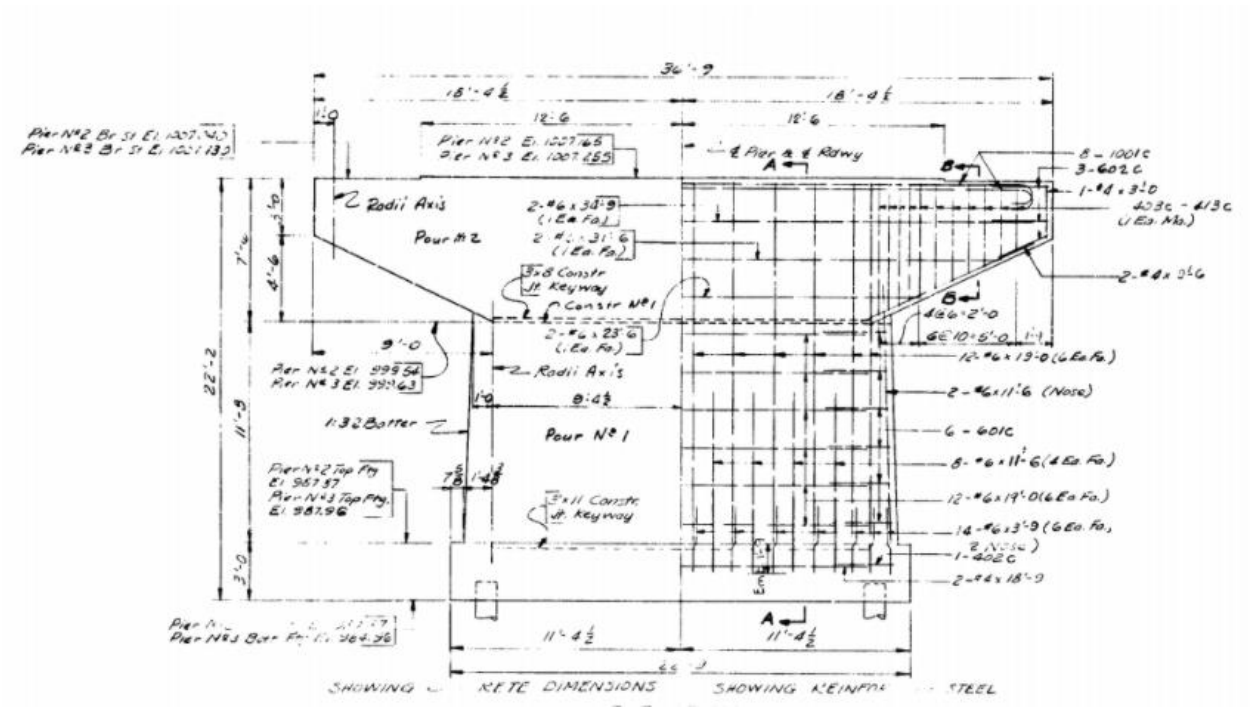

Figure A.3. Transverse Elevation of Interior Pier (NBI 13000) (1957)

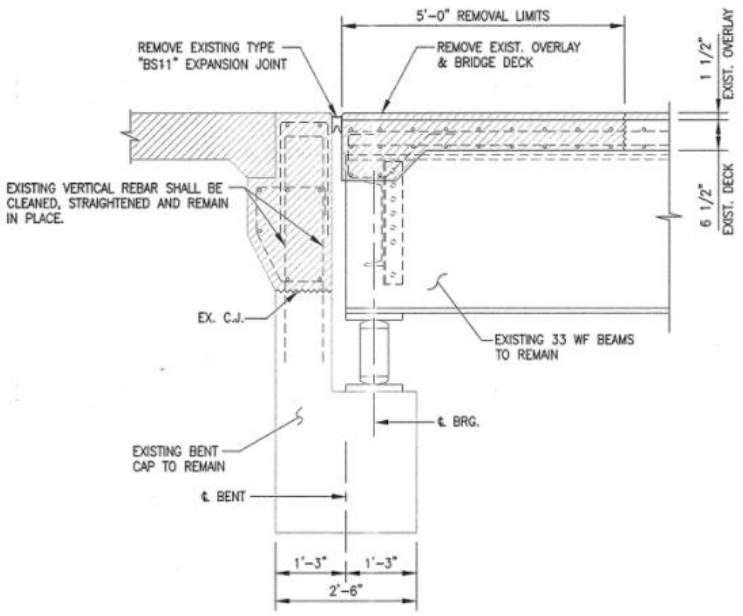

Figure A.4. Abutment Detail of the Bridge (NBI 13000) (2002)

Table A.2. Demand, Capacity, and Vulnerability of the Bridge (NBI 13000)

	Transverse Direction	**Longitudinal Direction**
Activated Mass (kips/g)	1.9	2.77
Total Stiffness (kips/in)	171252.8	1159.8
Period (s)	0.021	0.31
Base Shear Capacity	1.09; 1.09	0.13; 0.13
Shear Capacity (kips)	1636; 1636	787; 787
Shear Connection (kips)	209.7	
Vulnerability	Not Vulnerable	Highly Vulnerable – Potential for Brittle Failure

2. Bridge Asset Name: 041-82-05415 CSBL – NBI 14280

Table A.3. Specifications and Information on Bridge 041-82-05415 CSBLB (NBI 14280)

Geographical Information	Asset Name	041-82-05415 CSBL
	NBI Number	14280
	County	Vanderburgh
	District	Vincennes
	Year of Construction	1972
	Year of Reconstruction	2015
	Facility Carried	US 41 SB
	Feature Intersected	SR 66/62
Superstructure Information	No. Beams + Beam Type	8; Rolled Shape
	Number of Spans	2
	Span Lengths	76'-6", 76'-6"
	Deck Width	50'-6"
	Deck Thickness	8.75"
	Skew	04.00 degrees
Substructure Information	Sub. Type; No. of Elements	Frame Bent; 5
	Height of Wall	9'-0"
	Element Spacing	9'-0"
	Thickness of Wall	2'-0"
	Abutment Type	Semi-Integral
	Concrete Compressive Strength	3500 psi
	Yield Strength of Reinforcement	40000 psi

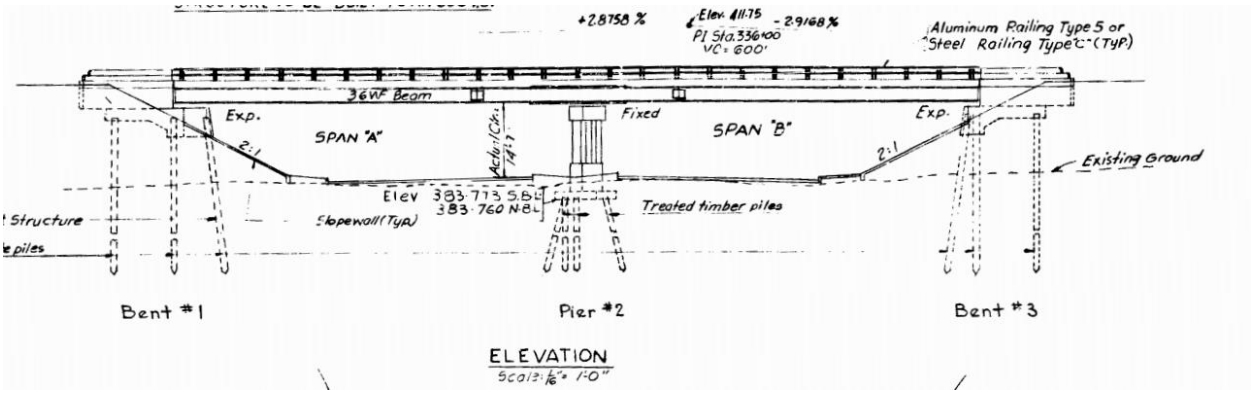

Figure A.5. Elevation View of the Bridge (NBI 14280) (1967)

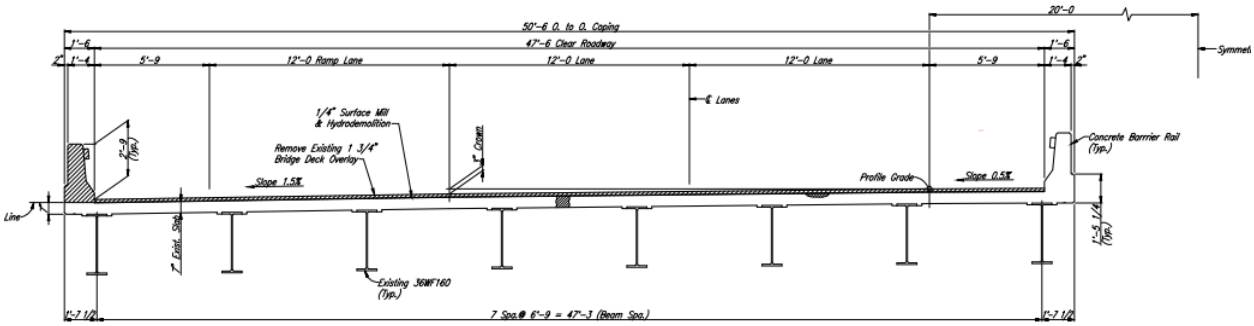

Figure A.6. Typical Section of the Bridge (NBI 14280) (2014)

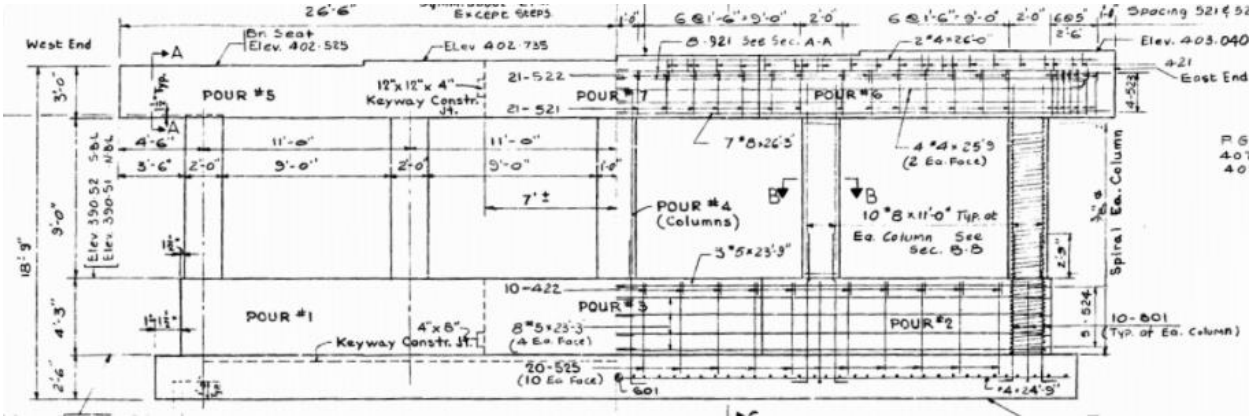

Figure A.7. Transverse Elevation of Interior Pier (NBI 14280) (1967)

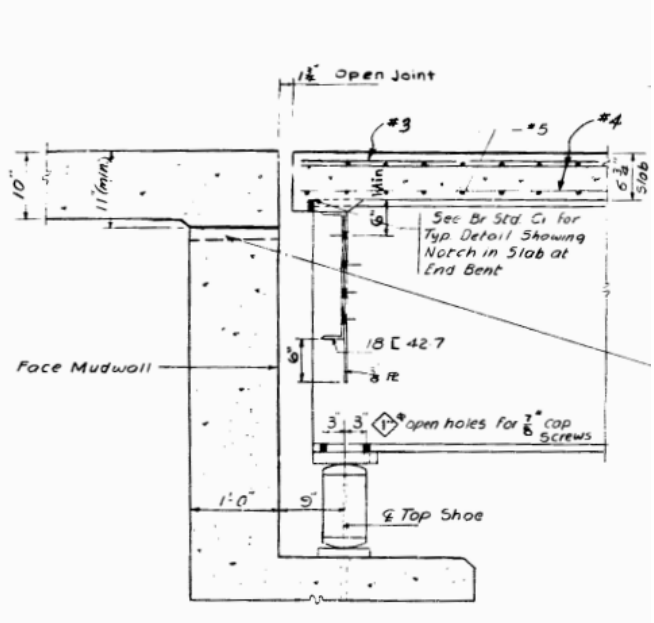

Figure A.8. Abutment Detail of the Bridge (NBI 14280) (1867)

Table A.4. Demand, Capacity, and Vulnerability of the Bridge (NBI 14280)

	Transverse Direction	**Longitudinal Direction**
Activated Mass (kips/g)	1.55	3.1
Total Stiffness (kips/in)	2535.1	416.4
Period (s)	0.155	0.54
Base Shear Capacity	0.44	0.19
Shear Capacity (kips)	308	308
Shear Connection (kips)	341.1	
Vulnerability	Moderately Vulnerable	Not Vulnerable due to Abutment

3. Bridge Asset Name: 041-77-03864 – NBI 14840

Table A.5. Specifications and Information on Bridge 041-77-03864 (NBI 14840)

Geographical Information	Asset Name	041-77-03864 JBNB
	NBI Number	14840
	County	Sullivan
	District	Vincennes
	Year of Construction	1973
	Year of Reconstruction	2005
	Facility Carried	US 41 NB
	Feature Intersected	MIDDLE FORK CREEK
Superstructure Information	No. Beams + Beam Type	7; Rolled Shape
	Number of Spans	3
	Span Lengths	50'-0", 60'-0", 50'-0"
	Deck Width	42'-6"
	Deck Thickness	9"
	Skew	25.00 degrees
Substructure Information	Substructure Type	Wall
	Height of Wall	28'-0", 28'-0"
	Width of Element (Base)	47'-1", 47'-1"
	Thickness of Wall	2'-0", 2'-0"
	Abutment Type	Semi-Integral
	Concrete Compressive Strength	3000 psi
	Yield Strength of Reinforcement	40000 psi

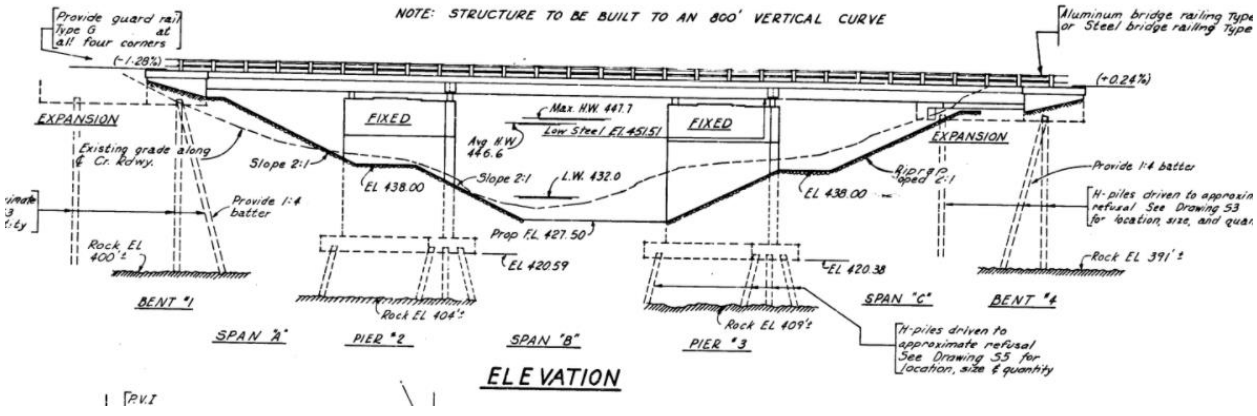

Figure A.9. Elevation View of the Bridge (NBI 14840) (1969)

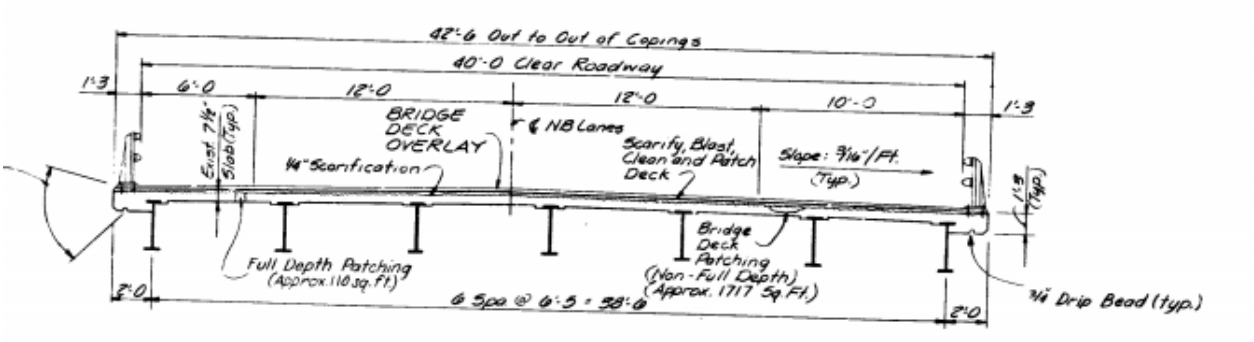

Figure A.10. Typical Section of the Bridge (NBI 14840) (1981)

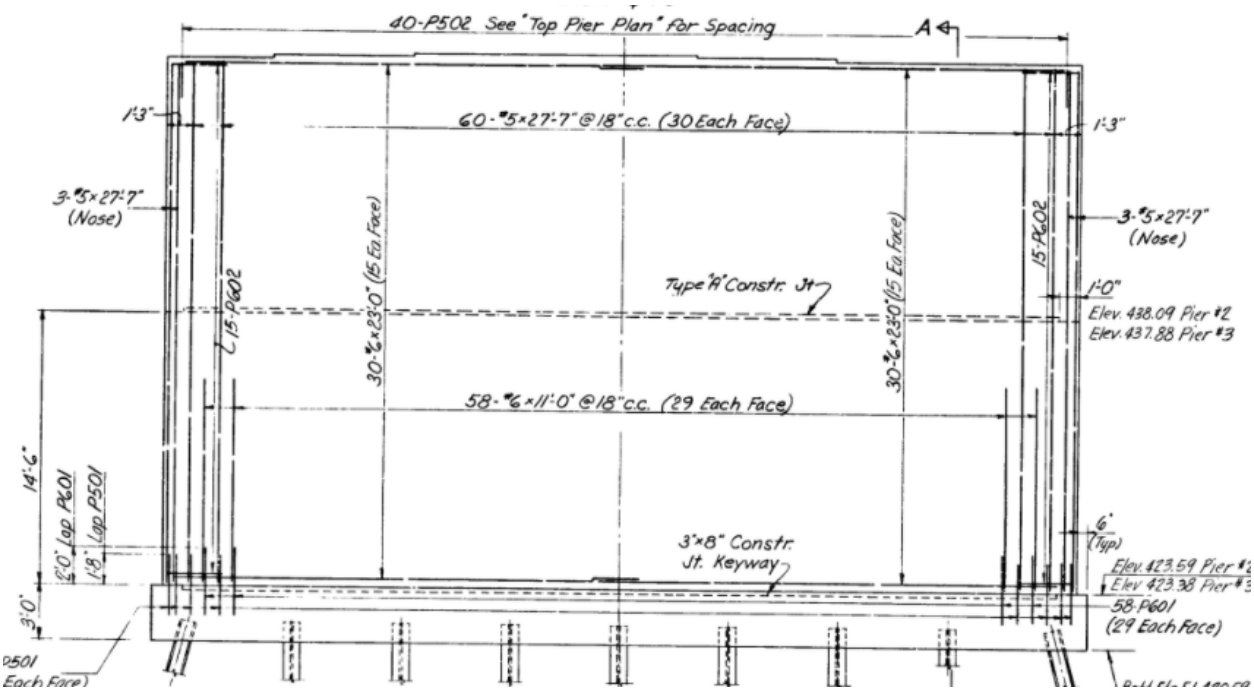

Figure A.11. Transverse Elevation of Interior Pier (NBI 14840) (1969)

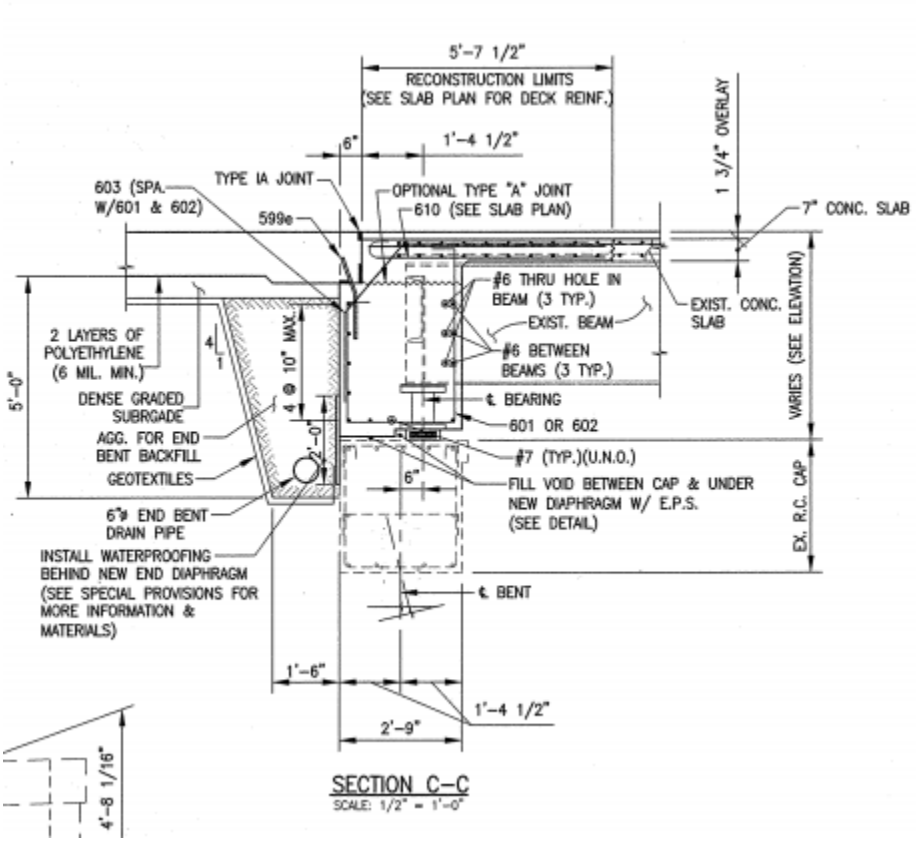

Figure A.12. Abutment Detail of the Bridge (NBI 14840) (2004)

Table A.6. Demand, Capacity, and Vulnerability of the Bridge (NBI 14840)

	Transverse Direction	Longitudinal Direction
Activated Mass (kips/g)	1.64	2.37
Total Stiffness (kips/in)	273311.6	325.4
Period (s)	0.015	0.54
Base Shear Capacity	5.31; 5.31	0.22; 0.22
Shear Capacity (kips)	3062; 3062	1133; 1133
Shear Connection (kips)	179.7	
Vulnerability	Not Vulnerable	Not Vulnerable due to Abutment

4. Bridge Asset Name: 062-82-02589 WBL – NBI 21985

Table A.7. Specifications and Information on Bridge 062-82-02589 WBL (NBI 21985)

Geographical Information	Asset Name	062-82-02589 WBL
	NBI Number	21985
	County	Vanderburgh
	District	Vincennes
	Year of Construction	1988
	Year of Reconstruction	N/A
	Facility Carried	SR 62 WB
	Feature Intersected	GOVERNOR ST, CSX RR
Superstructure Information	No. Beams + Beam Type	8; Plate Girder
	Number of Spans	4
	Span Lengths	65'-0", 90'-10", 90'-10", 91'-8"
	Deck Width	56'-6"
	Deck Thickness	8"
	Skew	00.00 degrees
Substructure Information	Sub. Type; No. of Elements	Frame Bent; 2
	Height of Wall	21'-5", 21'-3", 24'-3"
	Element Spacing	19'-9", 19'-9", 34'-0"
	Element Dimensions	3'-0" x 4'-0", 3'-0" x 4'-0", 4'-0" x 4'-0"
	Abutment Type	Expansion Shoe
	Concrete Compressive Strength	3500 psi
	Yield Strength of Reinforcement	40000 psi

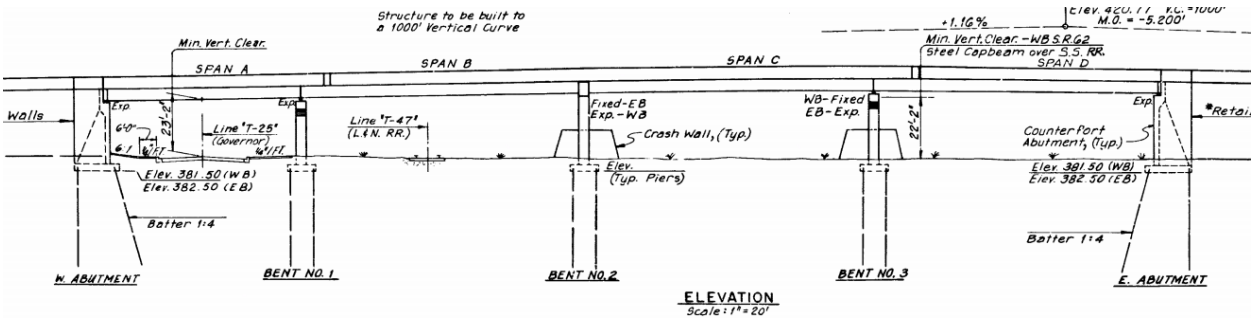

Figure A.13. Elevation View of the Bridge (NBI 21985) (1984)

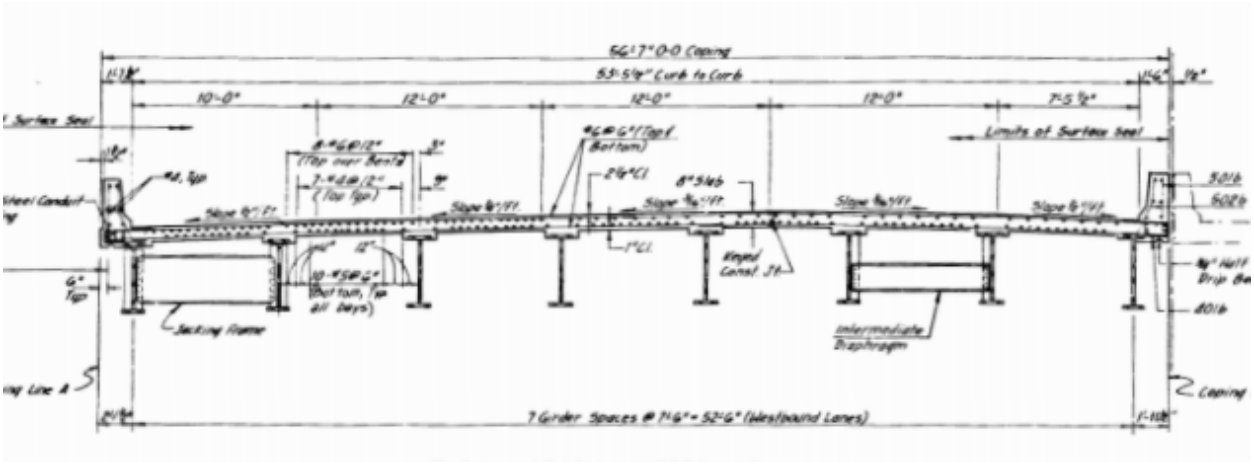

Figure A.14. Typical Section of the Bridge (NBI 21985) (1984)

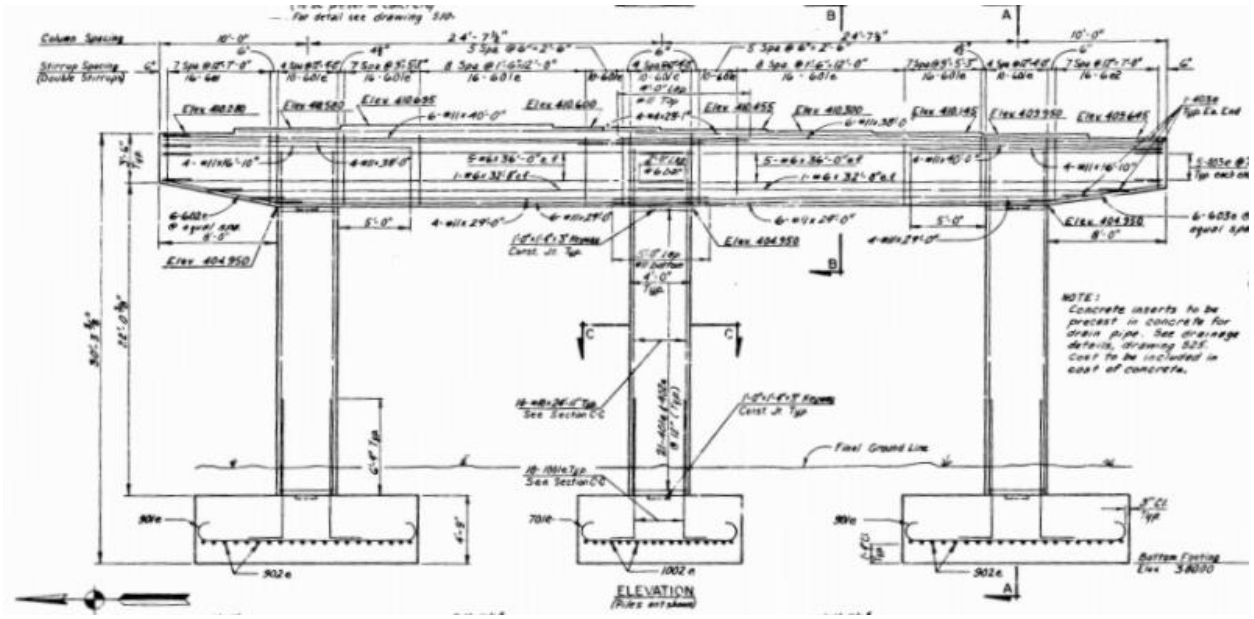

Figure A.15. Transverse Elevation of Interior Pier (Pier 2 and 3) (NBI 21985) (1984)

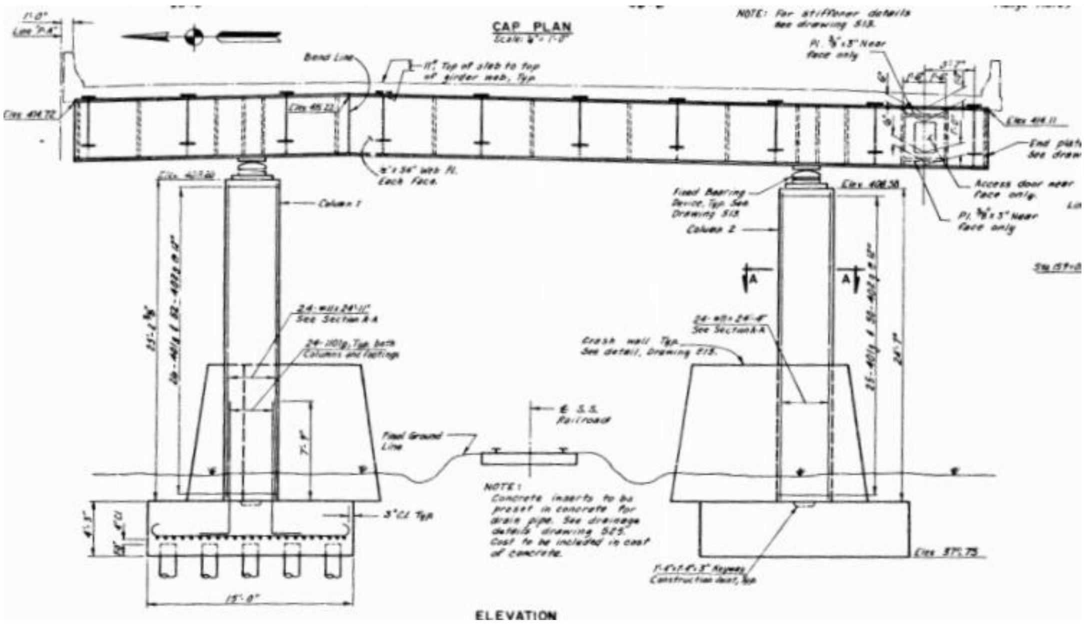

Figure A.16. Transverse Elevation of Interior Pier (Pier 4) (NBI 21985) (1984)

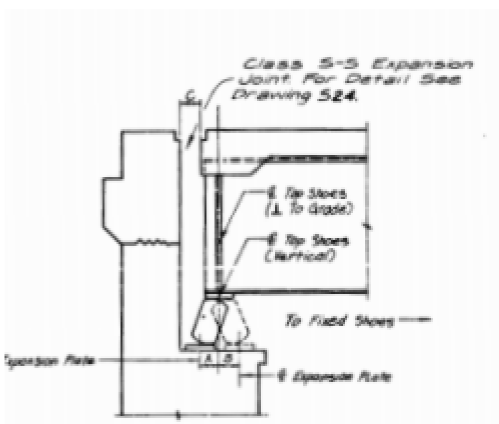

Figure A.17. Abutment Detail of the Bridge (NBI 21985) (1984)

Table A.8. Demand, Capacity, and Vulnerability of the Bridge (NBI 21985)

	Transverse Direction	Longitudinal Direction
Activated Mass (kips/g)	5.47	7.11
Total Stiffness (kips/in)	4399.3	366.8
Period (s)	0.221	0.87
Base Shear Capacity	0.7; 0.61; 0.66	0.36; 0.31; 0.33
Shear Capacity (kips)	483; 483; 407	552; 552; 407
Shear Connection (kips)	360.7	
Vulnerability	Moderately Vulnerable	Not Vulnerable

5. Bridge Asset Name: 062-74-06621 – NBI 22190

Table A.9. Specifications and Information on Bridge 062-74-06621 (NBI 22190)

Geographical Information	Asset Name	062-74-06621
	NBI Number	22190
	County	Spencer
	District	Vincennes
	Year of Construction	1982
	Year of Reconstruction	N/A
	Facility Carried	SR 62
	Feature Intersected	HURRICANE CREEK
Superstructure Information	No. Beams + Beam Type	8; Plate Girder
	Number of Spans	2
	Span Lengths	82'-0", 82'-0"
	Deck Width	46'-7"
	Deck Thickness	8"
	Skew	03.00 degrees
Substructure Information	Substructure Type	Hammerhead
	Height of Wall	17'-3"
	Width of Element (Base)	35'-0"
	Thickness of Wall	2'-6"
	Abutment Type	Expansion Shoe
	Concrete Compressive Strength	3000 psi
	Yield Strength of Reinforcement	40000 psi

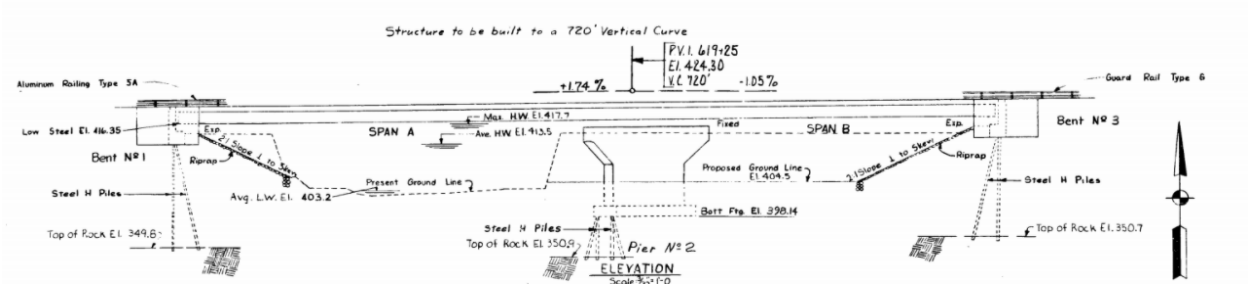

Figure A.18. Elevation View of the Bridge (NBI 22190) (1981)

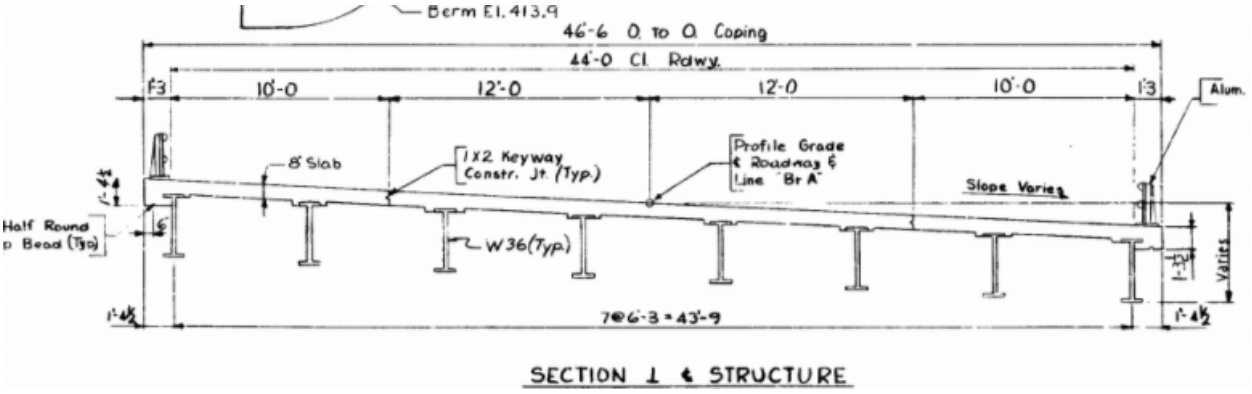

Figure A.19. Typical Section of the Bridge (NBI 22190) (1981)

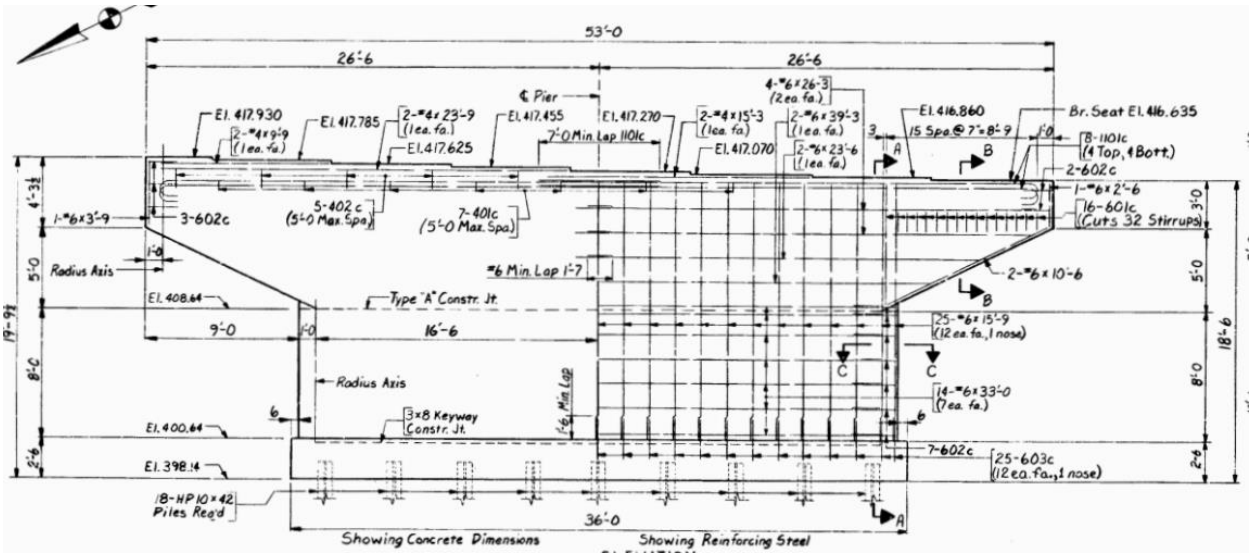

Figure A.20. Transverse Elevation of Interior Pier (NBI 22190) (1981)

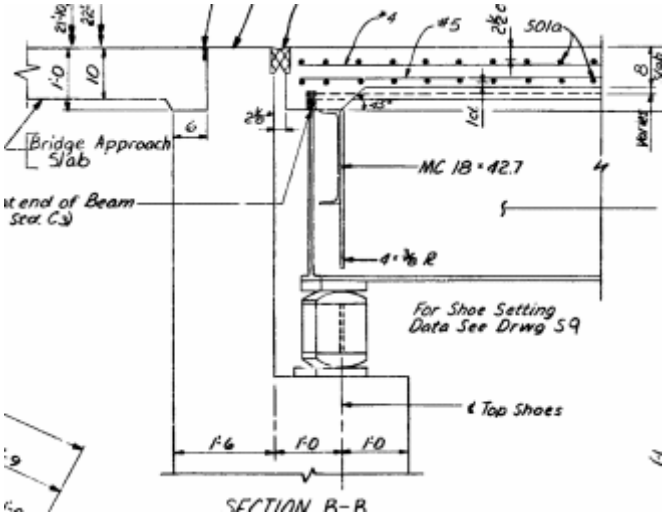

Figure A.21. Abutment Detail of the Bridge (NBI 22190) (1981)

Table A.10. Demand, Capacity, and Vulnerability of the Bridge (NBI 22190)

	Transverse Direction	Longitudinal Direction
Activated Mass (kips/g)	1.45	2.9
Total Stiffness (kips/in)	265701.7	1001.4
Period (s)	0.015	0.34
Base Shear Capacity	1.38	0.1
Shear Capacity (kips)	2892	1149
Shear Connection (kips)	319.7	
Vulnerability	Not Vulnerable	Highly Vulnerable – Potential for Brittle Failure

6. Bridge Asset Name: 062-13-07329 – NBI 22240

Table A.11. Specifications and Information on Bridge 062-13-07329 (NBI 22240)

Geographical Information	Asset Name	062-13-07329
	NBI Number	22240
	County	Crawford
	District	Vincennes
	Year of Construction	1994
	Year of Reconstruction	N/A
	Facility Carried	SR 62/SR 66
	Feature Intersected	LITTLE BLUE RIVER
Superstructure Information	No. Beams + Beam Type	6; Plate Girder
	Number of Spans	3
	Span Lengths	97'-0", 121'-0", 97'-0"
	Deck Width	40'-3"
	Deck Thickness	8"
	Skew	05.00 degrees
Substructure Information	Substructure Type	Hammerhead
	Height of Wall	33'-0", 33'-0"
	Width of Element (Base)	42'-6", 42'-6"
	Thickness of Wall	2'-6", 2'-6"
	Abutment Type	Elastomeric Bearing Pad
	Concrete Compressive Strength	3000 psi
	Yield Strength of Reinforcement	40000 psi

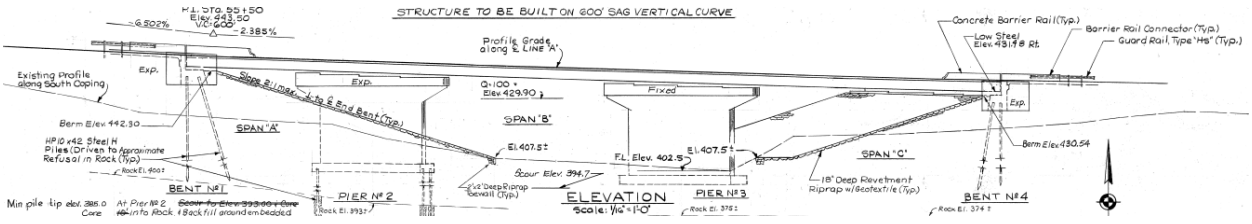

Figure A.22. Elevation View of the Bridge (NBI 22240) (1989)

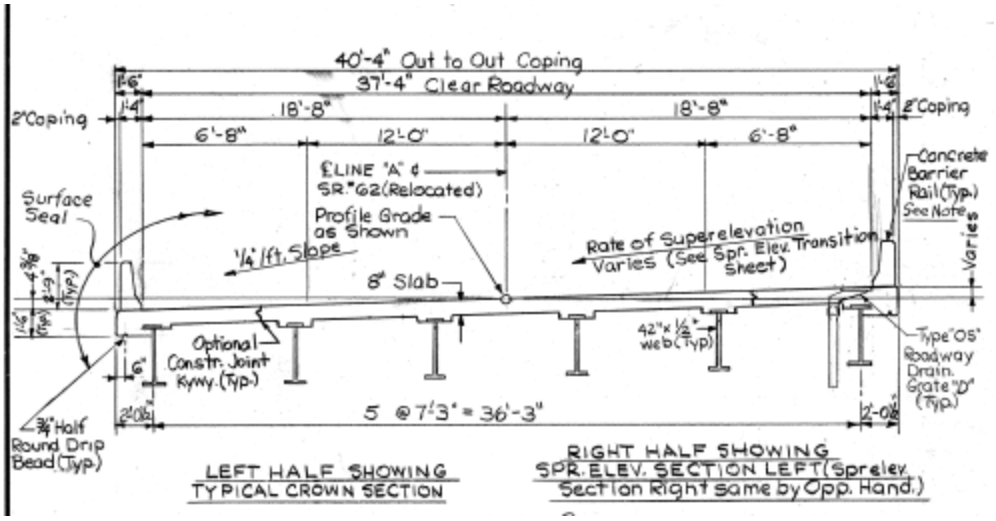

Figure A.23. Typical Section of the Bridge (NBI 22240) (1989)

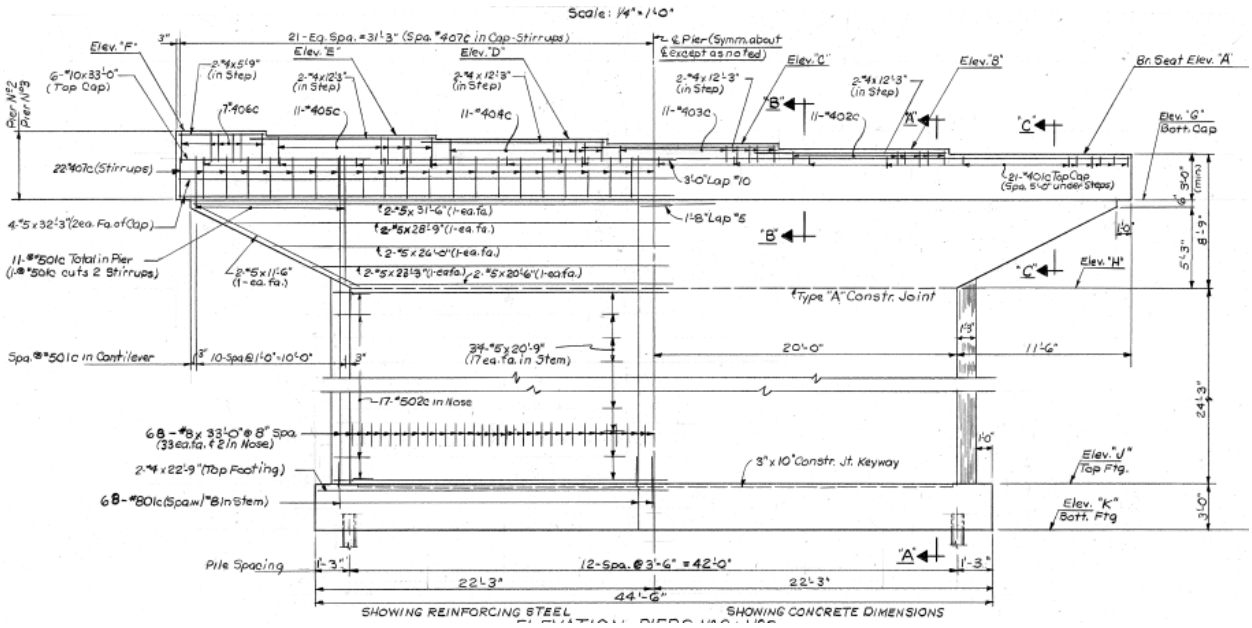

Figure A.24. Transverse Elevation of Interior Pier (NBI 22240) (1989)

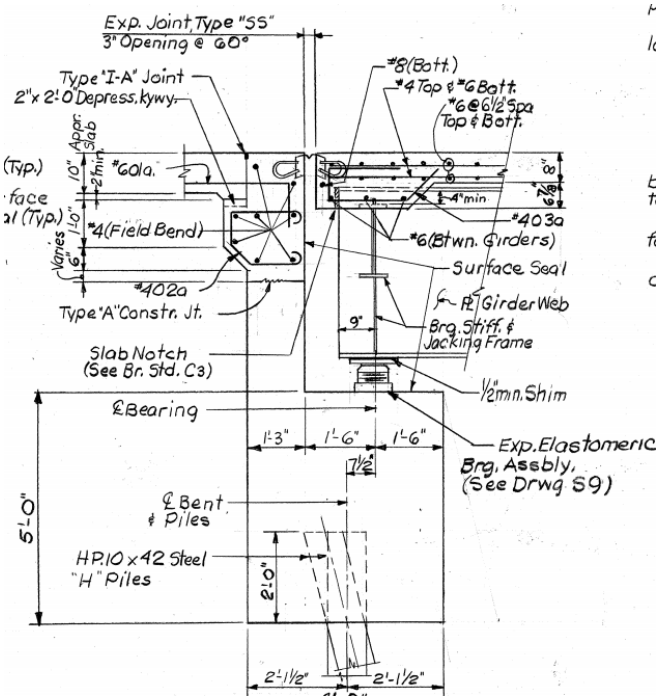

Figure A.25. Abutment Detail of the Bridge (NBI 22240) (1989)

Table A.12. Demand, Capacity, and Vulnerability of the Bridge (NBI 22240)

	Transverse Direction	Longitudinal Direction
Activated Mass (kips/g)	3.34	4.83
Total Stiffness (kips/in)	189423.4	174.9
Period (s)	0.026	1.04
Base Shear Capacity	3.45; 3.45	0.21; 0.21
Shear Capacity (kips)	3217; 3217	1279; 1279
Shear Connection (kips)	368.3	
Vulnerability	Not Vulnerable	Moderately Vulnerable

7. Bridge Asset Name: 067-18-05459 D – NBI 24210

Table A.13. Specifications and Information on Bridge 067-18-05459 D (NBI 24210)

Geographical Information	Asset Name	067-18-05459 D
	NBI Number	24210
	County	Delaware
	District	Greenfield
	Year of Construction	1973
	Year of Reconstruction	N/A
	Facility Carried	OLD SR 3/WALNUT ST
	Feature Intersected	SR 67
Superstructure Information	No. Beams + Beam Type	8; Plate Girder
	Number of Spans	2
	Span Lengths	91'-0", 91'-0"
	Deck Width	47'-0"
	Deck Thickness	8"
	Skew	05.00 degrees
Substructure Information	Substructure Type	Hammerhead
	Height of Wall	23'-6"
	Width of Element (Base)	27'-0"
	Thickness of Wall	2'-0"
	Abutment Type	Expansion Shoe
	Concrete Compressive Strength	3000 psi
	Yield Strength of Reinforcement	40000 psi

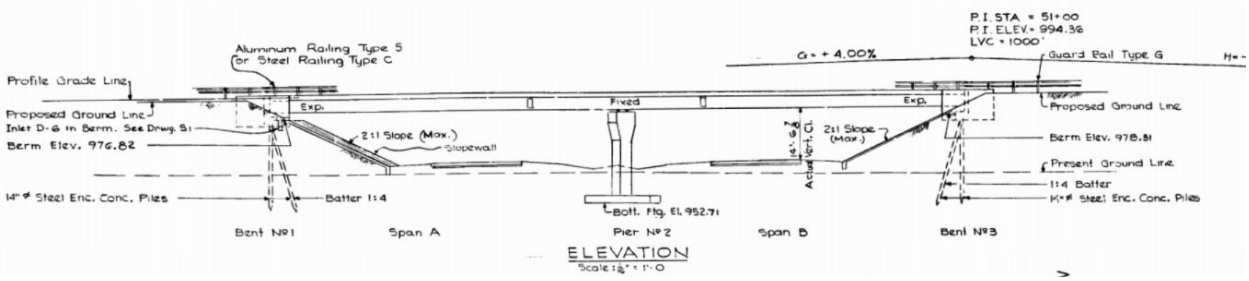

Figure A.26. Elevation View of the Bridge (NBI 24210) (1971)

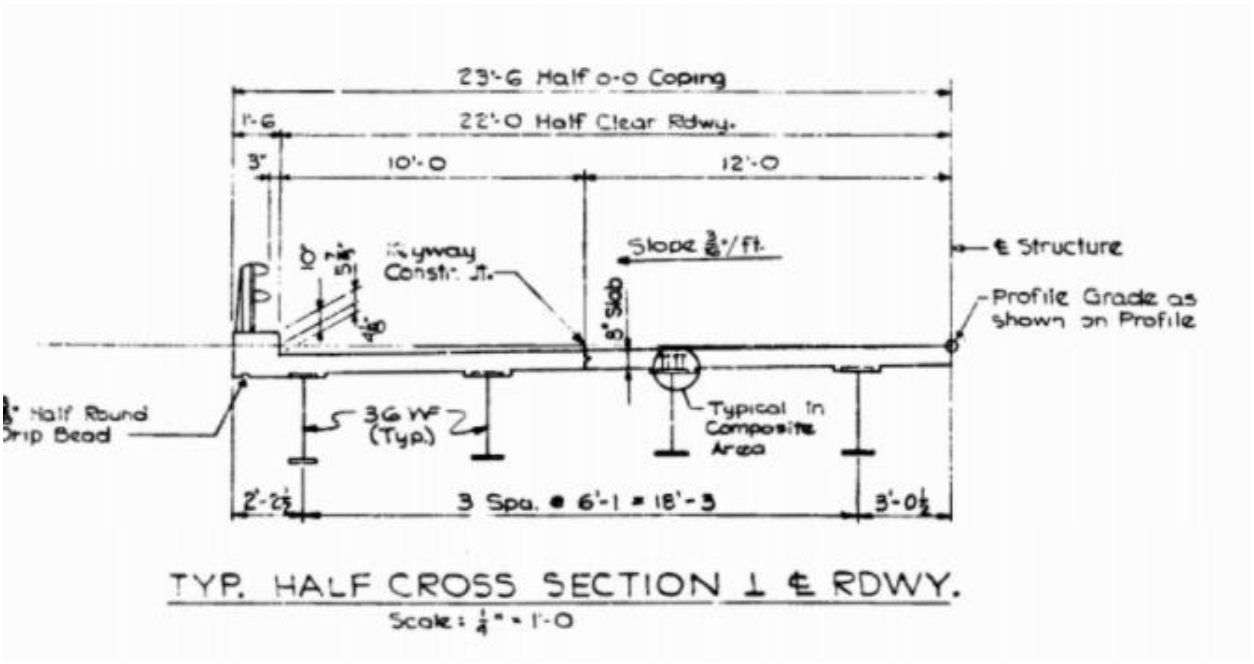

Figure A.27. Typical Section of the Bridge (NBI 24210) (1971)

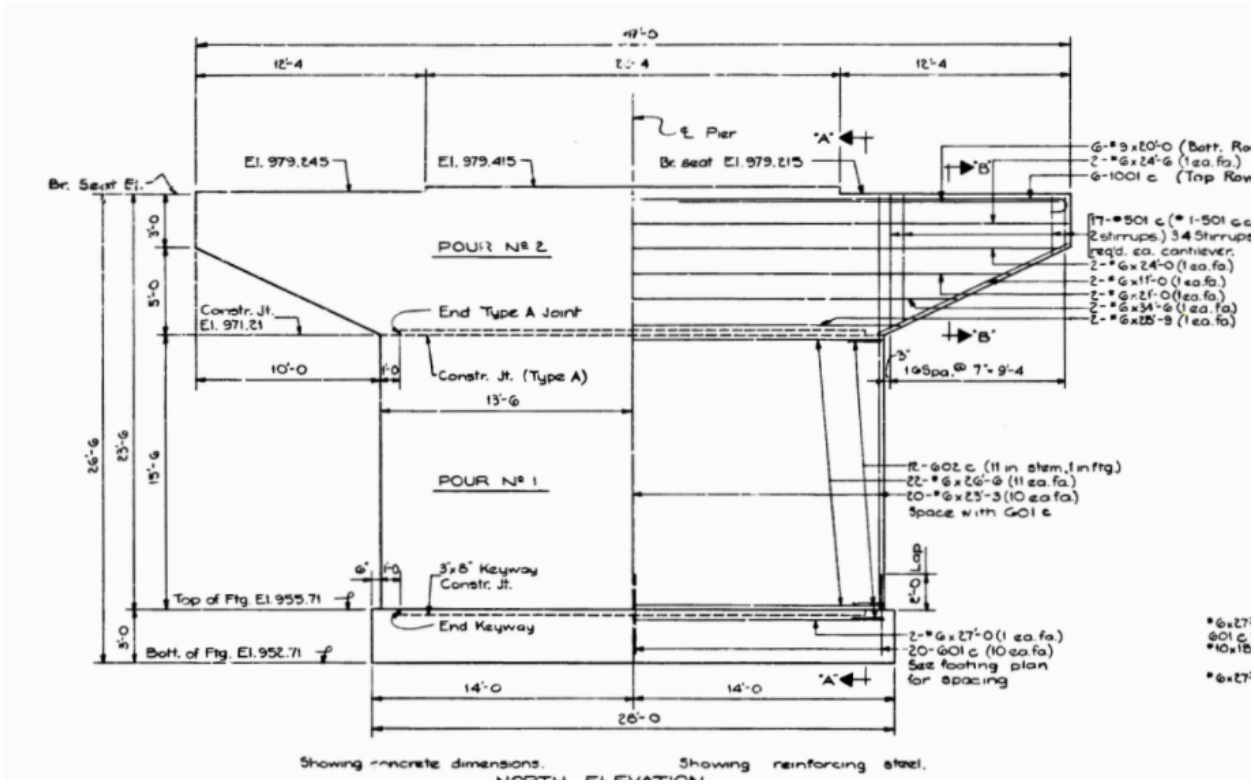

Figure A.28. Transverse Elevation of Interior Pier (NBI 24210) (1971)

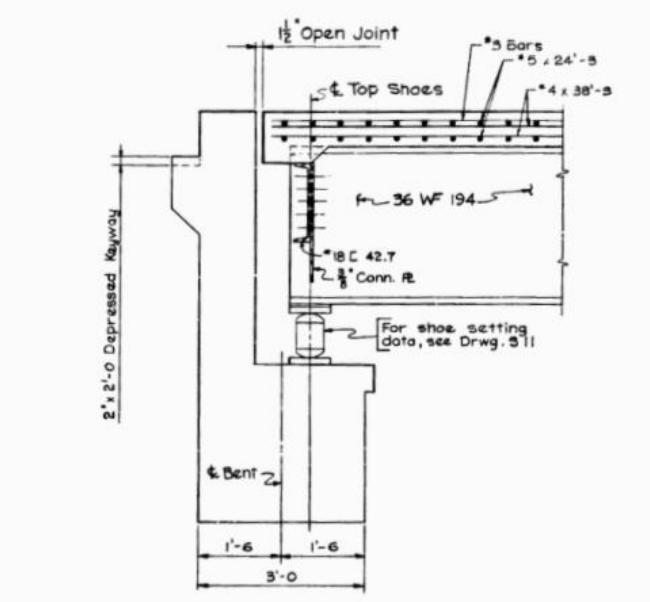

Figure A.29. Abutment Detail of the Bridge (NBI 24210) (1971)

Table A.14. Demand, Capacity, and Vulnerability of the Bridge (NBI 24210)

	Transverse Direction	**Longitudinal Direction**
Activated Mass (kips/g)	1.74	3.49
Total Stiffness (kips/in)	60231.2	157.5
Period (s)	0.034	0.93
Base Shear Capacity	0.53	0.04
Shear Capacity (kips)	1724	680
Shear Connection (kips)	371.2	
Vulnerability	Not Vulnerable	Highly Vulnerable – Potential for Brittle Failure

8. Bridge Asset Name: (421)39-12-01792 B – NBI 32200

Table A.15. Specifications and Information on Bridge (421)39-12-01792 B (NBI 32200)

Geographical Information	Asset Name	(421)39-12-01792 B
	NBI Number	32200
	County	Clinton
	District	Crawfordsville
	Year of Construction	1941
	Year of Reconstruction	1985
	Facility Carried	US 421
	Feature Intersected	S FORK WILDCAT CREEK
Superstructure Information	No. Beams + Beam Type	5; Truss
	Number of Spans	3
	Span Lengths	30'-0", 132'-0", 30'-0"
	Deck Width	30'-6"
	Deck Thickness	6.75"
	Skew	18.00 degrees
Substructure Information	Substructure Type	Wall
	Height of Wall	18'-1", 18'-1"
	Width of Element (Base)	36'-10", 36'-10"
	Thickness of Wall	3'-0", 3'-0"
	Abutment Type	Expansion Shoe
	Concrete Compressive Strength	3500 psi
	Yield Strength of Reinforcement	40000 psi

Bridge Modeling Assumptions:

Structure Number (421)39-12-01792 B is a three-span bridge. The first and the third span have reinforced concrete girder superstructures and the second span is a steel truss superstructure. There are two expansion joints which separate the bridge at each of the intermediate piers. Because of the expansion joints, the bridge is modeled as three single-span systems. However, due to the fixity of the connection between the substructure and the superstructure, at the locations of fixed connections, the substructure performance must be checked in the transverse direction. The bridge was modeled as a 3-span bridge with both intermediate piers adding stiffness. In the longitudinal direction, the three spans move separately and are treated as single span structures and therefore are not vulnerable.

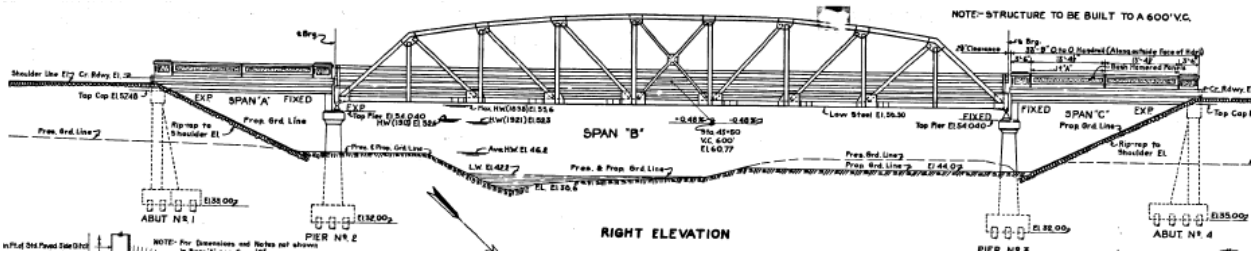

Figure A.30. Elevation View of the Bridge (NBI 32200) (1940)

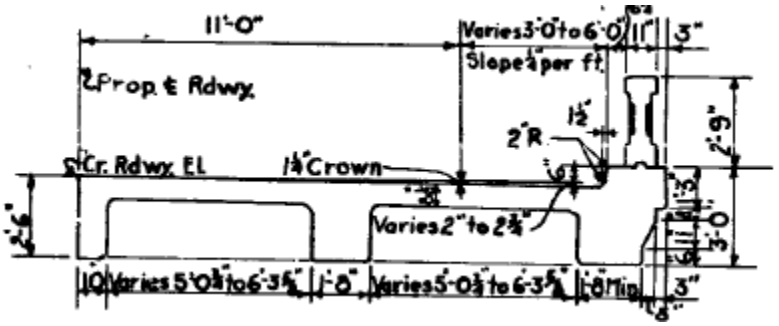

Figure A.31. Typical Section of Spans 1 and 3 of the Bridge (NBI 32200) (1940)

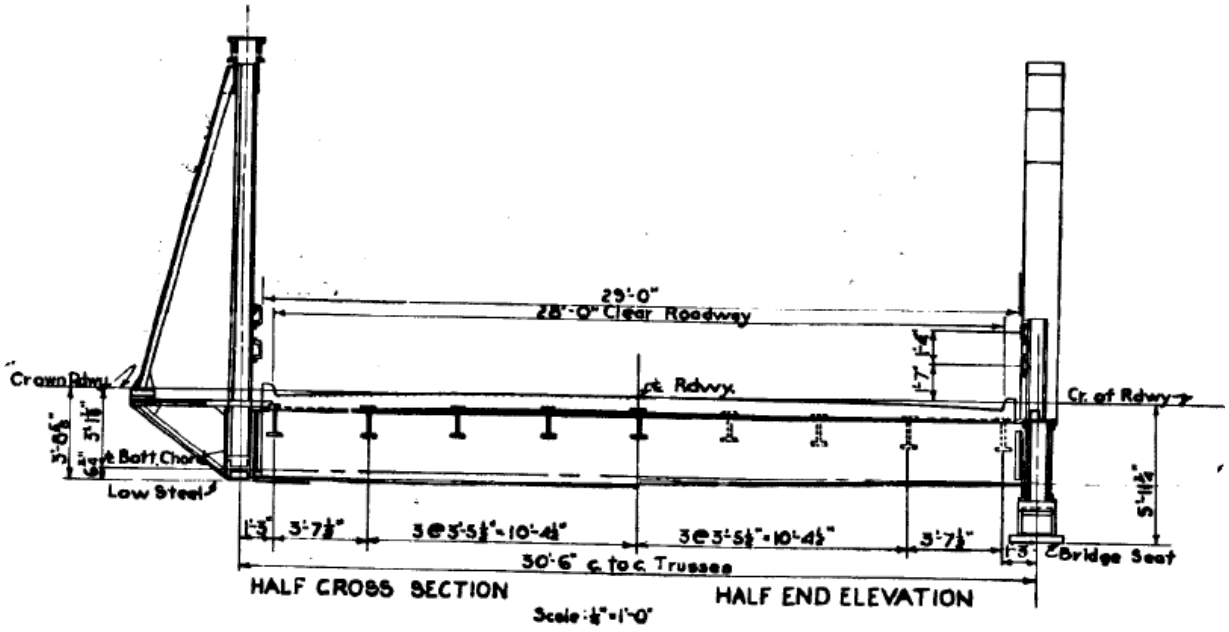

Figure A.32. Typical Section of Span 2 of the Bridge (NBI 32200) (1940)

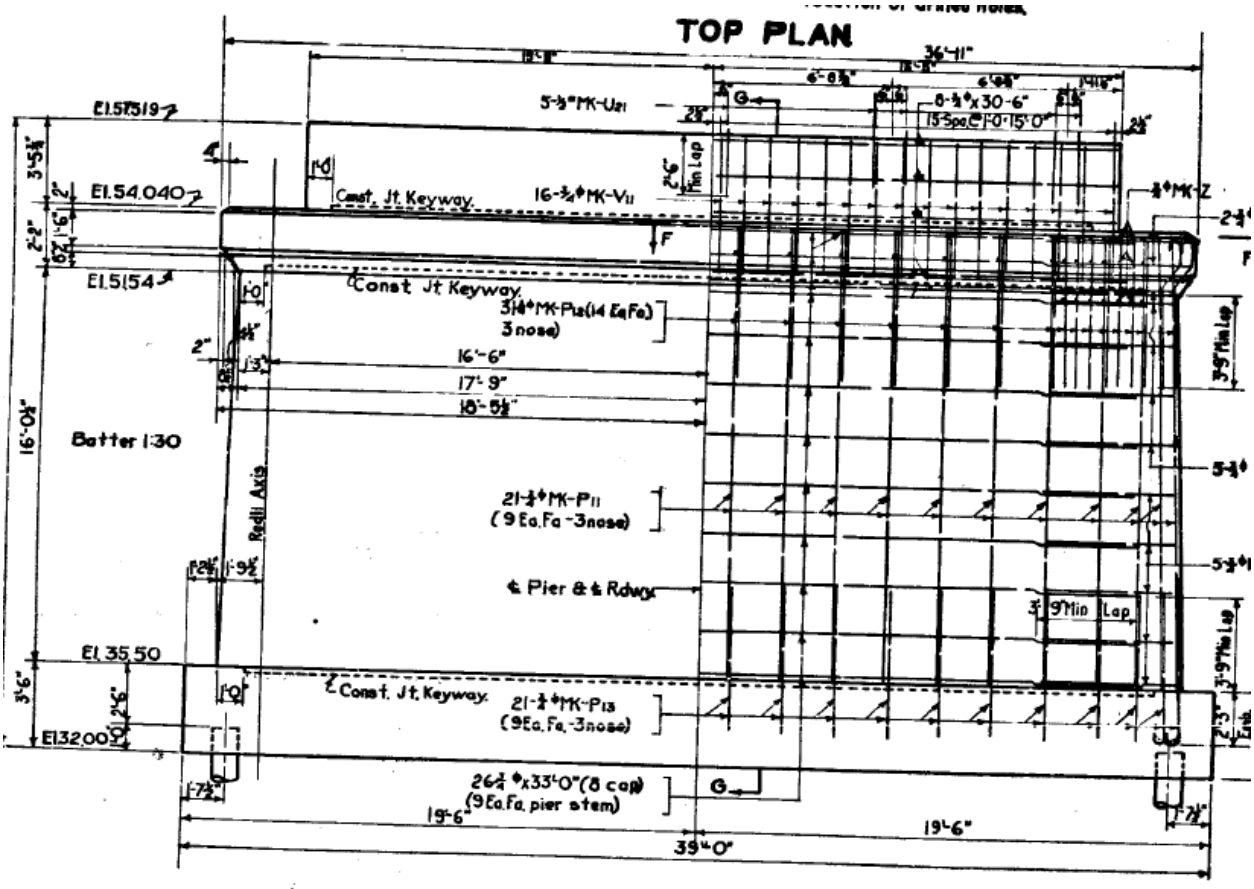

Figure A.33. Transverse Elevation of Interior Pier (NBI 24210) (1971)

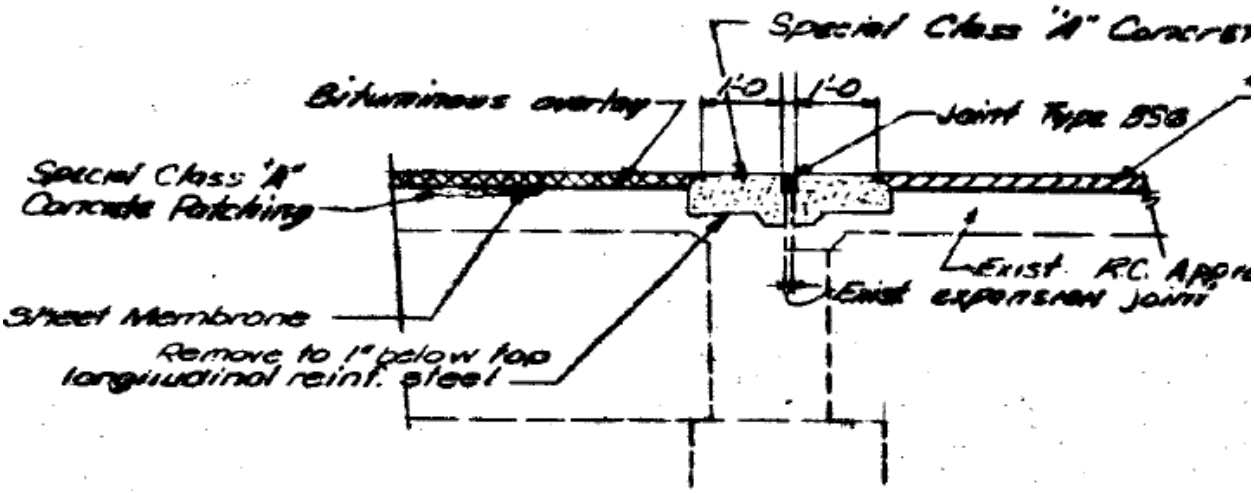

Figure A.34. Abutment Detail of the Bridge (NBI 32200) (1974)

Table A.16. Demand, Capacity, and Vulnerability of the Bridge (NBI 32200)

	Transverse Direction	Longitudinal Direction
Activated Mass (kips/g)	2.18	2.59
Total Stiffness (kips/in)	696164	3404.6
Period (s)	0.011	0.17
Base Shear Capacity	3.51; 3.51	0.29; 0.29
Shear Capacity (kips)	3480; 3480	1534; 1534
Shear Connection (kips)	240.9	
Vulnerability	Not Vulnerable	Not Vulnerable

9. Bridge Asset Name: I469-12-06974 AEB – NBI 32841

Table A.17. Specifications and Information on Bridge I469-12-06974 AEB (NBI 32841)

Geographical Information	Asset Name	I469-12-06947 AEB
	NBI Number	32841
	County	Allen
	District	Fort Wayne
	Year of Construction	1990
	Year of Reconstruction	2016
	Facility Carried	I-469 EB
	Feature Intersected	US 27 NB/SB
Superstructure Information	No. Beams + Beam Type	7; Plate Girder
	Number of Spans	2
	Span Lengths	123'-0", 123'-0"
	Deck Width	48'-8"
	Deck Thickness	7.5"
	Skew	20.00 degrees
Substructure Information	Sub. Type; No. of Elements	Frame Bent; 4
	Height of Wall	14'-9"
	Element Spacing	10'-3"
	Element Dimensions	2'-0" x 3'-0"
	Abutment Type	Semi-Integral
	Concrete Compressive Strength	3500 psi
	Yield Strength of Reinforcement	40000 psi

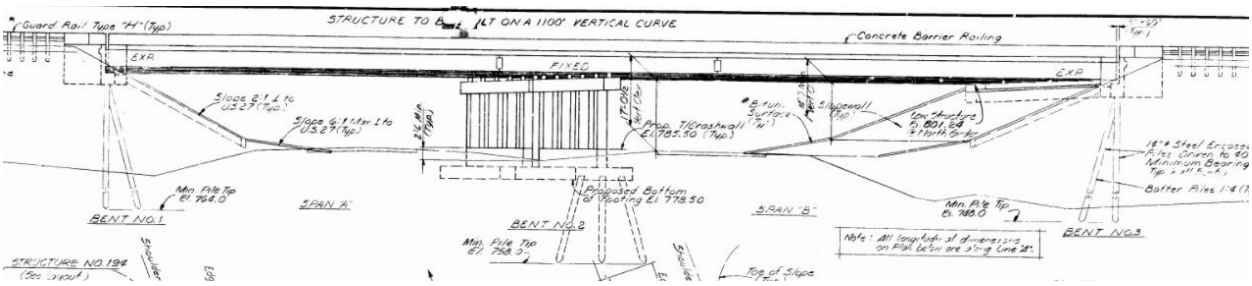

Figure A.35. Elevation View of the Bridge (NBI 32841) (1981)

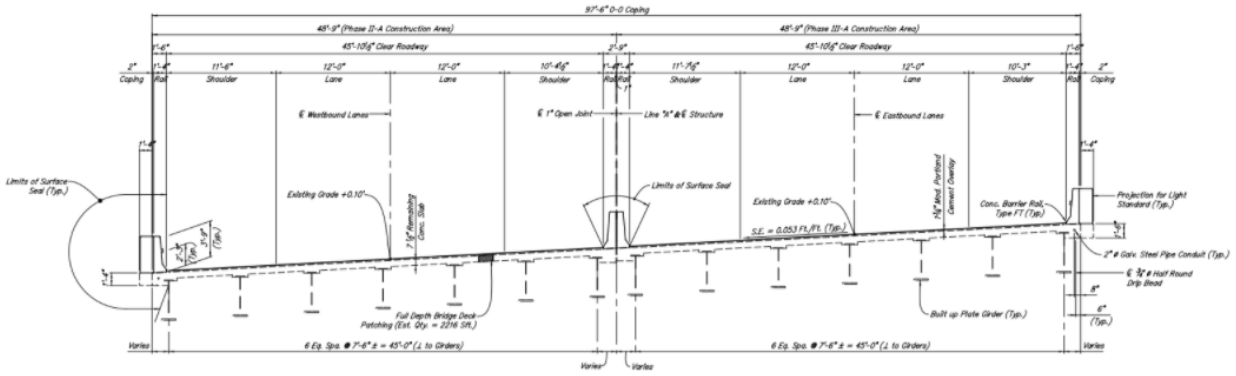

Figure A.36. Typical Section of the Bridge (NBI 32841) (2014)

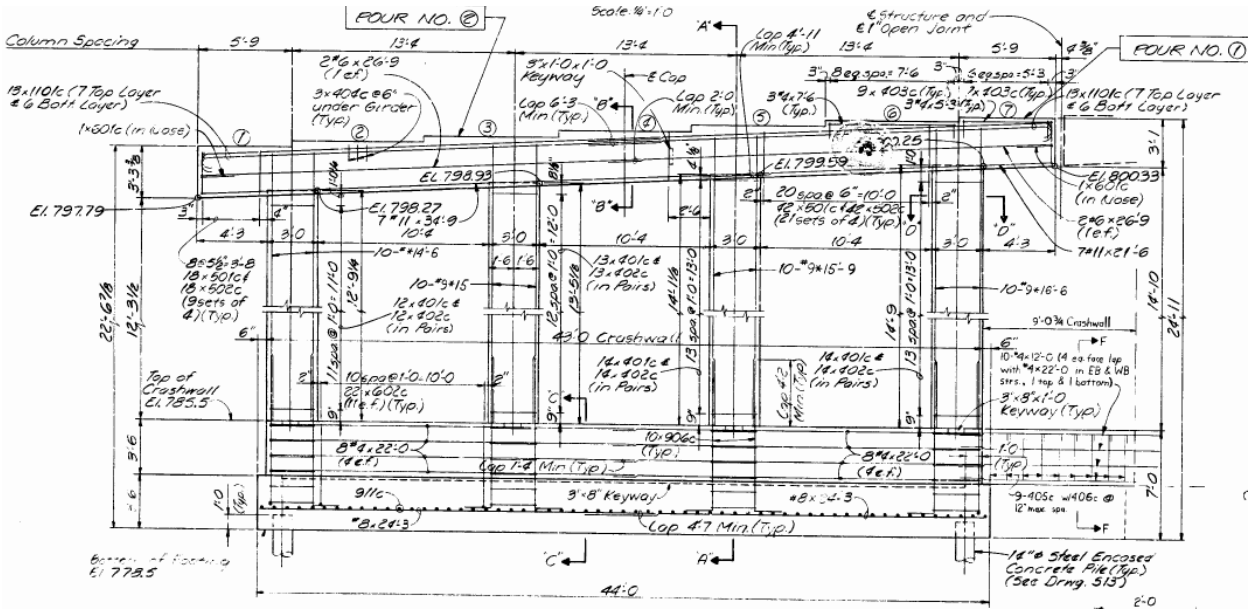

Figure A.37. Transverse Elevation of Interior Pier (NBI 32841) (1987)

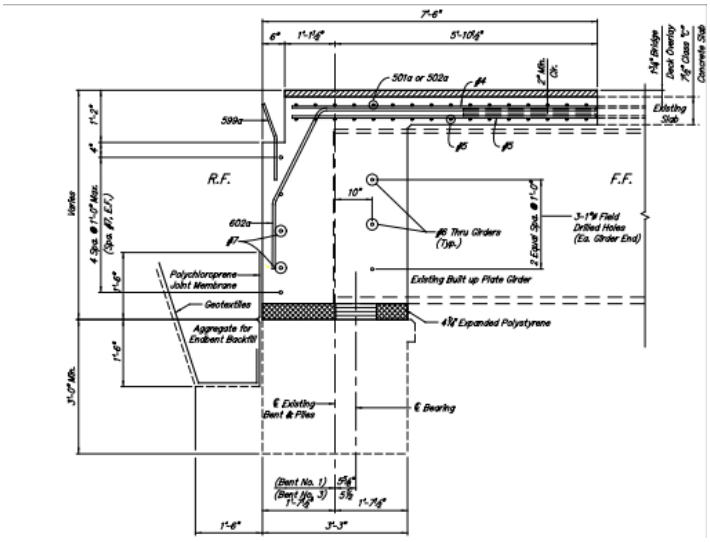

Figure A.38. Abutment Detail of the Bridge (NBI 32841) (2014)

Table A.18. Demand, Capacity, and Vulnerability of the Bridge (NBI 32841)

	Transverse Direction	**Longitudinal Direction**
Activated Mass (kips/g)	1.93	3.87
Total Stiffness (kips/in)	2312.9	225.4
Period (s)	0.182	0.82
Base Shear Capacity	0.36	0.1
Shear Capacity (kips)	328	268
Shear Connection (kips)	426.2	
Vulnerability	Moderately Vulnerable	Not Vulnerable due to Abutment

10. Bridge Asset Name: I65-118-02313 JCSB – NBI 36890

Table A.19. Specifications and Information on Bridge I65-118-02313 JCSB (NBI 36890)

Geographical Information	Asset Name	I65-118-02313 JCSB
	NBI Number	36890
	County	Marion
	District	Greenfield
	Year of Construction	1964
	Year of Reconstruction	2001
	Facility Carried	I-65 SB
	Feature Intersected	CSX RR, GUION ROAD
Superstructure Information	No. Beams + Beam Type	12; Plate Girder
	Number of Spans	4
	Span Lengths	44'-10", 83'-4", 82'-11", 44'-9"
	Deck Width	71'-5"
	Deck Thickness	8"
	Skew	10.00 degrees
Substructure Information	Substructure Type	Wall
	Height of Wall	26'-3", 27'-6", 21'-6"
	Width of Element (Base)	79'-3", 77'-6", 77'-0"
	Thickness of Wall	2'-0", 2'-0", 2'-0"
	Abutment Type	Semi-Integral
	Concrete Compressive Strength	3500 psi
	Yield Strength of Reinforcement	60000 psi

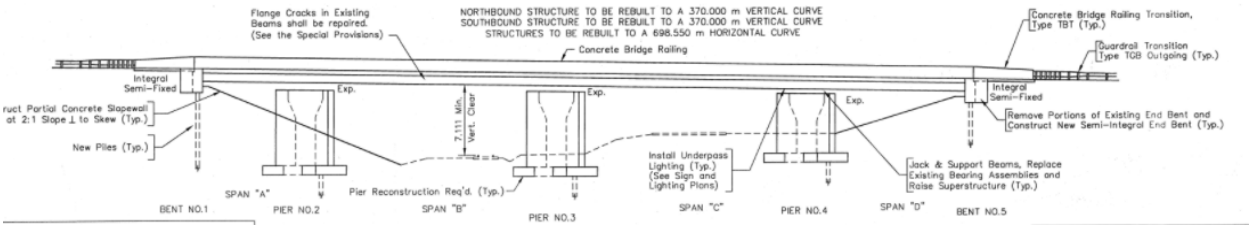

Figure A.39. Elevation View of the Bridge (NBI 36890) (2001)

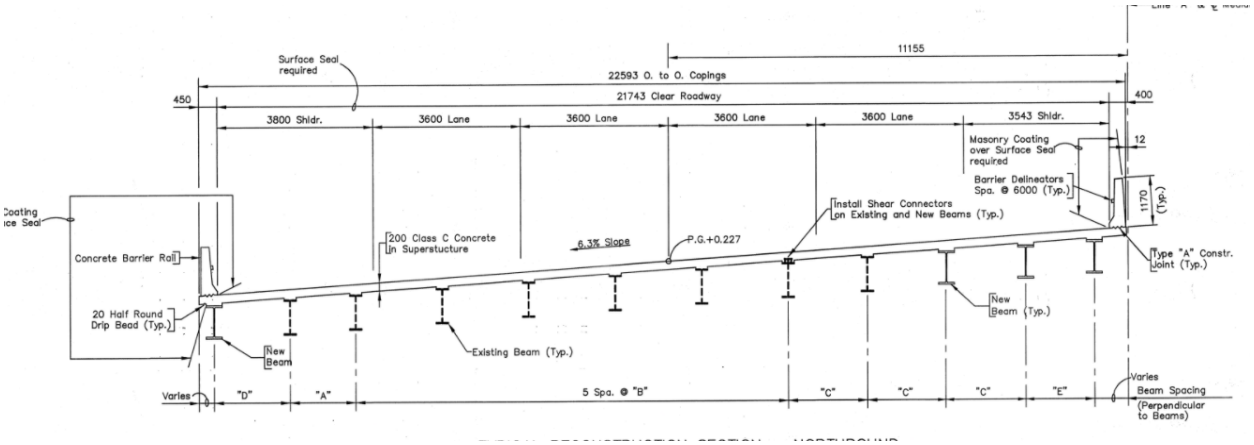

Figure A.40. Typical Section of the Bridge (NBI 36890) (2001)

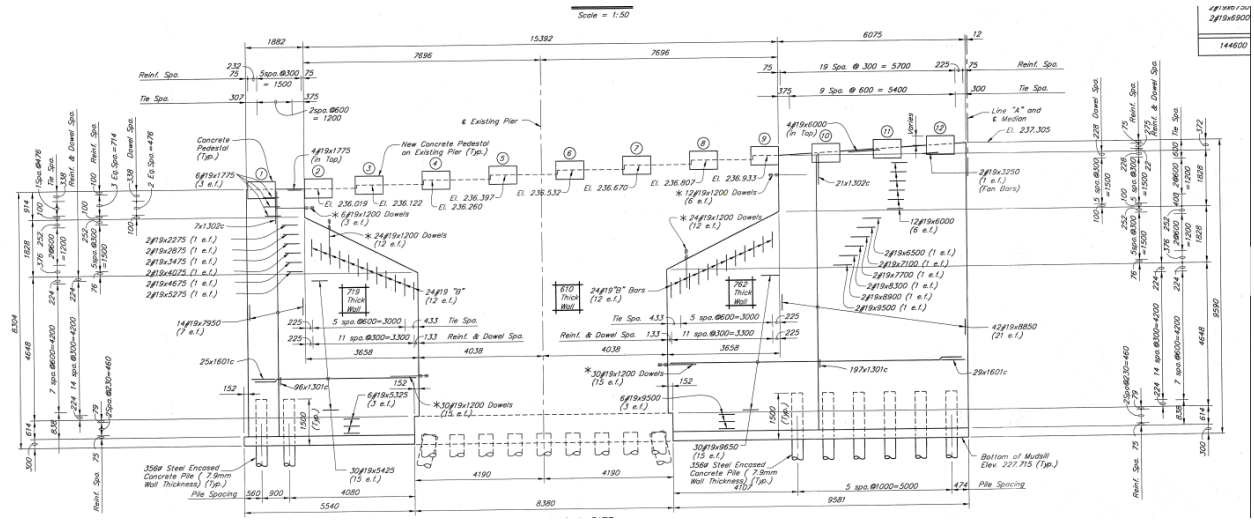

Figure A.41. Transverse Elevation of Interior Pier (NBI 36890) (2001)

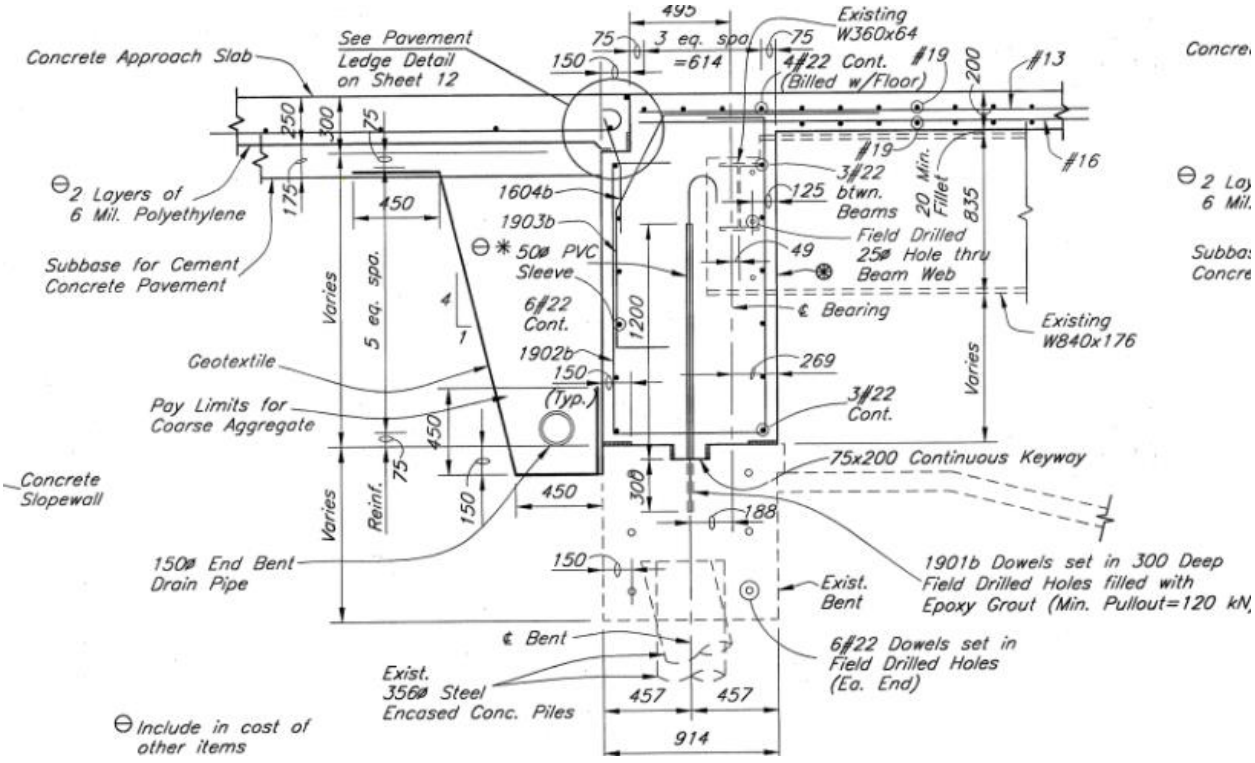

Figure A.42. Abutment Detail of the Bridge (NBI 36890) (2001)

Table A.20. Demand, Capacity, and Vulnerability of the Bridge (NBI 36890)

	Transverse Direction	Longitudinal Direction
Activated Mass (kips/g)	5.05	6.12
Total Stiffness (kips/in)	2242943.1	1297.8
Period (s)	0.009	0.43
Base Shear Capacity	8.45; 5.7; 12.2	0.21; 0.15; 0.31
Shear Capacity (kips)	8237; 8056; 8010	2116; 2074; 2031
Shear Connection (kips)	337.5	
Vulnerability	Not Vulnerable	Not Vulnerable due to Abutment

11. Bridge Asset Name: I69-309-04548 – NBI 40300

Table A.21. Specifications and Information on Bridge I68-309-04548 (NBI 40300)

Geographical Information	Asset Name	I69-309-04548 B
	NBI Number	40300
	County	Allen
	District	Fort Wayne
	Year of Construction	1960
	Year of Reconstruction	1988
	Facility Carried	HILLEGAS ROAD
	Feature Intersected	I-69 NB/SB
Superstructure Information	No. Beams + Beam Type	7; Plate Girder
	Number of Spans	4
	Span Lengths	65'-0", 104'-3", 104'-3", 49'-0"
	Deck Width	33'-3"
	Deck Thickness	6.25"
	Skew	51.00 degrees
Substructure Information	Sub. Type; No. of Elements	Frame Bent; 4
	Height of Wall	10'-9", 10'-6", 8'-7"
	Element Spacing	11'-0", 11'-0", 11'-0"
	Element Dimensions	2'-0" x 3'-0", 2'-0" x 3'-0", 2'-0" x 3'-0"
	Abutment Type	Expansion Shoe
	Concrete Compressive Strength	3500 psi
	Yield Strength of Reinforcement	40000 psi

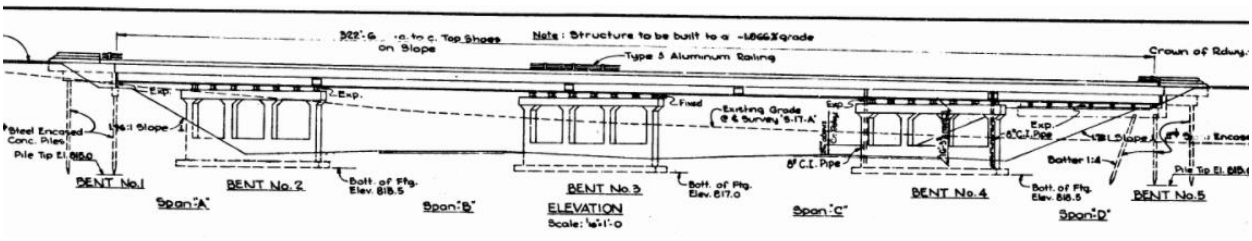

Figure A.43. Elevation View of the Bridge (NBI 40300) (1960)

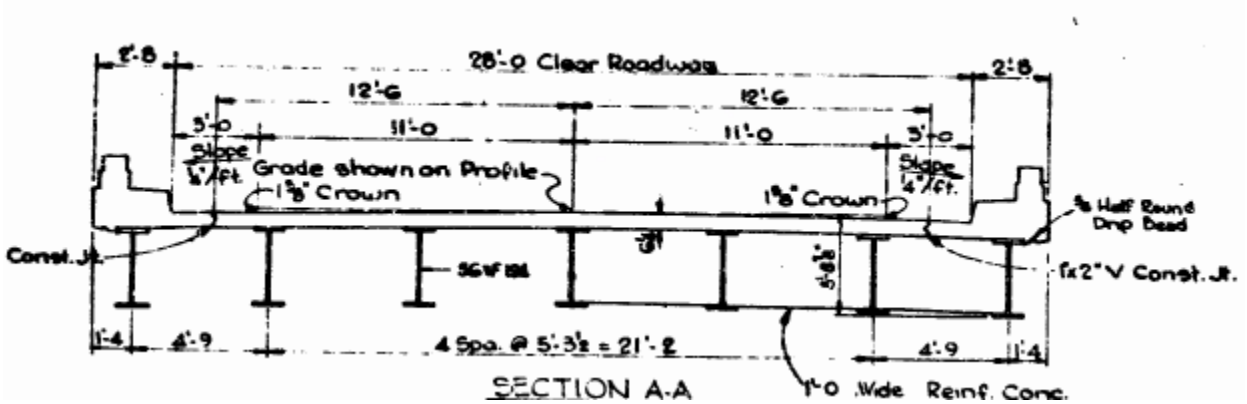

Figure A.44. Typical Section of the Bridge (NBI 40300) (1960)

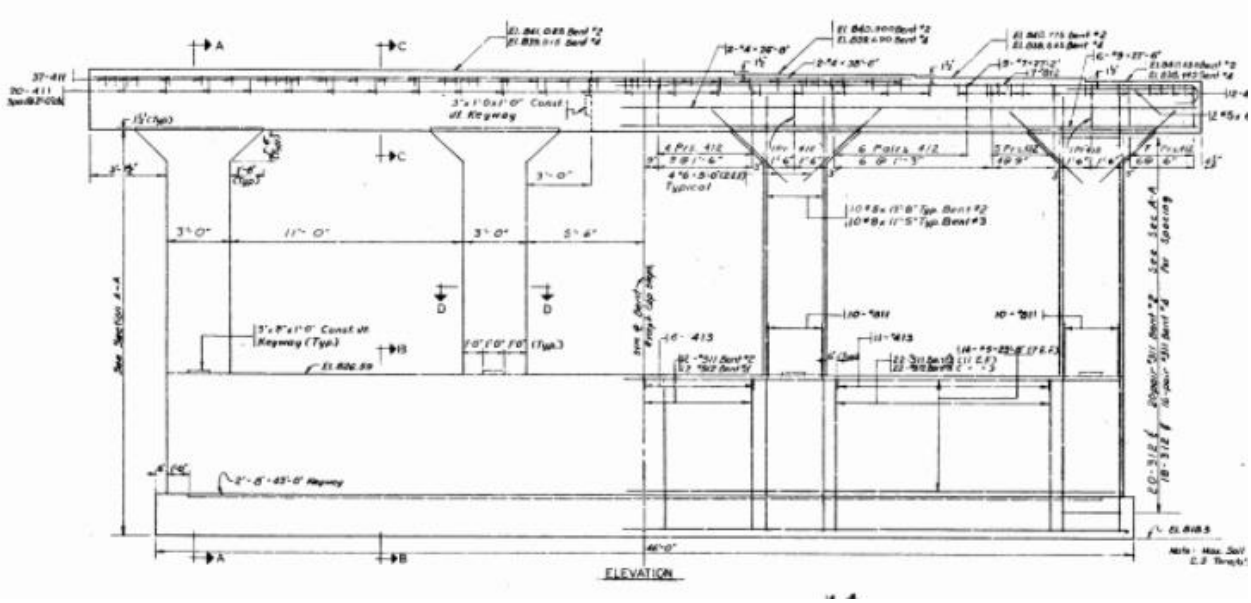

Figure A.45. Transverse Elevation of Interior Pier (NBI 40300) (1960)

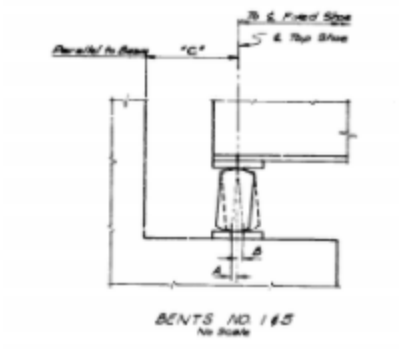

Figure A.46. Abutment Detail of the Bridge (NBI 40300) (1960)

Table A.22. Demand, Capacity, and Vulnerability of the Bridge (NBI 40300)

	Transverse Direction	Longitudinal Direction
Activated Mass (kips/g)	3.37	4.1
Total Stiffness (kips/in)	22455.8	556.7
Period (s)	0.077	0.54
Base Shear Capacity	0.74; 0.61; 1.02	0.05; 0.04; 0.07
Shear Capacity (kips)	304; 304; 304	268; 268; 268
Shear Connection (kips)	227.5	
Vulnerability	Not Vulnerable	Moderately Vulnerable

12. Bridge Asset Name: I70-006-04712 BEBL – NBI 41130

Table A.23. Specifications and Information on Bridge I70-006-04712 BEBL (NBI 41130)

Geographical Information	Asset Name	I70-006-04712 BEBL
	NBI Number	41130
	County	Vigo
	District	Crawfordsville
	Year of Construction	1964
	Year of Reconstruction	1980
	Facility Carried	I-70 EB
	Feature Intersected	US 41 SB/NB
Superstructure Information	No. Beams + Beam Type	8; Rolled Shape
	Number of Spans	4
	Span Lengths	39'-0", 58'-9", 58'-9", 39'-0"
	Deck Width	44'-6"
	Deck Thickness	8"
	Skew	18.00 degrees
Substructure Information	Substructure Type	Wall
	Height of Wall	18'-4", 20'-3", 18'-4"
	Width of Element (Base)	45'-3", 45'-3", 45'-3"
	Thickness of Wall	2'-0", 2'-0", 2'-0"
	Abutment Type	Semi-Integral
	Concrete Compressive Strength	3500 psi
	Yield Strength of Reinforcement	60000 psi

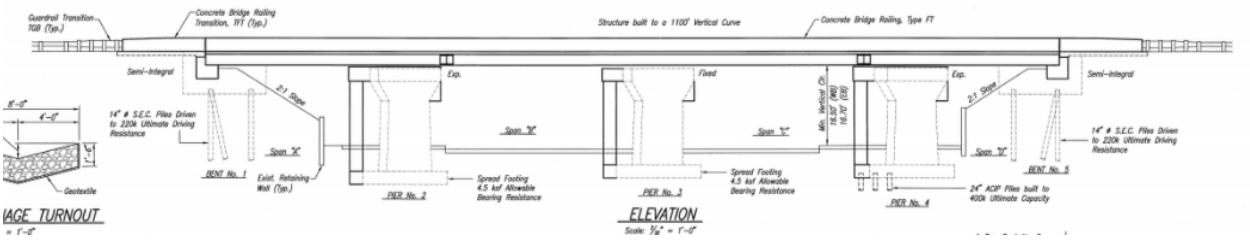

Figure A.47. Elevation View of the Bridge (NBI 41130) (2015)

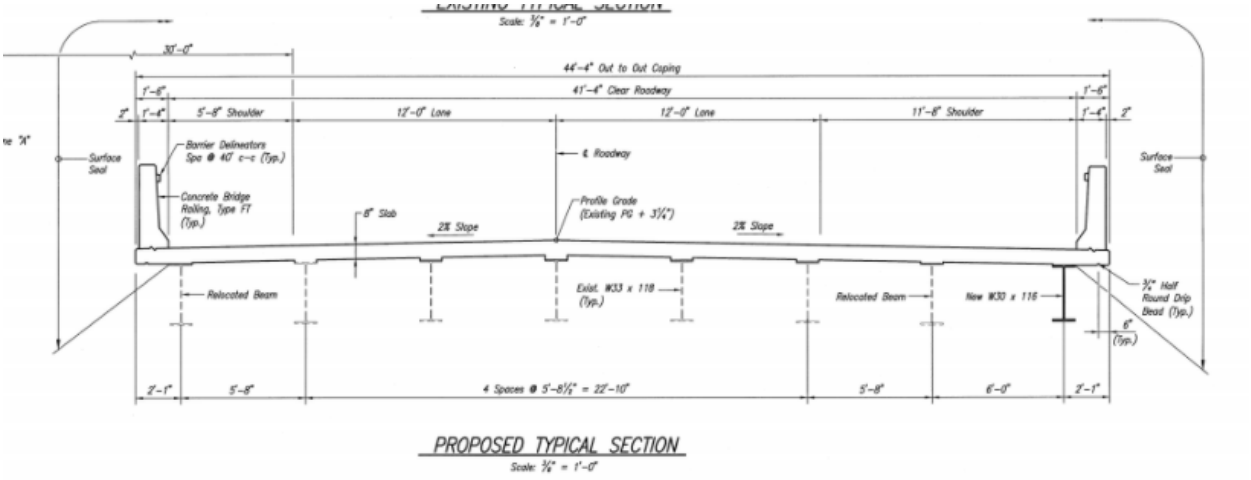

Figure A.48. Typical Section of the Bridge (NBI 41130) (2015)

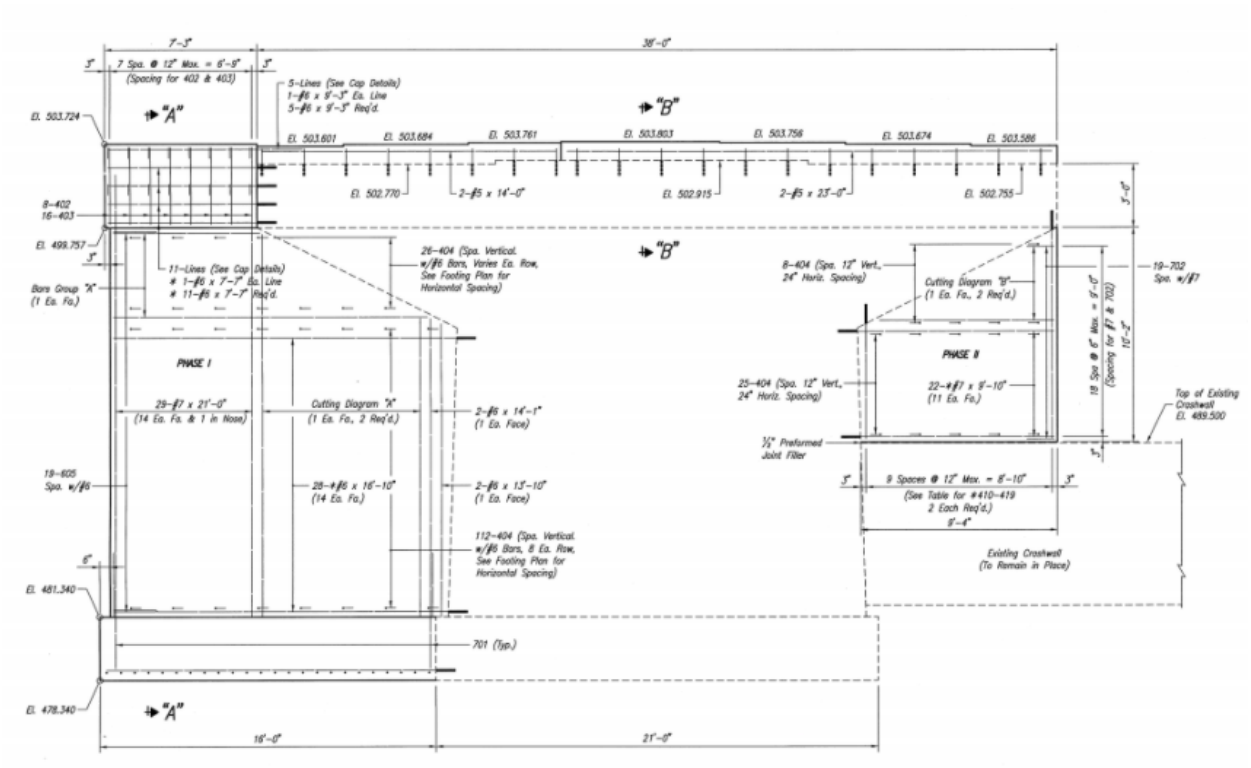

Figure A.49. Transverse Elevation of Interior Pier (NBI 41130) (2015)

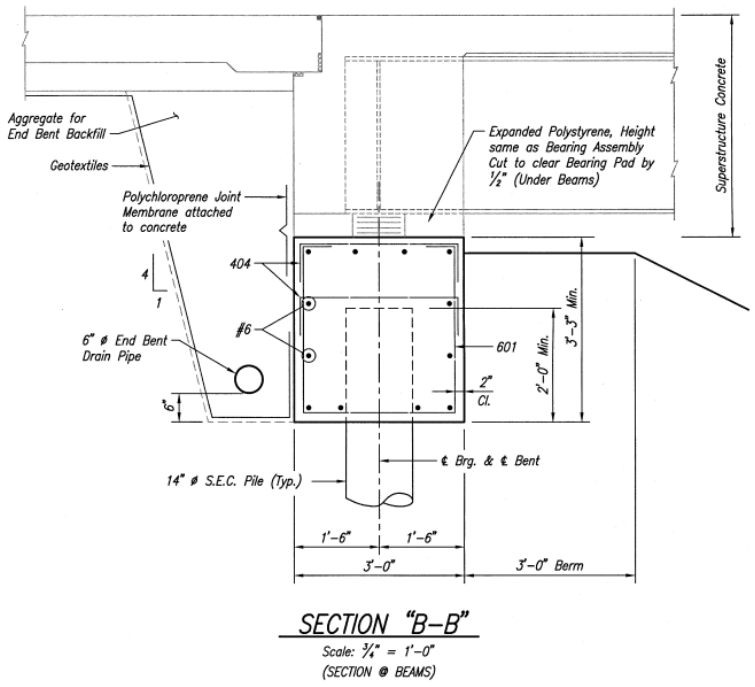

Figure A.50. Abutment Detail of the Bridge (NBI 41130) (2015)

Table A.24. Demand, Capacity, and Vulnerability of the Bridge (NBI 41130)

	Transverse Direction	**Longitudinal Direction**
Activated Mass (kips/g)	2.66	3.32
Total Stiffness (kips/in)	1046452.8	1630.1
Period (s)	0.01	0.28
Base Shear Capacity	9.12; 6.88; 9.12	0.4; 0.3; 0.4
Shear Capacity (kips)	3508; 3508; 3508	1191; 1191; 1191
Shear Connection (kips)	182.8	
Vulnerability	Not Vulnerable	Not Vulnerable due to Abutment

13. Bridge Asset Name: I70-008-02344 BEBL – NBI 41230

Table A.25. Specifications and Information on Bridge I70-008-02344 BEBL (NBI 41230)

Geographical Information	Asset Name	I70-008-02344 BEBL
	NBI Number	41230
	County	Vigo
	District	Crawfordsville
	Year of Construction	1964
	Year of Reconstruction	1980
	Facility Carried	I-70 EB
	Feature Intersected	THOMPSON DITCH, RR
Superstructure Information	No. Beams + Beam Type	7; Plate Girder
	Number of Spans	4
	Span Lengths	58'-9", 75'-3", 75'-3", 58'-9"
	Deck Width	44'-3"
	Deck Thickness	8"
	Skew	48.00 degrees
Substructure Information	Substructure Type	Wall
	Height of Wall	28'-2", 38'-0", 29'-3"
	Width of Element (Base)	50'-3", 50'-3", 50'-3"
	Thickness of Wall	2'-0", 2'-0", 2'-0"
	Abutment Type	Semi-Integral
	Concrete Compressive Strength	4000 psi
	Yield Strength of Reinforcement	60000 psi

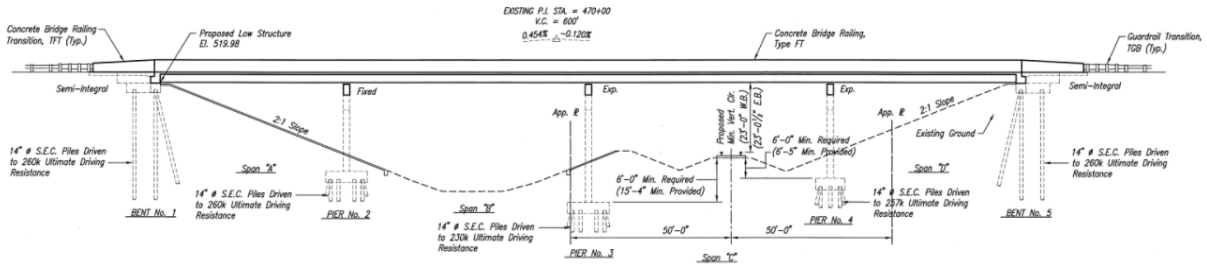

Figure A.51. Elevation View of the Bridge (NBI 41230) (2015)

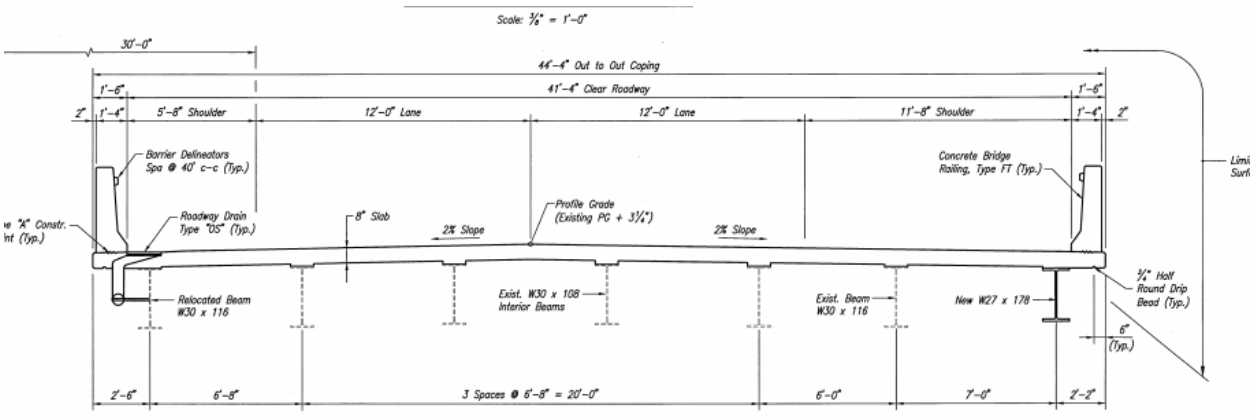

Figure A.52. Typical Section of the Bridge (NBI 41230) (2015)

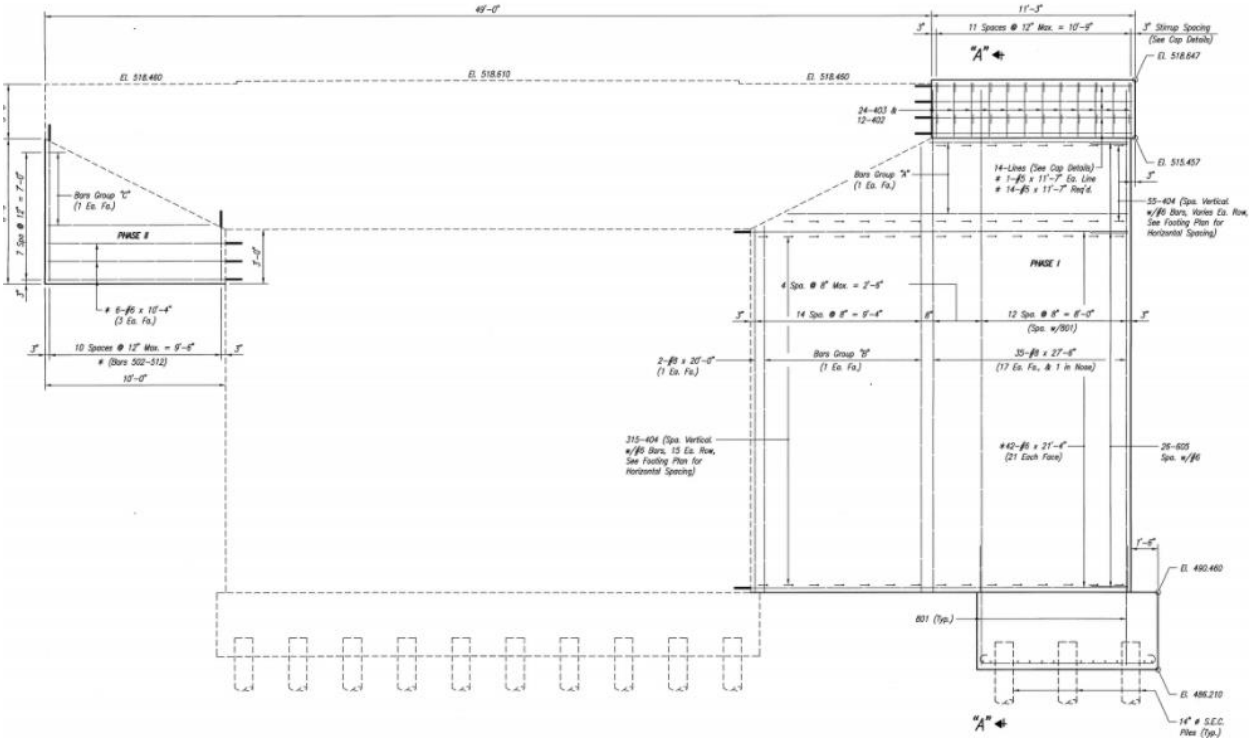

Figure A.53. Transverse Elevation of Interior Pier (NBI 41230) (2015)

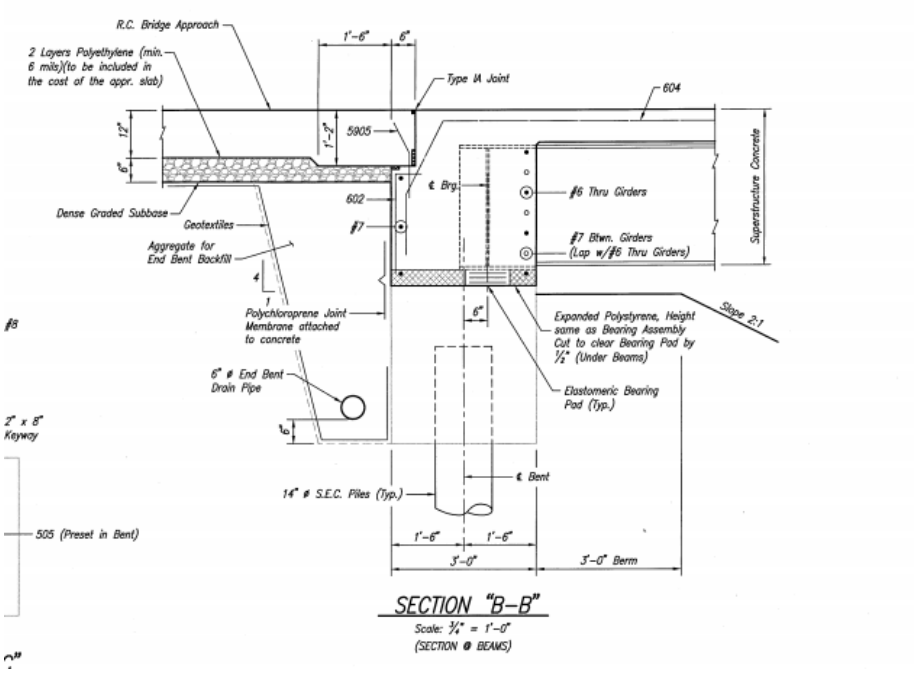

Figure A.54. Abutment Detail of the Bridge (NBI 41230) (2015)

Table A.26. Demand, Capacity, and Vulnerability of the Bridge (NBI 41230)

	Transverse Direction	**Longitudinal Direction**
Activated Mass (kips/g)	3.37	4.32
Total Stiffness (kips/in)	436999	450.4
Period (s)	0.017	0.62
Base Shear Capacity	6.89; 4.54; 6.62	0.27; 0.18; 0.26
Shear Capacity (kips)	5399; 5399; 5399	1402; 1402; 1402
Shear Connection (kips)	237.9	
Vulnerability	Not Vulnerable	Not Vulnerable due to Abutment

14. Bridge Asset Name: I70-074-05231 B – NBI 42020

Table A.27. Specifications and Information on Bridge I70-074-05231 B (NBI 42020)

Geographical Information	Asset Name	I70-074-05231 B
	NBI Number	42020
	County	Marion
	District	Greenfield
	Year of Construction	1967
	Year of Reconstruction	1981
	Facility Carried	LYNHURST DRIVE
	Feature Intersected	I-70
Superstructure Information	No. Beams + Beam Type	14; Rolled Shape
	Number of Spans	4
	Span Lengths	44'-0", 94'-0", 94'-0", 47'-0"
	Deck Width	82'-0"
	Deck Thickness	8"
	Skew	46.00 degrees
Substructure Information	Sub. Type; No. of Elements	Frame Bent; 6
	Height of Wall	6'-3", 8'-0", 7'-0"
	Element Spacing	13'-0", 13'-0", 13'-0"
	Element Dimensions	2'-0" x 6'-6", 2'-0" x 6'-6", 2'-0" x 6'-6"
	Abutment Type	Semi-Integral
	Concrete Compressive Strength	3500 psi
	Yield Strength of Reinforcement	40000 psi

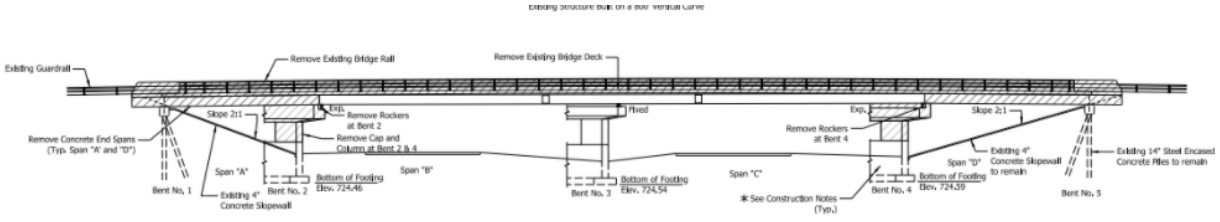

Figure A.55. Elevation View of the Bridge (NBI 42020) (2016)

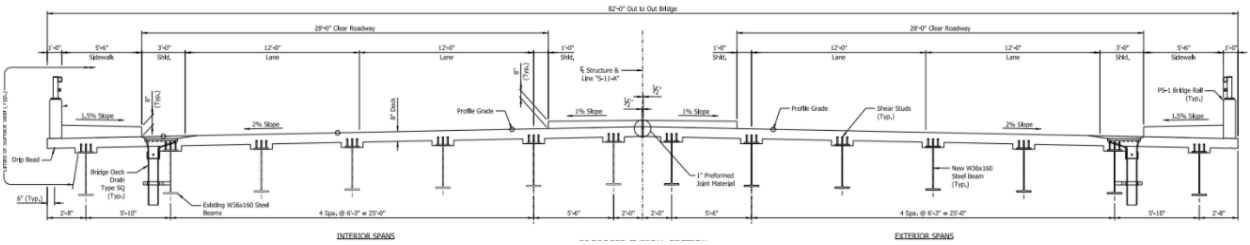

Figure A.56. Typical Section of the Bridge (NBI 42020) (2016)

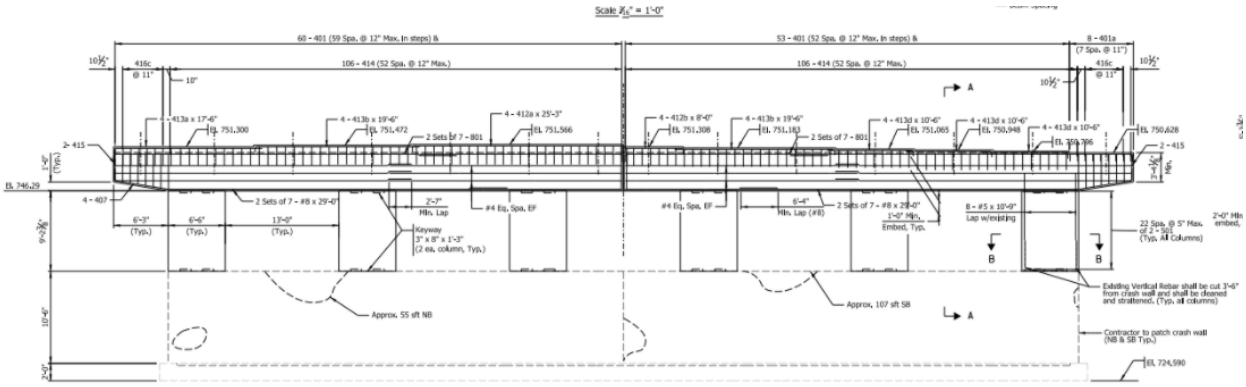

Figure A.57. Transverse Elevation of Interior Pier (NBI 42020) (2016)

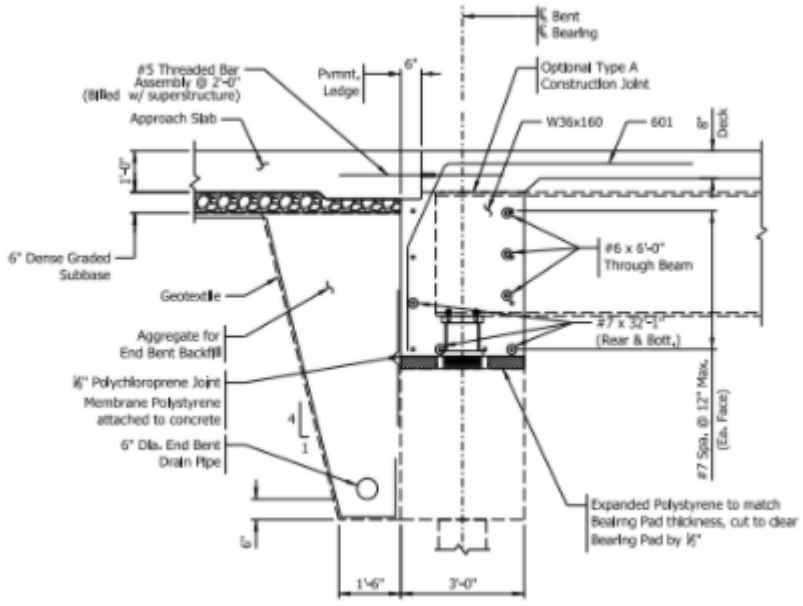

Figure A.58. Abutment Detail of the Bridge (NBI 42020) (2016)

Table A.28. Demand, Capacity, and Vulnerability of the Bridge (NBI 42020)

	Transverse Direction	Longitudinal Direction
Activated Mass (kips/g)	7.01	8.38
Total Stiffness (kips/in)	448196.9	8928.3
Period (s)	0.025	0.19
Base Shear Capacity	1.25; 0.8; 1.15	0.14; 0.09; 0.12
Shear Capacity (kips)	5304; 5304; 5304	1071; 1071; 1071
Shear Connection (kips)	456.3	
Vulnerability	Not Vulnerable	Not Vulnerable due to Abutment

15. Bridge Asset Name: I94-29-04469 CEB – NBI 49120

Table A.29. Specifications and Information on Bridge I94-29-04469 CEB (NBI 49120)

Geographical Information	Asset Name	I94-29-04469 CEB
	NBI Number	49120
	County	Porter
	District	La Porte
	Year of Construction	1969
	Year of Reconstruction	2014
	Facility Carried	I-94 EB
	Feature Intersected	BEAM STREET
Superstructure Information	No. Beams + Beam Type	9; Rolled Shape
	Number of Spans	3
	Span Lengths	55'-6", 84'-9", 48'-6"
	Deck Width	65'-2"
	Deck Thickness	8"
	Skew	09.00 degrees
Substructure Information	Sub. Type; No. of Elements	Frame Bent; 8
	Height of Wall	10'-0", 12'-9"
	Element Spacing	12'-0", 12'-0"
	Thickness of Wall	2'-0", 2'-0"
	Abutment Type	Semi-Integral
	Concrete Compressive Strength	3500 psi
	Yield Strength of Reinforcement	40000 psi

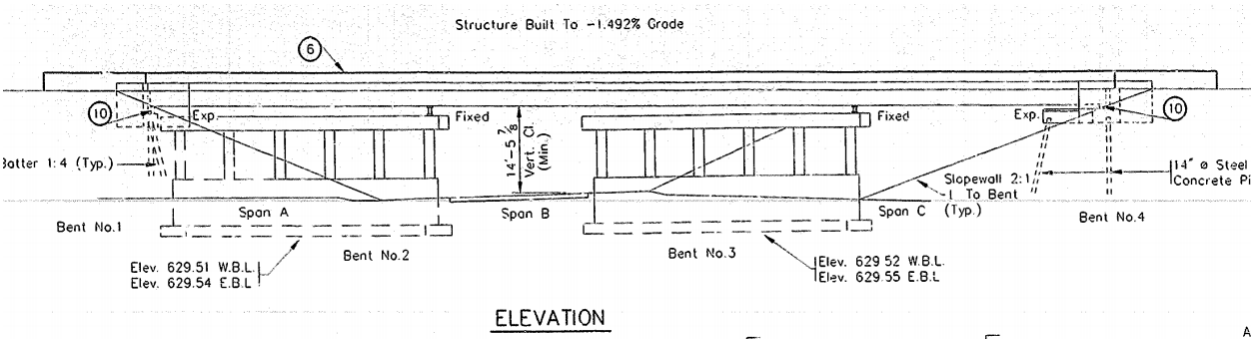

Figure A.59. Elevation View of the Bridge (NBI 49120) (1991)

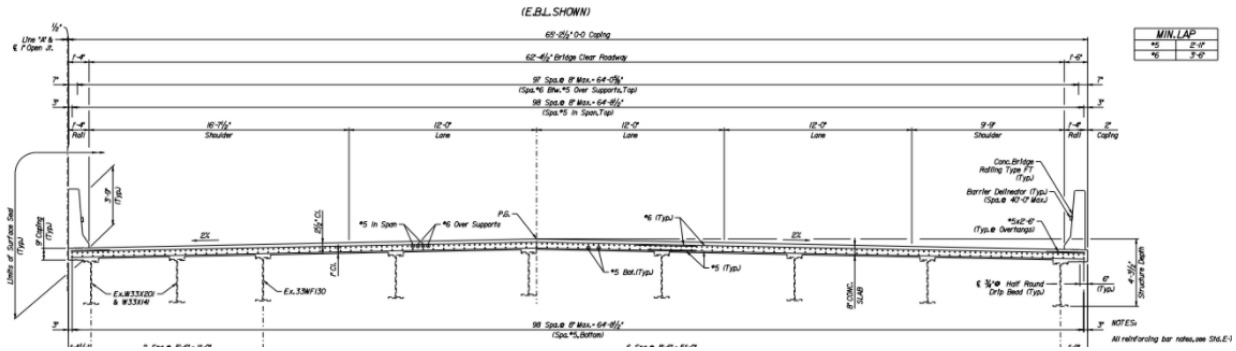

Figure A.60. Typical Section of the Bridge (NBI 49120) (2012)

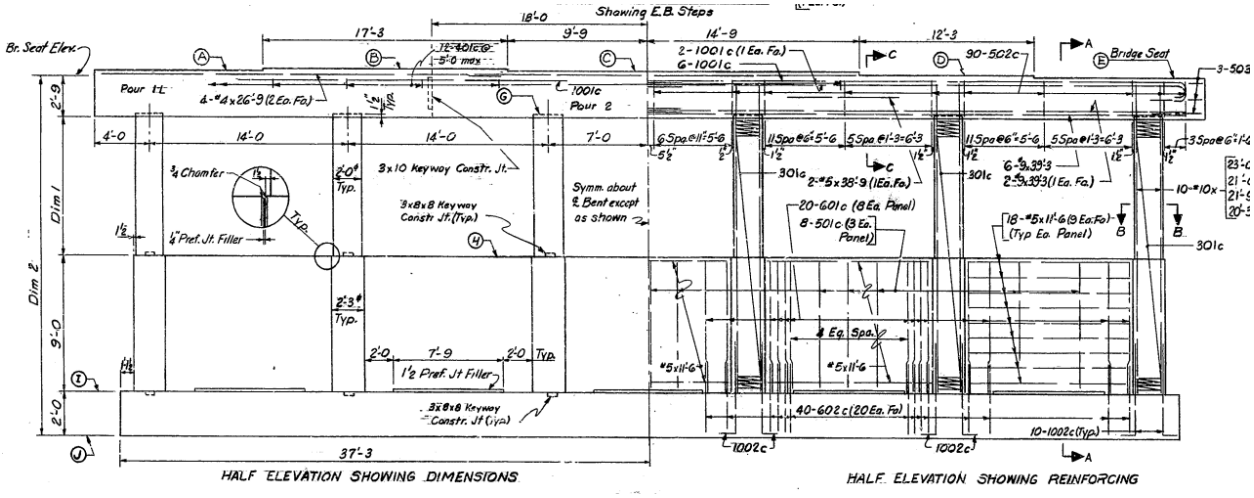

Figure A.61. Transverse Elevation of Interior Pier (NBI 49210) (1968)

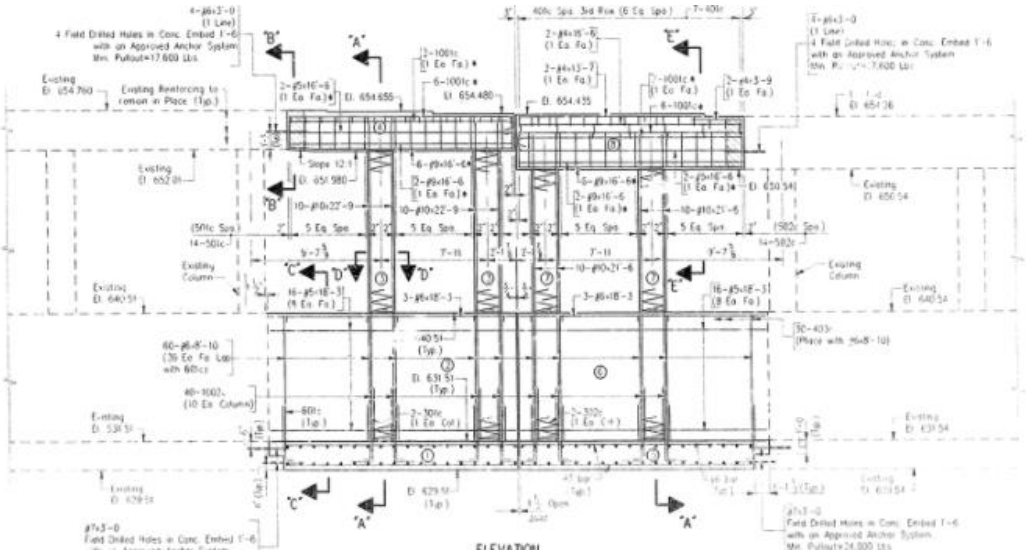

Figure A.62. Transverse Elevation of Interior Pier (NBI 49210) (1991)

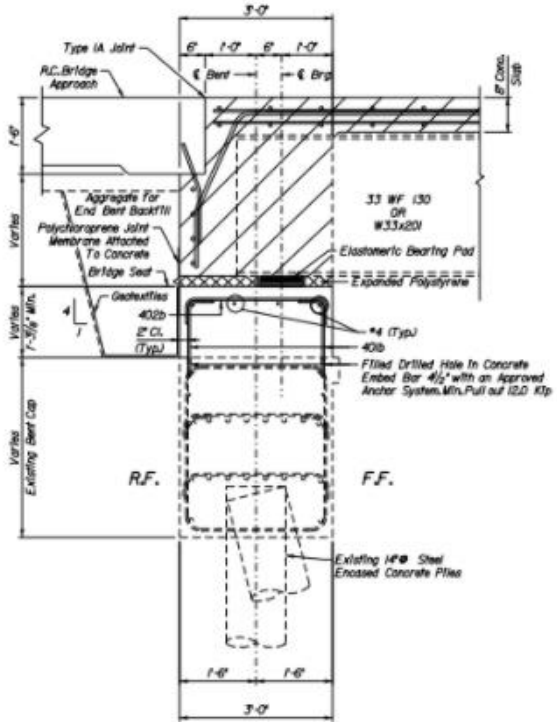

Figure A.63. Abutment Detail of the Bridge (NBI 49120) (2012)

Table A.30. Demand, Capacity, and Vulnerability of the Bridge (NBI 49120)

	Transverse Direction	Longitudinal Direction
Activated Mass (kips/g)	3.08	4.25
Total Stiffness (kips/in)	4344.9	797.8
Period (s)	0.167	0.46
Base Shear Capacity	0.93; 0.77	0.41; 0.35
Shear Capacity (kips)	458; 458	458; 458
Shear Connection (kips)	347.4	
Vulnerability	Not Vulnerable	Not Vulnerable due to Abutment

16. Bridge Asset Name: I465-127-05274 DEBL – NBI 50340

Table A.31. Specifications and Information on Bridge I465-127-05274 DEBL (NBI 50340)

Geographical Information	Asset Name	I465-127-05274 DEBL
	NBI Number	50340
	County	Marion
	District	Greenfield
	Year of Construction	1967
	Year of Reconstruction	2010
	Facility Carried	I-465 EB
	Feature Intersected	CARMEL CREEK
Superstructure Information	No. Beams + Beam Type	15; Plate Girder
	Number of Spans	3
	Span Lengths	35'-0", 44'-0", 35'-0"
	Deck Width	88'-4"
	Deck Thickness	8"
	Skew	00.00 degrees
Substructure Information	Substructure Type	Wall
	Height of Wall	23'-6", 26'-8"
	Width of Element (Base)	88'-4", 88'-4"
	Thickness of Wall	1'-6", 1'-6"
	Abutment Type	Semi-Integral
	Concrete Compressive Strength	4000 psi
	Yield Strength of Reinforcement	40000 psi

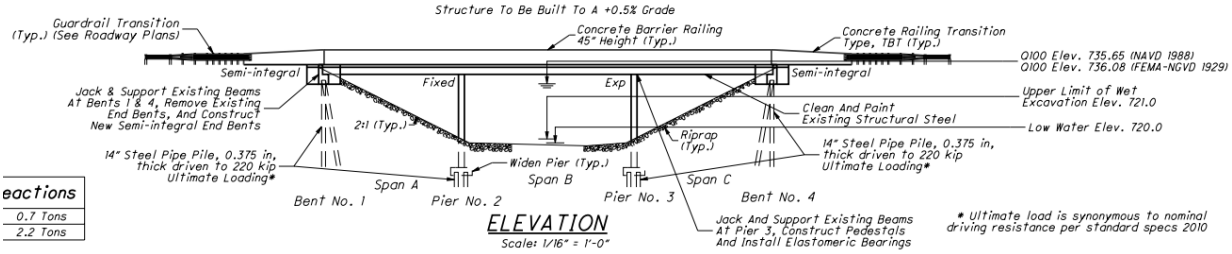

Figure A.64. Elevation View of the Bridge (NBI 50340) (2009)

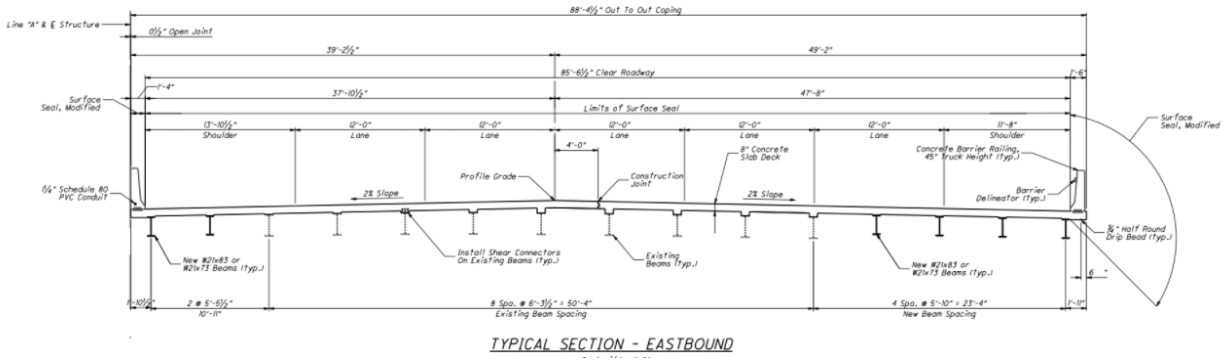

Figure A.65. Typical Section of the Bridge (NBI 50340) (2009)

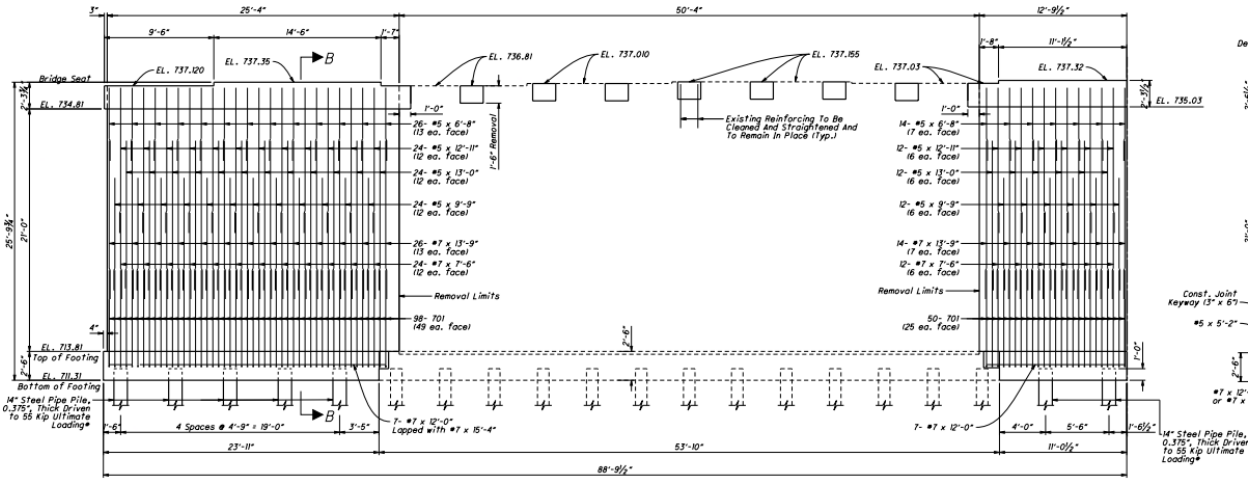

Figure A.66. Transverse Elevation of Interior Pier (NBI 50340) (2009)

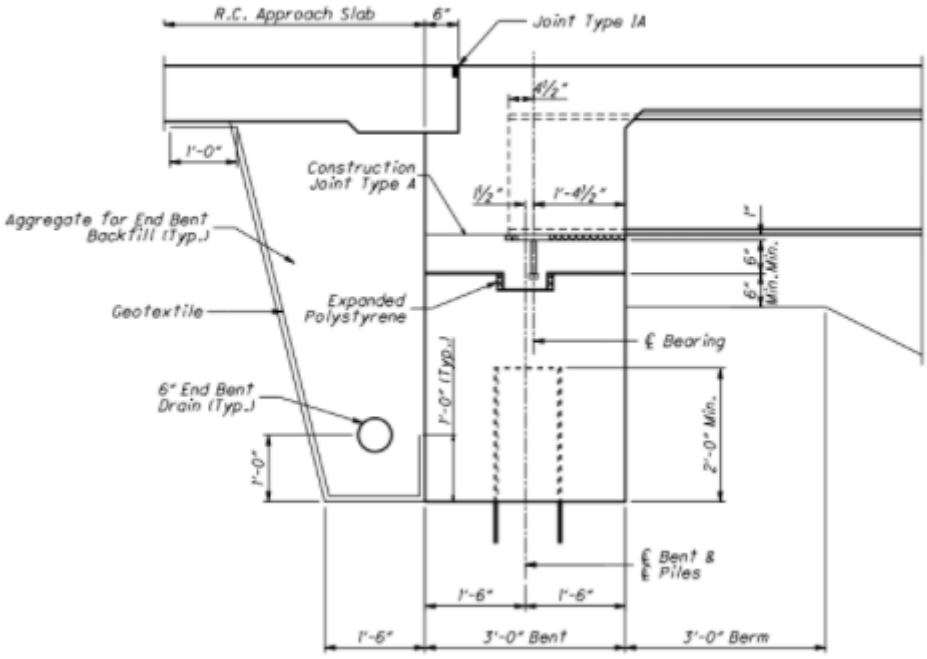

Figure A.67. Abutment Detail of the Bridge (NBI 50340) (2009)

Table A.32. Demand, Capacity, and Vulnerability of the Bridge (NBI 50340)

	Transverse Direction	**Longitudinal Direction**
Activated Mass (kips/g)	2.24	3.24
Total Stiffness (kips/in)	1628548.7	420.8
Period (s)	0.007	0.55
Base Shear Capacity	15.93; 14.03	0.27; 0.23
Shear Capacity (kips)	5177; 5177	1727; 1727
Shear Connection (kips)	247.5	
Vulnerability	Not Vulnerable	Not Vulnerable due to Abutment

17. Bridge Asset Name: I69-050-09497 NB – NBI 80182

Table A.33. Specifications and Information on Bridge I69-050-09497 NB (NBI 80182)

Geographical Information	Asset Name	I69-050-09497 NB
	NBI Number	80182
	County	Pike
	District	Vincennes
	Year of Construction	2012
	Year of Reconstruction	N/A
	Facility Carried	I-69 NB
	Feature Intersected	MUD CREEK
Superstructure Information	No. Beams + Beam Type	4; Plate Girder
	Number of Spans	3
	Span Lengths	130'-0", 190'-0", 130'-0"
	Deck Width	43'-3"
	Deck Thickness	8"
	Skew	18.00 degrees
Substructure Information	Substructure Type	Wall
	Height of Wall	24'-3", 23'-5"
	Width of Element (Base)	43'-0", 43'-0"
	Thickness of Wall	3'-0", 3'-0"
	Abutment Type	Semi-Integral
	Concrete Compressive Strength	3500 psi
	Yield Strength of Reinforcement	60000 psi

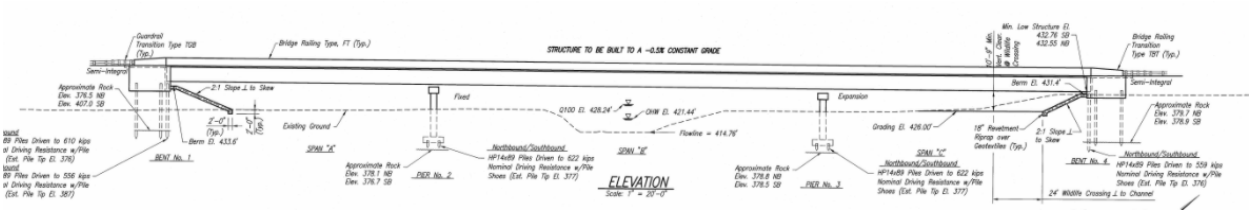

Figure A.68. Elevation View of the Bridge (NBI 80182) (2010)

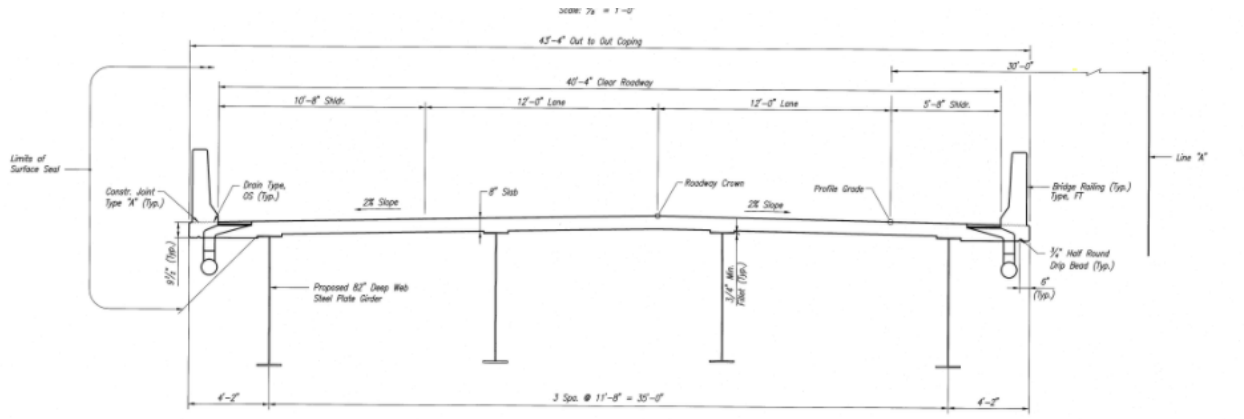

Figure A.69. Typical Section of the Bridge (NBI 80182) (2010)

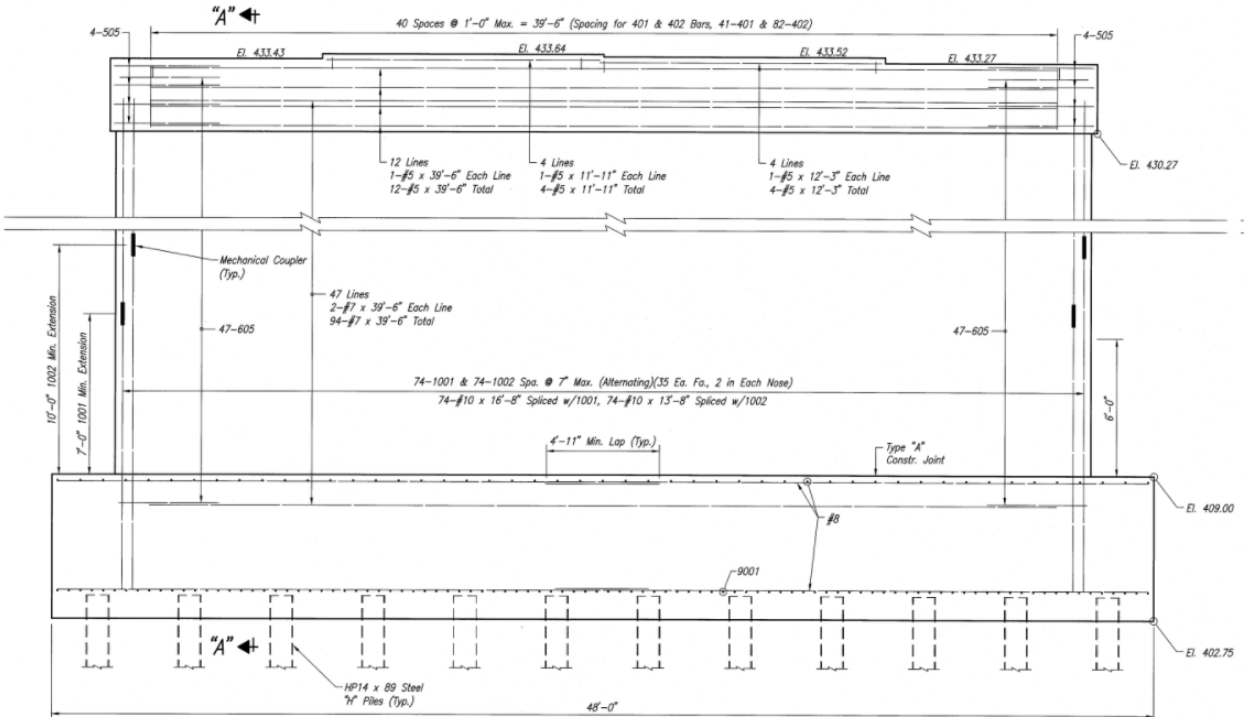

Figure A.70. Transverse Elevation of Interior Pier (NBI 80182) (2010)

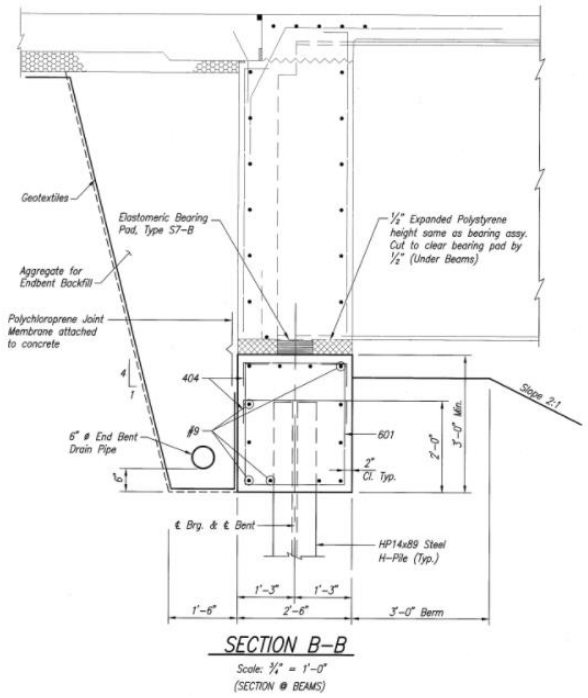

Figure A.71. Abutment Detail of the Bridge (NBI 80182) (2010)

Table A.34. Demand, Capacity, and Vulnerability of the Bridge (NBI 80182)

	Transverse Direction	**Longitudinal Direction**
Activated Mass (kips/g)	5.58	7.83
Total Stiffness (kips/in)	520616.3	1753.3
Period (s)	0.021	0.42
Base Shear Capacity	3.85; 3.98	0.28; 0.29
Shear Capacity (kips)	4432; 4432	1761; 1761
Shear Connection (kips)	613.5	
Vulnerability	Not Vulnerable	Not Vulnerable due to Abutment

APPENDIX B. SPECIAL MODELLING CASE: EXPANSION JOINTS

Bridge Information

Structure Number I64-05-05201 CEBL (NBI 033240) is a thirteen-span steel girder bridge located in the Posey county of the Vincennes District. Originally constructed in 1966, the bridge has had three rehabilitations. In 1984, the bridge deck overlay was replaced. In 2003, the bridge deck was patched and repaired and in 2016, a sealer was applied, and other general bridge rehabilitations were done. The super structure for spans 1-4 and 8-13 is composed of six W36x135 beams with a 7 ¾-*inch* reinforced concrete deck (Figure B.3). The superstructure for spans 5-7 is composed of four plate girders with a 7 ¾-*inch* reinforced concrete deck (Figure B.4). The bridge is skewed at 15-degress, has span lengths of 60’-0” , 75’-0”, 75’-0”, 60’-0”, 120’-0”, 160’-0”, 120”-0”, 60’-0”, 75’-0”, 75’-0”, 75’-0”, 75’-0”, and 60’-0”, and is 33’-6” wide.

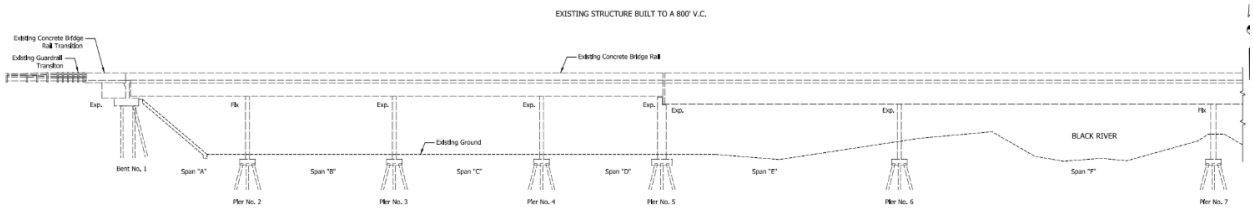

Figure B.1. Elevation View of Spans 1-6 of the Bridge (NBI 33240) (2015)

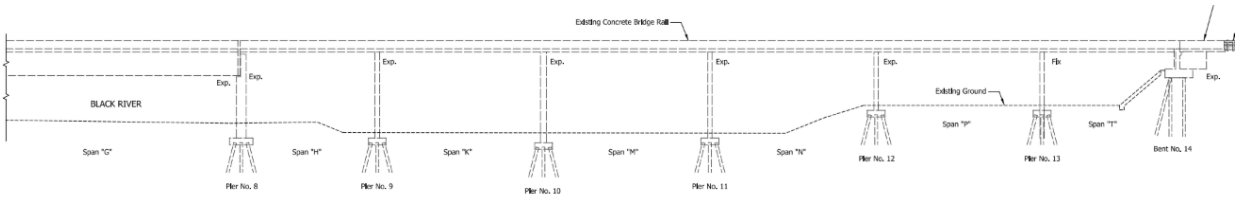

Figure B.2. Elevation View of Spans 7-13 of the Bridge (NBI 33240) (2015)

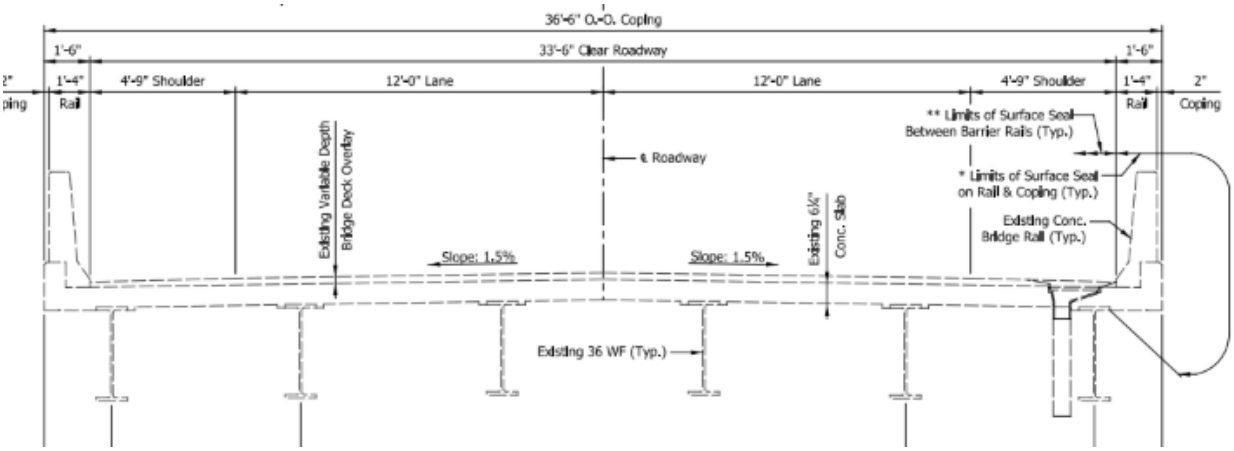

Figure B.3. Typical Section of Spans 1-4 and 8-13 of the Bridge (NBI 33240) (2014)

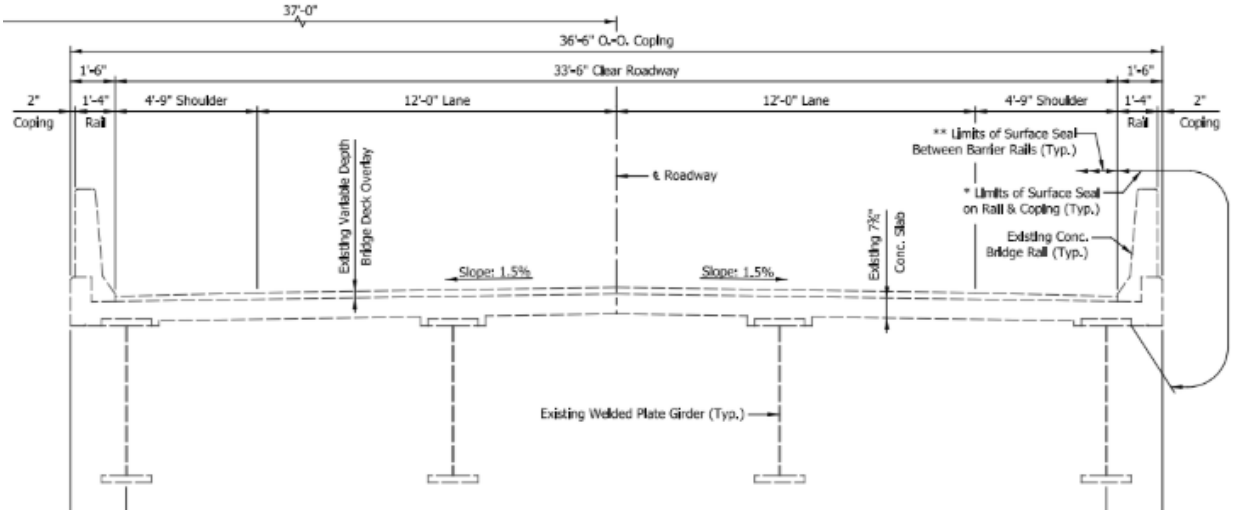

Figure B.4. Typical Section of 5-7 of the Bridge (NBI 33240) (2014)

The bridge is supported by two abutments and twelve interior piers shown in Figure B.1 and Figure B.2. Piers 2-4, and 9-13 are hammerhead piers. Piers 5-8 are wall piers. At each abutment and Piers 3-6, and 8-12, the superstructure is supported by expansion shoes (Figure B.5). At Piers 2, 7, and 13, the super structure is supported by fixed shoes (Figure B.6).

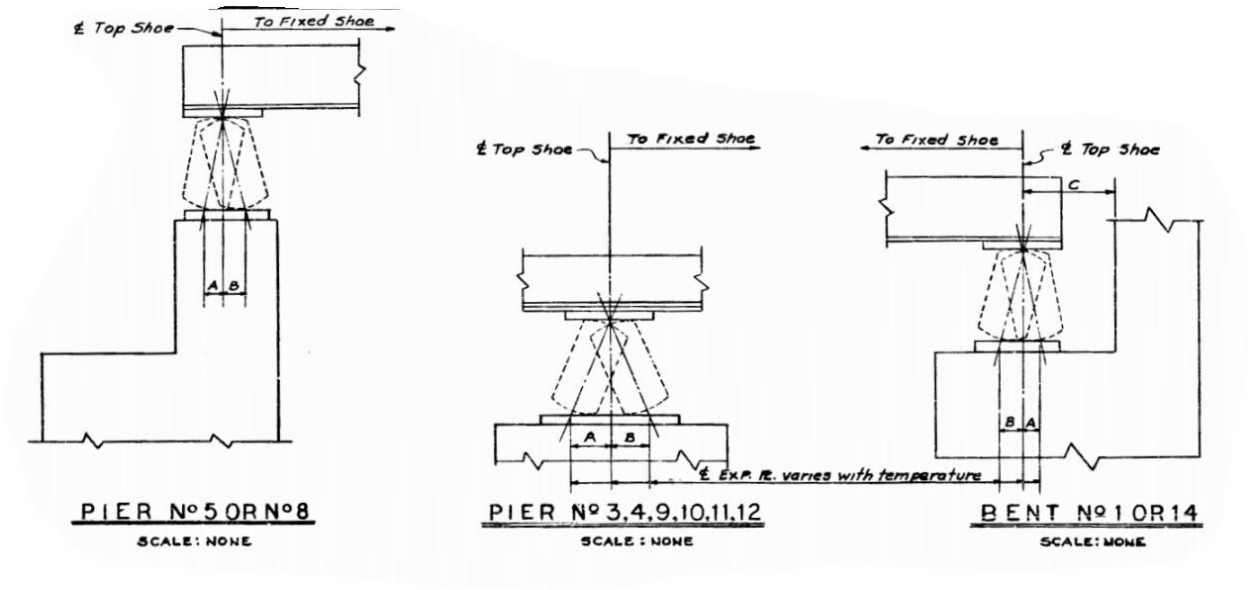

Figure B.5. Expansion Shoes for the Bridge (NBI 33240) (1966)

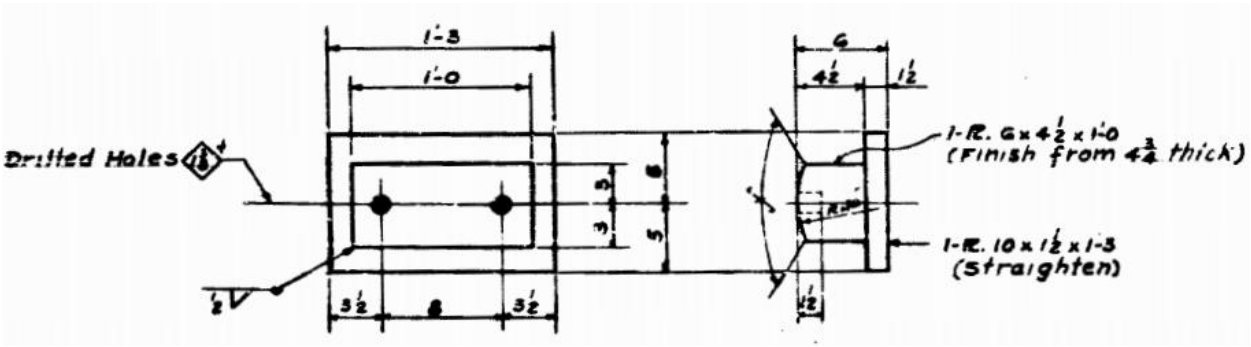

Figure B.6. Fixed Shoes for the Bridge (NBI 33240) (1966)

Over Piers 5 and 8, the bridge deck is broken up by expansion joints, shown in Figure B.7. The presence of the expansion joints allows the bridge deck to move as three separate bodies and therefore the bridge is modeled as three separate systems. System A includes spans 1-4 and Piers 2-4. Pier 5 is not included due to the expansion shoe connecting the superstructure to the substructure. System B includes spans 5-7 and Piers 6 and 7. Like in System A, Pier 5 and Pier 8 are not included in the model because of the expansion shoe. System C includes spans 8-13 and Piers 9-13, again, Pier 8 is not included because of the expansion shoe.

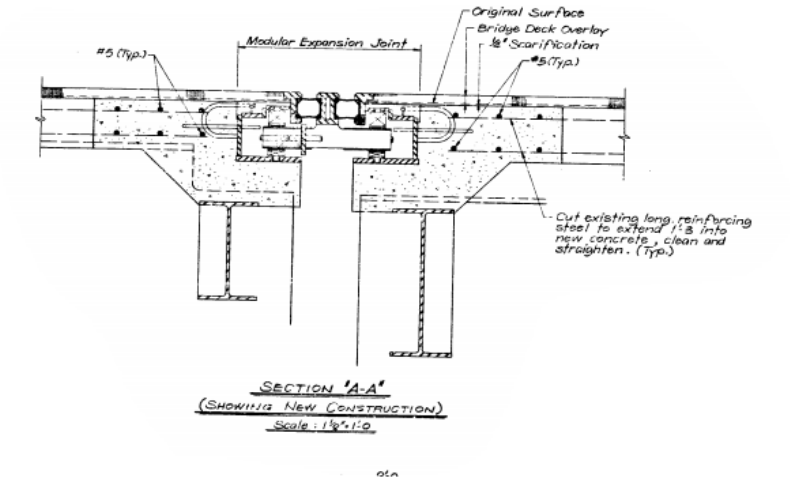

Figure B.7. Expansion Joints over Piers 5 and 8 for the Bridge (NBI 33240) (1978)

System A:

The substructure for System A is a hammerhead wall. For this substructure type, the geometries relevant to the calculations are wall length at the base, wall thickness, and wall height. Each pier has a uniform thickness of 2'-0", and an equivalent rectangular base length of 21'-6". The typical pier elevation is shown in Figure B.8. The heights of Piers 2, 3 and 4 are 22'-0", 21'-3", and 21'-3".

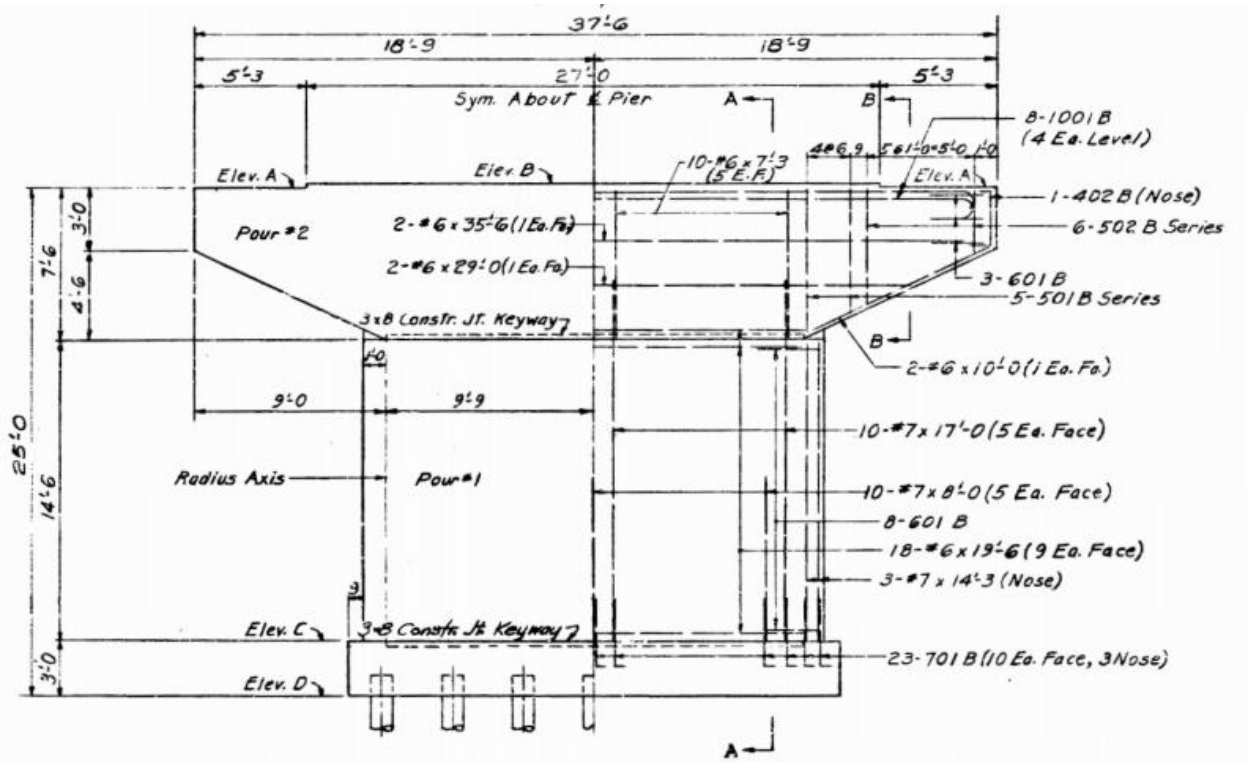

Figure B.8. System A: Transverse Elevation of an Interior Pier (NBI 33240) (1978)

Capacity

Identify Collapse Mechanism

As discussed in Chapter 3.5.2, the controlling mechanism of hinge formation for all fixed-free or fixed – semi-free hammerheads is identified as the formation of a plastic hinge at the base of the pier.

Base Shear

Walls in the transverse direction with aspect ratios less than 2.5 are controlled by shear. The aspect ratio for this bridge is 1.02. This This means that the bridge will not develop a hinge in the transverse direction

In the longitudinal direction, the base shear, controlled by the flexure mechanism, of each pier is calculated using the reinforcement layout shown in Figure B.1. The elongated oval shape is modeled as an equivalent rectangular section with a total reinforcement ratio of 0.20 percent or 0.6

in^2*/ft.* A 12 *inch* section of the wall is used for the longitudinal direction calculations and then multiplied by the total length to get the total base shear.

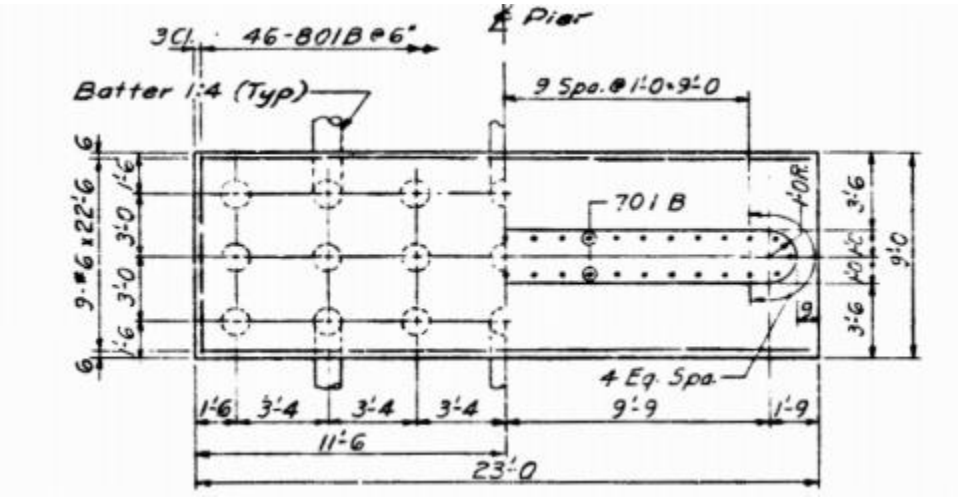

Figure B.9. System A: Cross Section of Typical Interior Pier of the Bridge (NBI 33240)

Table B. 1. System A: Moment-Curvature Results for the Longitudinal Direction for the Bridge (NBI 3324)

	Pier 2		**Pier 3**		**Pier 4**	
	Moment (*kip*ft*)	φ	**Moment (*kip*ft*)**	φ	**Moment (*kip*ft*)**	φ
Cracking	847.87	1.09E-5	847.87	1.09E-5	847.87	1.09E-5
Yield	831.64	7.68E-5	319.40	7.13E-5	319.40	7.13E-5
Ultimate	898.03	4.95E-4	340.34	4.79E-4	340.34	4.79E-4

The cracking moment exceeds the yield moment and the ultimate moment for Pier 3 and 4 and brittle failure my occur unless an alternate load path can be established. The cracking moment is therefore conservatively taken as the controlling moment for Piers 3 and 4. For Pier 2, the ultimate moment is larger than the cracking moment and therefore it is controlled by the base shear resulting from flexure. The shear force, over the entire length of the wall, that causes cracking or yielding (for Pier 2) of the three piers in the longitudinal direction is 62 *kips*, 62 *kips*, and 62 *kips*,

Shear Capacity of the Pier

Using the equations given in Chapter 3.5.2, the shear capacity of each pier is calculated. An α_c value of 3 is used based on the height to length ratio and a lambda (λ) value of 1 is used for normal-

weight concrete. The reinforcement ratio for each pier is 0.20%. The yield strength of the longitudinal reinforcement is assumed to be 40 *ksi* because the bridge was built during or after 1945 (Manual for Bridge Evaluation Table 6A.5.2.2-1). The shear capacity of each pier in the transverse direction is 1275 *kips*, 1200 *kips*, and 1200 *kips*. In the longitudinal direction, the shear capacity of each pier is 545 *kips*, 570 *kips*, and 570 *kips*.

Shear Capacity Connection

As mentioned in Case Study 2, the shear capacity of the connection is conservatively taken as the frictional force between the substructure and the superstructure and it is the same in the transverse and the longitudinal direction. The shear capacity of the connections of Piers 2, 3, and 4 are 170 *kips*, 190 *kips*, and 190 *kips*.

Identify Limiting Capacity

Table B.2 and Table B.3 show the limiting capacity and the controlling failure mechanism for all of the piers in the transverse and the longitudinal direction, respectively.

Table B.2. System A: Limiting Capacity of the Substructure in the Transverse Direction for the Bridge (NBI 33240)

Pier No.	Capacity – Trans.	Mechanism
2	170 kips	Shear Connection Failure
3	190 kips	Shear Connection Failure
4	170 kips	Shear Connection Failure

Table B.3. System A: Limiting Capacity of the Substructure in the Longitudinal Direction for the Bridge (NBI 33240)

Pier No.	Capacity – Long.	Mechanism
2	61.93 kips	Base Shear
3	61.66 kips	Brittle Failure of Pier
4	61.66 kips	Brittle Failure of Pier

Additional Longitudinal Displacement Capacity

In the longitudinal direction, when expansion shoe bearings are present, we consider the allowable displacement of the expansion shoe bearing as an additional displacement threshold. This threshold is 5.42 *inches*.

Demand

Longitudinal Mass

The entire mass is activated in the longitudinal direction. The mass consists of the entire mass of the deck, the mass of the beams and the mass of the railings. The longitudinal mass is 3.12 *kips/g*.

Transverse Mass

The activated mass of the bridge in the transverse direction is calculated using the superstructure geometry and the beam properties. The mass attributed to each pier is based on the mass calculated using the tributary area, taken as half of each span length adjacent to the pier, and the mass of the deck and the beams. Using the information used to calculate the mass in the longitudinal direction, the mass of the superstructure over Pier 2, 3, and 4 are 0.78 *kip/g*, 0.78 *kip/g*, and 0.78 *kip/g*.

Longitudinal Stiffness

As described previously, piers with expansion shoes connecting the superstructure to the substructure do not add to the overall stiffness of the system. Because of this, only Pier 2 contributes to the system's stiffness. Using the process and equations shown in Chapter 3.5.2, the stiffness of the bridge in the longitudinal direction is 152.9 *kip/in*.

Transverse Stiffness

The stiffness of hammerhead piers in the transverse direction is calculated using the equations found in Chapter 3.5.2. The resulting stiffness of each pier is 44480 *kip/in*, 47360 *kip/in*, and 47360 *kip/in*.

Equation-of-Motion

The equation-of-motion in the longitudinal direction is

$$3.12\frac{kips}{g}\ddot{x} + \left(2.19\frac{kips * s}{in}\right)\dot{x} + \left(152.9\frac{kips}{in}\right)x = -3.12\frac{kips}{g}\ddot{x}_g.$$

The equation-of-motion in the transverse direction is

$$2.43\frac{kips}{g}\ddot{x} + \left(58.16\frac{kips * s}{in}\right)\dot{x} + \left(139206.9\frac{kips}{in}\right)x = -2.43\frac{kips}{g}\ddot{x}_g.$$

Pushover Analysis

As mentioned previously, because the cracking moment of each pier is larger than the yield moment, the bridge will remain in the linear region until brittle failure. Because of this, no pushover analysis is needed.

Apply Ground Motions

This bridge did not have any available geotechnical information, so 100 synthetic ground motions were developed for the dynamic analysis. The site class for this bridge was determined from the IGS map (Figure 3.7) and is classified as site class D and the corresponding ground motions were used to assess the performance of the bridge.

Compare Demand to Capacity

In each direction, the maximum force resulting from the application of each of the seismic ground motions is compared to the capacity to assess if the capacity is exceeded. In the longitudinal direction, the maximum force resulting from 100 ground motions exceeds the capacity controlled by brittle failure of the pier. In the transverse direction, the maximum force resulting from 100 ground motions exceeds the capacity in the transverse direction, controlled by the shear connection between the substructure and superstructure, 9% of the time.

System B:

The substructure for System B is a wall. For this substructure type, the geometries relevant to the calculations are wall length, wall thickness, and wall height. Each pier has a uniform thickness of 2’-6” and an equivalent rectangular base length of 40’-6”. The typical pier elevation is shown in Figure B.10. The heights of Piers 6 and 7 are 30’-6” and 30’-6”, respectively.

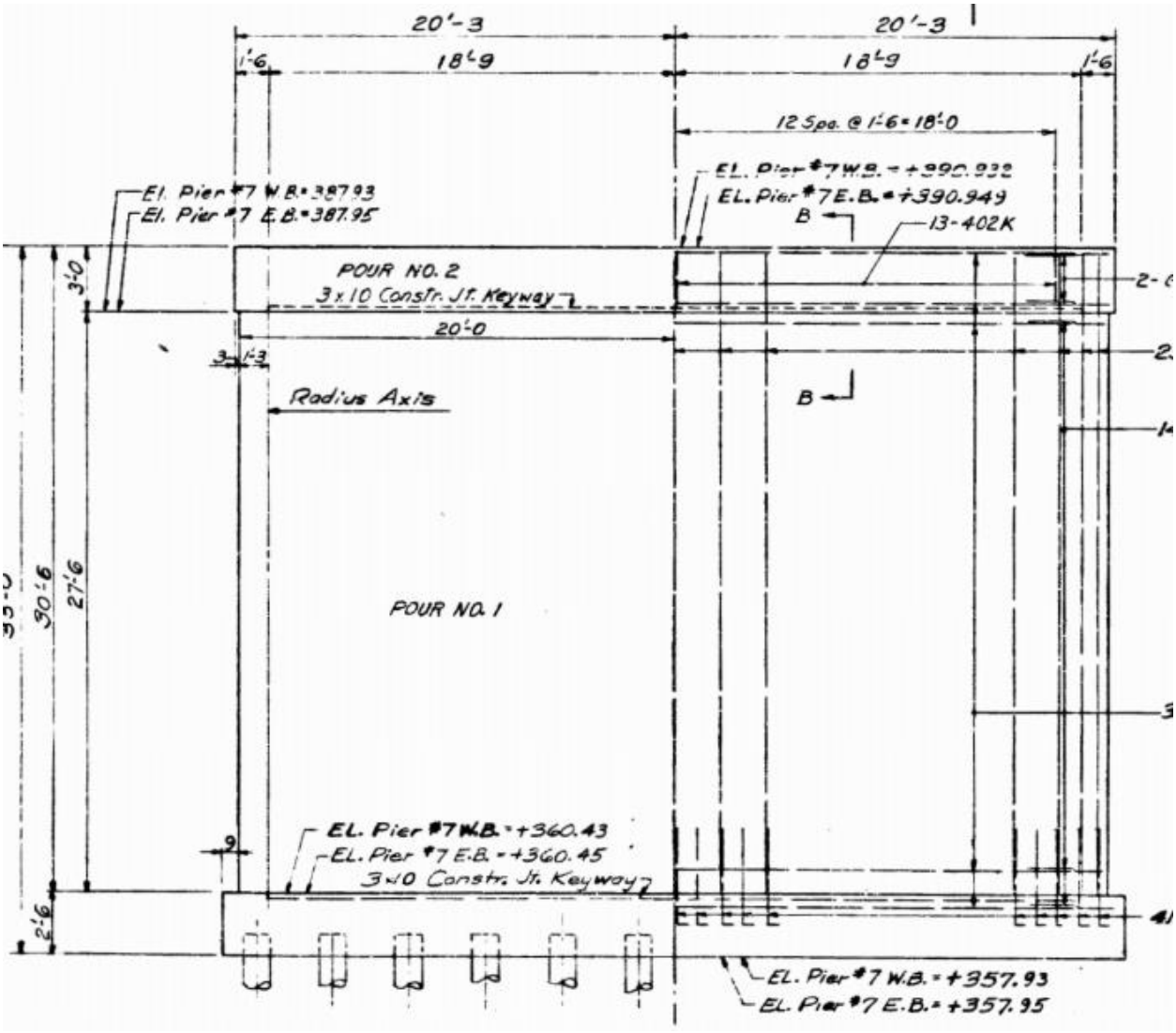

Figure B.10. System B: Transverse Elevation of an Interior Pier of the Bridge (NBI 33240) (1978)

Capacity

Identify Collapse Mechanism

As discussed in Chapter 3.5.1, the controlling mechanism of hinge formation for all fixed-free or fixed – semi-free walls is identified as the formation of a plastic hinge at the base of the pier.

Base Shear

Walls in the transverse direction with aspect ratios less than 2.5 are controlled by shear. The aspect ratio for this bridge is 0.75. This means that the bridge will not develop a hinge in the transverse direction

In the longitudinal direction, the base shear, controlled by the flexure mechanism, of each pier is calculated using the reinforcement layout shown in Figure B.11. The elongated oval shape is modeled as an equivalent rectangular section with a total reinforcement ratio of 0.20 percent or 0.6 in^2/ft. A 12 *inch* section of the wall is used for the longitudinal direction calculations and then multiplied by the total length to get the total base shear.

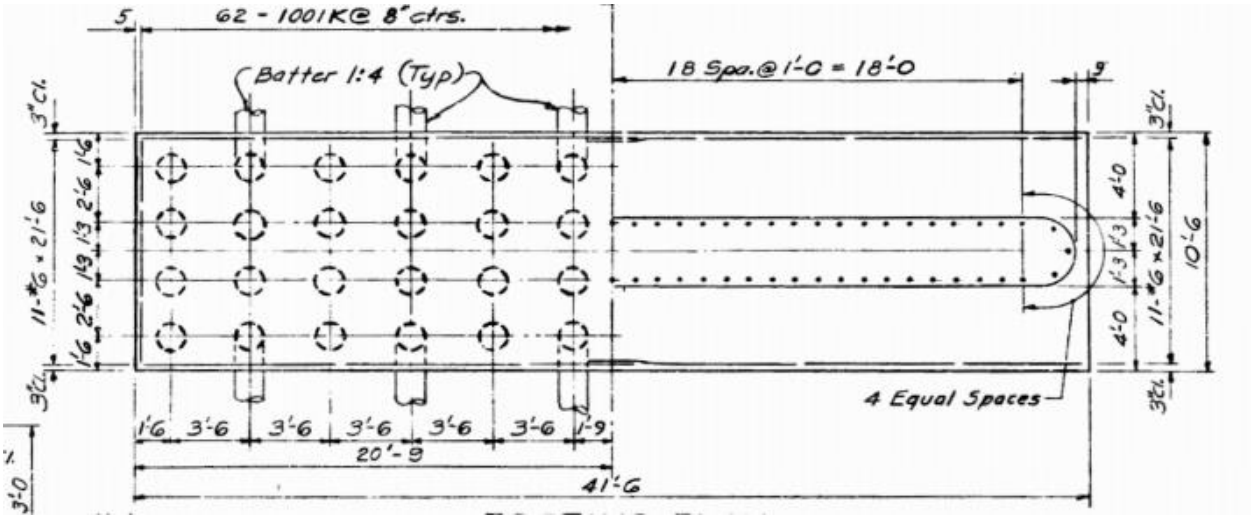

Figure B.11. System B: Cross Section of Typical Interior Pier of the Bridge (NBI 33240)

Table B. 4. System B: Moment-Curvature Results for the Longitudinal Direction for the Bridge (NBI 3324)

	Pier 6		**Pier 7**	
	Moment (kip*ft)	**φ**	**Moment (kip*ft)**	**φ**
Cracking	2695.5	8.7E-6	2695.5	8.7E-6
Yield	1925.8	1.01E-4	1925.8	1.01E-4
Ultimate	2033.1	4.51E-4	2033.1	4.51E-4

the cracking moment exceeds the yield moment and the ultimate moment for every pier and brittle failure my occur unless an alternate load path can be established. The cracking moment is therefore conservatively taken as the controlling moment for this bridge and a linear response of the bridge is used in all further calculations. The shear force, over the entire length of the wall, that causes cracking of Pier 6 and Pier 7 in the longitudinal direction is 88 *kips* and 88 *kips.*

Shear Capacity of the Pier

Using the equations given in Chapter 3.5.1, the shear capacity of each pier is calculated. An α_c value of 3 is used based on the height to length ratio and a lambda (λ) value of 1 is used for normal-weight concrete. The reinforcement ratio for each pier is 0.20%. The yield strength of the longitudinal reinforcement is assumed to be 40 *ksi* because the bridge was built during or after 1945 (Manual for Bridge Evaluation Table 6A.5.2.2-1). The shear capacity of each pier in the transverse direction is 3122 *kips* and 3122 *kips.* In the longitudinal direction, the shear capacity of each pier is 1242 *kips* and 1242 *kips.*

Shear Capacity Connection

As mentioned in Case Study 2, the shear capacity of the connection is conservatively taken as the frictional force between the substructure and the superstructure and it is the same in the transverse and the longitudinal direction. The shear capacity of the connections of the piers are 457 *kips* and 457 *kips.*

Identify Limiting Capacity

Table B.5 and Table B.6 show the limiting capacity and the controlling failure mechanism for all of the piers in the transverse and the longitudinal direction, respectively.

Table B.5. System B: Limiting Capacity of the Substructure in the Transverse Direction for the Bridge (NBI 33240)

Pier No.	Capacity – Trans.	Mechanism
6	457.5 kips	Shear Connection Failure
7	457.5 kips	Shear Connection Failure

Table B.6. System B: Limiting Capacity of the Substructure in the Longitudinal Direction for the Bridge (NBI 33240)

Pier No.	Capacity – Long.	Mechanism
6	88.37 kips	Brittle Failure of Pier
7	88.37 kips	Brittle Failure of Pier

Additional Longitudinal Displacement Capacity

In the longitudinal direction, when expansion shoe bearings are present, we consider the allowable displacement of the expansion shoe bearing as an additional displacement threshold. This threshold is 5.42 *inches*.

Demand

Longitudinal Mass

The entire mass is activated in the longitudinal direction. The mass consists of the entire mass of the deck, the mass of the beams and the mass of the railings. The cross-section for the plate girder can be seen in Figure B.12. The longitudinal mass is calculated as 5.95 *kips/g*.

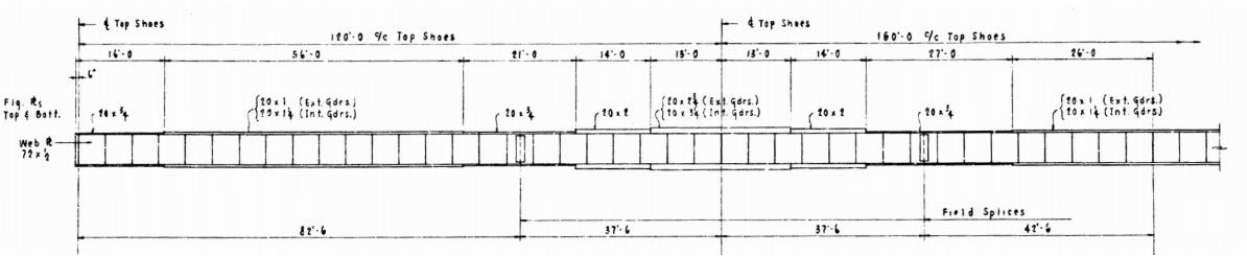

Figure B.12. System B: Typical Plate Girder Elevation for the Bridge (NBI 33240)

Transverse Mass

The activated mass of the bridge in the transverse direction is calculated using the superstructure geometry and the beam properties. The mass attributed to each pier is based on the mass calculated using the tributary area, taken as half of each span length adjacent to the pier, and the mass of the deck and the beams. Using the information used to calculate the mass in the longitudinal direction, the mass of the superstructure over each pier is 2.08 *kips/g* and 2.08 *kips/g*.

Longitudinal Stiffness

As described previously, piers with expansion shoes connecting the superstructure to the substructure do not add to the overall stiffness of the system. Because of this, only Pier 7 contributes to the system's stiffness. Using the process and equations shown in Chapter 3.5.2, the stiffness of the bridge in the longitudinal direction is 228 *kip/in*.

Transverse Stiffness

The stiffness of hammerhead piers in the transverse direction is calculated using the equations found in Chapter 3.5.2. The resulting stiffness of each pier is 109100 *kip/in,* and 109100 *kip/in.*

Equation-of-Motion

The equation-of-motion in the longitudinal direction is

$$5.94\frac{kips}{g}\ddot{x} + \left(3.68\frac{kips * s}{in}\right)\dot{x} + \left(228.2\frac{kips}{in}\right)x = -5.94\frac{kips}{g}\ddot{x}_g.$$

The equation-of-motion in the transverse direction is

$$4.16\frac{kips}{g}\ddot{x} + \left(95.27\frac{kips * s}{in}\right)\dot{x} + \left(218195.4\frac{kips}{in}\right)x = -4.16\frac{kips}{g}\ddot{x}_g.$$

Pushover Analysis

As mentioned previously, because the cracking moment of each pier is larger than the yield moment, the bridge will remain in the linear region until brittle failure. Because of this, no pushover analysis is needed.

Apply Ground Motions

This bridge did not have any available geotechnical information, so 100 synthetic ground motions were developed for the dynamic analysis. The site class for this bridge was determined from the IGS map (Figure 3.7) and is classified as site class D and the corresponding ground motions were used to assess the performance of the bridge.

Compare Demand to Capacity

In each direction, the maximum force resulting from the application of each of the seismic ground motions is compared to the capacity to assess if the capacity is exceeded. In the longitudinal direction, the maximum force resulting from 100 ground motions exceeds the capacity controlled by brittle failure of the pier. In the transverse direction, the maximum force resulting from 100 ground motions exceeds the capacity in the transverse direction, controlled by the shear connection between the substructure and superstructure, 12% of the time.

System C:

The substructure for System C is a hammerhead wall. For this substructure type, the geometries relevant to the calculations are wall length at the base, wall thickness, and wall height. Each pier has a uniform thickness of 2'-0", and an equivalent rectangular base length of 21'-6". The typical pier elevation is shown in Figure B.13. The heights of Piers 9, 10, 11, 12 and 13 are 25'-6", 25'-6", 25'-6", 15'-3", and 16'-0", respectively.

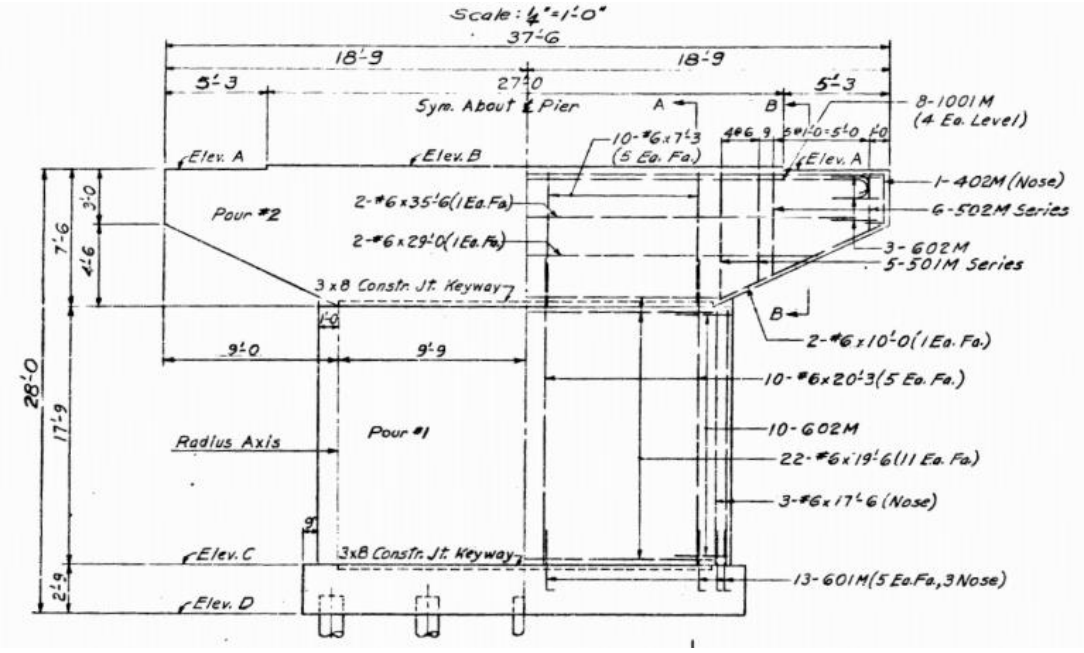

Figure B.13. System C: Transverse Elevation of an Interior Pier (NBI 33240) (1978)

Capacity

Identify Collapse Mechanism

As discussed in Chapter 3.5.2, the controlling mechanism of hinge formation for all fixed-free or fixed – semi-free hammerheads is identified as the formation of a plastic hinge at the base of the pier.

Base Shear

Walls in the transverse direction with aspect ratios less than 2.5 are controlled by shear. The aspect ratio for this bridge is 1.18. This This means that the bridge will not develop a hinge in the transverse direction.

In the longitudinal direction, the base shear, controlled by the flexure mechanism, of each pier is calculated using the reinforcement layout shown in Figure B.14. The elongated oval shape is modeled as an equivalent rectangular section with a total reinforcement ratio of 0.20 percent or 0.6 in^2/ft. A 12-*inch* section of the wall is used for the longitudinal direction calculations and then multiplied by the total length to get the total base shear.

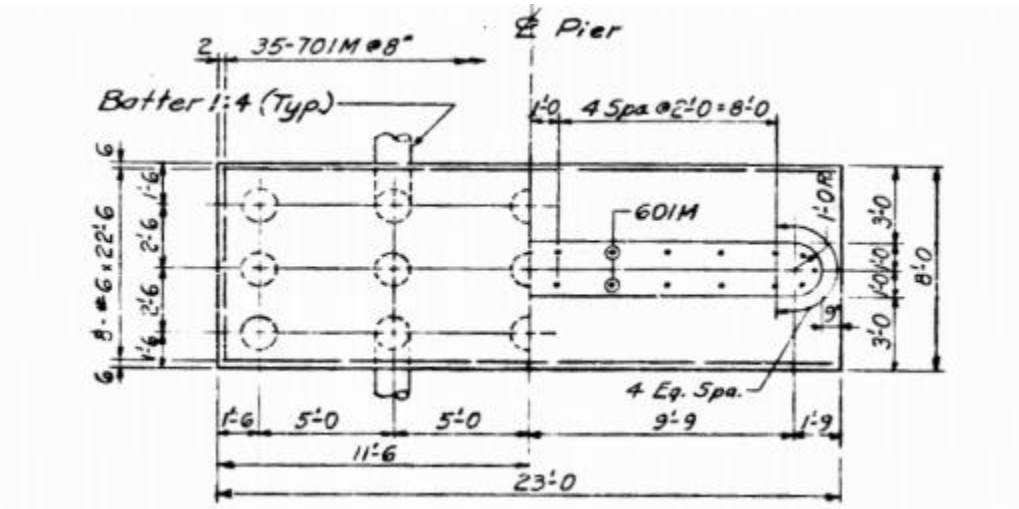

Figure B.14. System C: Cross Section of Typical Interior Pier of the Bridge (NBI 33240) (1986)

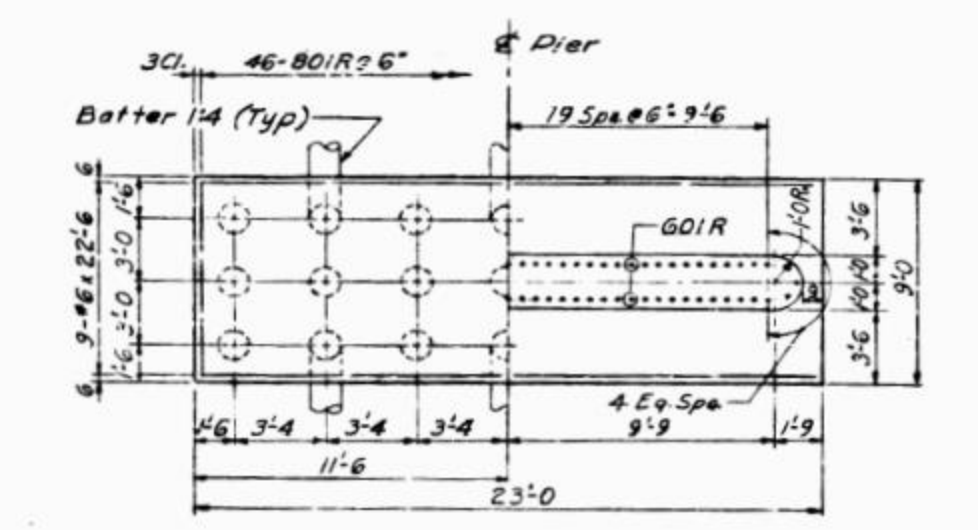

Figure B.15. System C: Cross Section of Pier 13 of the Bridge (NBI 33240) (1986)

Table B. 7. System A: Moment-Curvature Results for the Longitudinal Direction for the Bridge (NBI 3324)

	Pier 9, 10, 11 and 12		**Pier 13**	
	Moment (kip*ft)	**φ**	**Moment (kip*ft)**	**φ**
Cracking	847.87	1.09E-5	847.9	1.09E-5
Yield	319.40	7.13E-5	1196.5	8E-5
Ultimate	340.34	4.79E-4	1300.3	5.04E-4

Piers 9, 10, 11, and 12 and brittle failure may occur unless an alternate load path can be established. This does not occur in Pier 13 due to the increased amount of reinforcement, shown in Figure B.15. For Pier 9-12, the cracking moment is therefore conservatively taken as the controlling moment for this bridge and a linear response of the bridge is used in all further calculations. For Pier 13, the resulting base shear, calculated using the ultimate moment, is taken as the capacity. The shear fore, over the entire length of the was, that causes cracking or yielding of the five piers in the longitudinal direction is 47 *kips*, 47 *kips*, 47 *kips.* 110 *kips*, and 150 *kips.*

Shear Capacity of the Pier

Using the equations given in Chapter 3.5.2, the shear capacity of each pier is calculated. An α_c value of 3 is used based on the height to length ratio and a lambda (λ) value of 1 is used for normal-

weight concrete. The reinforcement ratio for each pier is 0.20%. The yield strength of the longitudinal reinforcement is assumed to be 40 *ksi* because the bridge was built during or after 1945 (Manual for Bridge Evaluation Table 6A.5.2.2-1). The shear capacity of each pier in the transverse direction is 1206 *kips*, 1206 *kips*, 1206 *kips*, 1206 *kips* and 1206 *kips*. In the longitudinal direction, the shear capacity of each pier is 572 *kips*, 572 *kips*, 572 *kips*, 572 *kips* and 572 *kips*.

Shear Capacity Connection

As mentioned in Case Study 2, the shear capacity of the connection is conservatively taken as the frictional force between the substructure and the superstructure and it is the same in the transverse and the longitudinal direction. The shear capacity of the connections of Piers 9, 10, 11, 12, and 13 are 170 *kips*, 190 *kips*, 190 *kips*, 190 *kips*, and 170 *kips*.

Identify Limiting Capacity

Table B.8 and Table B.9 show the limiting capacity and the controlling failure mechanism for all of the piers in the transverse and the longitudinal direction, respectively.

Table B.8. System C: Limiting Capacity of the Substructure in the Transverse Direction for the Bridge (NBI 33240)

Pier No.	Capacity – Trans.	Mechanism
9	171.9 kips	Shear Connection Failure
10	191.0 kips	Shear Connection Failure
11	191.0 kips	Shear Connection Failure
12	191.0 kips	Shear Connection Failure
13	171.9 kips	Shear Connection Failure

Table B.9. System C: Limiting Capacity of the Substructure in the Longitudinal Direction for the Bridge (NBI 33240)

Pier No.	Capacity – Long.	Mechanism
9	47.76 kips	Brittle Failure of Pier
10	47.76 kips	Brittle Failure of Pier
11	47.76 kips	Brittle Failure of Pier
12	109.40	Brittle Failure of Pier
13	152.97	Base Shear

Additional Longitudinal Displacement Capacity

In the longitudinal direction, when expansion shoe bearings are present, we consider the allowable displacement of the expansion shoe bearing as an additional displacement threshold. This threshold is 5.42 *inches*.

Demand

Longitudinal Mass

The entire mass is activated in the longitudinal direction. The mass consists of the entire mass of the deck, the mass of the beams and the mass of the railings. The longitudinal mass is 4.86 *kips/g*.

Transverse Mass

The activated mass of the bridge in the transverse direction is calculated using the superstructure geometry and the beam properties. The mass attributed to each pier is based on the mass calculated using the tributary area, taken as half of each span length adjacent to the pier, and the mass of the deck and the beams. Using the information used to calculate the mass in the longitudinal direction, the mass of the superstructure over Piers 9, 10, 11, 12, and 13 are 0.78 *kip/g*, 0.87 *kip/g*, 0.87 *kip/g*, 0.87 *kip/g*, and 0.78 *kip/g*.

Longitudinal Stiffness

As described previously, piers with expansion shoes connecting the superstructure to the substructure do not add to the overall stiffness of the system. Because of this, only Pier 13 contributes to the system's stiffness. Using the process and equations shown in Chapter 3.5.2, the stiffness of the bridge in the longitudinal direction is 400 *kip/in*.

Transverse Stiffness

The stiffness of hammerhead piers in the transverse direction is calculated using the equations found in Chapter 3.5.2. The resulting stiffness of each pier is 35000 *kip/in*, 35000 *kip/in*, 91700 *kip/in*, and 82700 *kip/in*.

Equation-of-Motion

The equation-of-motion in the longitudinal direction is

$$4.86\frac{kips}{g}\ddot{x} + \left(4.39\frac{kips * s}{in}\right)\dot{x} + \left(397.5\frac{kips}{in}\right)x = -4.86\frac{kips}{g}\ddot{x}_g.$$

The equation-of-motion in the transverse direction is

$$4.17\frac{kips}{g}\ddot{x} + \left(107.99\frac{kips * s}{in}\right)\dot{x} + \left(279661.6\frac{kips}{in}\right)x = -4.17\frac{kips}{g}\ddot{x}_g.$$

Pushover Analysis

As mentioned previously, because the cracking moment of each pier is larger than the yield moment, the bridge will remain in the linear region until brittle failure. Because of this, no pushover analysis is needed.

Apply Ground Motions

This bridge did not have any available geotechnical information, so 100 synthetic ground motions were developed for the dynamic analysis. The site class for this bridge was determined from the IGS map (Figure 3.7) and is classified as site class D and the corresponding ground motions were used to assess the performance of the bridge.

Compare Demand to Capacity

In each direction, the maximum force resulting from the application of each of the seismic ground motions is compared to the capacity to assess if the capacity is exceeded. In the longitudinal direction, the maximum force resulting from 100 ground motions exceeds the capacity controlled by brittle failure of the pier. In the transverse direction, the maximum force resulting from 100 ground motions exceeds the capacity in the transverse direction, controlled by the shear connection between the substructure and superstructure, 8% of the time.

Vulnerability Assessment

Structure Number I64-05-05201 CEBL (NBI 033240) is found to be not vulnerable in the transverse direction. In the longitudinal direction, the bridge is found to be highly vulnerable because demand exceeded the maximum base shear based on brittle failure for all the ground motions considered.

APPENDIX C. DEVELOPMENT OF THE UNIFORM HAZARD SPECTRUM

Introduction

INSAT utilizes the uniform hazard spectra (UHS) for a given return period, in this case, 1,000 years. A probabilistic seismic hazard analysis is completed to compute the hazard curves for each site, and then using the desired return period, and corresponding annual frequency of exceedance, the UHS at each bridge site is computed for a range of spectral periods. The unique characteristic of the UHS is that every point on the curve has an equal probably of being exceeded, however, it is an envelope of separate spectral accelerations at different period values which may have come from different events (Baker, 2008).

Methods and Tools for Determining the UHS

USGS has developed two tools to determine the UHS for a given return period and location. The first tool is the Unified Hazard Tool. This tool is available online and outputs the hazard curve and the UHS. However, it only calculates the spectral acceleration (SA) for three spectral periods and can only handle one site at a time. The other tool is the nshmp-haz tool. This is a java-based platform that is compatible with seven spectral periods and can handle multiple sites at one time. Unlike the Unified Hazard Tool, the nshmp-haz tool only computes the hazard curve; additional calculations are needed to convert the hazard curve to the UHS for the chosen return period. The hazard curve plots different levels of accelerations (in *g*) against the annual frequency of exceedance. Each spectral period has a different hazard curve. Because of its ability to handle multiple sites at a given time, the nshmp-haz tool was chosen over the Unified Hazard Tool for this project.

Using the nshmp-haz Tool

The nshmp-haz platform was developed by the National Seismic Hazard Mapping Project (NSHMP) within the U.S. Geological Survey's (USGS) earthquake hazards program (EHP) (https://github.com/usgs/nshmp-haz/wiki). At the time of application, the nshmp-haz tool required the following software programs: Java 8, Any, Guava, and Gson. The IntelliJ IDEA CE interface includes all the software requirements and was used to run the nshmp-haz tool.

The first step is downloading and assembling the nshmp-haz platform. At the time of writing, the nshmp-haz platform was available for download from GitHub and the specific instructions for assembling it were available on the GitHub wiki. For this project, the 2014 Central and Eastern US Seismic Hazard Map was used as the source model.

Each source model contains a config.json file which contains model initialization and calculation configuration properties. The default file is set up to calculate the hazard curves for three intensity measure types: PGA, 0.2s SA, and 0.1s SA at their default intensity measure levels (in terms of g). However, the nshmp-haz tool is compatible with more intensity measure types and is compatible with an intensity measure level. For this project, seven intensity measure types were specified in an edited config.json file: PGA, 0.1s SA, 0.2s SA, 0.3s SA, 0.5s SA, 1.0s SA, and 2.0s SA. Since this project needs the ground motion level at a desired return period and nshmp-haz calculates he return period for a given ground motion level, additional intensity measure levels are used to prevent error during interpolation. The edited config.json file contains custom intensity measure levels from 0.01g to 1.0g with a step size of 0.01g.

In addition to the config.json file, the other input into the nshmp-haz platform is a sites.csv file. This is where the location of each bridge is specified. The file must be named sites.csv and must contain a name, a longitude, and a latitude column, in that order. The name is how each site is distinguished and the longitude and latitude are what determine the hazard, using the chosen seismic hazard map.

Once the config.json file and the sites.csv file contain the required information, the next step is running hazard calculations. This consists of setting up an alias for the hazard tool, and then running the hazard tool. Using the edited config.json file discussed above, it takes approximately six seconds to run each site. The output is a hazout folder in the location where the sites.csv file is stored. The hazout folder contains a subfolder for each intensity measure type specified in the config.json file. Each intensity measure type subfolder contains a curves.csv file which holds the data for the hazard curve for each site at that intensity measure type. Figure C.1 shows the outputted hazard curves for a site in the Vincennes district.

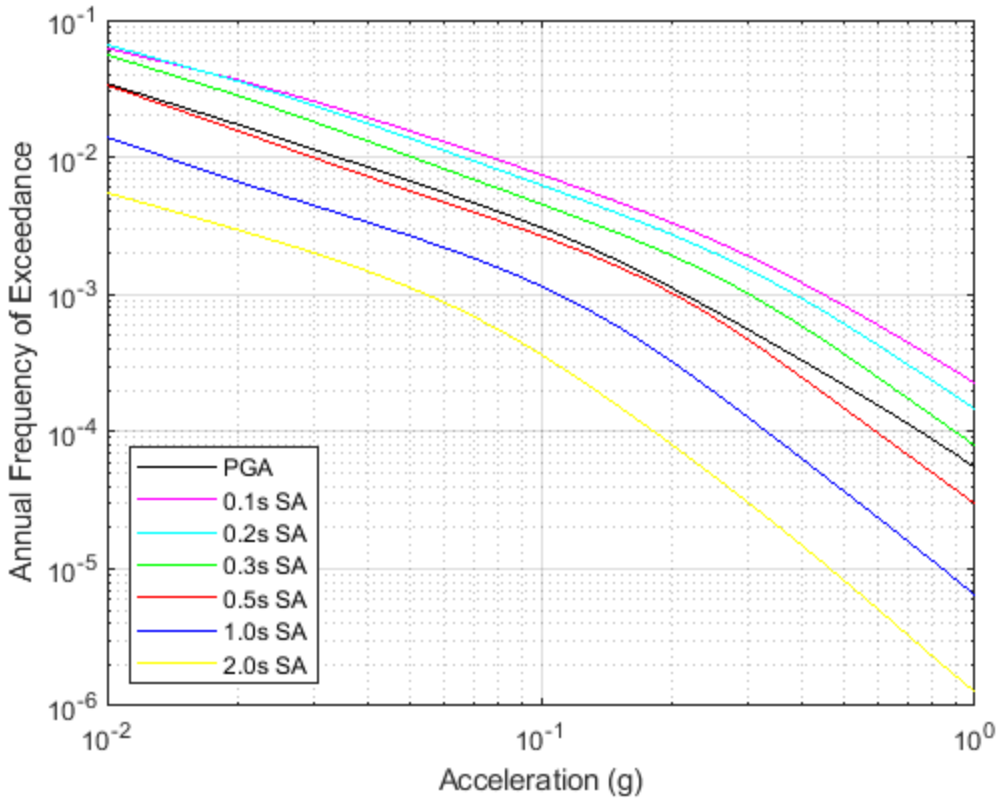

Figure C.1. Hazard Curve Output from nshmp-haz for a Site in the Vincennes District

As mentioned previously, interpolation calculations are needed to convert the hazard curve to the UHS for each site. To be consistent with the current AASHTO design specifications (2017), a return period of 1000 years (corresponding to a 7% probability of exceedance in 75 years) is considered. This corresponds to an annual frequency of exceedance (ν) of $9.68*10^{-3}$, calculated using Equation C. 1. Where P_E is the probability of exceedance of a given amplitude of ground motion, in this case 7% and t is the lifetime of the bridge, in this case 75 years.

$$\nu = \frac{-\ln(1 - P_E)}{t}. \qquad (C.1)$$

The UHS for a site is the ground accelerations for the desired annual frequency of exceedance plotted against the intensity measure type. Figure C.2 shows the UHS for the same site in the Vincennes district.

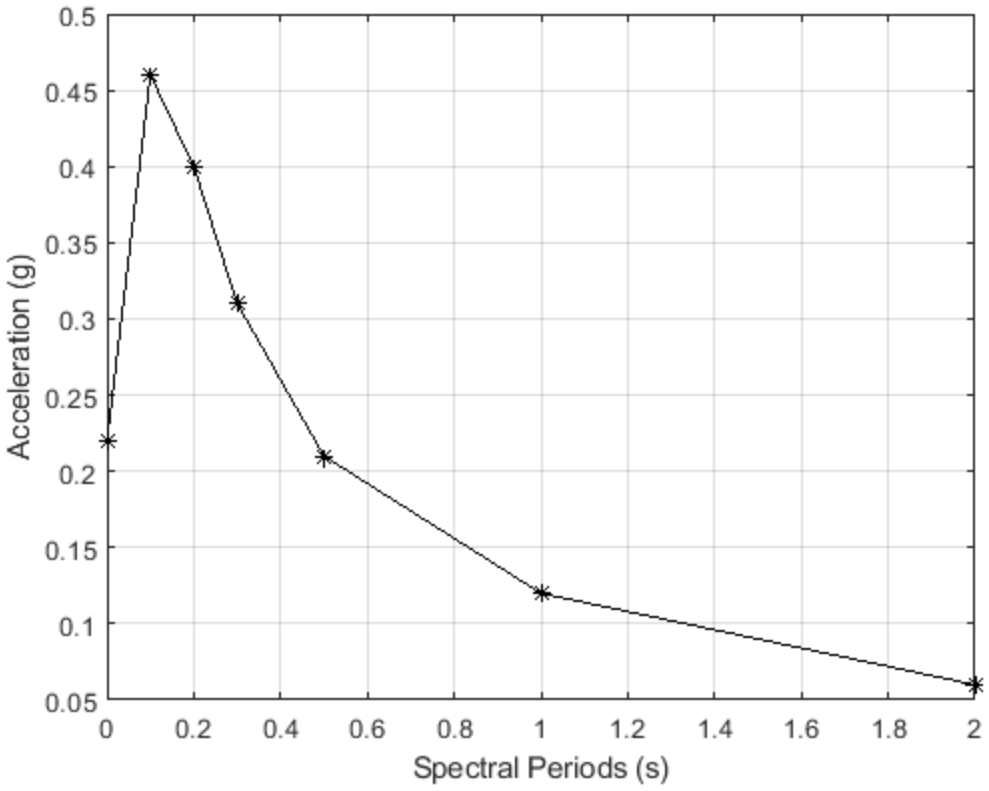

Figure C.2. Uniform Hazard Spectra for a Site in the Vincennes District, Site Class B/C

One of the shortfalls of nshmp-haz is that it is only compatible for NEHRP site class B/C, so the calculated UHS must be adjusted for local site conditions. AASHTO specifies site factors to amplify/de-amplify the ground acceleration based on the site class and the structure period (AASHTO, 2017). Figure C.3 shows the effects of the site class on the UHS for the same site in the Vincennes district.

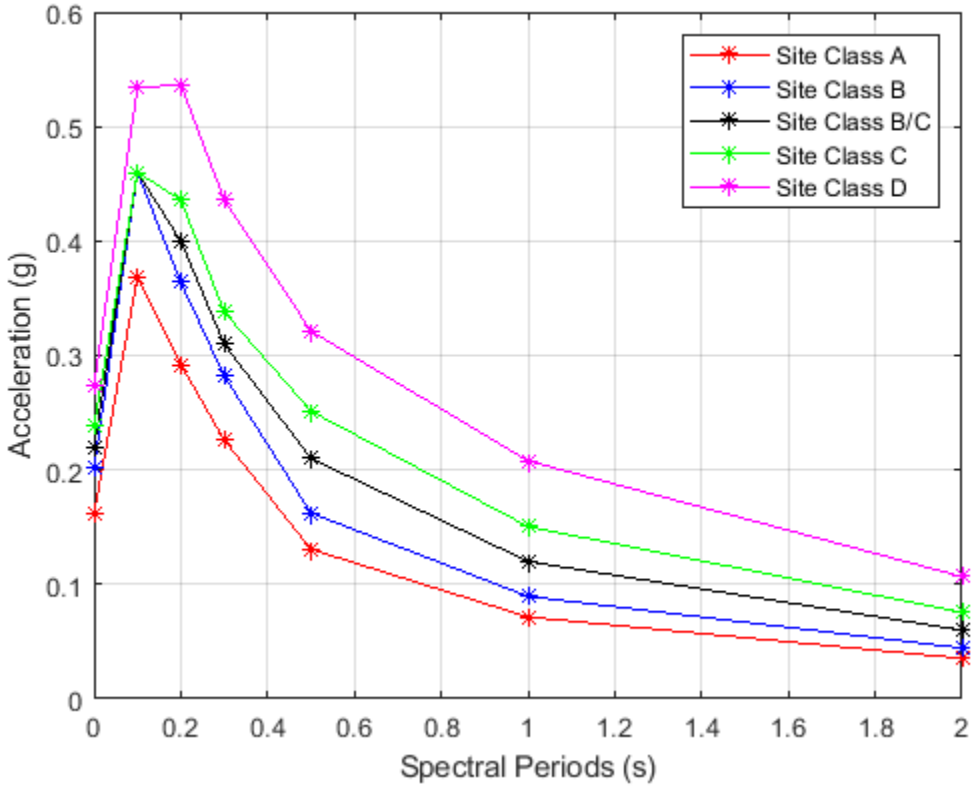

Figure C.3. Uniform Hazard Spectrum for a Site in the Vincennes District, All Site Classes